THE UNIVERSITY
of EDINBURGH

ORGANISATION OF THE FEATHER PERIODIC PATTERN THROUGH PROPAGATING MOLECULAR WAVES

WILLIAM KA WING HO

THE UNIVERSITY *of* EDINBURGH

Thesis submitted to the University of Edinburgh for the degree of Doctor of Philosophy

September 2015

CONTENTS

LIST OF FIGURES

LIST OF ABBREVIATIONS

ACVR	Activin A Receptor
ALK	Activin Receptor-Like Kinase
A-P	Anterior-Posterior
APC	Adenomatous Polyposis Coli
ASLV	Avian Sarcoma Leukosis Virus
BCIP	5-Bromo-4-Chloro-3-Indolyl Phosphate
BLAST	Basic Local Alignment Search Tool
BMP	Bone Morphogenetic Protein
BMPR	Bone Morphogenetic Protein Receptor
Bp	Base Pair
BrdU	Bromodeoxyuridine
BSA	Bovine Serum Albumin
Ca	Calcium
$CaCl_2$	Calcium Chloride
CaMKII	Calcium/Calmodulin-Dependent Protein Kinase II
cDNA	Complementary Deoxyribonucleic Acid
CEF	Chick Embryonic Fibroblast
CO_2	Carbon Dioxide
CRISPR	Clustered Regularly Interspaced Short Palindromic Repeats

DAPI	4 4', 6-Diamidino-2-Phenylindole
DEPC	Diethylpyrocarbonate
DIG	Digoxigenin
DKK	Dickkopf
DM	Dermomyotome
DMEM	Dulbecco's Modified Eagle's Medium
DMSO	Dimethyl Sulfoxide
DNA	Deoxyribonucleic Acid
DNP	2, 4-Dinitrophenol
dNTP	Deoxyribonucleoside Triphosphate
DTT	Dithiothreitol
E (#)	Embryonic Day
EDA	Ectodysplasin
EDAR	Ectodysplasin Receptor
EDARADD	Ectodysplasin Receptor-Associated Death Domain
EDTA	Ethylenediaminetetraacetic Acid
EGF	Epidermal Growth Factor
EMT	Epithelial-Mesenchymal Transition
ERK	Extracellular Signal-Regulated Kinase
ETS	E26 Transformation-Specific Transcription Factor

ETV	E26 Transformation-Specific Transcription Factor Translocation Variant
FBS	Foetal Bovine Serum
FGF	Fibroblast Growth Factor
FGFR	Fibroblast Growth Factor Receptor
FGFRL	Fibroblast Growth Factor Receptor Like
FRS	Fibroblast Growth Factor Receptor Substrate
GDF	Growth Differentiation Factor
GFP	Green Fluorescent Protein
GRB	Growth Factor Receptor-Bound
GSK	Glycogen Synthase Kinase
H & E	Haematoxylin and Eosin
HCl	Hydrochloric Acid
HED	Hypohidrotic/Anhidrotic Ectodermal Dysplasia
HH	Hamburger and Hamilton
HISS	Heat Inactivated Sheep Serum
HSPG	Heparin Sulphate Proteoglycan
IgG	Immunoglobulin G
IKK	Inhibitor of κB Kinase
INT	2-(4-Iodophenyl)-5-(4-Nitrophenyl)-3 Phenyltetrazolium
JNK	c-Jun N-Terminal Kinase

KCl	Potassium Chloride
KH_2PO_4	Potassium Dihydrogen Phosphate
LB	Lysogeny Broth
Lef	Lymphoid Enhancer-Binding Factor
LRP	Lipoprotein Receptor-Related Protein
MAD	Mothers Against Decapentaplegic
MAPK	Mitogen Activated Protein Kinase
MEK	Mitogen/Extracellular Signal-Regulated Kinase
Mg	Magnesium
$MgSO_4$	Magnesium Sulphate
mRNA	Messenger Ribonucleic Acid
Na	Naked Neck
NaOH	Sodium Hydroxide
$NaHCO_3$	Sodium Bicarbonate
NaH_2PO_4	Sodium Dihydrogen Phosphate
NARF	National Avian Research Facility
NBT	Nitroblue Tetrazolium
NC	Notochord
NEMO	NF- κB Essential Modulator
NFAT	Nuclear Factor of Activated T-Cells
NT	Neural Tube

NTMT	Alkaline Phosphatase Buffer
NTP	Nucleoside Triphosphate
OCT	Optimal Cutting Temperature
ORF	Open Reading Frame
PBS	Phosphate Buffered Saline
PBST	Phosphate Buffered Saline containing Tween 20
PCP	Planar Cell Polarity
PCR	Polymerase Chain Reaction
PFA	Paraformaldehyde
PKC	Protein Kinase C
PLCγ	Phospholipase Cγ
qRT-PCR	Quantitative Reverse Transcription Polymerase Chain Reaction
Ras	Rat Sarcoma
RCAS	Replication Competent ASLV Long Terminal Repeat with a Splice Receptor
rh	Recombinant Human
RNA	Ribonucleic Acid
RNAi	RNA Interference
ROR	Tyrosine-Protein Kinase Transmembrane Receptor
RT	Reverse transcriptase
RTK	Receptor Tyrosine Kinase

RYK	Related to Receptor Tyrosine Kinase
Sc	Scaleless
SHH	Sonic Hedgehog
SMA	Small body
SMAD	Portmanteau of SMA and MAD
SOS	Son of Sevenless
STAT	Signal Transducer and Activator of Transcription
TAB	TGFβ-Activated Kinase Binding Protein
TAK	TGFβ-Activated Kinase
TALEN	Transcription Activator-Like Effector Nuclease
TBS	Tris buffered Saline
TBST	Tris buffered Saline containing Tween 20
TCF	T-Cell Factor
TE	Tris-EDTA
TGF	Transforming Growth Factor
TNF	Tumour Necrosis Factor
TRAF	TNF Receptor Associated Factor
Tris	2-Amino-2-Hydroxymethyl-1, 3-Propanediol
U	Unit
UTR	Untranslated Region
v/v	Volume/Volume

WNT	Wingless-Related Integration Site
WT	Wild Type
w/v	Weight/Volume

DECLARATION

I declare that no portion of the work presented in this has been or will be submitted for any degree or qualification in this or any other university or institute. All work presented in this thesis is my own, unless otherwise stated.

LAY ABSTRACT

The evolution of birds and flight has been a major subject of debate within the scientific community ever since the discovery of archaeopteryx, a bird-like dinosaur with both avian and reptilian features. Since then, many more fossils of feathered dinosaurs have been discovered and it now appears that many of the dinosaurs we previously imagined as large scaly lizards may in fact be more similar to large chickens. Many studies have looked at how the shape of individual feathers may enable flight but do not examine how the arrangement of these feathers on the body is controlled. In flighted birds, feathers are arranged in a highly repeatable pattern of hexagons which is thought to streamline the body for increased flight efficiency. In bird species which have lost the ability to fly over the course of evolutionary history, the feather arrangement is less organised. This feather arrangement develops while the bird is still in the egg. In this project I study how the feather arrangement is laid out using the developing chicken as a model. I discover that wave-like movement across the skin of expression of a gene called *EDA*, a gene previously linked to hair and tooth formation in humans and mice, promotes the formation of a hexagonal pattern of feathers. If the wave-like movement of *EDA* is blocked in chicken then the arrangement of feathers becomes unorganised, similar to that seen in the non-flighted ostrich and emu, suggesting that gradual movement of *EDA* across the skin is responsible for the precise hexagonal arrangement of feathers.

ABSTRACT

Members of the class Aves possess integumentary structures which distinguish them from other vertebrate lineages. The characteristic integumentary structure that defines the Aves from other vertebrates are the feathers, whose functions include insulation, camouflage, visual display, gliding, and powered flight. The recent discoveries of theropod dinosaur fossils displaying feather-like structures have led to interest in the morphological innovations of the feathers, which are associated with the evolution of flight in Aves. Most modern birds, display a highly ordered, hexagonal arrangement of feather follicles, which aids in the streamlining of the body to increase aerodynamic efficiency. Using the chicken embryo as a developmental model, I address the cellular and molecular processes involved in the initiation and formation of a high fidelity periodic pattern of feather primordia. From my studies, I propose a model in which the induction of individual feather primordia begins with the activation of *FGF20* expression. This gene encodes a protein that serves as a chemoattractant. Aggregation of cells towards sources of FGF20 stimulates and reinforces *FGF20* expression and also induces the expression of *BMP4*. Via a reaction-diffusion-like mechanism, *BMP4* acts to limit the growth of the cell aggregate and promotes lateral inhibition to prevent fusions between neighbouring feather primordia through transcriptional regulation of *FGF20*. In order to achieve a high fidelity periodic pattern of feather primordia, three components are required; 1) a competent epidermis displaying *β-Catenin* and *EDAR* expression, 2) wave-like propagation of *EDA* expression, which acts synergistically with *β-Catenin* expression to activate *FGF20* expression at the *β-Catenin*/*EDA* junction, 3) and a dermis of sufficient cell density. The spatiotemporal wave-like propagation of *EDA* expression, specifically, promotes the sequential induction of new feather primordium rows and is associated with the formation of a high fidelity periodic pattern. The importance of these three components appears to be evolutionarily conserved among the Aves and differences in the periodic pattern of feather primordia between species can be explained by how the three components are expressed or regulated in individual species. Independent losses of flight in ratites, such as ostriches and emus, are associated with the loss of feather pattern fidelity. In

emus, this loss of pattern fidelity results from the delayed formation of a dermis of sufficient cell density, which prevents the induction of feather primordium formation within the dorsal tract, despite the presence of a fully primed and competent epidermis. These studies demonstrate how the precise feather pattern arises during embryonic development in birds, and how feather patterns can be modified through differential regulation of the molecular and cellular toolkit involved in feather primordium induction in different bird species.

ACKNOWLEDGEMENTS

Numerous people have supported and guided me over the last four years, without whom the completion of this thesis would not be possible. I am truly grateful to these people and will be forever indebted to them.

I would first like to thank my supervisor Dr. Denis Headon for giving me the opportunity to take part in this research project. His advice and guidance has been invaluable throughout this project.

To the late Professor Steven Bishop, whose advice and support kept me going during the early days of my PhD.

Thanks to the members of the Headon group, past and present, whose friendship and technical guidance over the last four years helped me progress to where I am today.

Over the last four years many people have helped me throughout this project in some way, be it technical support or general advice for surviving a PhD. In particular, I would like to thank the past and present members of the Burdon, Clinton, Davey, McGrew, Hohenstein, and Sang groups.

Thank you to all my family and friends who have supported me throughout this project. Special mention must go to the members of the hot-pot group, whose support and distractions kept me sane, especially during the writing of this thesis.

Honorable mentions should go to Claire Stenhouse, Selene Jarrett, and Dr. James Glover.

Finally, my greatest thanks should go to my partner Gwen Tsang, who has constantly had to put up with me during the most stressful times of my PhD.

INTRODUCTION

1. INTRODUCTION

1.1 General Introduction

The integument, or skin, is the largest organ of the body in most vertebrate organisms and its basic function is to act as a physical and chemical barrier between the organism and environment. The integument consists of two distinct layers, the epidermis and dermis, and protects the organism against desiccation, infection and mechanical trauma. In birds, the integument does not refer to the skin only, but also encompasses the integumentary derivatives such as feathers, scales, comb, beak, wattle, claws, and the uropygial (preen) gland. These integumentary structures are derived from the epidermis and dermis, and serve to broaden the range of functions of the integument in mature birds to include insulation, camouflage, visual display, gliding and powered flight. The avian skin itself shows regional variations in terms of thickness and the type of integumentary structure it bears based on the local roles the region of skin in question plays, such as the presence of scales on the feet and feathers on the wings. These regional variations are established during embryonic development and have long been a subject of interest for study (reviewed by (Johansson and Headon, 2014)). Although distinct types of integumentary appendages appear on different regions of skin, a common developmental theme exists between them, they all arise through epidermal-dermal interactions during embryonic development (Dhouailly *et al.*, 1978; Dhouailly, 1984; Saunders, 1958). Due to the accessibility of the developing chicken embryo and its amenability to experimental manipulation, the developing chicken embryo offers a powerful tool for the study of tissue interactions involved in the formation of the avian integument.

This thesis primarily focuses on the early development of the feather follicle precursors, and how the hexagonal arrangement of feathers arises during embryonic development, as such, these topics are reviewed in more detail below.

1.1.1 Structure of the Epidermis

The epidermis is a multi-layered, stratified epithelium, originating from the embryonic ectoderm, and which eventually gives rise to the epithelial appendages such as feathers and scale during embryogenesis (**Figure 1**). The thickness of the avian epidermis varies throughout the body and is thickest on feather bearing skin but thinnest on bare skin (Spearman, 1966). However, even at its thickest point, the avian epidermis throughout most of the body is thinner than the epidermis of other vertebrates, consisting of only two to three layers of cells. Due to the presence of feathers which can provide mechanical protection, it is thought that a reduction in epidermal thickness may reduce the overall weight of the bird, which can be advantageous for flight (Spearman, 1966). Another possible explanation for the requirement of a thin epidermis may be related to thermoregulation. Birds lack sweat glands, and a thinner "leaky" epidermis may facilitate evaporation and cooling to reduce body temperatures during flight (Menon *et al.*, 1996). The thin epidermis makes distinguishing the intermediate epidermal layers in birds, if present, very difficult compared to that of mammalian epidermis which can be clearly separated into four distinct layers based on their morphology and the keratins they produce (Fuchs and Green, 1980; Fuchs, 2007). Similar to the mammalian epidermis though, avian epidermis contains stratified layers of keratinocytes (keratin containing cells) composed of a basal layer, the stratum germinativum, and a suprabasal layer which terminates at the stratum corneum, a layer of flattened cornified keratinocytes on the surface of the epidermis (Spearman, 1966). The stratum corneum is continually sloughed off from the surface and is constantly replaced by the upward migration of keratinocytes produced by the underlying proliferating stratum germinativum.

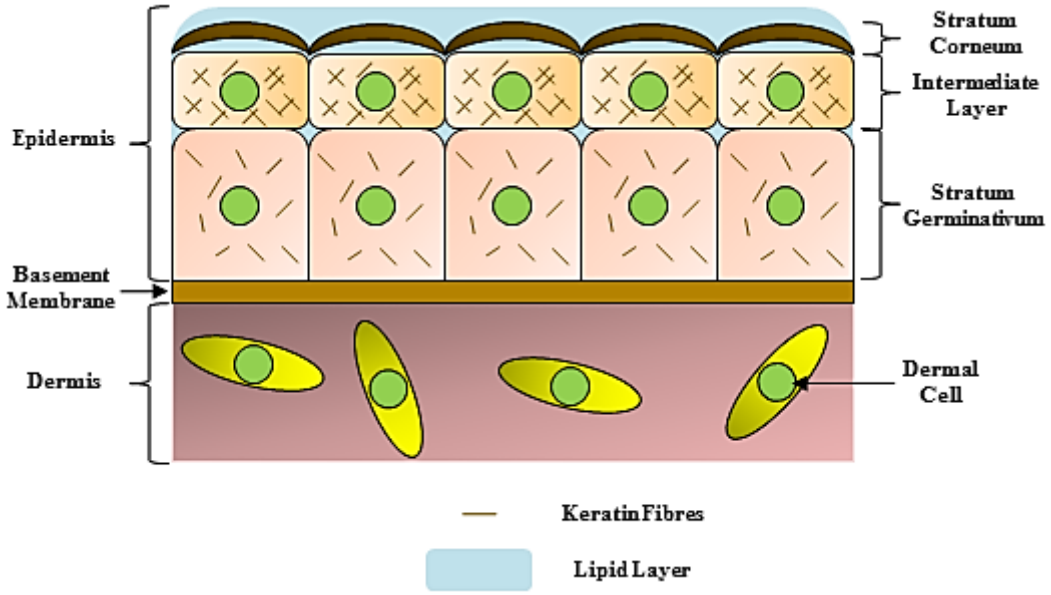

Figure 1. Structure of the skin. The adult chicken skin is composed of two main layers, a stratified epidermis and an underlying dermis. The epidermis and dermis are separated by a basement membrane. The epidermis is composed of either two or three distinct layers, but will always contain a basal layer called the stratum germinativum, and an exposed upper layer called stratum corneum

Keratins are structural proteins that are the main constituents of vertebrate epidermal appendages such as hair, nails, feather, and scales, of which there are two main forms; α-keratin and β-keratin (Baden and Maderson, 1970; Bell and Thathachari, 1963; Greenwold *et al.*, 2014; Rogers, 1985). The two forms of keratin proteins can be distinguished from their basic structure. α-keratins are fibrous proteins made up of α-helices, while β-keratins are made up of stacked, pleated sheets (Pauling and Corey, 1951; Pauling *et al.*, 1951). Structurally, this means that epidermal appendages made up of α-keratin, such as hair, are more pliable compared to those structures composed mainly of β-keratin e.g. feathers and scales, which are stiffer in comparison. α-keratins can be found in all vertebrates and are separated into two groups, type I and type II. Type I and type II α-keratins form obligate heterodimers and are the structural basis of the stratum corneum in both mammals and birds (Baden and Lee, 1978; Fuchs and

Marchuk, 1983; Hatzfeld and Franke, 1985; Sawyer *et al.*, 1986). β-keratins, on the other hand, are found exclusively in birds and reptiles (Greenwold and Sawyer, 2010; 2013; Sawyer *et al.*, 2000) and are the main structural components of feathers and scales (Haake *et al.*, 1984). In birds, there are four phylogenetically overlapping subfamilies of β-keratins: claw, feather, scale and epidermal β-keratin, each of which are differentially expressed during embryogenesis (Greenwold *et al.*, 2014). Of all four subfamilies of β-keratins, the genes of the feather β-keratins shows the greatest level of expansion and diversity among bird species (Greenwold and Sawyer, 2013; Greenwold *et al.*, 2014), and it has been hypothesised that the evolution and expansion of β-keratin genes within bird and reptile lineages led to the emergence of new innovative morphological structures such as feathers of birds and turtle/tortoise shells (Greenwold and Sawyer, 2010; Greenwold *et al.*, 2014; Li *et al.*, 2013)

The basic processes of proliferation and differentiation of keratinocytes from the stratum germinativum into the flattened, anucleated cells of the stratum corneum is common to all vertebrates. The basal layer is anchored to the basement membrane which separates the epidermal and dermal layers. Keratinocytes within the basal layer undergo rapid, continual proliferation and upward migration to form the suprabasal layers of the epidermis. To begin migration towards the surface of the epidermis, basal keratinocytes must detach from the basement membrane. Current models suggest that the detachment of the keratinocytes can occur in two ways: 1) delamination; proliferating cells gradually reduce their ability to adhere to the basement membrane and neighbouring cells, and are eventually pushed upwards as cell numbers in the stratum germinativum increase (Watt and Green, 1982), or 2) orientated mitosis; proliferating keratinocytes orientate themselves so that cell division causes the formation of two daughter cells that are stacked upon one another, which results in the upward migration of the apical daughter cell, while the basal daughter cell remains anchored to the basement membrane (Lechler and Fuchs, 2005; Smart, 1970) (**Figure 2)**. As suprabasal layers of keratinocytes migrate upwards, the keratinocytes undergo a terminal differentiation programme which results in the synthesis of keratin filaments, and gradual programmed cell death, leading to the formation of a layer of

dead, flattened, anucleated, keratin filled cells at the surface of the epidermis (Watt, 1998).

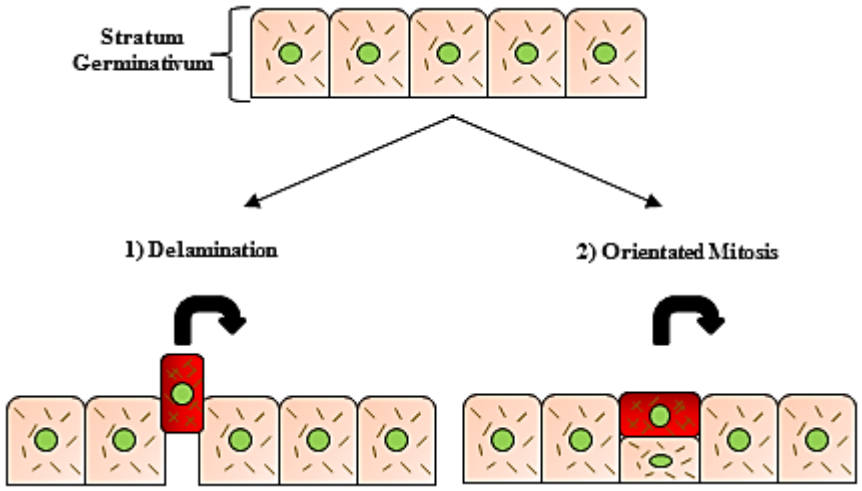

Figure 2. Models of development and upwards migration of new cells from the stratum germinativum. Models of how cell layers of the epidermis are replenished by the stratum germinativum; **1)** delamination and **2)** orientated mitosis. In delamination, as the cells of the stratum germinativum proliferate, some cells within the layer gradually lose their adhesion to the basement membrane and neighbouring cells and are eventually pushed upwards (red cell). Orientated mitosis involves the directed orientation of the dividing cell, prior to mitosis, which results in the formation of two daughter cells stacked one upon another. The basal daughter cell remains attached to the basement membrane, while the apical daughter cell migrates upwards into the upper layers (red cell).

As mentioned above, the epidermis of birds is relatively thin compared to other vertebrate species. The stratum corneum of birds is only one cell layer thick and composed of a layer of dead keratinised cells (Spearman, 1966). A thin epidermal layer may result in the increased permeability of the skin. The skin of birds lacks sebaceous glands which in mammals lubricates the skin and forms a permeability barrier (Lucas and Stettenheim, 1972). To compensate for this, in some birds, the epidermis is extremely lipogenic and the keratinocytes themselves are able to produce and secrete

a variety of lipids as the keratinocytes undergo differentiation during their upward migration towards the stratum corneum (Freinkel, 1972; Matoltsy, 1969; Menon and Menon, 2000). These lipid secreting keratinocytes have been termed "sebokertinocytes" due to their ability to synthesis both keratin and lipids (Wrench *et al.*, 1980). The lipids produced by the sebokertinocytes function analogously to mammalian sebum, resulting in the stratum corneum having an organisation that has been described as "brick and mortar" like (Elias and Menon, 1991; Nemes and Steinert, 1999). The dead keratinised cells form the bricks and the surrounding lipids excreted by the maturing keratinocytes form the mortar which lubricates and waterproofs the skin, forming a permeability barrier.

1.1.2 Development of the Epidermis

During chicken embryogenesis, the epidermis develops from the surface ectoderm at around stages 9 to 11 of Hamburger and Hamilton (HH stage) (Hamburger and Hamilton, 1952; Hamilton, 1952). (Note: developmental stages of chicken embryos will be described according to the HH staging system, unless they were not stated by the original authors, otherwise the number of days of incubation will be used instead). The ectoderm begins as monolayer and serves as the initial interface between the amniotic fluid and the developing embryo. The ectoderm is highly proliferative throughout embryogenesis to cope with the rapidly growing embryo during its development. At around HH stage 29, similar to mammals (between E9 - E12 in mouse), the ectoderm becomes a bilayer which consists of a lower basal layer of cuboidal cells which eventually gives rise to the stratum germinativum and an apical layer of flattened cells called the periderm, which can be identified by keratin 5 expression (Boneko and Merker, 1988; Hamilton, 1952; Saathoff *et al.*, 2004; Sawyer *et al.*, 1986). However, unlike mammals, at HH 38 an additional layer of cells begins to form between the periderm and the basal layer of cells called the subperiderm which associates with the periderm forming a periderm/subperiderm unit. (Saathoff *et al.*, 2004; van Echten-Deckert *et al.*, 2007). It is thought that the periderm/subperiderm unit functions as an impermeable barrier to diffusion between the embryo and amniotic fluid, through the formation of tight junctions between the cells of the

periderm/subperiderm unit, prior to the formation of a mature stratified epidermis in the developing embryo (Saathoff *et al.*, 2004). The periderm/subperiderm may also function to prevent the adhesion of immature epithelia of different skin regions, as demonstrated in experiments using mice with dysfunctional periderm formation which show fusions between adjacent skin regions such as the developing upper and lower jaws (Richardson *et al.*, 2014). At HH stage 39, the basal layer begins to rapidly proliferate, starting the process of keratinization and stratification of the epidermis (Mcloughlin, 1961). By HH stage 44, keratinisation of the epidermis is completed forming the mature epidermis. After the formation of a mature stratified epidermis, containing a layer of cornified keratinocytes surrounded by lipids, the peridermal and subperidermal layers are sloughed off through simultaneous programmed cell death around two days prior to hatching (Saathoff *et al.*, 2004; Sawyer *et al.*, 1986; van Echten-Deckert *et al.*, 2007) (**Figure 3**).

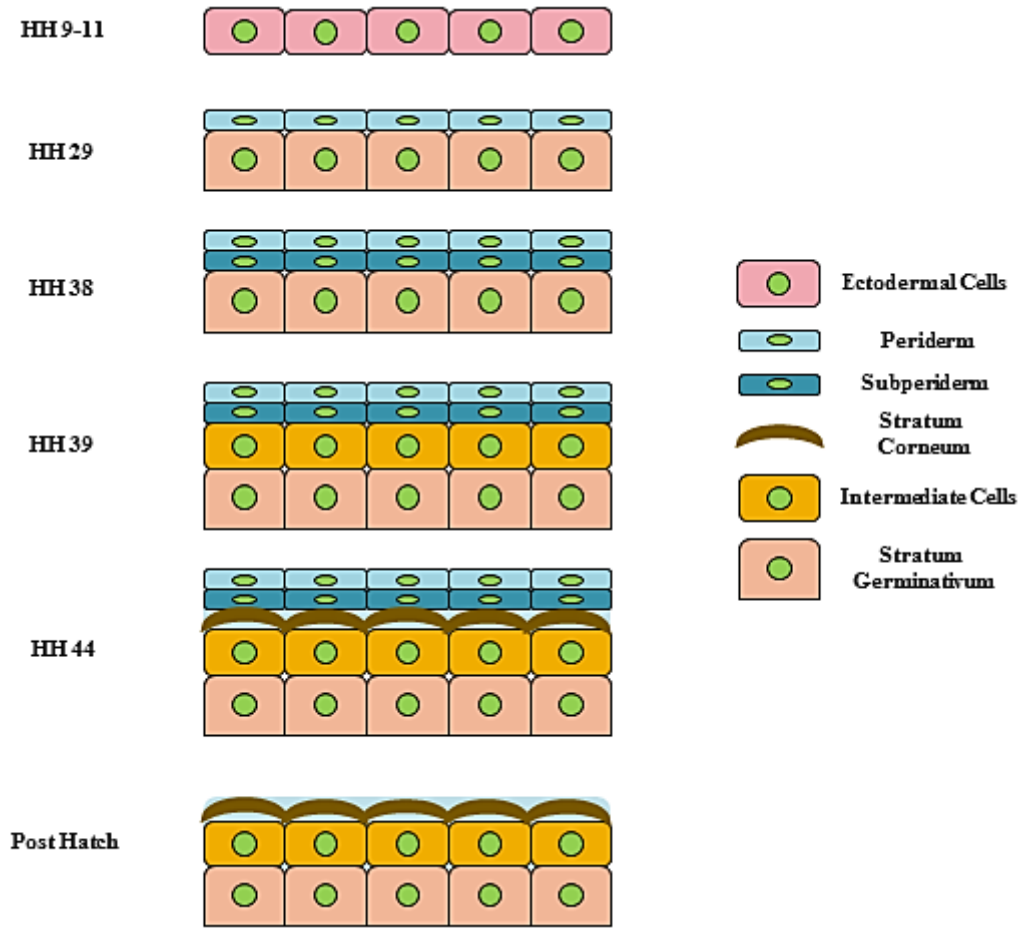

Figure 3. Embryonic development of the epidermis. The epidermis is derived from the embryonic ectoderm which consists of a single layer of cells. From HH 29, the ectoderm undergoes stratification to produce the single layered epidermis and peridermal layers (periderm/subperiderm). The peridermal layers are sloughed off prior to hatch. When the peridermal layers are established, the single layered epidermis begins to stratify and the apical cells undergo terminal differentiation to form the keratinised stratum corneum of the mature epidermis.

1.1.3 Structure of the Dermis

The dermis functions as the structural support for the epidermis and its appendages. The dermis is located beneath the basement membrane but above lamina elastica, an elastic layer of collagen fibres which separates the dermis from the underlying

subcutaneous tissue, and is in general much thicker than the overlying epidermis. The overall thickness of the dermis can vary throughout the body of adult chickens. Similar to the epidermis, the dermis is thickest in feather forming skin but is much thinner on bare regions of skin. The dermis contains three main cells types: fibroblasts, fat containing adipocytes and macrophages. The dermis is composed of mainly connective tissue, rich in collagen and elastin fibres, and can be divided into two distinct layers: the superficial dermis and deep dermis, which itself can be subdivided into the deep upper dense and lower loose dermis. The superficial dermis serves as the interface between the basement membrane and the dermis. The superficial dermis is composed of layered collagen fibres, and contains blood vessels and can vary in density and thickness between different skin regions. The upper dense layer of the deep dermis is thicker than the superficial layer and is composed of a dense network of collagen fibres, interspersed with elastin fibres and also contains blood vessels. The deep loose dermis, as the name implies, is the most basal layer of the dermis and is composed of relatively loose connective tissue. The deep loose dermis is made up of loose collagen fibres and contains the blood vessels, muscles, sensory nerves which are associated with the feather follicle and the movement of individual feathers (Bereiter-Hahn *et al.*, 1984; Lucas and Stettenheim, 1972; Sawyer *et al.*, 1986).

1.1.4 Development of the Dermis

The dermis is primarily of mesodermal origin, underlying the surface ectoderm. The dermis of the main body originates from various sources during embryonic development. The head and neck dermis is derived from neural crest cells (Couly and Le Douarin, 1988), while the dermis of the lateral and ventral body regions are derived from the lateral plate mesoderm (Fliniaux *et al.*, 2004b; Mauger, 1972a; b). The dermis of the dorsal region (the main region of interest in this thesis) is derived from the dermomyotome (a derivative of the somites) (Dhouailly *et al.*, 2004; Mauger, 1972b; Morosan-Puopolo *et al.*, 2014; Olivera-Martinez *et al.*, 2000; Olivera-Martinez *et al.*, 2002). Within the dorsal region of HH 19-20 chick embryos, the first visible sign of dermis formation is the migration of dermomyotome derived dermal progenitor cells beneath the surface ectoderm (**Figure 4**). To begin the process of migration, dermal

progenitor cells from the dermomyotome undergo epithelial-mesenchymal transition, whereby the cells decrease their adhesiveness to neighbouring cells and gain invasive and migratory properties (Delfini *et al.*, 2009). By HH 26 the dermal progenitors have invaded and formed a layer of loosely dispersed mesenchymal cells between the ectoderm and the neural tube in the medial-dorsal region of the embryo. The process of dermal progenitor cell migration can be detected by the presence of *Dermo-1* expression, a known marker of early dermis formation in chickens (Scaal *et al.*, 2001). At this stage a recognisable dermis cannot be distinguished (Dhouailly *et al.*, 2004). From HH 26 onwards, the upper part of the mesenchymal layer begins to thicken, forming the dense dermis beginning at the midline of the dorsal region of the embryo, directly above the spine (Dhouailly *et al.*, 2004). Formation of dense dermis spreads bilaterally from the midline, gradually forming a layer of dense dermis across the entire dorsal region of the embryo (Mayerson and Fallon, 1985). As the wave of dense dermis thickening travels laterally across the skin on the dorsal side of the embryo, feather formation is induced through interactions between the epidermis and dermis. The formation of a dense dermis is a requirement for the induction of feather formation (Sengel, 1990). This was demonstrated by *in vitro* experiments where dermal cell numbers were artificially altered, showing that a minimal density of dermal cells is required for the induction of feather formation (Jiang *et al.*, 1999). It was recently shown that inhibition of dense dermis formation, by blocking dermal cell progenitor migration from the dermomyotome, prevented the induction of feather primordia (Morosan-Puopolo *et al.*, 2014).

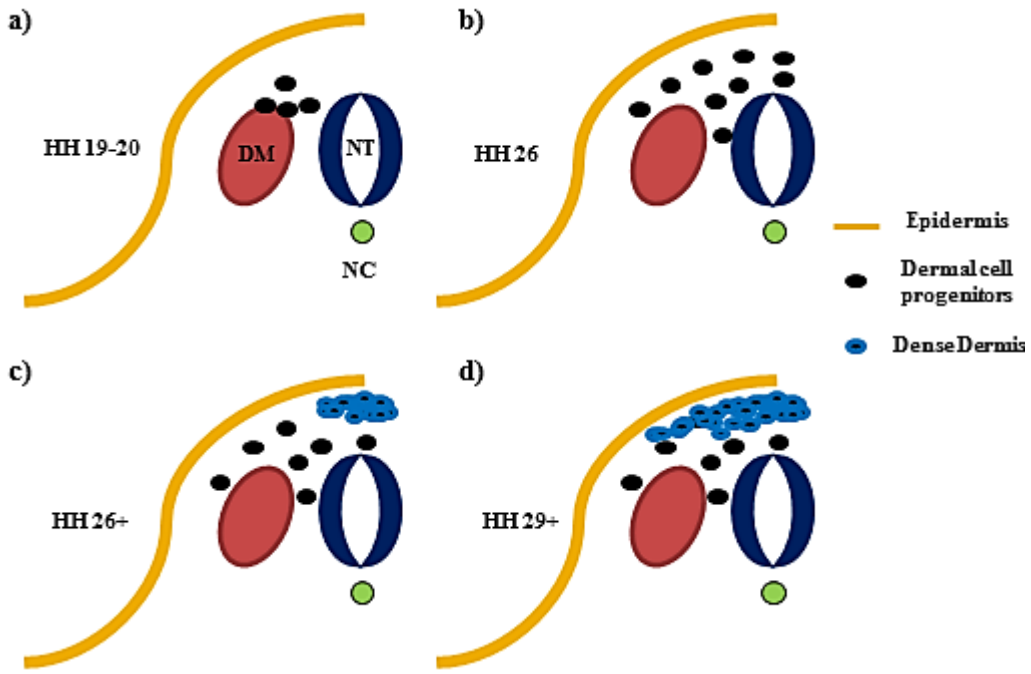

Figure 4. Development of the dorsal dermis. The dermis originates from the embryonic mesoderm. The dermal cell progenitors are produced from the dermomyotome (DM), which is a derivative of the somite. **a-b)** From HH 19-20, dermal cell progenitors migrate and fill the subectodermal space. **c-d)** From HH 26 onwards, dermal cells gather at the dorsal midline closest to the epidermis, forming a layer of dense dermis. The formation of dense dermis spreads in a bilateral direction across the embryo. NT - neural tube, NC - notochord.

1.2 Induction of Epithelial Appendage Formation

The process of epithelial appendage formation occurs through a number of hierarchical steps during the embryonic development of birds (Lucas and Stettenheim, 1972) (**Figure 5**). Firstly, regionalisation of the skin occurs throughout the body, forming distinct areas of skin, which are capable of appendage formation, separated by bare skin. Secondly, the formation of feathers or scales are induced within the previously specified skin regions. Both feather and scale formation are induced through interactions between the epidermis and the underlying dermis, resulting in the formation of a patterned array of either feather follicle precursors (feather primordia), or scale precursors (scale primordia). Thirdly, once feather or scale primordia are established, the primordia undergo differentiation and outgrowth to form the feather filament and the underlying feather follicle or a definitive scale ridge. Finally, in feather formation, differentiation and proliferation within the feather follicle, produces the structures of the mature feather. In scale formation, proliferation of the definitive scale ridge results in the formation of a series of overlapping scales.

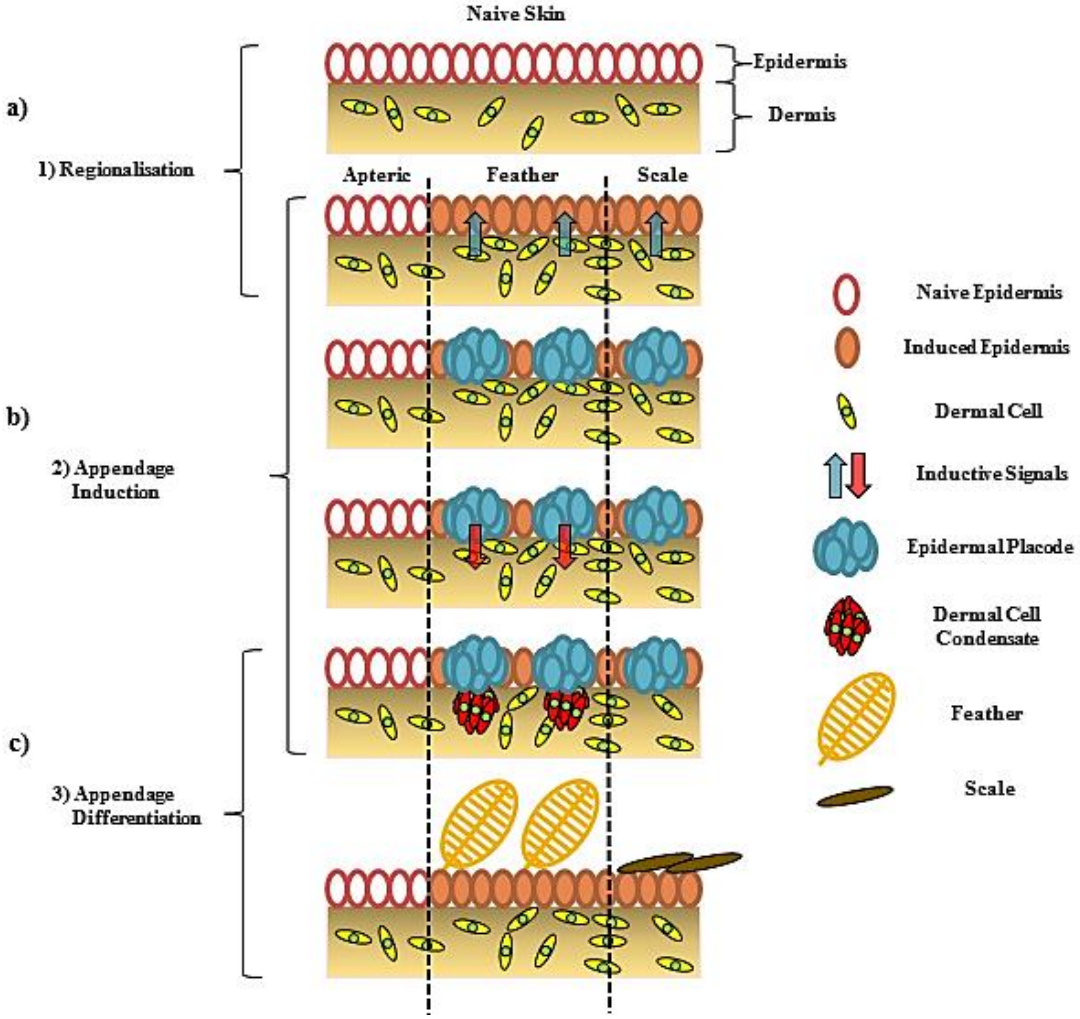

Figure 5. Induction of epithelial appendage formation. The process of epithelial appendage formation occurs through a series of hierarchical steps. **a)** First, the skin undergoes regionalisation to determine which parts of the skin of the body will bear epithelial appendages (scale or feathers). **b)** In response to a dermal signal, the overlying epidermis of appendage forming skin will form periodic thickenings (epidermal placodes), which in feather formation will signal down to the underlying dermal cells to induce the formation of cell condensates. The epidermal placodes and dermal cell condensates constitute the feather primordia which eventually gives rise to the mature feather follicles. Scale formation does not involve dermal cell condensate formation. **c)** The feather and scale primordia differentiate to form the mature appendage

1.2.1 Epidermal-Dermal Interactions during Epithelial Appendage Induction.

The formation of epithelial appendages arises through interactions between the developing epidermis and dermis during embryogenesis. The epidermal and dermal layers of the skin are separated by a thin layer of fibrous connective tissue known as the basement membrane. The distinct separation between the two skin layers allowed early developmental biologists attempting to understand the basis of epithelial appendage induction to study the inductive properties of each individual tissue layer or the other (Cadi *et al.*, 1983; Chuong *et al.*, 1996; Novel, 1973a; Rawles, 1963; Sengel and Abbott, 1963; Sengel, 1990). The epidermal and dermal layers can be mechanically separated through treatment of dissected skin prior to appendage formation with proteases to digest the basement membrane or with ion chelating agents such as ethylenediaminetetraacetic acid (EDTA), which prevents calcium^{2+} ion dependent cadherin binding between neighbouring cells. Epidermis and dermis from different regions of the body from individuals of different ages, and even between different species, can then be recombined and cultured to determine the role of each tissue layer in the formation of epithelial appendages.

From these early studies, it was demonstrated that the epidermis and dermis have distinct roles during the early induction of appendage formation. The epidermis determines the orientation of the appendage. In most feather tracts, individual feathers are oriented in an anterior-posterior direction. When feather forming epidermis is rotated and recombined with dermis from the same region of skin, the orientation of the feathers that form always follows the original orientation of the donor epidermis (Novel, 1973a). The dermis on the other hand determines the identity, placement (patterning), and size of the induced appendage. In chickens, when dermis from the feather forming regions are recombined with scale forming epidermis, feather formation is induced. Conversely in the reverse recombination, scale forming dermis with feather forming epidermis results in the formation of scales (Sengel, 1975; 1990) (**Figure 6**). Recombination of epidermis and dermis between epithelial appendage forming tracts and apteric regions also revealed the dermal effect on epithelial appendage formation (Cadi *et al.*, 1983; Sengel, 1990). Dermis from appendage

forming tracts always induced the formation of appendages specific to the origin of the dermis used in the recombination, while dermis from apteric regions failed to induce appendage formation. Based on epidermal-dermal recombination experiments, it was proposed that the formation of epidermal appendages, such as feathers, are induced by a signal of dermis origin, after dermis formation has taken place (Dhouailly, 1973; 1975; 1977),

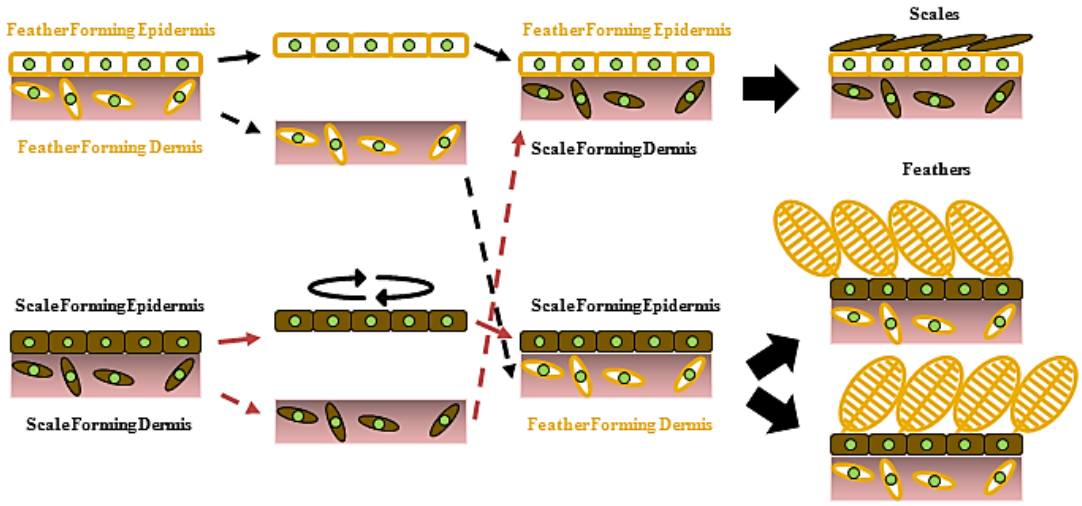

Figure 6. Diagrammatic representation of epidermal/dermal recombination experiments. Epidermis and dermis from feather or scale forming skin regions are separated and recombined to form chimeric skin explants. The resulting appendages that are formed on the chimeric skins are dictated by the dermis while the orientation of the appendage is under epidermal control.

On the other hand, when epidermis and dermis from different species are recombined (hetero-specific), such as feather forming dermis from chicken and hair forming epidermis from mouse, abnormal hair formation was induced, but the arrangement of individual hairs followed the chicken pattern (Dhouailly, 1973). The result suggested that different species may utilise similar inductive signals to induce appendage formation. However, formation of specific appendages such as complete hair and feathers requires species specific epidermal-dermal interactions.

Hetero-chronic recombination experiments (recombination of epidermis and dermis of different ages) demonstrated that the inductive properties of both skin layers in the formation of specific epithelial appendages is transient (Hughes *et al.*, 2011; Rawles, 1963; Song and Sawyer, 1996). When HH 35-37 scale epidermis is recombined with HH 31 feather forming dermis, feather formation is induced but the ability of the scale forming epidermis to respond to feather forming signals from the dermis reduces as the age of the epidermis used in the recombination increases. The use of older scale forming epidermis results in the formation of smaller, abnormal feathers, suggesting that there is only a small window of opportunity for the dermis to induce the formation of appendages on the overlying epidermis (Hughes *et al.*, 2011). Feather forming epidermis, on the other hand, shows a peak competence to feather induction from the developmental period between HH 31-35.

An interesting property of the chicken epidermis was observed during hetero-chronic epidermal-dermal recombination experiments between feather forming epidermis and scale forming dermis (Rawles, 1963). During chicken embryonic development, scale formation is induced a few days after feather formations has begun, and the hetero-chronic epidermal-dermal recombination experiments suggest that the ability of the scale forming dermis to induce scale formation in the overlying epidermis is transient. When feather forming epidermis from E5-E7.5 chicken embryos were recombined with E9-E12 scale forming dermis, feathers formed. However, when E13-E15 scale forming dermis was recombined with E5-E7.5 epidermis, scale formation was induced. Taken together with the reciprocal recombination (scale forming epidermis with feather forming dermis), the results show that the epidermis of chickens is primed to form feathers and that scale formation is a result of inhibition of feather identity which requires the active inhibition of feather induction (Dhouailly, 2009). This is supported by evidence of the ease by which epidermis from scale forming regions, and even extraembryonic membranes, can be experimentally manipulated to form feathers through alterations to various unrelated signalling pathways during embryonic development or after experimental epidermal-dermal recombination (Crowe and Niswander, 1998; Dhouailly, 1978; Dhouailly and Hardy, 1978; Harris *et al.*, 2004;

Widelitz *et al.*, 2000; Zou and Niswander, 1996). Other supporting evidence comes from chicken breeds which display the replacement of scales on the feet with feathers (a condition known as ptilopody), such as the scaleless high line (Abbott, 1965), and the silkie breed (Sawyer *et al.*, 2005) which show feathering of the legs and feet.

1.2.2 Regionalisation of the Skin (Feather Tract Specification)

On the body of most birds, distinct skin regions of the skin are covered in feathers, separated by patches of bare skin where little to no feathers occur. These regions are termed the pterylae and apterylae, or feather tracts and apteric regions respectively, and are a common feature to all bird species (Clench, 1970; Nitzsch, 1867; Stettenheim, 2000). The distinct pattern of feather tract distribution on birds is termed the "macropattern" (Sengel, 1975) and is established during embryonic development. The size and shape of the feather tracts and apteric regions vary greatly between different species of birds which may reflect the differences in their life styles related to flight or thermoregulation. However the basic topology of feather bearing tracts separated by apteric regions is maintained in different bird species. Most species display feather tracts among similar regions of the body, and the tracts are termed based on their location on the body, such as the spinal (dorsal) tract, alar (wing) tracts, and humeral (shoulder) tracts (**Figure 7**). Other feather tracts also exist and are common among most bird species. The distribution, arrangement, and types of individual feathers in each feather tract can also vary (Clench, 1970; Nitzsch, 1867; Stettenheim, 2000). Flighted bird species generally have wider apteric regions that separate the feather tracts compared to those of less flighted or non-flighted bird species. During flight, the body of a bird generates a lot of heat, and a wider region of bare skin would be able to radiate excess heat more effectively than feather covered skin (Stettenheim, 2000). On the other hand, adult penguins and ratite species such as emus, are completely covered in a tightly packed arrangement of feathers with no visible apteric regions in adult birds, which increases insulation in these species. Although adult penguins and ratites do not display a visible apteric region, the boundaries of each feather tract can be detected during embryogenesis of each species (Stettenheim, 2000).

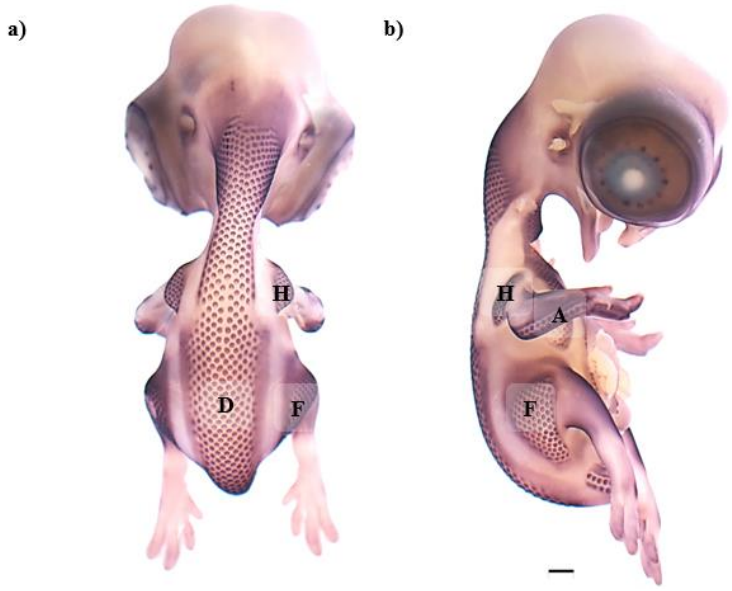

Figure 7. Distribution of embryonic feather tracts. a) Dorsal and **b)** lateral view of a HH 33 chicken embryo hybridised with *β-Catenin* antisense RNA probes. **H,** humeral tract; **F,** femoral tract; **D,** dorsal tract; **A,** alar tract. Scale bar - 1 mm.

Feather tract specification determines the regions of skin which are competent to the induction of feather formation. The first sign of feather tract formation is indicated by the thickening of the underlying dermis within each presumptive tract region, forming a layer of dermal cells of noticeable thickness (Dhouailly *et al.*, 2004). As mentioned previously, the density of dermal cells is much greater in appendage bearing tract regions compared to apteric regions in adult birds, forming a defined boundary between tract and apteric regions. Histological examination revealed that prior to feather formation, the underlying dermis within the feather tract regions displayed a dermal cell density of 2.6 nuclei/ mm^3, whereas apteric regions show a dermal cell density of 1.98 nuclei/ mm^3 (Wessells, 1965). The feather tracts are specified during the early stages of embryonic development, around E2 (Dhouailly *et al.*, 1998; Fliniaux *et al.*, 2004a). The specification of each tract region is not fixed and can be altered by experimental manipulation. When formation of the dorsal tract is inhibited through excision of part of the spinal cord during early embryogenesis, the neighbouring femoral tract dermis was observed to migrate into skin regions normally

occupied by dorsal tract dermis, suggesting that tract specification during development is plastic (Sengel, 1990). Previous studies have described the process of dense dermis formation within the tracts during embryonic development, (described in section **1.1.4**), but the mechanisms underlying tract specification and induction are not well understood. Similarly, the mechanisms underlying the specification of the featherless apteric regions are also relatively unknown.

1.2.3 Induction of the Feather Follicle Formation and Patterning

Following tract specification and the beginnings of dense dermis formation within each tract, the induction of the feather primordia takes place. During this time, beginning at around HH stage 28-30 of chicken development, the placement and arrangement of the final feather pattern in adult birds takes place. As mentioned above, the regionalisation of distinct skin regions of the body, tract and apteric regions is termed the "macropattern", but within the tracts the arrangement of individual feathers is termed the "micropattern" (Sengel, 1975). The process of micropatterning converts the initially homogenous skin field into a hexagonally patterned array of feather primordia separated by interbud spaces, within each feather bearing tract (Davidson, 1983).

In regions of skin within the tract where the presence of an epidermis and a dense dermis coincide, the formation of feather primordia is induced through reciprocal epidermal-dermal interactions. Within the dorsal tract, the first signs of feather primordium induction are observed within the dorsal midline region directly above the spinal cord, where formation of dense dermis initially takes place, and occurs over a period of two days (Lucas and Stettenheim, 1972). Based on epidermal-dermal recombination experiments, it has been suggested that a signal originating from the dermis instructs the overlying epidermis to form a localised epidermal thickening, an epidermal placode (Dhouailly, 1973; 1975; 1977). The epidermal placode then sends a signal to the underlying dermal cells to stimulate cell migration and aggregation, resulting in the formation of a dermal cell condensate directly underneath the epidermal placode. The epidermal placode and dermal condensate forms one unit, the

feather primordium, which later gives rise to the feather follicle. Cell proliferation within the growing dermal cell condensate ceases, until the formation of the feather primordium is complete (Jiang and Chuong, 1992; Michon *et al.*, 2008; Wessells, 1965). The process is repeated across the entirety of feather tracts until an organised hexagonal arrangement of feather primordia, separated by interbud spaces, has formed across the tracts (Davidson, 1983). The process is represented in **Figure 8**.

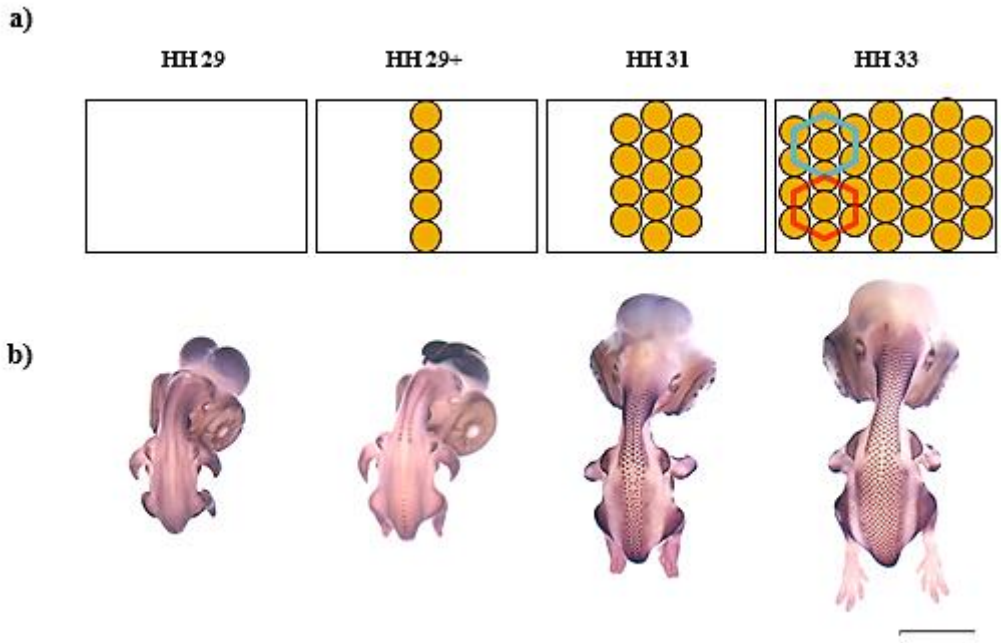

Figure 8. Primordium formation during embryonic development. Time series of feather primordium formation during chicken embryonic development in HH 29, HH 29+, HH 31 and HH 33 embryos. **a)** Diagrammatic representation of the sequential addition of new feather primordium rows in the developing dorsal tract. **b)** The process visualised on whole embryos through detection of *β-Catenin* expression. Orange circles - feather primordia, blue and red hexagons - outline the hexagonality of the primordium arrangement. Scale bar - 5 mm.

Within different feather forming tracts, the induction of feather primordia occurs in a spatiotemporal sequence through epidermal-dermal interactions. In the dorsal tract, the first feather primordia are induced along the dorsal midline towards the caudal end of

the dorsal tract, where dermal cell density is highest. Initially, a stripe of high dermal cell density is formed along the dorsal midline of the tract, which gradually breaks up to produce a primary row of feather primordia. As the density of the underlying dermis increases bilaterally from the midline, new rows of feather primordia are added sequentially in a wave-like manner across the tract lateral to the previous row. New feather primordium rows are added approximately every 6-8 hours and align themselves relative to the previous row of feather primordia (Jung and Chuong, 1998; Jung *et al.,* 1998). The sequential wave-like addition of new feather primordium rows across the tract results in a skin which bear feather primordia of different developmental stages. Medial rows are always developmentally more mature than lateral rows. The addition of new feather primordium rows terminates at the tract margins in front of the apteric region.

The wave-like propagation of feather primordium formation results in the formation of a hexagonal, high fidelity periodic arrangement of the feather primordia (Cruywagen *et al.*, 1992; Davidson, 1983). However, *in vitro* studies demonstrated that a hexagonal arrangement of feather primordia can arise without the need of wave-like addition of new feather primordium rows (Jiang *et al.*, 1999). Jiang *et al* showed, through the modulation of dermal cell density in a reconstituted mesenchymal skin explant culture that a hexagonal pattern can arise simultaneously across the skin explant when dermal cell density is high enough. Although the formed pattern is hexagonal in pattern, the spacing of the feather primordia across the skin is not even and primordia show slight variations in size. They propose that an optimal packing density is the underlying process behind the formation of a hexagonal arrangement of feather primordia in their reconstituted explants.

Feather follicle formation involves the differentiation and outgrowth of the feather primordium (**Figure 9**) (Lucas and Stettenheim, 1972). The initially induced feather primordium displays a dome-shape which is radially symmetric. The feather primordium gradually develops an anterior-posterior polarity, increasing cell proliferation within the posterior region of the feather primordium (Chodankar *et al.*, 2003). Outgrowth of feather primordium results in the formation of a short feather bud

that grows in an anterior to posterior direction. During outgrowth of the short feather bud, the region of cell proliferation is shifted from the posterior end of the feather bud to the distal tip of the short feather bud, which drives further outgrowth of the feather bud to form the long feather bud. The long feather bud continues to extend and the feather bud epidermis at the base of the long feather bud begins to invaginate into the underlying dermis to begin the process of feather follicle formation. As the feather bud epidermis invaginates, it envelops the underlying dermis, establishing a boundary between the outer and inner part of the feather follicle at the base of the feather bud, while the feather bud itself matures into a feather filament. During epidermal invagination, the region of cell proliferation gradually descends towards the base of the long feather bud forming a ring of cells. (Chodankar *et al.*, 2003). This basal ring of cells displays high rates of proliferation cells and is known as the collar bulge. The collar bulge houses the epithelial stem cells which through rapid cellular proliferation, contributes the keratinocytes for the formation of the mature feathers (Lucas and Stettenheim, 1972; Yue *et al.*, 2005).

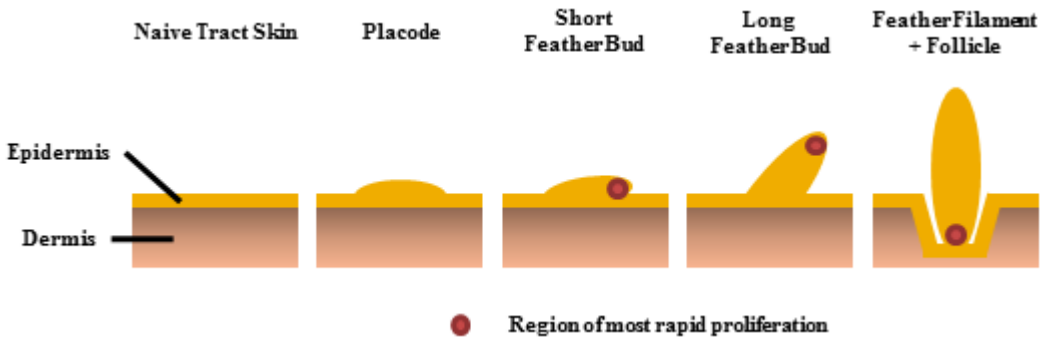

Figure 9. The morphogenic events of embryonic feather development. After initial signalling from the dermis, the epidermis undergoes thickening to form the epidermal placode. As the placode differentiates, it develops an anterior-posterior polarity, increasing cell proliferation at the posterior end of the placode, forming the short feather bud. Further outgrowth of the feather bud forms the long feather bud. Once the long feather bud has been established, the zone of proliferation migrates downwards towards the base of the feather bud. During this time the epidermis surrounding the feather bud/filament invaginates to form the feather follicle. Future morphogenetic events regulates the formation of the mature feather.

1.2.4 Development of the Mature Feather

After the feather follicle has been established, formation of the mature feather begins. The feather follicle sustains the growth of the developing feather during embryonic development. In adult birds, the feather follicle can start the regeneration of a new feather within the same follicle if the feather is removed through either plucking or molting (Yu *et al.*, 2004). As mentioned above, the epidermis of individual feather filaments invaginates into the underlying dermis to form the feather follicle. This results in the formation of distinct epidermal and dermal layers within feather follicle, which is shaped like a cylinder.

There are many different feather types on the various body regions of a bird, but they can be separated into two main groups; plumulaceous and pennaceous (Lucas and Stettenheim, 1972). Each feather type serve distinct functions. Plumulaceous feathers are the down feathers which display radial symmetry. The barbs (filaments) of down feathers are not connected to a main shaft (rachis) but extend from a structure called the calamus which is embedded in the skin. Down feathers form loose tufts which provide an insulative function. Pennaceous feathers on the other hand, are the stereotypical vaned flight feathers. The barbs are all connected to a central rachis and each barb contains barbules. Barbules can be separated into two types, cilia and hooklets which can interlock, linking together neighbouring barbs to form vane. Although the structure of each type of feather may differ, each feather is composed of similar elements that arise through similar developmental processes during embryogenesis (**Figure 10**).

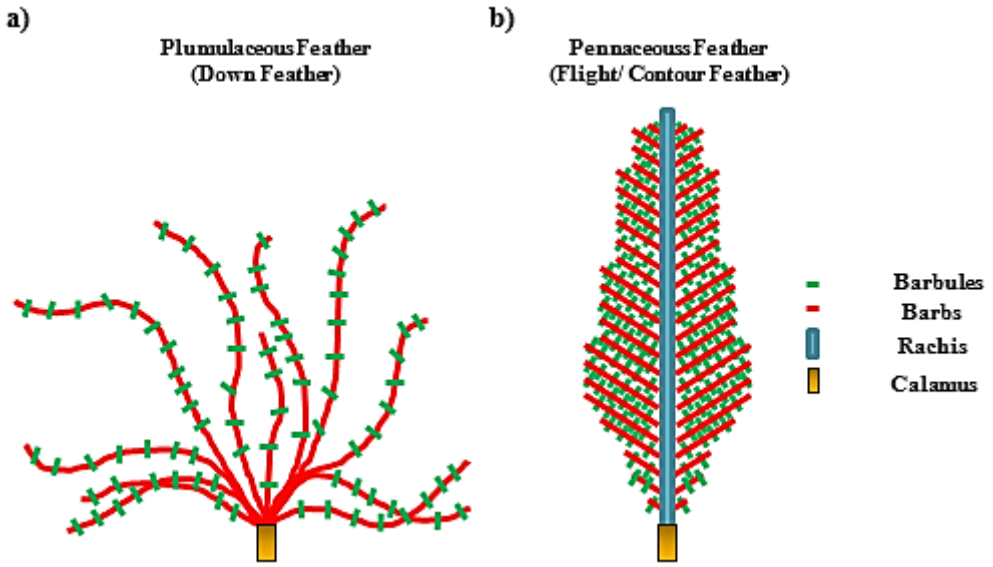

Figure 10. Diagrammatic representation of feather types. There are two basic feather types that exist on adult birds. **a)** Plumulaceous feathers are radially symmetric and lack a rachis. The barbs emerge from the calamus and may contain barbules, forming a loose tuft structure. Plumulaceous feathers are the stereotypical down feathers and primarily function to insulate the adult bird. **b)** Pennaceous feathers, on the other hand, are the flight/contour feathers found on the surface of adult birds. Barbs are fused to the rachis and individual barbs may interlock via the barbules to form a feather vane. Pennaceous feather are primarily used for flight or streamlining.

In chickens the first feathers produced throughout the body are all down feathers. Vaned feathers are only produced after the second and third molts and are produced from the same initial feather follicles. Additionally, during the adult life of some birds, the size, shape, or colouration of the feathers may be altered under the influence of seasonal hormonal changes to develop the secondary sexual characteristics which are used for display during the breeding season (Mayer *et al.*, 2004; Witschi, 1935). This demonstrates that feather follicles are not strictly programmed to form one type of feather but can alter the type of feathers the follicle produces throughout life.

During development, feathers form as a cylindrical tube which opens up after feather maturation. The epidermis of the feather follicle consists of three layers. The outer most layer forms the follicle wall (outer root sheath). The intermediate layer forms the feather sheath (inner root sheath) which degrades after the formation of the mature feather to allow the feathers to open. The third epidermal layer consists of two parts. The most basal part of the third epidermal layer forms the collar bulge, which is the source of new keratinocytes for the growing feather. Directly above the collar bulge, the epidermis thickens and differentiates to form the ramogenic zone. The ramogenic zone gives rise to the barbs of the mature feather, which are the keratinised filaments that make up the vane of the feather (**Figure 11**) (Chuong *et al.*, 2000; Prum, 1999; Prum and Williamson, 2001).

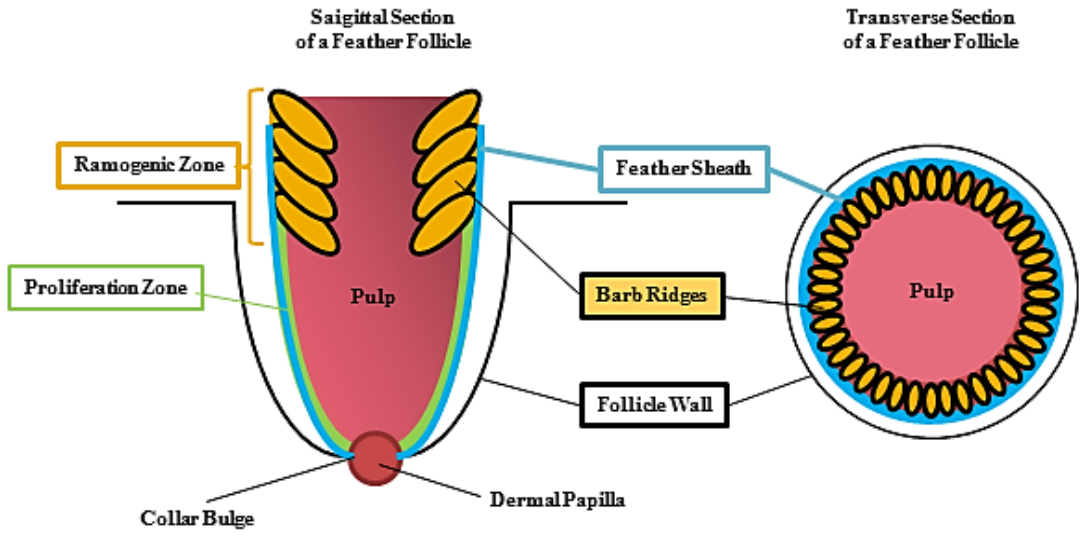

Figure 11. Diagrammatic representation of developing feather follicles. a) Sagittal and **b)** transverse section of a feather follicle in the midst of feather development. The epidermal component of the feather follicle can be divided into three distinct layers: the outer layer (follicle wall), the intermediate layer (feather sheath) and the inner layer (proliferating zone). At the base of the feather follicle is the collar bulge which proliferates to provide cells for the developing barb ridges (future barbs of the mature feathers). The developing/maturing barb ridges are supplied with nutrients by the dermal pulp at the centre of the follicle which contains a network of blood vessels.

At the centre of the feather follicle are the dermal components, consisting of the dermal papilla at the base of the feather follicle and the dermal pulp above it, which fills the internal space of the feather filament. These dermal components are filled with blood vessels that supply the growing and developing feather filaments (the barb ridges) with nutrients. As the growing feather filament extends away from the feather follicle, the dermal pulp within the feather filament gradually degrades. This cuts off the nutrient supply to the growing feather filament, which cause cell death of the barb keratinocytes within the feather filament, leaving behind the dead keratinised cells, which make up the mature feather and also allows the mature feather to open.

The growing feather forms as a cylindrical tube due to the cylindrical structure of the feather follicle. The collar bulge which houses the stem cells exists as a ring at the base of the feather follicle, and during proliferation of the stem cells "older" keratinocytes are gradually pushed upwards by "newer" keratinocytes from below as they are generated by the proliferating collar bulge. As the daughter cells of the collar bulge are pushed distally upwards into the ramogenic zone, the keratinocytes differentiate to form the barb ridges (individual barbs of the mature feather), which are arranged between the periphery of the dermal pulp and the feather sheath. In plumulaceous feathers (down feathers), the barb ridges grow parallel to one another throughout the formation of the feather. In the pennaceous feathers (vaned feathers), barb ridges are generated at the posterior end of the feather follicle. As the barb ridges grow, however, new keratinocytes are added to the base of the growing barb ridges in a wave-like/helical manner that moves bilaterally around the collar bulge, gradually converging and fusing at anterior end of the feather follicle to form the rachis (**Figure 12**).

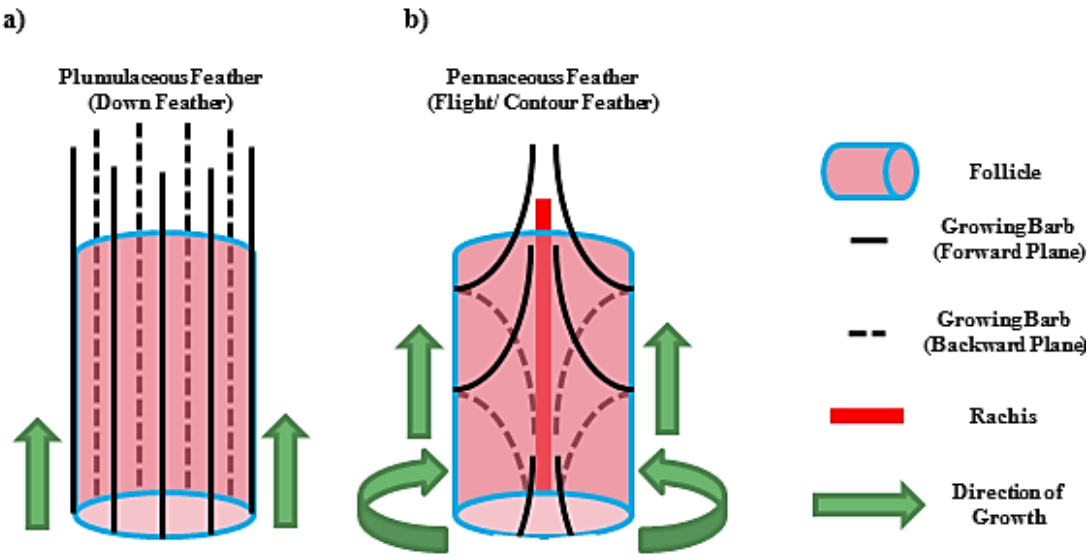

Figure 12. Diagrammatic representation of barb growth. a) In plumulaceous feathers, barb ridges grow vertically, parallel to one another. **b)** In pennaceous feathers, new barb ridges are formed at the posterior end of the feather follicle. Growth of individual barbs occurs helically and they grow bilaterally from each other. Once the barbs reach the anterior side of the follicle, the barbs fuse, giving rise to the rachis of the mature feather. In both feather types, cell death between maturing barbs begin in the distal regions of the follicle to allow the separation of individual barbs from their neighbours.

The basic process that forms both types of feathers are the same (described below), and differ only in the topology of the collar bulge. In follicles of down feathers, the collar bulge lies horizontally across the base of the follicle. The distance between the collar bulge and the ramogenic zone is equal across the feather follicle, allowing the parallel upward growth of barb ridges. Whereas in follicles of vaned feathers, the collar bulge is tilted towards the anterior end of the feather follicle, altering the distance of the ramogenic zone between the anterior and posterior part of the collar bulge. This creates a molecular gradient across the anterior and posterior parts of the collar bulge, resulting in the helical growth of the barbs and the convergence of the growing barb ridges at the anterior end of the feather follicle (Yue *et al.*, 2005). It was discovered in the same study, that the type of feather produced by the feather follicle was controlled

by the dermal papilla. When dermal papilla from a vaned feather producing follicle was replaced with the dermal papilla from a down feather producing follicle, the chimeric follicle produced a radially symmetric down feather (Yue *et al.*, 2005).

As the barb ridges within the growing feather filament extend, keratinocytes within the barb ridges closest to the feather sheath within the distal parts of the growing feather undergo proliferation and further differentiation to form three different cell types which are aligned longitudinally within each barb ridge (**Figure 13**). At the outer edges of each barb ridge are the marginal plates, between the marginal plates are the barbule plates and at the centre lies the axial plates. In the medial stages of feather development, the marginal plate and axial plate cells undergo apoptosis, while the barbule plate cells fuse to each other and to the barb ridge which eventually giving rise to the barbules of the mature feather. As the barb ridges continue to grow, during the later stages of feather formation, the keratinocytes undergo keratinisation and programmed cell death, beginning at the most distal end of the growing barb ridges, to form the individual keratinised elements of the mature feather (Haake *et al.*, 1984).

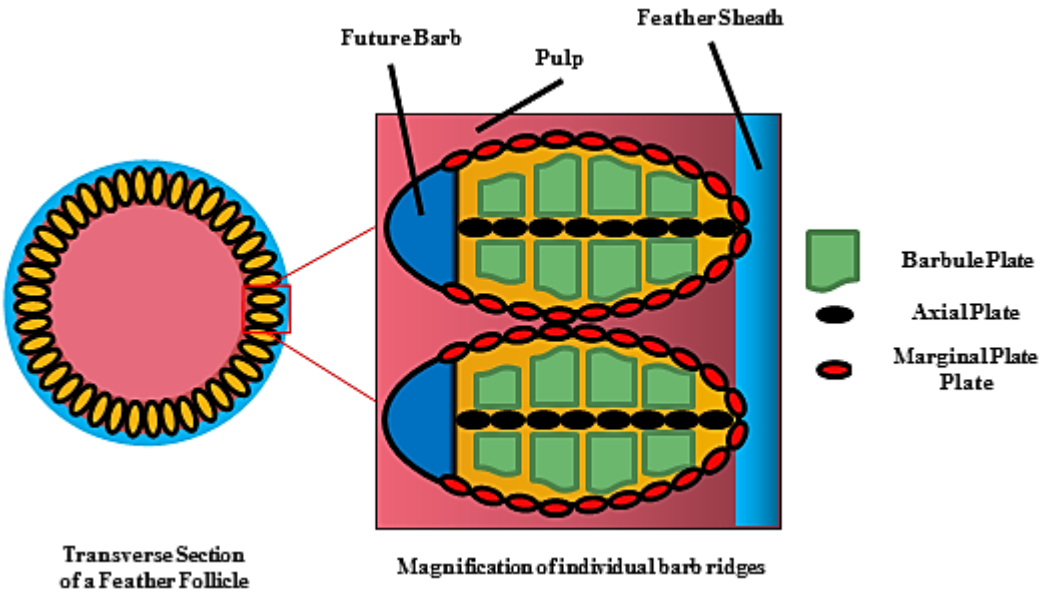

Figure 13. Diagrammatic representation of barb ridge differentiation. Transverse section of a developing feather follicle. The cells of individual barb ridges differentiate to form three distinct cell types called barbule plates, axial plates and marginal plates.

The barbule plates eventually fuse together to form the individual barbule filaments. As the barb ridges mature, the axial plate and marginal plate cells degrade to allow the barbules to open.

Feather formation is terminated when the collar bulge begins the formation of the calamus. The calamus is the structure which connects the base of the barbs or rachis to the skin of the body of adult birds. After the calamus has been formed, the base of the calamus is capped, cutting off the nutrient supply to the keratinocytes which make up the calamus and cell proliferation within the collar bulge ceases. The collar bulge and dermal papilla shrink in size after the termination of feather formation. The cells within the calamus keratinise and undergo programmed cell death, leaving behind a keratinised hollow tube.

Throughout the life of a bird, feather follicles constantly regenerate feathers that have been lost through plucking or after a moult to replace worn feathers (Lucas and Stettenheim, 1972), but the process is relatively understudied compared to mammalian hair follicle regeneration (Harris *et al.*, 2002; Prum, 1999; Yu *et al.*, 2004). Each individual feather follicle functions like a mini-organ that undergoes two distinct phases, growth and rest. During the resting phase, the collar bulge and dermal papilla are much smaller in size compared to the size of the structures during the growth phase and active cell proliferation has stopped. The resting phase can last anywhere between two days and fourteen months (Yu *et al.*, 2004). At the end of the rest phase, cell proliferation within the collar bulge is induced and the collar bulge and dermal papilla grow in size to begin the process of feather formation (as described above). The length of the growth phase varies depending on the type of feather being produced and can last from anywhere between two days to several years (Yu *et al.*, 2004).

1.2.5 Origin and Evolution of Feathers

The development and evolution of the avian integument in birds has garnered much interest in recent years due to the discoveries of theropod dinosaur fossils displaying avian characteristics, such as wings and feathers (Brusatte *et al.*, 2014; Hu *et al.*, 2009a; Lü and Brusatte, 2015; Norell and Xu, 2005; Xu *et al.*, 2003; Xu *et al.*, 2004; Xu and Zhang, 2005; Xu *et al.*, 2012; Zhou *et al.*, 2003). Over the last 20 years, fossils from the Liaoning Province in China has yielded many well preserved specimens from the Jehol biota of the early Cretaceous era, which illustrate the evolutionary innovations that led to the evolution of modern birds from theropod dinosaurs.

Both mammals and birds evolved from a common basal amniote ancestor and later diverged into two distinct groups. Mammals belong to the synapsid lineage while birds and reptiles belong to the diapsid lineage. The two lineages are defined by the presence of either one (synapsid) or two (diapsid) openings on either side of their skulls, behind the eyes. Members of the diapsids are represented by an extremely diverse group of extant and extinct animal species such as reptiles, birds and non-avian dinosaurs. All birds are members of the archosaur group of diapsids, which also includes all the members of extinct dinosaur lineages. Currently, the only extant members of the archosaur group are birds and crocodilians (Dhouailly, 2009).

To better understand the origin and evolution of feathers, studies into the evolution of avian β-keratins were performed (Greenwold and Sawyer, 2011). Molecular dating methods were performed to compare the β-keratin sequences of several different species such as chickens, zebra finch, Nile crocodile, anole lizards, and redbelly turtles, to assess when the avian specific β-keratins began to diverge from the common archosaur ancestor. Through these methods it was determined that avian β-keratins began to diverge from their archosaur ancestor around 216 million years ago, but the sub-family of feather β-keratins did not begin to diverge until around 143 million years ago, long after the first appearance of feather-like structures in the fossil record (*Anchiornis huxleyi* was dated to around 155 million years old (Hu *et al.*, 2009a)). The results suggest that the first feathers that appeared did not contain any β-keratin from

the feather β-keratin subfamily but contained other avian β-keratins. Feather β-keratins only evolved later, to increase the plasticity of the feather structure, which may have aided the evolution of powered flight.

The structure of the feather itself and its role in the evolution of flight has been a focus of recent studies. Models theorising the structural evolution of feather forms that lead to the development of modern flight feathers were proposed based on studies and observations of feather development during embryogenesis (**Figure 14**) (Brush, 2000; Prum, 1999; Prum and Williamson, 2001). The models predicted that the collar bulge within the feather follicle underwent a series of transitional changes, which resulted in the formation of different types of proto-feathers (Prum, 1999; Prum and Williamson, 2001). They proposed that the first feather follicles formed a continuous hollow structure without barbed ridges, resulting in the formation of hollow hair like filaments. Next, the feather follicle developed the ability to form the barb ridges that grew out of the feather follicle to form proto-feathers resembling down-like tufts consisting of just feather barbs that do not contain barbules. The next stage can be separated into two parts and involves the evolution of two different novel structures: 1) the barb ridges evolved the ability to further differentiate to produce the barbules, forming branched barbs within the down feathers, and 2) feather follicles developed the posterior to anterior growth of barb ridges to form a primitive rachis. Which occurred first cannot be discerned from the model. When these two structural innovations evolved, the two processes could be combined to form an open pennaceous feather vane (similar to flight feathers but lack interlocking barbules. Lastly, barbules differentiated into the cilia and hooklets, allowing the barbs to interlock, forming a closed pennaceous vane (Greenwold and Sawyer, 2011; Prum, 1999; Prum and Williamson, 2001).

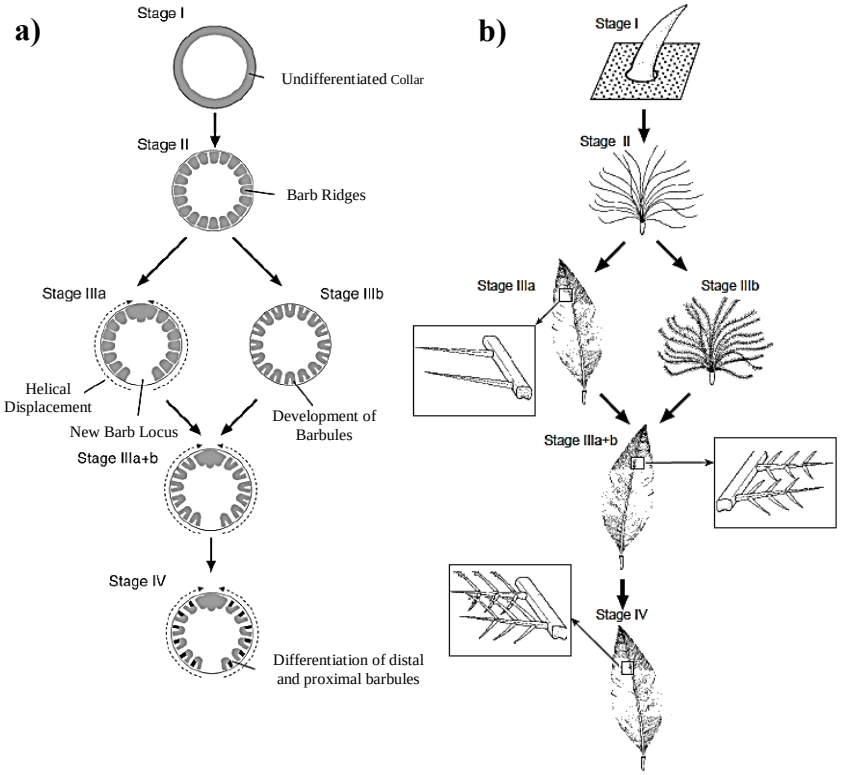

Figure 14. Schematic of the evolution of feather forms. Adapted and modified from Prum, 1999 (Prum, 1999). The evolution of feathers is described as a series of stages. Each stage describes the appearance of a new developmental novelty which gave rise to new feather forms. **a)** The model of feather development is illustrated as cross sections of feather follicles, while **b)** depicts the structure of the proto-feather. Stage I, the evolution of the undifferentiated feather collar forming a hollow hair like structure. Stage II, evolution of barb ridges resulted in the formation of a feather with unbranched barbs. Stage III involved the evolution of either the development of helical barb ridge growth to produce a rachis or the development of barbules within the barb ridges. Stage IV, differentiation of proximal and distal barbs which allowed the neighbouring barbs to interlock, producing a closed pennaceous vane.

These hypothetical models are now supported by the identification of the transitional proto-feathers described in the models, on some of the above referenced fossil specimens. However, although these specimens bear proto-feather like appendages, the arrangement of these structures on the bodies cannot be deduced due to deformation of body structure during the process of fossilisation. In modern birds capable of flight, feathers are arranged in a high fidelity hexagonal pattern which is established during embryonic development and persist throughout life (Homberger and de Silva, 2000; Lucas and Stettenheim, 1972; Stettenheim, 2000). When this arrangement of feather pattern evolved is unknown. Not many studies have been performed to explain the adaptive significance of a hexagonal array of feathers in birds, but it has been suggested that the arrangement may increase the aerodynamic efficiency of birds for flight (Pennycuick *et al.*, 1996).

1.2.6 Induction of Scale Formation

On the legs and feet of most species of birds are scales. Scales are flattened epidermal structures that protect the legs and feet of the bird from abrasion. (Sengel, 1976). In chickens, there are three main types of scales; scuta, scutella, and reticula (**Figure 15**) (Lucas and Stettenheim, 1972). The scuta are large, overlapping oblong scales which cover the dorsal surface of the tarsometatarsus and also extend in a single row along the dorsal side of each toe. The scutella are smaller compared to the scuta and are also oblong in shape. The scutella cover the ventral side of the tarsometatarsus. On the ventral surface of each foot are the reticulate scales. Reticula are small and rounded, and do not overlap with one another. Apart from shape differences, the scales can also be differentiated by the keratins they express. Scuta and scutella express both α and β keratins while reticula express only α-keratins post hatch (reticula initially express both α and β keratins but the expression of β-keratin is restricted to the peridermal layers which are shed just prior to hatch) (O'Guin and Sawyer, 1982).

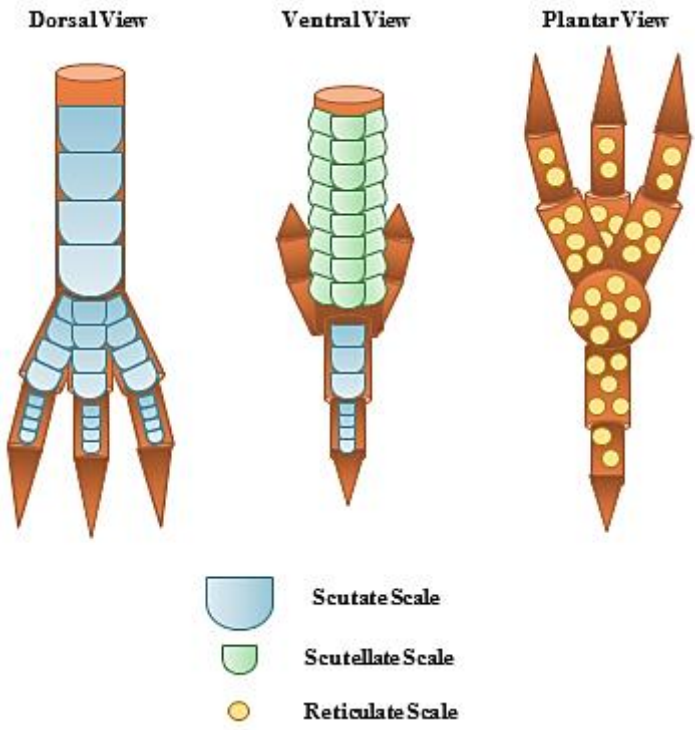

Figure 15. Scale types on the feet of adult chickens. In adult birds, there are three scale types, each morphologically distinct. The scuta scale are large oblong scales that overlap one another and cover the dorsal surfaces of the legs and feet. The scutella are similar in shape to scuta but are smaller in size and cover the ventral side of the legs. Reticula are small and round and are located on the underside of each foot.

As mentioned in section **1.2.1**, epidermis from scale forming regions appear to be primed for the formation of feather primordia and that scale formation is the result of inhibition of feather fate by the underlying dermis (Dhouailly, 2009). This was demonstrated by the ease of which feather formation can be induced experimentally, and the existence of various chicken breeds that display natural feathering of the legs and feet. This suggests the possibility that, evolutionarily, avian scales are structures derived from avian feathers rather being analogous to reptilian scales, which had been the prevailing theory (Maderson, 1972). With the discovery of several bird-like dinosaur fossils from the Liaoning Province which bear flight feathers on the legs (Han

et al., 2014; Hu *et al.*, 2009a; Xu *et al.*, 2003; Xu and Zhang, 2005), it appears that the leg scales of modern birds are essentially modified feathers.

Scales, similar to feathers, also arise through epidermal-dermal interactions, but later during embryogenesis than feathers. Similar to feather formation, the skin regions that are specified to form scales show densification of the underlying dermis prior to the induction of scale formation (Tanaka and Kato, 1983). However, unlike the morphogenesis of feathers, scale formation does not involve the formation of dermal cell condensates (Wessells, 1965) (**Figure 16**).

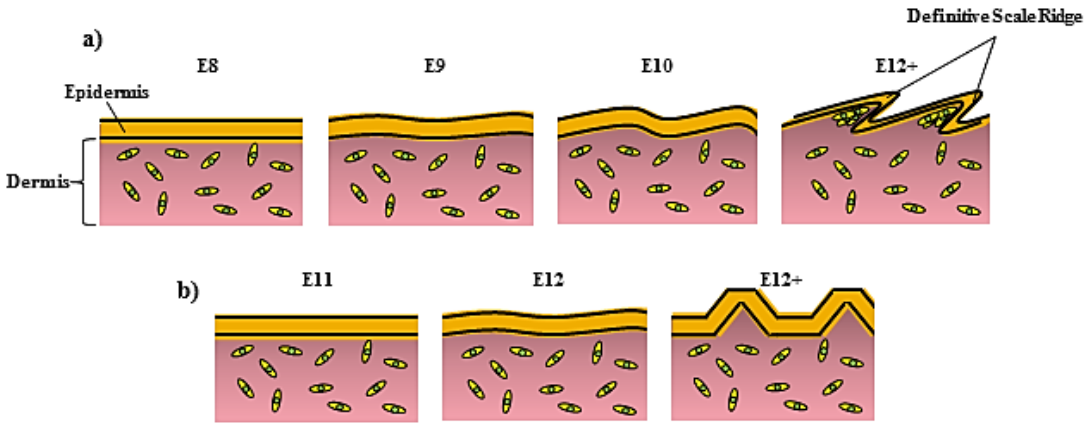

Figure 16. The morphogenetic events of embryonic scale development in chickens. Unlike feather formation, dermal cell condensates do not form during scale formation. **a)** Formation of scuta and scutella scales. At E9, epidermal placodes form on the surface of the skin. At E10, outgrowth is localised to the distal edge of the forming placode which eventually give rise to individual definitive scale ridges by E12. Further outgrowth results in the formation of overlapping scales. **b)** Reticula scales form as symmetrical elevations on the plantar side of the foot of E12 embryos. The elevations grow outwards forming radially symmetric scales.

The first sign of scuta and scutella scale development are indicated by the formation of epidermal scale placodes on the third digit of the tarsometatarsus at around E9 of embryonic chick development, followed by the subsequent formation of new

epidermal placodes in surrounding skin regions. These initial epidermal placodes eventually give rise to the definitive scale ridges. At around E10, the epidermal scale placodes develop a proximal-distal axis and show outgrowth of the distal edge of the placodes. At this stage the scale placodes are visible as elevations on the skin (Sengel, 1976). Over the next two days, the continued elongation of the distal edge of the epidermal placode results in the formation of the definitive scale ridge. During the formation of the definitive scale ridge, dermal condensate formation can be observed at the distal tip of the scale ridge, but the structure is transient and disappears by E13 (Dwyer, 1971). Further elongation of the definitive scale ridge until E13 to E16 of chicken development, eventually results in the formation of overlapping scuta and scutella scales.

The process of reticulate scale formation occurs slightly differently to that of scuta and scutella scale formation. Unlike the scutate and scutellate scales, reticulate scales do not begin with the formation of an epidermal placode or dermal condensate. The reticula form as symmetrical elevations on the plantar side of the foot and do not show asymmetric outgrowth during the formation of the mature reticula. The first sign of reticula formation appear around E12 and over the next four days, through proliferation and differentiation, form the mature reticula (Sawyer and Craig, 1977).

1.3 Molecular Requirements for Feather Primordium Morphogenesis

Based on previous classical embryological studies it was shown that epithelial appendage morphogenesis required the reciprocal communication between the epidermis and the underlying dermis (Dhouailly *et al.*, 1978; Dhouailly, 1984; Saunders, 1958). From these early studies, it was determined that the signals that govern epithelial appendage induction were conserved among vertebrates and that the initial inductive signal was of dermal origin (Dhouailly, 1973; 1975). With the advent of tools which allowed researchers to study the molecular basis of epithelial appendage formation through a variety of methods, researchers began to dissect the molecular mechanisms underlying epithelial appendage morphogenesis in chickens. From these studies it was established that some of the molecules involved in feather primordium formation are expressed exclusively in either the epidermis or dermis, and that these molecules can either promote or repress feather fate. To date, protein members within the following signalling pathways have been demonstrated to be involved in the various stages of feather formation; WNTs (Chang *et al.*, 2004b; Chodankar *et al.*, 2003; Morosan-Puopolo *et al.*, 2014; Noramly *et al.*, 1999; Widelitz *et al.*, 1999; Widelitz *et al.*, 2000), fibroblast growth factors (FGFs) (Jung *et al.*, 1998; Patel *et al.*, 1999; Song *et al.*, 1996; Song *et al.*, 2004; Wells *et al.*, 2012), bone morphogenetic proteins (BMPs) (Jung *et al.*, 1998; Michon *et al.*, 2008; Mou *et al.*, 2011; Noramly and Morgan, 1998; Patel *et al.*, 1999; Scaal *et al.*, 2002), ectodysplasin A (EDA) and its receptor (EDAR) (Drew *et al.*, 2007; Houghton *et al.*, 2005), sonic hedgehog (SHH) (Morgan *et al.*, 1998; Ting-Berreth and Chuong, 1996), epidermal growth factors (EGFs) (Atit *et al.*, 2003), Dermo-1 (Hornik *et al.*, 2005; Scaal *et al.*, 2001), Delta-1 (Viallet *et al.*, 1998) and Notch-1 (Chen *et al.*, 1997; Crowe *et al.*, 1998) among others. However, even with these major advancements, the molecular identity of the initial inductive dermal signal that initiates feather primordium induction, as suggested by recombination experiments, remains elusive.

As previously mentioned (section **1.2**), the process of feather formation occurs in key hierarchical steps. Many of the identified signalling pathways involved in feather formation are used repeatedly at different stages and may have stage dependent effects.

A prime example is the BMP family. During tract formation, bead-mediated delivery of recombinant BMP2 protein to HH stage 17-21 chicken embryos was able induce the formation of an ectopic feather tract around the bead (Scaal *et al.*, 2002), whereas after tract formation, ectopic expression of *BMP2* within the tract, inhibited the formation of feather primordia in the local area (Noramly and Morgan, 1998). Depending on the context, a pathway may either promote or inhibit the formation of feathers.

1.3.1 Variations in Feather Development in Different Chicken Breeds

The generation of transgenic mouse models to study the effects of modulated gene function in development is used extensively in research, offering a valuable tool for the study of the molecular basis of tissue development in mammalian systems (as reviewed by (Capecchi, 2005)). With the recent development and advancements of gene editing technologies such as transcription activator-like effector nuclease (TALENs) (Boch *et al.*, 2009; Miller *et al.*, 2011), and clustered regularly interspaced short palindromic repeats (CRISPR) systems (Jinek *et al.*, 2012), generating transgenic mice with targeted genomic mutations has become faster and simpler than ever (Shen *et al.*, 2013; Sung *et al.*, 2013; Wang *et al.*, 2013; Yang *et al.*, 2013).

However, the development of technologies for the generation of transgenic chicken models have not shown a similar level of advancement compared to mammalian systems and the process remains time consuming (Nishijima and Iijima, 2013). Due to the lack of transgenic chicken models for the study of epidermal appendage development, studies using chicken breeds displaying various feathering defects, such as the scaleless (Abbott and Asmundson, 1957), and naked neck (Somes Jr, 1990), have been important for dissecting the molecular and cellular mechanisms involved in the generation of epidermal appendage formation (**Figure 17**).

Scaleless is an autosomal recessive trait and chicken mutants with the scaleless phenotype display almost complete loss of feathering across the body of the bird, and also the complete loss of scale formation in the legs (**Figure 17a**). The first scaleless chickens were sired at the University of California, Davis, from a flock of New

Hampshire chickens (Abbott and Asmundson, 1957). From this original scaleless line, two separate scaleless lines were developed through outcrossing and selection to generate scaleless lines with varying levels of feather loss; the low-line and high-line (Abbott, 1965). Both scaleless lines display complete loss of scale formation on the legs. The scaleless low line, displays almost complete feather loss on the body, but some abnormal feathers can form on the thigh. The scaleless high-line can generate feathers on most tracts of the body and also on the feet and toes.

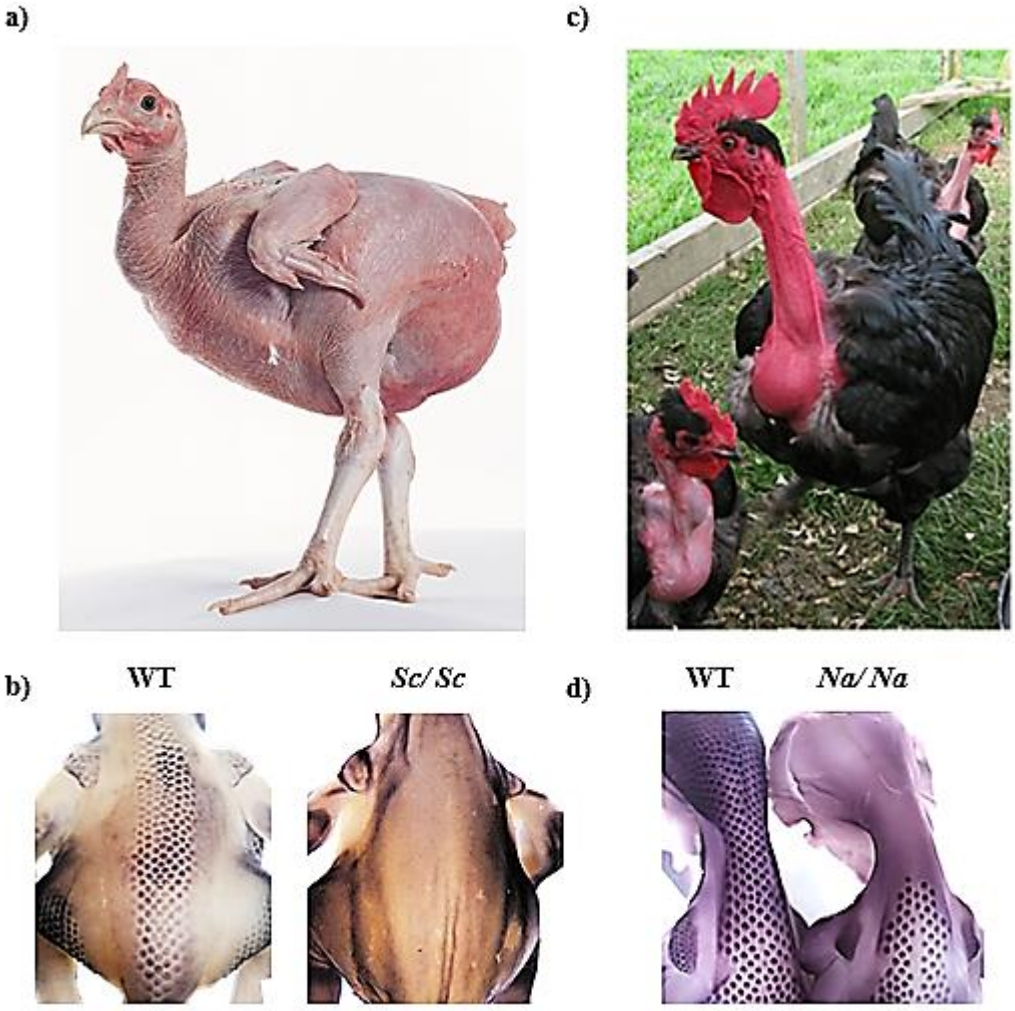

Figure 17. Chicken breeds displaying feathering defects. a) The scaleless breed is characterised by the near complete loss of all feathers and scales. **b)** *In situ* hybridisation for *β-Catenin* expression in wild type and scaleless at HH 31. HH 31 embryos, displaying the scaleless, trait do not develop a restricted *β-Catenin* expression pattern due to loss of feather primordium induction. **c)** Birds displaying the naked neck phenotype display a complete lack of feathering on the neck. **d)** Naked neck chicken embryos fail to develop feather primordia in the neck during development as indicated by the absence of focalised *β-Catenin* expression in the neck region. Adapted from **a)** Wells *et al*, 2012, **b)** Widelitz *et al,* 2000 and **c) & d)** Mou *et al*, 2011.

Due to the almost complete loss of feathering, the scaleless low-line has been the subject of intense research in the study of epidermal-dermal interactions during the induction of epidermal appendages (Drew *et al.*, 2007; Sengel and Abbott, 1963; Song *et al.*, 1996; Song *et al.*, 1994; Song and Sawyer, 1996; Viallet *et al.*, 1998; Wells *et al.*, 2012; Widelitz *et al.*, 2000). The feathering and scale defects of the adult scaleless lines arise during embryonic development and are the result of the failure of feather primordium and scale induction (**Figure 17b**). Histological examination of the scaleless low-line skin during embryonic development demonstrated that the process of tract specification and dense dermis formation is unaffected by the scaleless mutation (Sengel and Abbott, 1963; Viallet *et al.*, 1998). However, epidermal placode and dermal condensate induction does not occur after dense dermis formation. Epidermal-dermal recombination experiments revealed that the feathering defect originated in the epidermis (Sengel and Abbott, 1963). When scaleless low-line dermis was transplanted under wild type chicken epidermis, feather primordia were induced, whereas the reciprocal recombination resulted in bare skin, demonstrating that the appendage induction ability of the scaleless low-line dermis was intact, and that the defect was epidermal (Sengel and Abbott, 1963). The results suggested that the epidermis of the scaleless low-line either lost the ability to respond to the initial dermal induction signal or else lost the ability to subsequently signal to the dermis to induce cell migration and aggregation to form the dermal condensate. Subsequent studies revealed that the scaleless low-line phenotype was the result of a loss of function mutation of an epidermally expressed gene that encodes *FGF20* (Wells *et al.*, 2012).

The naked neck trait in birds is characterised by the complete loss of feathering of on the neck (**Figure 17c**). A naked neck trait has arisen independently in various bird species, such as vultures, ostriches, emus, rheas, and some tropical storks, and is thought to have evolved in response for increased heat-tolerance (Merat, 1986; N'dri *et al.*, 2007; Singh *et al.*, 2001). Some domestic chicken breeds also display the naked neck phenotype and have been used as models to study the mechanisms underlying regionalisation of different feather tracts in birds (Mou *et al.*, 2011; Pitel *et al.*, 2000).

The naked neck trait in chickens was found to be the result of an incompletely dominant mutation which results in the different feathering phenotypes of birds which are either heterozygous or homozygous for the allele. Heterozygous and homozygous naked neck chickens display varying degrees of feather loss. Chickens heterozygous for the trait display reduced feathering of the neck while homozygous birds show a complete loss of feathers on the neck and reduced feathering within the feather bearing tracts (Somes Jr, 1990). Similar to the scaleless trait, the adult phenotype arises during embryonic development due to the failure of feather primordium induction in the neck (**Figure 17d**). The genetic basis of the naked neck chicken phenotype was characterised by Mou, *et al* (Mou *et al.*, 2011). The naked neck trait in chickens was found to be the result of increased expression of *BMP12* that has the ability to block feather primordium induction. Coupled with the selective sensitivity of the neck to the proteins' inhibitory properties, this results in the restricted loss of feathering to the neck of chickens with the trait.

1.3.2 Molecular Signalling during Feather Tract Formation

Several signalling molecules have been implicated in tract formation, but how the process is initiated and how feather tracts are defined are still under investigation. What is currently known is that prior to the induction of feather primordium formation the densification of the underlying dermis of the presumptive feather tract is required.

The earliest known molecular marker for dermis formation within the dorsal tract is *Dermo-1* (Scaal *et al.*, 2001). The expression of *Dermo-1* can be detected within the dermal cell progenitors in the subectodermal space around the midline of the tract as early as HH 24, prior to the migration of the dermal cell progenitors from the dermomyotome. *Dermo-1* expression is readily detected and increases in signal intensity throughout the process of dense dermis formation of the dorsal tract. Based on the *Dermo-1* expression pattern within the dorsal tract, it was suggested that *Dermo-1* may have an active role in the formation of the dense dermis and subsequent feather development. Overexpression of *Dermo-1* during chicken embryogenesis, through retroviral delivery of an over-expression construct containing the coding region of

Dermo-1, resulted in the formation of dense dermis and subsequent formation of ectopic feathers or scales (Hornik *et al.*, 2005).

How *Dermo-1* induces the formation of dense dermis is unknown but in subsequent studies it was demonstrated that *Dermo-1* expression itself was regulated by BMP2 (Scaal *et al.*, 2002). Bead-mediated delivery of recombinant BMP2 protein to skin regions outside of the presumptive feather tracts resulted in the ectopic expression of dense dermis markers, such as *Dermo-1*, and the formation of ectopic feather tracts around the bead. The ectopic feather tracts were capable of feather induction. Co-application of BMP2 protein and Noggin, an antagonist of BMPs, did not result in the induction of *Dermo-1* expression or the formation of dense dermis, demonstrating that *Dermo-1* is a downstream target of BMP signalling during dorsal tract dermis formation.

Recently, it was shown that the directed migration of the *Dermo-1* expressing dermal cell progenitors from the dermomyotome was dependent on WNT11 activity (Morosan-Puopolo *et al.*, 2014). Inhibition of WNT11 protein synthesis within the dermomyotome through gene silencing using RNA interference (RNAi), resulted in the failure of dense dermis formation. This was due to the failure of migration of the dermal cell progenitors from the dermomyotome towards the subectodermal space. As described in section **1.1.4** epithelial-mesenchymal transition (EMT) is required for the migration of dermal cell progenitors from the dermomyotome. The authors suggest that WNT11 is required for dermal cell progenitors to undergo EMT, without which, the progenitors cannot migrate. When *WNT11* expression was silenced within the dermomyotome, the expression of the EMT marker gene, *SNAIL1*, was decreased within the *WNT11* silenced regions, demonstrating that without WNT11 activity, EMT of dermal cell progenitor is reduced.

On the epidermis, the early expression of *β-Catenin*, within the presumptive feather tracts, suggests its involvement in epidermal tract specification (Widelitz *et al.*, 2000). The appearance of *β-Catenin* expression on the epidermis of developing chicken embryos is a reliable marker of feather tract boundaries. *β-Catenin* is only expressed

within the presumptive feather tract regions but is excluded from the apteric regions. How *β-Catenin* expression within the epidermis of the tracts is regulated and what the function of *β-Catenin* during tract specification, is currently unknown. However, forced expression of stabilised β-Catenin protein resulted in the formation of ectopic feather buds in both tract and apteric regions, indicating that β-Catenin protein is capable of inducing the formation of feather bearing skin (Noramly *et al.*, 1999).

1.3.3 Molecular Signalling during Feather Primordium Induction

Feather follicles are arranged in a high fidelity periodic pattern in adult birds. The precise arrangement of feather follicles arises during embryonic development and persists throughout the adult life of the bird. Feather primordium formation is induced in a spatiotemporal sequence across the presumptive feather tracts, through the sequential addition of new feather primordium rows lateral to the previously induced row (as described in section **1.2.3**). From experimental observations of dorsal tract patterning, it was suggested that a morphogenetic wave sweeps bilaterally across the dorsal tract from the midline, inducing the formation of feather primordia in its wake (Davidson, 1983; Ede, 1972; Patel *et al.*, 1999). The components of the morphogenetic wave would function as permissive factors to allow the induction and formation of feather primordia.

Through experimental manipulation of dorsal tract skin prepared from HH 29+ chicken embryos (which contains only one row of feather primordia), the mechanism of the morphogenetic wave was revealed (Patel *et al.*, 1999). Removal of skin lateral to the existing row of feather primordia resulted in the failure of feather primordium formation on the operated side, showing that without the inductive signals from the morphogenetic wave, feather formation cannot be induced. The results showed that the expression/activity of the morphogenetic wave is spatiotemporally restricted. The morphogenetic wave had, at that stage, not travelled beyond the operated skin regions, resulting in the failure of feather primordium formation on the operated side of the skin. From this observation it was suggested that visible formation of feather primordia within the dorsal tract is preceded by a wave of induction which travels bilaterally

from the midline. The cellular and molecular basis of the morphogenetic wave is currently unknown.

Detection of RNA transcripts within the developing feather tracts, through *in situ* hybridisation analysis, revealed that the genes which encode the proteins known to be involved in the induction of feather primordia, display two different but distinct patterns of expression. These were termed "restrictive mode" and "*de novo*" mode pattern of expression (Jiang *et al.*, 2004) (**Figure 18**).

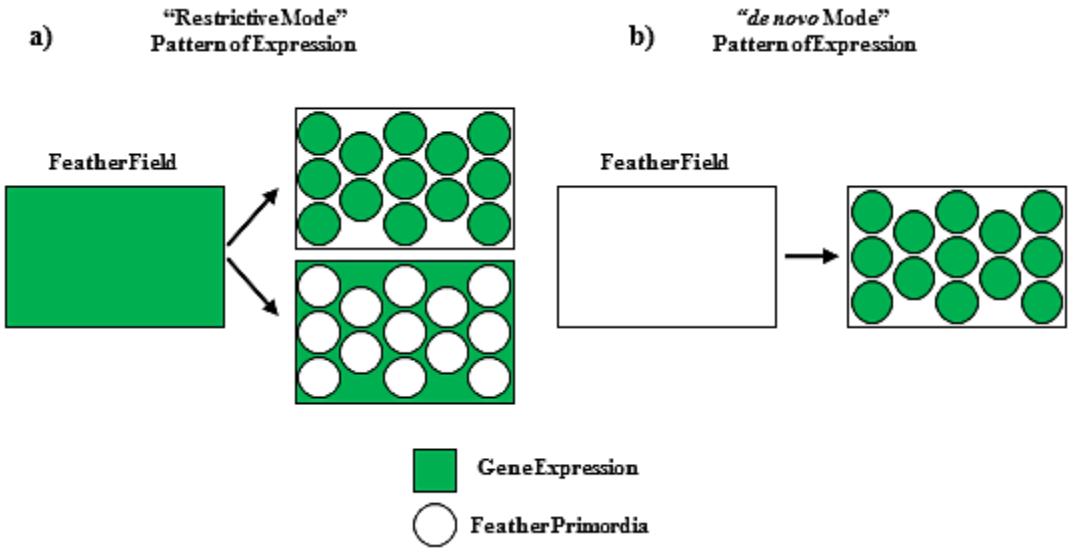

Figure 18. Gene expression patterns during feather primordium formation. Genes involved in feather primordium formation can be grouped based on their expression pattern. **a)** Genes that are initially expressed throughout the feather field but are then subsequently focalised into either the feather primordia or interbud domains are termed "restrictive mode" pattern of expression. **b)** Genes that are only expressed within the feather primordia, after their formation, are termed "*de novo*" mode pattern of expression.

Genes that are initially expressed throughout the tract, but are subsequently focalised into either primordia or inter-primordia regions, show a "restrictive mode" expression pattern. *β-Catenin* is a prime example of a gene that displays a "restrictive mode" expression pattern (Widelitz *et al.*, 2000). The presence of *β-Catenin* expression on

developing chicken skin defines the feather tracts and distinguishes regions of skin competent to feather primordium formation from the apteric skin regions. During the formation of feathers, the initially homogenous expression of *β-Catenin* across the tracts show focalisation and restriction of expression to the forming primordium domain but is inhibited in the inter-placode domain. Genes expressed in the "restrictive mode" may function as inducers of feather primordium formation.

Genes which show a "*de novo*" mode expression pattern are not expressed homogenously across the tract initially, but are expressed within the forming feather primordia, after induction has taken place. Genes which display a "*de novo*" pattern of expression are believed to not be involved in the process of feather primordium induction but are involved in later events, such as stabilisation of the forming feather primordia or directing primordium outgrowth and differentiation. The *SHH* gene shows a "*de novo*" mode expression pattern (Ting-Berreth and Chuong, 1996). Its expression first appears within the forming feather primordia and is then restricted to the distal tip of the feather primordia, directing the outgrowth of the developing feather bud. Ectopic expression of *SHH* results in the loss of anterior-posterior polarity of the developing feather primordia, changing the orientation of feather outgrowth.

During feather primordium induction, several signalling molecules and their associated pathways such as, WNTs/β-Catenin, FGFs, BMPs, and EDA have all been shown, in multiple studies, to be important for the normal induction of feather primordium formation (of which the role and function of these genes, during feather induction will be individually reviewed below).

1.3.4 WNT Signalling during Feather Primordium Induction

The WNT signalling pathway has been one of the most extensively studied signalling pathways in skin and feather morphogenesis. Different members of the WNT protein family members have been associated with various stages of epithelial appendage induction. As such, various processes have been attributed to the function of WNT proteins during avian skin and feather formation, including cell polarity, cell migration, cell adhesion, proliferation, and differentiation.

WNT proteins are a family of secreted signalling molecules, which have potent morphogenetic properties and have been implicated in various biological processes such as embryogenesis and cancer development (Logan and Nusse, 2004; MacDonald *et al.*, 2009). The WNT proteins are highly conserved across various species such as humans, mice, frogs, and flies (Nusse and Varmus, 2012). In humans and mice, there are currently nineteen known WNT protein family members (Malbon *et al.*, 2001), while around ten family members of the WNT transmembrane receptor (Frizzled) have been identified (Wang *et al.*, 1996). The binding of WNT ligands to Frizzled receptors is mediated through the interaction of various co-receptors which include, lipoprotein receptor-related protein (LRP) (Gordon and Nusse, 2006; Tamai *et al.*, 2000), related to receptor tyrosine kinase (RYK), and tyrosine-protein kinase transmembrane receptor (ROR2) (Komiya and Habas, 2008). When an extracellular WNT ligand binds to its transmembrane Frizzled receptor and its associated co-receptor, a signal cascade is induced. WNTs can activate at least three different signalling cascades: the canonical WNT/β-Catenin pathway, the non-canonical WNT/Ca^{2+} pathway and the non-canonical WNT/planar cell polarity (PCP) pathway (Gordon and Nusse, 2006; Komiya and Habas, 2008; Nelson and Nusse, 2004). As their name implies, the WNT signalling pathways can be separated into two categories: the canonical pathway, which is dependent on the translocation of β-Catenin protein to the nucleus to induce the transcription of downstream signalling targets, and the non-canonical pathways which are β-Catenin independent. Other non-canonical WNT pathways have been described but have not been as well characterised as the three mentioned above (Komiya and Habas, 2008).

Which pathway is stimulated is not strictly dictated by the binding of a specific WNT ligand, as demonstrated by the ability of WNT5a protein to stimulate both the canonical and non-canonical WNT pathways (Mikels and Nusse, 2006; Nishita *et al.*, 2010; Nomachi *et al.*, 2008). Instead, it has been suggested that it is the specific combination of WNT ligand, co-receptor, and Frizzled receptor that determines the pathway stimulated (Verkaar and Zaman, 2010). However, which WNT/co-receptor/Frizzled combinations stimulate which pathway is currently unknown due to technical limitations in the purification of most WNT proteins (Willert and Nusse, 2012), preventing the analysis of WNT protein/Frizzled binding affinities.

Of the different WNT signalling pathways, the canonical WNT/β-Catenin pathways is one of the best characterised and relies on β-Catenin protein to exert its signalling activities. However, the functional role of β-Catenin protein is not restricted to signal transduction. The β-Catenin protein is known to be associated with the cadherin protein complex where it mediates calcium dependent adhesion between cells (Choi *et al.*, 2006). Most studies have focused on the function of β-Catenin in cell signalling and its effect on feather induction and formation (Noramly *et al.*, 1999; Widelitz *et al.*, 2000).

The canonical WNT/β-Catenin signalling pathway regulates cellular processes through its effects on intracellular concentrations of β-Catenin protein. In the absence of WNT signalling the intracellular concentration of β-Catenin is regulated via proteosomal degradation by the β-Catenin destruction complex, which prevents the accumulation of β-Catenin protein in the cytoplasm (Aberle *et al.*, 1997). The β-Catenin destruction complex is a multi-protein complex comprising axin, glycogen synthase 3β kinase (GFK3β), and adenomatous polyposis coli (APC). The β-Catenin destruction complex binds and phosphorylates β-Catenin which marks the protein for degradation by the ubiquitin-mediated proteasome pathway (**Figure 19a**).

During canonical WNT/β-Catenin signalling, the binding of WNT ligands to their associated Frizzled receptor is mediated by the LRP5 or LRP6 co-receptors (Gordon and Nusse, 2006; Tamai *et al.*, 2000). Preventing LRP6 association during

WNT/Frizzled binding by a WNT signalling antagonist, Dickkopf-1 (DKK1), inhibited the induction of WNT/β-Catenin signalling (Bafico *et al.*, 2001). Upon successful binding of WNT to its Frizzled receptor, an intracellular protein, Dishevelled, is activated which inhibits the formation of the β-Catenin destruction complex through the inhibition of GSK3β activity. The inhibition of the formation of the β-Catenin destruction complex prevents the phosphorylation and targeted destruction of β-Catenin protein, allowing the accumulation of β-Catenin protein within the cytoplasm of the cell. As cytoplasmic concentrations of β-Catenin protein increase, β-Catenin proteins may translocate to the nucleus, forming a complex with lymphoid enhancer-binding factors (Lefs) and T-cell factors (TCFs), to induce the transcription of downstream target genes (Staal and Clevers, 2000; van de Wetering *et al.*, 1997) (**Figure 19b**).

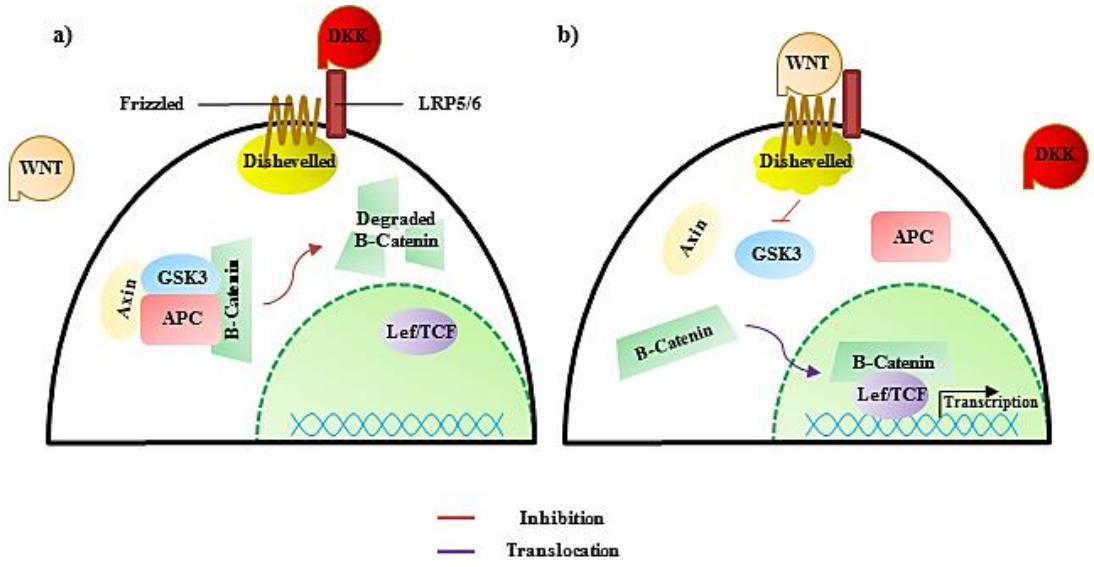

Figure 19. Canonical WNT/β-Catenin signalling pathway. a) Absence of WNT signalling due to lack of WNT ligand or inhibition by DKK results in the targeted degradation of β-Catenin protein by the β-Catenin destruction complex. **b)** When WNT singling is stimulated, Dishevelled is activated which inhibits the formation of the β-Catenin destruction complex via the inhibition of GSK3β activity. This allows cytoplasmic β-Catenin protein concentrations to increase resulting in the eventual translocation of β-Catenin protein to the nucleus. In the nucleus, β-Catenin interacts with Lef/TCF to mediate the transcription of downstream signalling targets.

There are various different non-canonical WNT pathways, however, what they all have in common is their independence from β-Catenin protein (Gordon and Nusse, 2006; Komiya and Habas, 2008; Nelson and Nusse, 2004). The function of the non-canonical WNT pathways during feather induction and formation has not been well studied, and as such will be described in a simplified manner for the purposes of this thesis. As mentioned above, the main focus of previous studies has been the effects of WNT/β-Catenin signalling on feather induction and formation.

In the WNT/Ca^{2+} pathway, the binding of WNT ligand to a Frizzled receptor is also required to induce the signal cascade. However, unlike the canonical WNT/β-Catenin pathway, the binding of WNT to Frizzled is mediated through the ROR2 co-receptor rather than LRP5/6 (Kohn and Moon, 2005; Kuhl *et al.*, 2000; Wang and Malbon, 2003). The binding of WNT ligand to Frizzled results in the release of intracellular Ca^{2+} through stimulation of a trimeric G protein. The increase in intracellular Ca^{2+} activates protein kinase C (PKC) or calcium/calmodulin-dependent protein kinase II (CaMKII) leading to the activation of various transcription factors, such as nuclear factor of activated T- cells (NFAT), to exert the signalling effects of the pathway. The WNT/Ca^{2+} pathway has previously been shown to be involved in cellular processes such as cell adhesion and migration, and has also been shown to inhibit the canonical WNT/β-pathway through GSK3β independent degradation of β-protein (Komiya and Habas, 2008) (**Figure 20a**).

The WNT/PCP pathway has been demonstrated to be involved in the regulation of cytoskeleton structure (Strutt, 2003), and in various mouse studies, has been shown to be involved in the differentiation and orientation of hair follicles, hair follicle maintenance and cycling, and wound healing (reviewed by (Chen and Chuong, 2012)). Activation of the WNT/PCP pathway requires the binding of WNT ligand to a Frizzled receptor, which is mediated through the co-receptors RYK and ROR2. Stimulation of the WNT/PCP pathway also lead to the activation of Dishevelled, but unlike the canonical WNT/β-Catenin pathway, does not lead to the inhibition of GSK3β. Activation of dishevelled during the WNT/PCP pathway instead, activates a signalling

cascade which leads to the eventual activation of c-Jun N-terminal kinase (JNK), leading to gene transcription (Komiya and Habas, 2008) (**Figure 20b**).

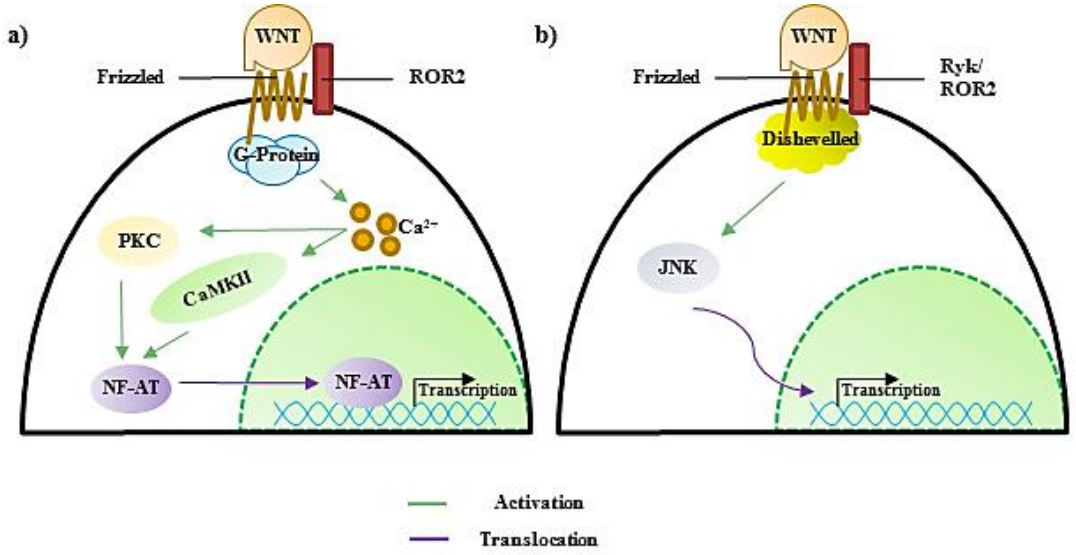

Figure 20. Non-Canonical WNT signalling pathways. a) WNT/Ca^{2+} signalling pathway. Activation of this pathway stimulates the release of Ca^{2+} ions into the cytoplasm. This causes the activation of Ca^{2+} dependent kinases, leading to the activation of transcription factors which mediate the transcription of downstream signalling targets. **b)** The WNT/PCP pathway, stimulation of this pathways results in the activation of a signalling cascade which leads to the eventual activation of JNK. Activation of JNK leads to scaffold protein modifications or the activation of transcription factors which mediate the transcription of target genes.

As noted above, β-Catenin protein and various WNT protein members have been demonstrated to be involved in the various stages of feather induction and formation. In previous studies, the function of WNT1, WNT3a, WNT5a, WNT7a, WNT11, and β-Catenin during the different stages of feather formation were tested.(Chang *et al.*, 2004b; Huelsken *et al.*, 2001; Noramly *et al.*, 1999; Widelitz *et al.*, 1999). Based on *in situ* hybridisation analysis of skin after feather tract specification, it was revealed that all the above WNT proteins and β-Catenin were expressed in a "restrictive mode" of pattern expression, suggesting all the examined molecules may have a role in the

feather induction. Although all the WNT proteins were expressed in a "restrictive mode", different *WNTs*, and *β-Catenin* were localised to different skin regions. *WNT1*, *WNT3a*, *WNT7a*, and β-Catenin, were all expressed homogenously across the presumptive feather tracts prior to feather primordium formation and were later focalised within the developing feather primordia (Chang *et al.*, 2004b; Chuong *et al.*, 1996). *WNT5a* was also initially detected in the epidermis but was later restricted to the interbud domains. *WNT11* expression was only ever detected in the dermis, and similar to *WNT5a*, was later restricted to the interbud domains (Tanda *et al.*, 1995). The differences in the observed expression patterns may indicate distinct functions for individual WNT proteins or β-Catenin.

Through perturbation of expression of *β-Catenin* and various *WNTs* from a retroviral vector (replication competent ASLV long terminal repeat with a splice receptor (RCAS), the function of the molecules during feather induction and formation were tested either *in ovo* or *ex vivo* (Chang *et al.*, 2004b; Huelsken *et al.*, 2001; Noramly *et al.*, 1999; Widelitz *et al.*, 1999). Also, the ability of each WNT to stimulate either the canonical or non-canonical WNT pathway was tested to determine how the WNT proteins and the pathway(s) they stimulate may affect feather induction (with the exception of WNT7a) (Chang *et al.*, 2004b). These studies demonstrated that the majority of WNT proteins appear to specifically induce the activity of only one of the WNT signalling pathways, and that each WNT protein/pathway may exert different effects during feather primordium induction and formation. However, as revealed through *in situ* hybridisation analysis, the expression of the individual *WNTs* or *β-Catenin* were localised specifically to either the epidermis or dermis. Retroviral mediated delivery of overexpression vectors may result in the expression of *WNT* genes or *β-Catenin* in both skin layers, and may not fully reflect the *in vivo* function of the genes.

During *ex vivo* feather induction, overexpression of both *WNT1*, and *WNT3a* showed similar effects on reconstituted mesenchymal skin explants. *WNT1* overexpression caused the formation of enlarged feather buds, whereas expression of a dominant negative form of *WNT1* resulted in the formation of a thin feather bud with increased

interbud spacing, suggesting that *WNT1* does not function as a feather primordium inducer but affects primordium development and differentiation. *WNT3a* overexpression induced the formation of enlarged feather buds but reduced interbud spacing. However, the effects of inhibiting *WNT3a* expression on feather primordium induction were not tested in this study. The overlapping expression pattern of the two *WNTs* suggest they may serve similar functions during the induction and formation of feather primordia. Conversely, when the effects of *WNT1* and *WNT3a* overexpression were tested *in ovo* at an earlier stage of feather development, the two *WNTs* displayed contrasting effects. *WNT1* expression inhibited dense dermis formation resulting in a truncated dorsal tract. Feather primordium formation was also affected, with only a few widely dispersed feather buds being present on the affected areas of the tract. *WNT3a*, on the other hand, increased dermal thickening in affected skin regions and expanded the dorsal tract region. Within the expanded tract regions, enlarged feather buds were observed (similar to the *ex vivo* assay) (Chang *et al.*, 2004b). In the *in ovo* assays, the effects of overexpression of the *WNTs* on feather structure were probably due to the upstream effects of dense dermis formation rather than a direct effect of the WNT proteins, due to the requirement of dense dermis for the normal formation of feathers (Jiang *et al.*, 1999). Through TCF-luciferase assays, using chicken embryonic fibroblasts (CEFs), it was shown that both WNT1 and WNT3a proteins exert their effects through the canonical WNT/β-Catenin pathway (Chang *et al.*, 2004b). The results further demonstrate the stage specific effects of various proteins during feather formation, even if the proteins in question show similar expression profiles and signals through the same pathways.

WNT5a, although expressed within the skin and showed a "restrictive mode" pattern of expression, had no apparent effects on feather tract size or feather structure when overexpressed (Chang *et al.*, 2004b). The result suggest that *WNT5a* does not function in the induction or formation of feather primordia. However, in their cell proliferation assays using CEFs, WNT5a was able to induce cell proliferation via signalling through the non-canonical WNT/Ca^{2+} and WNT/PCP pathways, as detected through PKC

activity assays and western blot for JNK protein respectively. The lack of phenotypic effects on feather formation is unexpected and requires further study.

In *ex vivo* reconstituted mesenchymal explant cultures, the overexpression of *WNT7a* caused the formation of enlarged feather primordia with reduced interbud spacing and occasional fusions between neighbouring primordia (Widelitz *et al.*, 1999). The resulting feather buds displayed abnormal morphologies. During normal outgrowth, feather buds show oriented proximal-distal extension in an anterior-posterior (A-P) direction, resulting in the formation of a feather bud displaying bilateral symmetry which tapers distally. The *WNT7a* transduced feather buds however, are plateau-shaped and display radial symmetry indicating *WNT7a* functions to induce A-P orientation and outgrowth of forming feather primordia/buds.

WNT11 overexpression resulted in the inhibition of feather primordium formation in both *in ovo* and *ex vivo* experiments, suggesting that *WNT11* functions to inhibit feather fate through WNT/PCP signalling, as indicated through immuno-detection of JNK proteins via western blot analysis (Chang *et al.*, 2004b). This contrasts with the study performed by Morosan-Puopolo *et al*, 2014, who demonstrated through RNAi, when *WNT11* expression was silenced, feather bud formation was reduced in transduced skin regions (Morosan-Puopolo *et al.*, 2014). However, *WNT11* silenced skin regions display a lack of dense dermis formation, and inhibition of feather formation in their experiment may reflect the requirement of dense dermis formation for the induction of feather primordia rather than a direct effect of the lack of *WNT11* gene activity. The direct effect of *WNT11* gene silencing on feather induction was not tested in their study. Morosan-puopolo *et al*, 2014 also showed that *WNT11* expression is required for the EMT of dermal cell progenitors and cell migration during dorsal tract formation (Morosan-Puopolo *et al.*, 2014). Chang *et al*, 2004 demonstrated that WNT11 induced migration of CEFs in culture, and suggested that the inhibition of feather formation after *WNT11* overexpression *in ovo* and *ex vivo* was the result of increased cell migration, which inhibited the formation of stable dermal cell aggregates during feather induction (Chang *et al.*, 2004b).

Prior to HH 29, β-Catenin protein can be detected in the cytoplasm of the cells in both the epidermis and in the underlying dermis, however, little to no nuclear staining of β-Catenin in these cells can be detected at these stages, suggesting that there is no WNT/β-Catenin signalling in these cells (Noramly *et al.*, 1999). The detection of β-Catenin protein in the dermis is transient however, and by HH 29, β-Catenin protein can only detected within the cells of the epidermis in both the cytoplasm and nucleus, indicating WNT/β-Catenin signalling activity is restricted to the epidermis during feather primordium induction. During feather primordium induction, *β-Catenin* expression is initially restricted to the epidermis of the presumptive feather tracts but is excluded from the apteric regions and is later focalised to the forming feather primordia (Noramly *et al.*, 1999; Widelitz *et al.*, 2000). Forced expression of a stabilised form of β-Catenin protein, through RCAS transduction, resulted in the formation of ectopic feather primordia in both the feather tracts and apteric regions (Noramly *et al.*, 1999). The ectopic feather primordia in the apteric regions express genes associated with endogenous feather primordium formation, such as *SHH* (Morgan *et al.*, 1998), *BMP2* (Jung and Chuong, 1998), and *BMP4* (Noramly and Morgan, 1998). This indicates that forced activation of WNT/β-Catenin signalling in skin, alone, is capable of inducing feather primordia, despite the lack of a dense dermis.

In ovo overexpression of the WNT/β-Catenin signalling antagonist, *DKK1*, through RCAS-mediated transduction, resulted in the failure of dense dermis formation and induction of feather primordia in the affected skin regions. In the *ex vivo* skin cultures, overexpression of *DKK1* did not prevent the induction of feather primordia, but prevented the subsequent outgrowth of the primordia (Chang *et al.*, 2004b).

In summary, based on these studies, it was established that the various WNT signalling pathways have distinct roles during the induction and formation of feather primordia, such as dense dermis formation, feather primordium growth and polarity. However, based on the inhibition experiments through the use of *DKK1* and dominant negative *WNT1* expression vectors (expressing a truncated version of the WNT1 protein), WNT signalling appears to be dispensable for the induction of feather primordia, suggesting

other signalling pathways may function as permissive factors during feather induction (Chang *et al.*, 2004a).

1.3.5 FGF Signalling during Feather Primordium Induction

Fibroblast growth factors (FGFs) are a family of proteins which have been implicated in various biological processes such as organogenesis and tissue homeostasis in different species (reviewed by (Ornitz and Itoh, 2015)). In epithelial appendage formation, FGF signalling has been shown to be indispensable for the formation of hairs, feathers and scales of mice, chicken and fish respectively (Casas *et al.*, 2013; Huh *et al.*, 2013; Rohner *et al.*, 2009; Wells *et al.*, 2012), indicating that FGF signalling is required for the induction and formation of epithelial appendages.

To date, in mammals, 22 *FGF* genes have been identified which can be separated in to seven distinct subfamilies based on phylogenetic analysis (Itoh and Ornitz, 2004; Itoh, 2010; Ornitz and Itoh, 2001; Oulion *et al.*, 2012). The seven subfamilies can be further subdivided into three distinct groups based on the way they exert their effects. Secreted FGFs signal through receptor tyrosine kinase (RTK) signal transduction pathway after a FGF ligand binds to its associated FGF receptor (FGFR). Intracellular FGFs, which are not secreted and do not bind to FGFRs, function as co-factors to regulate the ion-gating properties of ion channels and other molecules such as microtubules. Finally, endocrine FGFs, which also exert their signalling effects through the binding of FGF ligand to FGFR, but require a different set of co-factors compared to secreted FGFs for receptor binding. Compared to the other two types of FGFs, the study of endocrine FGFs and their functions have begun only relatively recently, (within the last ten years), and so their role and functions in epithelial appendage formation are currently unknown (Ornitz and Itoh, 2015). In feather morphogenesis, only the function of secreted FGFs have been explored and so the function of intracellular and endocrine FGFs will not be reviewed below.

There are five subfamilies of secreted FGF proteins which comprise of 15 of the 22 known *FGF* genes. During embryogenesis, various *FGFs* are expressed throughout the developing embryo and function as paracrine factors which can regulate cellular

proliferation, migration, survival and differentiation. FGF signal transduction is stimulated through the binding of a secreted FGF ligand to its associated extracellular FGFR. FGFRs are members of the tyrosine kinase superfamily, and to date, five members have been identified, FGFR1-4, and FGFR-like1 (FGFRL1) (Trueb, 2011). The binding affinities of the FGFRs are dependent on the structure of their extracellular immunoglobulin-like domains which can regulate ligand binding specificities (Johnson and Williams, 1993; Wang *et al.*, 1995). *FGFR1-3* have been shown to generate two major splice variants within their immunoglobulin-like III domains and so are referred to as *FGF IIIb* or *IIIc* variants. Each has its own distinct FGF ligand binding affinities (Miki *et al.*, 1992; Werner *et al.*, 1992). *FGFR4* does not generate different splice variants (Partanen *et al.*, 1991). FGFRL1 has been demonstrated to bind secreted FGF ligands but, due to the lack of a cytoplasmic tyrosine kinase domain, ligand binding does not stimulate signal transduction, suggesting that FGFRL1 may function as a decoy receptor to inhibit FGF signalling (Trueb, 2011). During feather morphogenesis, the various *FGFR* genes are differentially expressed in a tissue specific manner which suggest that each tissue layer may bind a specific subset of FGF proteins and indicate different roles for the receptors during feather induction and formation (Noji *et al.*, 1993; Noramly and Morgan, 1998; Patstone *et al.*, 1993). *FGFR1* is expressed within the dermis of forming dermal cell condensates. *FGFR2* is expressed throughout the epidermis prior to feather primordium formation but is later restricted to the interbud domains (Noramly and Morgan, 1998). *FGFR3* is expressed ubiquitously throughout the dermis of feather tracts (Noji *et al.*, 1993).

Secreted FGF ligands contain a heparin sulphate proteoglycan (HSPG) binding domain, and are tightly bound to HSPG proteins found on the cell surfaces and ECM. The ECM is a network of molecules that are excreted into the extracellular space by cells and provide structural support for the surrounding cells. This property limits their diffusion and therefore the active range of the secreted FGF proteins. However, HSPGs appear to play a pivotal role in FGF signalling and have been demonstrated to function as co-factors, which can regulate the binding affinities between certain FGF and

FGFRs (Ornitz and Leder, 1992; Rapraeger *et al.*, 1991; Yayon *et al.*, 1991). FGF proteins can bind and stimulate the activation of more than one type of FGFR, and so, different FGF proteins may function redundantly to one another, such as FGF9 and FGF20 in the maintenance of the stemness of nephron progenitors in mammalian species (Barak *et al.*, 2012). The binding of FGF proteins to FGFRs causes homo- or hetero-dimerization of the receptor monomers resulting in the trans-phosphorylation and activation of tyrosine within the cytoplasmic region of the receptors (Bellot *et al.*, 1991). The stimulation of tyrosine activation regulates the recruitment of different signalling complexes, and depending on the combination of complexes, activates one of four distinct intracellular signalling cascades; 1) the RAS-MAPK (rat sarcoma-mitogen activated protein kinase), 2) PI3K-AKT, 3) phospholipase Cγ (PLCγ), and 4) the signal transducer and activator of transcription (STAT) (Hart *et al.*, 2000; Kouhara *et al.*, 1997; Mohammadi *et al.*, 1992; Ong *et al.*, 2000; Peters *et al.*, 1992). Currently, the signalling outcomes of different combinations of FGF/FGFR binding is unknown. Each pathway can stimulate the activation of its own set of transcription factors, which mediate the transcription of downstream targets to exert specific cellular responses, such as cell proliferation, migration, and survival.

In the context of feather morphogenesis, FGF1, FGF2, FGF4, FGF10, and FGF20 have all been shown to be involved or to be able to modulate feather induction and formation (Lin *et al.*, 2009; Mandler and Neubuser, 2004; Song *et al.*, 1996; Song *et al.*, 2004; Tao *et al.*, 2002; Wells *et al.*, 2012; Widelitz *et al.*, 1996). FGF signalling has been shown to be crucial for the morphogenesis of feathers, and in general, have been demonstrated to promote feather fate. Blocking FGF signalling through the use of a chemical inhibitor, SU5402 (Sun *et al.*, 1999), or forced expression of soluble FGFR1/2 in developing embryonic chicken skin explants (Mandler and Neubuser, 2004), results in the complete loss of feather formation.

Each of the above tested FGFs represent four distinct FGF subfamilies and may exert different FGF signalling outcomes due to their differing binding affinities to FGFRs. FGF1 and FGF2 belong to the FGF1 subfamily, FGF4 is within the FGF4 subfamily, FGF10 is part of the FGF7 subfamily, and FGF20 is part of the FGF9 subfamily (Itoh

and Ornitz, 2004). During feather induction, the *FGF* genes examined thus far are believed to be expressed in a "restrictive mode" of pattern expression (Lin *et al.*, 2009). However, the expression profiles of the above genes have not all been shown and different FGFs may be expressed in different patterns/modes. *FGF10* is expressed in the dermis and displays a "restrictive mode" of pattern expression where expression is focalised to developing feather primordia (Tao *et al.*, 2002). In contrast, *FGF20* appears to be only expressed within the epidermis of forming feather primordia and does not show homogenous expression outwith the primordium generating region within the presumptive feather tracts, suggesting that not all *FGFs* are expressed in a "restrictive mode" (Wells *et al.*, 2012).

Exogenous application of recombinant FGF1 protein to embryonic chick dorsal skin explants, prior to appearance of visible feather primordia, resulted in the formation of enlarged feather primordia which often fuse with their direct neighbours (Widelitz *et al.*, 1996).

Bead-mediated delivery of recombinant FGF4 protein within the presumptive dorsal tract displayed similar effects as FGF1 and caused the formation of fused feather buds in the area surrounding the bead due to the local effects of the treatment. When FGF4 coated beads were applied to apteric regions, small, discrete feather buds formed within the vicinity of the bead, suggesting that FGF4 is able to induce the formation of skin that is capable of feather induction (Widelitz *et al.*, 1996).

The effects of recombinant FGF2 protein on embryonic chick dorsal skin, prior to feather primordium induction, has similar effects to those induced by FGF1 protein application (Widelitz *et al.*, 1996). Feather buds are enlarged and show occasional fusions but fusions are limited to the medial regions of the presumptive tracts while no fusions are observed in more lateral skin regions. This suggests that FGF2 may have stage specific effects. Due to the spatiotemporal sequence of feather primordium formation, medial regions of the feather tract are more developmentally "mature" compared to lateral regions and so, experimental manipulation of *ex vivo* skin cultures may show spatial differences (Davidson, 1983). When FGF2 protein is applied to more

mature skin explants (after primordium formation), established feather primordia develop into enlarged feather buds, while lateral regions form smaller, discrete feather buds.

In embryonic skin cultures prepared from scaleless embryos, which fail to form dermal condensates due to an ectodermal defect (Sengel and Abbott, 1963), bead-mediated delivery of FGF2 protein rescued feather formation (Song *et al.*, 1996). The ability of FGF2 protein to rescue the feather forming capabilities of scaleless skin suggest that the ectodermal defect may be attributed to loss of FGF signalling during feather induction in chickens displaying the scaleless trait, and that FGFs may function in the formation of dermal condensates. Indeed, when FGF2 protein coated beads were applied to denuded dermis, prepared from wild type and scaleless embryos, the beads were able to stimulate dermal cell aggregation and expression of *BMP2* (a feather primordium marker gene) in the local area around the bead (Song *et al.*, 2004). This demonstrates, that even in the absence of endogenous signalling from an overlying epidermis, FGF2 can functionally mimic epidermal functions to stimulate the formation of dermal aggregates, suggesting that FGFs can function as a permissive factor in the induction of feather primordia.

Recently, the genetic basis of the scaleless trait was determined through gene sequencing (Wells *et al.*, 2012). Well *et al*, identified a nonsense mutation within the *FGF20* gene which was predicted to result in the production of a truncated protein lacking the motifs associated with receptor and HSPG binding (as described in section **1.3.1**). The result suggest that FGF20 protein within chickens displaying the scaleless trait is non-functional, and that the function of *FGF20* is fundamental to the induction of epithelial appendage formation. The ability of FGF2 protein to rescue feather formation in *ex ovo* culture of scaleless skin, as demonstrated in studies by Song *et al*, (Song *et al.*, 1996; Song *et al.*, 1994), suggests that FGF2 and FGF20 can function redundantly to exert their effects on the dermis and stimulate the formation of dermal aggregates. Both FGF2 and FGF20 belong to different subfamilies of FGF proteins, and both families are able to bind similar FGFRs with differing levels of binding

specificities (Ornitz and Itoh, 2015). As of the writing of this thesis, the ability of FGF20 proteins to induce feather induction experimentally, has not been shown.

FGF1, FGF2, FGF4, and *FGF20* are all expressed within the epidermis during feather induction and formation, and exert their morphogenetic effects on the dermis (Nohno *et al.*, 1995; Song *et al.*, 1996; Wells *et al.*, 2012; Xu *et al.*, 2004). Although, the above *FGFs* are expressed in the same skin layer, due to differing binding specificities to different FGFRs, each may have distinct functions during feather induction/formation. *FGF10* however, is expressed within the underlying dermis during feather morphogenesis and is shown to have an epidermal effect (Tao *et al.*, 2002). Overexpression of *FGF10* using RCAS, resulted in the stimulation of epidermal thickening and formation of abnormal feather buds in affected skin regions. Feather buds were structurally bulbous and outgrowth was inhibited by the overexpression of *FGF10*. In *FGF10* misexpressing skin, staining for membrane associated β-Catenin protein within the epidermis increased, but nuclear staining of β-Catenin was not observed in *FGF10* overexpressing regions, indicating that increased *FGF10* activity does not result in the stimulation of canonical WNT/β-Catenin signalling. As previously described, localisation of β-Catenin protein to the nucleus, and thus, active WNT/β-Catenin signalling appears to be a pre-requisite for epidermal competence for feather induction, suggesting that *FGF10* may alter cellular adhesion and differentiation of the epidermis. Blocking FGF10 protein activity, through the use of FGF10 specific antibodies, on the other hand, resulted in the complete inhibition of feather primordium formation in treated *ex vivo* skin explants (Mandler and Neubuser, 2004). The results demonstrate that *FGF10* is required for the initiation of feather primordium development and may function as the primary inductive dermal signal. However, based on current evidence, such as the lack of ectopic feather formation in tract and apteric regions after forced expression of *FGF10*, suggests that *FGF10* may function in the regulation of epidermal competence rather than a direct inductive signal for feather morphogenesis.

As mentioned above, stimulation of FGF signalling can result in the activation different signalling cascades. The RAS-MAPK signalling cascade has been implicated

in a variety of biological processes such as wound healing, kidney branching, and somitogenesis (Delfini *et al.*, 2005; Fisher *et al.*, 2001; Matsubayashi *et al.*, 2004; Sawada *et al.*, 2001). During RAS-MAPK signalling, dimerization of the FGFRs stimulates tyrosine kinase activity leading to the phosphorylation and activation of the adapter protein, FGFR substrate 2α (FRS2α). Activated FRS2α then binds to growth factor receptor-bound 2 (GRB2), which recruits son of sevenless (SOS) to activate Ras. Ras in turn, phosphorylates and activates Raf, mitogen/extracellular signal-regulated kinase (MEK), and extracellular signal-regulated kinase (ERK). Following activation of ERK, ERK translocates to the nucleus and phosphorylates E26 transformation-specific transcription factors (ETS), such as ETS translocation variant 4 and 5 (ETV4 and ETV5), which results in the transcription of downstream target genes of the RAS-MAPK signalling cascade (McCormick, 1993; Ong *et al.*, 2000; Roberts, 1992; Sharrocks, 2001; Wasylyk *et al.*, 1998) (**Figure 21**).

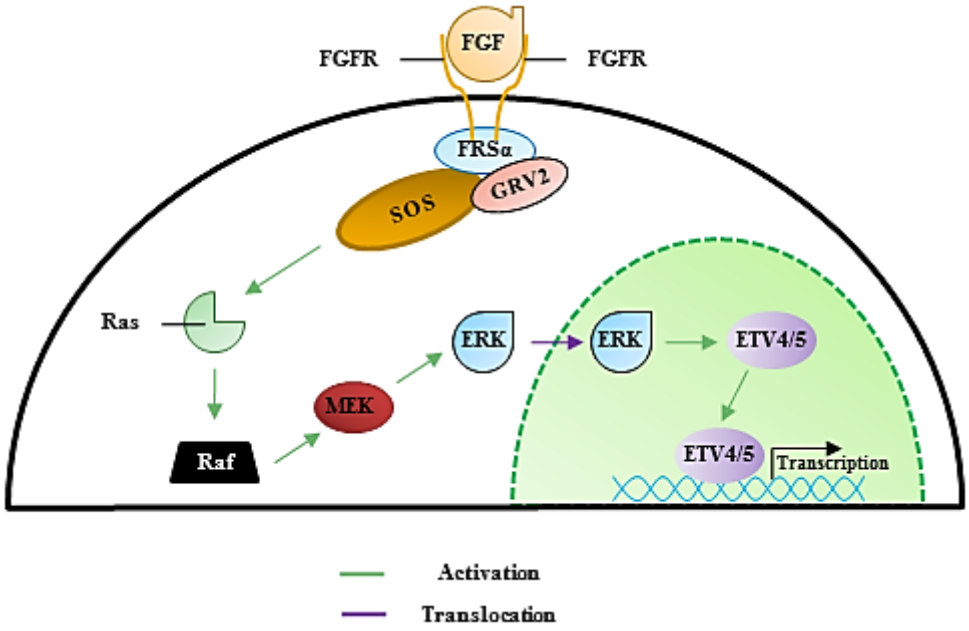

Figure 21. FGF signalling pathway. Activation of the FGF signalling pathway results in the activation and recruitment of several proteins such as FRSα, GRV2 and SOS. This leads to the eventual activation of ERK through the activation of Ras, Raf, and MEKs. Activated/phosphorylated ERK translocates to the nucleus and activates

transcription factors, such as ETV4/5, to mediate the transcription of downstream target gene.

During feather development, Widelitz *et al*, 1996 showed that downstream signalling components of the RAS-MAPK cascade are activated within forming feather primordia, indicating that the pathway may be involved in feather morphogenesis (Widelitz *et al.*, 1996). Lin *et al*, 2009 demonstrated that altering p-ERK activity (a downstream signalling component of the RAS-MAPK cascade), through gene silencing and the use of chemical inhibitors, altered the inductive capabilities of treated dorsal skin explants and altered feather morphologies (Lin *et al.*, 2009). p-ERK activities were modulated in skin explants with established feather primordia in the medial region of the skin, while lateral regions were still bare (morphogenetic wave had yet to induce feather formation). Inhibiting p-ERK activity at this stage, converted the round, discrete feather buds into fused stripes, in a dose dependent manner, while feather primordium induction in lateral regions were inhibited. At the highest dose of the p-ERK inhibitor, all pre-existing feather were lost and markers of feather primordium fate disappeared. The results indicate that the RAS-MAPK signalling cascade is required for feather primordium induction and stability. They further show that both recombinant FGF4 and FGF10 protein are capable of inducing p-ERK expression, and that FGF4 protein can stimulate cell migration and aggregation which is dependent on RAS-MAPK signalling (Lin *et al.*, 2009). The authors suggest, based on their data, that formation of dermal cell aggregates is dependent on FGF activation of the RAS-MAPK signalling pathway. However, the effects of FGF activation of the other three signalling cascade on feather morphogenesis have not been demonstrated as of yet.

FGFs are not the only proteins that can activate the RAS-MAPK pathway. Epidermal growth factors (EGFs) also signal through RTK related receptors which can also activate the RAS-MAPK signalling cascade (Oda *et al.*, 2005). The effects of EGF stimulation of the RAS-MAPK pathways, specifically, has not yet been examined. However, the effects of exogenous EGF application is restricted to the epidermis, inhibiting feather formation while promoting interbud fate, and did not show any

obvious effects on the underlying dermis (Atit *et al.*, 2003). When separated skin layers were treated individually with EGF and recombined with their untreated reciprocal skin layer, only the epidermis treated recombination displayed inhibition of feather primordia. The dermis treated recombinants were unaffected by the treatment and were comparable to control recombinants after culture. The data suggests that EGFs are not involved in the induction of dermal cell condensates, indicating that the effects of RAS-MAPK induced cell migration and aggregation is not the result of EGF signalling, but is instead FGF mediated.

1.3.6 BMP Signalling during Feather Primordium Induction

The BMPs are a family of secreted proteins, and along with members of the transforming growth factors (TGFβs) and activin families, are part of the TGFβ superfamily of proteins. As their name implies, the function of BMPs were primarily associated with bone and cartilage formation when first discovered (Urist, 1965; Wozney *et al.*, 1988), but have since been implicated in the formation of a variety of different organs such as the kidneys and eyes (Dudley *et al.*, 1995; Luo *et al.*, 1995). BMPs have also been implicated in the development of hair and teeth (Botchkarev, 2003; Wang *et al.*, 2012). Increasing BMP signalling activity through the genetic knockout of an antagonist of BMP protein function (*Noggin*), decreased hair follicle density (Botchkarev *et al.*, 2002). Decreased BMP activity in mice was achieved through the epidermal knockout of a gene which encodes a receptor of BMP protein ligands. These knockout mice displayed an increase in hair follicle density but also resulted in the arrest of tooth development (Andl *et al.*, 2004). The data suggests that BMP signalling may play an important role in the morphogenesis of epidermal appendages.

Currently, around twenty members of the BMP family have been identified which are further divided into distinct subgroups based on their gene homology, structure, and function (Reddi, 2005; Sánchez-Duffhues *et al.*, 2015). Of these, the functions of BMP2, BMP4, BMP7, and BMP12 or growth differentiating factor 7 (GDF7), have been implicated in feather morphogenesis (Harris *et al.*, 2004; Houghton *et al.*, 2005;

Jung *et al.*, 1998; Michon *et al.*, 2008; Mou *et al.*, 2011; Noramly and Morgan, 1998; Patel *et al.*, 1999).

BMP signalling is mediated through the binding of BMP ligands to a specific set of transmembrane serine/threonine kinase receptors, BMPRs (Massague, 2000; Reddi, 1998). There are two types of BMPRs, type I and type II, and signalling requires the dimerization of both type I and type II receptors in a single complex to mediate signalling. There are three type I receptors; activin A receptor type I (ACVRI) (or activin receptor-like kinase 2 (ALK2)), ALK3 (also known as BMPRIa) and ALK6 (or BMPRIb), and also three type II receptors; BMPRII, AVCRIIa and AVCRIIb. Each of these receptors have different binding affinities to various BMP ligands. Secreted BMP molecules exist as homodimeric or heterodimeric molecules, both forms are capable of binding type I and type II BMPRs to elicit a signalling response (Sampath *et al.*, 1990; Wang *et al.*, 1988). As mentioned above, BMPRs (both type I and type II) preferentially bind a different set of BMP proteins. This suggests that heterodimeric forms of BMP proteins would be more effective, compared to homodimeric forms of BMP proteins, in activating BMP signalling. Indeed, it was demonstrated that heterodimeric BMP proteins are more biologically active compared to homodimeric forms of BMP proteins (Israel *et al.*, 1996).

Intracellular signal transduction of TGFβ protein members such as BMPs is primarily mediated by a group of proteins known as SMADs, homologs of mothers against decapentaplegic (MAD) in *Drosophila* (Sekelsky *et al.*, 1995) and small body (SMA) in *Caenorhabditis elegans* (Savage et al., 1996). TGFβ protein family members are also able to induce SMAD independent pathways such as MAPK and JNK (Hartsough and Mulder, 1995; Hocevar *et al.*, 1999; Massague, 2003). SMADs are separated into three classes; receptor-regulated (R-SMADs), common-partner (co-SMADs) and inhibitory (I-SMADs). In BMP signalling, SMADs 1, 5, and 8 are the primary transducers of the pathway. Dimerisation of BMPRs, through the binding of a dimeric BMP ligand results in the phosphorylation of the kinase on the type I receptor by the type II receptor, thereby activating the type I receptor. The activated type I receptor can phosphorylate and activate the R-SMADs which recruits and forms a complex

with SMAD4 (a co-SMAD). Following the formation of the R-SMAD-co-SMAD complex, the complex translocates to the nucleus to activate the transcription of downstream signalling targets of BMP signalling (**Figure 22**).

BMPs have been implicated in the various stages of feather formation. Compared to the other molecules that have been reviewed thus far in the thesis, BMPs are generally associated with the inhibition of feather primordium formation (Houghton *et al.*, 2005; Jung *et al.*, 1998; Mou *et al.*, 2011; Noramly and Morgan, 1998; Patel *et al.*, 1999). As noted previously however, the function of BMPs may be context sensitive, promoting tract formation during the early stages, but inhibiting feather formation later (Noramly and Morgan, 1998; Scaal *et al.*, 2002).

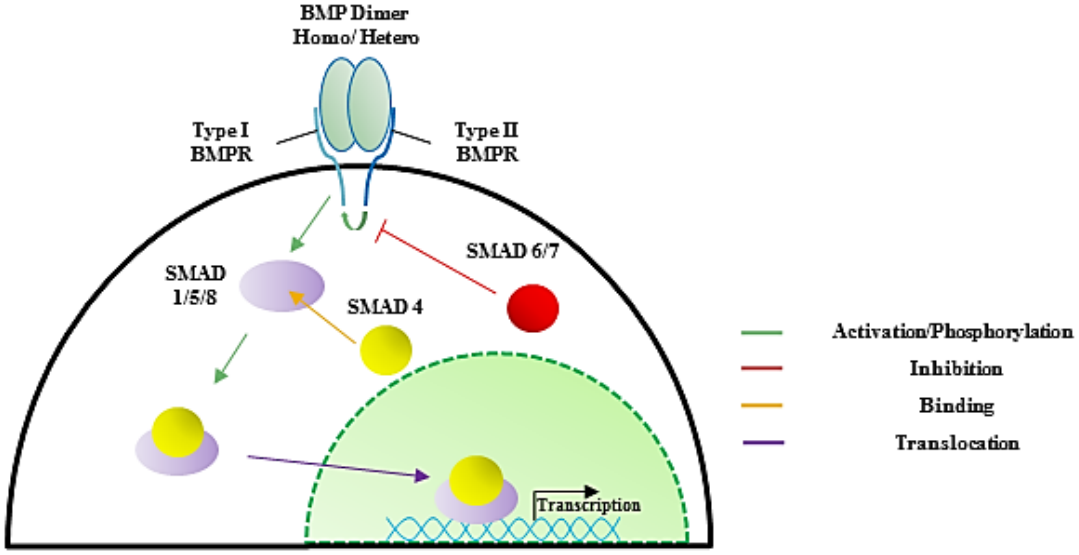

Figure 22. BMP signalling pathway. Stimulation of the BMP signalling pathway results in the phosphorylation of Type I BMPR by the Type II BMPR. This leads to the activation of SMAD 1/5/8 by phosphorylation. Activated SMAD 1/5/8 then forms a complex with SMAD 4 and translocated to the nuclease to induce transcription of target genes. Signalling is regulated by the inhibition of SMAD 1/5/8 phosphorylation by the inhibitory SMAD 6/7.

The expression patterns of the *BMPs* tested thus far vary from one *BMP* to another. *BMP2* shows a "restrictive mode "of pattern expression (Noramly and Morgan, 1998). It is expressed as a diffuse stripe within the presumptive feather tracts prior to feather primordium induction but is later restricted to the forming feather primordia. *BMP2* expression is initially observed within the epidermis prior to the formation of visible feather primordia. During the induction of dermal condensate formation, *BMP2* expression is detected in both the epidermal placode and in the underlying dermal condensate (Noramly and Morgan, 1998). *BMP4* expression coincides with the formation of dermal cell condensates but is only detected within the condensates themselves and is not detected in the overlying epidermis ("*de novo*" mode pattern of expression) (Jung *et al.*, 1998; Noramly and Morgan, 1998). The expression pattern of *BMP7* is very similar to that of *BMP2* during feather primordium induction (Harris *et al.*, 2004; Patel *et al.*, 1999). *BMP7* is also expressed in a "restrictive mode", but shows an initially broader, diffuse expression across the presumptive feather tracts compared to *BMP2*. Like *BMP2*, *BMP7* is initially expressed within the epidermis, but is later restricted to both the epidermis and dermis of the forming feather primordia. The expression pattern of *BMP12* is less clear. Mou *et al*, 2011 showed that *BMP12* is expressed in the skin of developing embryonic chickens (Mou *et al.*, 2011). *BMP12* appears to be expressed in a "restrictive mode" pattern of expression, across the entire presumptive feather tracts and later restricted to the feather primordia, but the signal is weak. The skin layer expressing *BMP12* during feather primordium induction is unknown.

The effects of BMP2 on feather induction were assessed through perturbation experiments of *BMP2* expression using RCAS, and also application of exogenous BMP2 protein through bead-mediated delivery (Jung *et al.*, 1998; Noramly and Morgan, 1998). Overexpression of *BMP2* in infected skin regions prevented the induction of feather primordium formation (Noramly and Morgan, 1998). The addition of recombinant BMP2 coated beads to HH 29-32 dorsal skin explants resulted in the formation of a zone of inhibition, an area of skin incapable of feather primordium induction, around the bead (Jung *et al.*, 1998). Michon *et al*, 2008 showed that

recombinant BMP2 proteins can inhibit cell migration of dissociated dermal fibroblasts in culture (Michon *et al.*, 2008). They suggest that BMP2 and BMP4 (which are in the same family subgroup), mediate their inhibitory response by preventing cell migration, which is required for the formation of dermal cell aggregates. The data indicates that *BMP2* functions to inhibit feather fate during feather primordium induction. However, when exogenous BMP2 protein was applied to earlier staged embryos (HH 17-23), the treatment caused the formation of ectopic feather bearing tracts (Scaal *et al.*, 2002), suggesting that BMP2 can also function to promote feather fate, indirectly through the induction of dense dermis formation, and that BMP2 may function differently based on the developmental context.

BMP4 is also primarily shown to inhibit the induction of feather primordia (Houghton *et al.*, 2005; Jung *et al.*, 1998; Mou *et al.*, 2011; Noramly and Morgan, 1998). Increasing BMP4 signalling through the use of RCAS and application of recombinant BMP4 protein prevented the formation of feather primordia in *in ovo* and *ex ovo* studies. It was suggested that the inhibitory effects of BMP4 were mediated through its ability to negatively regulate the expression of both FGF4 and FGFR1 (Jung *et al.*, 1998; Noramly and Morgan, 1998). As described in section **1.3.5**, blocking FGF signalling inhibited cell migration and the formation of dermal cell aggregates during feather primordium induction (Lin *et al.*, 2009). However, Michon *et al*, 2008 suggests that BMP2 (and possibly BMP4) may be inhibiting cell migration, as demonstrated by the inhibitory effects of BMP2 protein on BMP7 induced cell migration of disassociated fibroblasts (Michon *et al.*, 2008).

The effects of BMP7 on feather primordium formation during their induction is not as simply understood as the other BMPs. The current studies conflict with one another on whether BMP7 promotes or inhibits feather primordium fate (Harris *et al.*, 2004; Michon *et al.*, 2008; Patel *et al.*, 1999). Local application of BMP7, through bead-mediated delivery, to HH 29+ dorsal skin explants led to the formation of a zone of inhibition around the source of BMP7, similar to the effects observed with treatments of BMP2 or BMP4 protein (Patel *et al.*, 1999). Conversely, Harris *et al*, 2004, showed that BMP7 is required for the induction of feather primordium formation in femoral

skin explants through the use of a BMP7 blocking antibody (Harris *et al.*, 2004). Antibody treated explants failed to induce the formation of feather primordia, as detected by *BMP7* expression. In a third study, performed by Michon *et al,* 2008, when BMP7 protein coated beads were applied to feather forming dorsal skin explants, cell aggregation around the bead was observed (Michon *et al.*, 2008). They also show that BMP7 coated beads were capable of inducing cell migration and aggregation of dissociated dermal cell fibroblasts around the bead. They suggest that BMP7 is required for the induction of dermal cell condensates during feather primordium induction.

Increased expression of *BMP12,* is associated with the naked neck trait in affected individuals (see section **1.3.1**). Application of recombinant BMP12 protein to chicken skin explants, containing the neck and dorsal regions, results in the selective loss of feather induction in the neck while the dorsal regions remain largely unaffected, supporting the idea that the naked neck trait is the result of increased *BMP12* activity (Mou *et al.*, 2011). It has been demonstrated that the differing sensitivities to BMP12 activity, between the neck and dorsal regions, is the result of the selective production of retinoic acid (RA) in the neck which sensitises the neck skin to BMP signalling. Indeed, treatment of explants with both BMP12 and an inhibitor of RA synthesis (citral) (Connor, 1988), abolished the observed differences in BMP signalling sensitivities between the neck and dorsal regions. The increased expression of *BMP12* is the associated with the insertion of a non-coding region between *WNT11* and *UV radiation resistance-associated gene* (*UVRAG*) from chromosome 1, downstream of the *BMP12* gene on chromosome. How the insertion increases the expression of *BMP12* remains speculative, but it is possible that the *BMP12* gene gained enhancers from the *WNT11* gene as a result of the insertion, or the insertion may have abolished the activity of inhibitory elements of *BMP12* expression. How RA potentiates BMP signalling to inhibit feather primordium formation is currently unknown.

Under experimental conditions, the effects of BMPs were shown to mainly inhibit the formation of feather primordia, but what is the function of BMPs *in ovo*? Noramly and Morgan, 1998 (Noramly and Morgan, 1998), suggested that the actual function of

BMPs during feather primordium formation is to regulate the spacing between forming feather primordia through the process of lateral inhibition. In the simplest terms, lateral inhibition is a process whereby the activity of a cell inhibits the activity of other cells within the immediate vicinity. When BMP signalling was inhibited through RCAS-mediated expression of *Noggin* or via the application of a chemical inhibitor of BMP signalling, the forming feather primordia developed fusions between neighbouring primordia (Mou *et al.*, 2011; Noramly and Morgan, 1998). Increasing BMP signalling in a local area, via bead-mediated delivery of BMP proteins, on the other hand, resulted in the formation of a zone of inhibition (Jung *et al.*, 1998; Patel *et al.*, 1999). The results suggests that BMP-mediated lateral inhibition may regulate the spacing between forming feather buds and prevent fusion between neighbouring primordia.

1.3.7 EDA/EDAR Signalling during Feather Primordium Induction

EDA/EDAR signalling is required for the formation of a diverse range of epithelial appendages in a variety of species. The components of EDA/EDAR signalling consists of the EDA ligand, its receptor EDAR, and the cytoplasmic adapter molecule EDAR associated death domain (EDARADD). Loss of function in any of the components of the EDA/EDAR signalling pathway results in similar losses of epidermally derived structures in fish, and several mammalian species such as mice, rats, dogs, and humans (Atukorala *et al.*, 2010; Casal *et al.*, 2005; Charles *et al.*, 2009; Drogemuller *et al.*, 2001; Gaide and Schneider, 2003; Harris *et al.*, 2008; Headon and Overbeek, 1999; Kere *et al.*, 1996; Kondo *et al.*, 2001; Kuramoto *et al.*, 2011; Laurikkala *et al.*, 2002; Thesleff and Mikkola, 2002).

In humans, the loss of EDA/EDAR signalling causes a condition known as hypohidrotic/anhidrotic ectodermal dysplasia (HED), characterised by the reduced/complete loss or abnormal formation of hair, teeth, and sweat glands (Headon and Overbeek, 1999; Headon *et al.*, 2001; Kere *et al.*, 1996). HED-like phenotypes observed in other mammalian species have been attributed to the loss of function mutations in components of the EDA/EDAR signalling pathway (Casal *et al.*, 2005; Drogemuller *et al.*, 2001; Kuramoto *et al.*, 2011). In fish affected by the loss of

EDA/EDAR signalling, scale and teeth formation is reduced or lost during embryonic development (Atukorala *et al.*, 2010; Harris *et al.*, 2008; Kondo *et al.*, 2001). The similar phenotypes observed across the vertebrate species, as a direct result of the loss of EDA/EDAR signalling, suggests an evolutionarily conserved role of the pathway in the induction of epithelial appendages in animals. However, loss of function mutations in avian models have not yet been observed, suggesting that mutations within the EDA/EDAR signalling pathway in Aves may be lethal, or that the pathway has sufficient redundancy to avoid effects of single gene mutations, or that it is not involved in feather development.

EDA is a member of the tumour necrosis factor (TNF) superfamily of proteins (Headon and Overbeek, 1999; Mikkola *et al.*, 1999). Proteins from the TNF superfamily are normally involved in the activation of immunological responses, such as inflammation and apoptosis (Gaur and Aggarwal, 2003). However, EDA is unusual in the fact that it functions specifically in the formation of epithelial appendages. There are two functional variants of the EDA proteins, EDA-1 and EDA-2, which are the result of alternative splicing of the *EDA* gene (Bayes *et al.*, 1998). The two variants only differ by two amino acids within the TNF domain of the protein which impacts their receptor specificity. EDA-1 protein (hereon referred to as EDA), binds to EDAR, while EDA-2 protein binds to XEDAR (Yan *et al.*, 2000).

EDA protein itself is initially bound to the membranes of cell surfaces and requires proteolytic cleavage in order to function as a signalling factor (Schneider *et al.*, 2001). The overall outcome of stimulation of the EDA/EDAR signalling pathway is the activation and translocation of nuclear factor kappa-light-chain-enhancer of activated B-cells (NF-κB) to the nucleus to regulate the transcription of downstream signalling targets (**Figure 23**). When EDA/EDAR signalling is not active, NF-κB is tightly bound to inhibitors of κB (IκBs), which retain the NF-κB proteins within the cytoplasm of the cell, preventing nuclear translocation of NF-κB (**Figure 23a**). Signalling is activated through the interaction between the EDA ligand and its associated TNF receptor, EDAR, which trimerises the EDAR monomers. This stimulates the recruitment of EDARADD via the death domains of EDAR and EDARADD (Headon

and Overbeek, 1999; Tucker *et al.*, 2000). Activation of EDARADD leads to the recruitment and formation of a protein complex consisting of TNF receptor-associated factor (TRAF6), TGFβ-activated kinase 1 binding protein (TAB2) and TGFβ-activated kinase 1 (TAK1) (Morlon *et al.*, 2005). The protein complex recruits and activates another protein complex, the inhibitor of κB kinase (IKK) complex. The IKK complex is a multimeric complex consisting of two catalytic subunits, IKKα and IKKβ, and a regulatory subunit, NF-κB essential modulator (NEMO or also known as IKKγ) (Israel, 2000; Rothwarf *et al.*, 1998). The activated IKK complex phosphorylates the IκB which targets IκB for degradation, which releases the NF-κB protein, allowing it to translocate to the nucleus to exert its signalling function (Doffinger *et al.*, 2001) (**Figure 23b**).

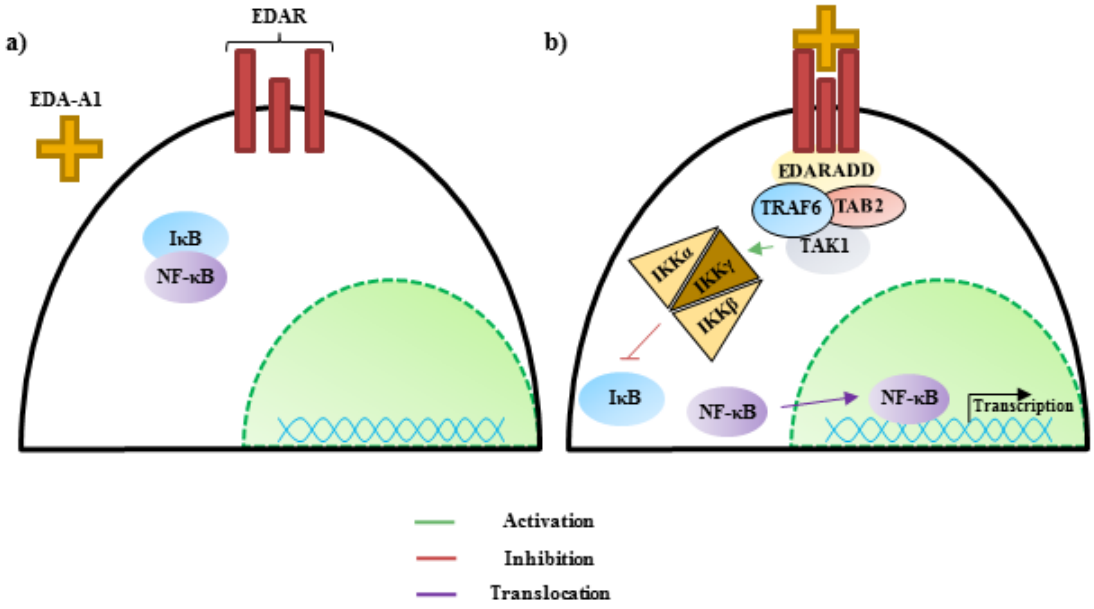

Figure 23. EDAR signalling pathway. a) When not stimulated, the effector protein of EDAR signalling, NF-κB, is prevented from translocating to the nucleus by IκB. **b)** Binding of an EDA ligand to the receptor, EDAR, results in the recruitment and formation of a protein complex consisting of EDARADD, TRAF6, TAB2 and TAK1. The protein complex then activates the IKK complex which inhibits IκB activity. Free of IκB, the NF-κB protein translocates to the nucleus to mediate the transcription of target genes.

Compared to the other signalling pathways described so far, the involvement of the EDA/EDAR signalling pathway in feather morphogenesis is relatively understudied. Inhibition of NF-κB signalling, through the use of a chemical inhibitor, BAY11-7082 (Pierce *et al.*, 1997) on developing dorsal skin explants resulted in the loss of visible feather primordium formation, indicating that EDA/EDAR signalling pathway may be critical for feather induction during embryogenesis (Drew, 2006).

During feather primordium induction, *EDA* and *EDAR* are both initially expressed within the epidermis of the feather forming tract (Drew *et al.*, 2007; Houghton *et al.*, 2005). *EDAR* displays a "restrictive mode" of pattern expression and is initially expressed diffusely across the presumptive feather tracts prior to the formation of feather primordia. During primordium formation, *EDAR* expression is focalised to within the epidermis of the feather primordia and excluded from interbud regions. The expression of *EDAR* completely overlaps the *β-Catenin* expression pattern and *EDAR* has been shown to be a downstream target of WNT/β-Catenin signalling pathway (Houghton *et al.*, 2005). *EDA* expression, on the other hand, is more complex. Unlike *EDAR, EDA* expression is not regulated by WNT/β-Catenin signalling in chicken and, also, *EDA* does not initially display diffuse expression across the feather tract, but is restricted to skin regions undergoing feather formation. When feather primordia are established, *EDA* expression is restricted to the dermis of the interbud regions and epidermal expression of *EDA* can no longer be detected (Houghton *et al.*, 2005).

Drew *et al*, 2007 showed that EDA/EDAR signalling is required for the initiation of feather primordium formation through the use of RCAS-mediated delivery of overexpression constructs of dominant negative (DN) and constitutively active (CA) forms of the EDAR receptor (Drew *et al.*, 2007). Regions of feather tracts overexpressing DN-*EDAR* showed loss of feather formation in affected skin regions, whereas, CA-*EDAR* was able to induce the formation of ectopic feather primordia in skin regions outwith the endogenous feather primordium forming zone. The findings show that EDA/EDAR signalling alone is sufficient in inducing the formation of feather primordia and is required for their induction.

How EDA/EDAR signalling is able to induce ectopic feather primordia is unknown. In mouse tooth development, stimulation of the EDA/EDAR signalling pathway stimulates *FGF20* expression (Haara *et al.*, 2012). As mentioned in section **1.3.5**, *FGF20* is required for feather induction (Wells *et al.*, 2012). However, a link between *FGF* expression and EDA/EDAR signalling activity has not yet been observed in avian models during feather morphogenesis.

1.3.8 Role of Cell Adhesion Molecules in Feather Primordium Induction

Cell adhesion molecules (CAMs), are a group of cell surface proteins involved in cell to cell adhesion or cell to ECM adhesion. CAM proteins belong one of four families; the immunoglobulin superfamily (IgSF) CAMs, integrins, cadherins, and selectins. The four families can be further classified into two distinct groups based on their dependence or independence from Ca^{2+}. IgSF function independently from Ca^{2+} while integrins, cadherins, and selectins all require Ca^{2+} to function (Brackenbury *et al.*, 1981). The primary role of CAMs are to promote the binding of cells to neighbouring cells or to their immediate surroundings and the regulation of their expression is critical for morphogenetic processes during embryogenesis, such as chick somitogenesis (Glazier *et al.*, 2008; Linask *et al.*, 1998). The CAMs mediate adhesion through their extracellular domains which can bind to other CAMs of the type (homophilic), or other types of CAMs or ECM (heterophilic).

In the study of feather primordium induction, the role and function of CAMs are relatively understudied, compared to those of signalling molecules. Currently, only the functions of neural cell adhesion molecules (N-CAM) and integrins have been examined experimentally (Jiang and Chuong, 1992; Michon *et al.*, 2007). N-CAM belongs to the IgSF family and function independently of Ca^{2+} while integrins rely on Ca^{2+} for adhesion.

The expression pattern of N-CAM during the process of feather primordium induction in the dorsal tract of chicken embryos of various developmental stages was examined in previous studies (Chuong and Edelman, 1985; Jiang *et al.*, 1999). Prior to primordium induction, N-CAM is expressed throughout the presumptive dorsal tract

of HH 29 embryos. During the wave-like propagation of feather primordium formation, N-CAM expression follows a "restrictive mode" of pattern expression. The initially homogenous expression of N-CAM is gradually restricted to the developing feather primordia while excluded from the interbud domains. Expression of N-CAM is localised to the dermis, and during feather primordium formation, expression is restricted to the dermal cell condensate. The early appearance of N-CAM prior to the visible formation of feather primordia, and its localised expression to within the dermal cell condensates, suggested that N-CAMs may be required for the early stages of feather primordium development. From these observations, it was proposed that N-CAMs may be involved in the stabilisation of dermal cell aggregates during dermal cell condensate formation (Jiang *et al.*, 1999). However, in previous studies, inhibition of N-CAM function through the use of anti-N-CAM antibodies, during feather primordium formation did not prevent their formation (Jiang and Chuong, 1992). Feather primordia were able to form and differentiate in to feather buds in the antibody treated explants, but the structure and size of the feather buds varied greatly. Also, the hexagonality of the feather arrangement was disrupted by the treatment. The result suggests that N-CAM may be required for the even segregation of dermal cells during dermal condensate formation.

Integrins exist as obligate heterodimers, comprising of one α and one β subunit (Huttenlocher *et al.*, 1995). The expression of both the integrin-α and integrin-β subunits were shown to be localised to the feather primordium domain during the development of the primordia (Jiang and Chuong, 1992; Michon *et al.*, 2008). The expression pattern of the two subunits prior to primordium induction, however, have not been shown. In transverse sections of developing dorsal skin explants, it was revealed that integrin-β expression is localised to the basement membrane, between the epithelial placode and dermal cell condensate specifically (Jiang and Chuong, 1992). The localisation of integrin- α expression has currently not been examined. Perturbation experiments modulating integrin adhesion between cells during feather primordium development demonstrated that integrins may be required for the stabilisation of dermal condensates (Jiang and Chuong, 1992; Michon *et al.*, 2007).

Under the *ex vivo* culture conditions utilised by Michon *et al,* 2007, existing feather primordia, on freshly dissected dorsal skin explants, disappear after eight hours in culture but reappear later after a total of twelve hours in culture (Michon *et al.*, 2007). Treatment of the explants with reagents that either increased intracellular concentrations of Ca^{2+} or converted the integrins to a high-affinity state, ionomycin or Mn^{2+} respectively, prevented the initial disappearance of existing primordia during culture (Michon *et al.*, 2007). Inhibition of integrin activity on HH 33 skin explants, through the use of an anti-integrin-β antibody, lead to the formation of underdeveloped dermal cell condensates (Jiang and Chuong, 1992). The initial observation suggests that integrin activity is required for the formation of dermal cell condensates, however, the skin regions displaying abnormal primordium formation also show separation of the epidermal and dermal cell layers. This suggests that the observed effect of inhibition of integrin activity is the result of the loss of epidermal-dermal interactions, due to the detachment of the epidermis from the dermis, rather than, a direct effect on dermal cell condensate formation (Jiang and Chuong, 1992).

Based on current studies, the function of CAMs during feather primordium induction and formation is unclear. Perturbation experiments, examining the two members of the CAM family, did not establish a direct correlation of the CAMs with stability of dermal cell condensates. The effect of stabilisation of dermal cell condensates during *ex vivo* culture, through the use of ionomycin, suggests that Ca^{2+} dependent CAMs are required for primordium formation (Michon *et al.*, 2007). However, as mentioned above, there are three families of CAMs that are dependent on Ca^{2+} for adhesion, and treatment of explants with ionomycin may stimulate any of the Ca^{2+} dependent CAMs. Further studies examining the functions of other CAM family members and how they are regulated during feather primordium are required to determine the role of CAMs in feather primordium development.

1.4 Generation of Periodic Patterns in Biology

The spatiotemporal patterning of the feather tracts during embryonic development occurs on a 2 dimensional field, producing a periodically arranged array of feather primordia. Over the last decade, many signalling molecules that govern feather primordium formation have been identified. Various molecules have been demonstrated to function as promoters or inhibitors of feather primordium fate, but how these molecules interact, and how they are regulated during the formation of a periodically arranged array of feather primordia, is currently not well understood.

As described in section **1.2.3**, feather follicles in adult chickens are arranged in a high fidelity hexagonal pattern, termed the micropattern (Homberger and de Silva, 2000; Lucas and Stettenheim, 1972; Sengel, 1975; Stettenheim, 2000). This arrangement of feather follicles arises spontaneously from a homogenous field of cells and self-organises during the development of the embryonic chicken. The development of the feather micropattern in chickens is one of the most well studied examples of periodic pattern formation in biological systems.

From the development of left-right body asymmetry to fur/feather pigment patterns, periodic patterning is a fundamental organisation process which occurs during embryogenesis and is essential for the development of a fully functioning organism. The development of most organisms begins with a single fertilised egg from which a vast array of various cells types are produced, each containing the same basic genetic blueprint. One of the fundamental questions in developmental biology is how these cells, using the same genetic tool kit, are able to self-organise and arrange themselves to give rise to distinct structures that constitute the working tissues and organs. Micropatterning of the feather follicles in avian skin has been a major model for the study of biological periodic patterning due to the accessibility and amenability to experimental manipulation of the developing chicken skin.

Many mathematical models have been developed to explain the process of biological pattern formation such as the molecular or mechanical based models. All these models are capable of reproducing the various patterns observed in biological systems but do

so through different means. In this section, I will review the major models which have been employed to understand the mechanisms underlying feather micropattern formation.

1.4.1 Turing's Reaction-Diffusion Model

In 1952, Alan Turing proposed a relatively simple and elegant model which described how interactions between two differentially diffusing chemical substances can generate a periodic pattern from an initially homogenous state in a biological system, called reaction-diffusion (Turing, 1952). The chemical substances, termed "morphogens" govern the patterning process through their effects on cell behaviours during morphogenesis such as migration, proliferation, and differentiation. In Turing's model, if diffusion rates were the same, two interacting morphogens would exist in a stable equilibrium within the system and the patterning field would remain homogenous. If diffusion rates differed between morphogen A and morphogen B, stochastic fluctuations within the system could be amplified to generate spatial patterns of regions displaying high morphogen concentrations separated by regions of low morphogen concentrations. This molecular pattern can then be utilised as a blueprint, from which cells in a tissue can acquire positional information cues to generate a structural pattern from a previously homogenous state. As such, in this model, cells within a tissue are dependent on the formation of a molecular pre-pattern prior to cellular reorganisation. However, the molecular pattern forms from a completely self-organisation process and its formation is completely independent of a pre-patterning system **(Figure 24)**.

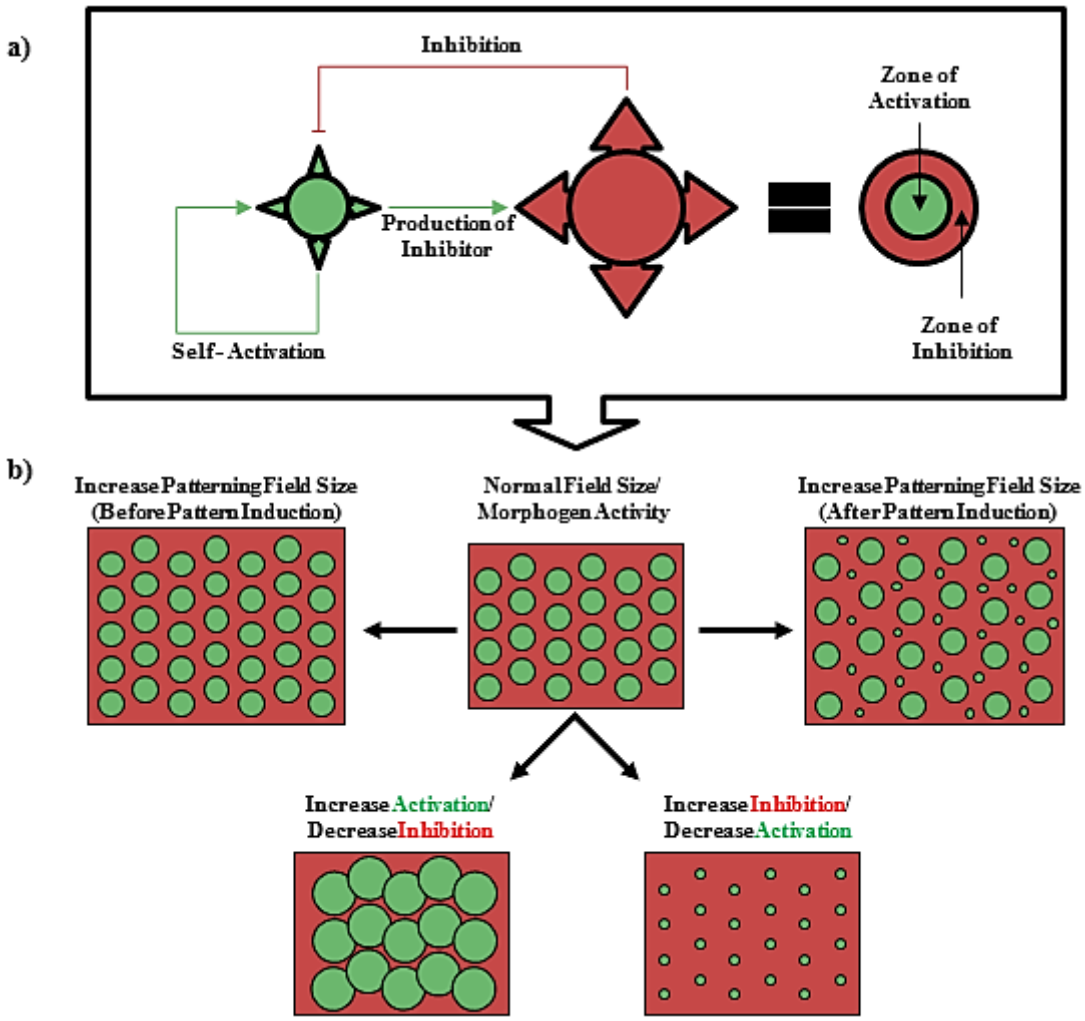

Figure 24. Reaction-diffusion Model. a) In reaction-diffusion based models, the short-range activator promotes its own production and the production of its own long-inhibitor. Due to differences in diffusion rates of the activators and inhibitors (activators generally cannot diffuse as far as inhibitors), two distinct zones are formed locally, a zone of activation and a zone of inhibition. The process is repeated multiple times across a patterning field resulting in the formation of a periodic pattern. **b)** Patterns produced by reaction-diffusion based models are subject to modulation. Depending on how and when the patterning is modulated, different patterns may be produced.

The model is capable of generating periodic patterns *in silico*, which are analogous to those observed in biological systems. However, patterns generated by a pure reaction-diffusion system, as described by Turing, are in a state of unstable equilibrium, as such, minute changes to the system or differing initial conditions would generate slightly different patterns. The model is likely to be an oversimplification of real biological systems. The reaction-diffusion model ignores the cellular components of biological systems, and how they can affect the diffusion of the morphogens is not taken into account. Due to the irreproducibility of patterns, the over simplification of the model, and the lack of molecular evidence at the time of publication, the reaction-diffusion model for biological pattern formation was not widely accepted by the scientific biological community for a time (Bard and Lauder, 1974; Bunow *et al.*, 1980).

Turing's model was later refined by Gierer and Meinhardt and become capable of generating reproducible and stable periodic patterns, based on a somewhat different activator-inhibitor or substrate-depletion model (Gierer and Meinhardt, 1972). The basis of the model is identical to the one proposed by Turing, differentially diffusing morphogens underlie the pattern generating properties of the system. The Gierer and Meinhardt models proposes, however, that the two morphogens are separated into two groups; activators, which promote the formation of periodic structures, and inhibitors, which inhibit their formation. Activators have a shorter active range compared to inhibitors (possibly due to either shorter diffusion or higher of depletion rates), and stimulate the production of more activators (local self-activation) and the production of its own inhibitor. Due to the wider active range of the inhibitor, local concentrations of inhibitor never reach as high as the short range activator (due to a wider dispersal of the inhibitor compared to the locally active activator). This difference results in the formation of spatial patterns of local regions of high activation/low inhibition separated by regions of low activation/high inhibition. The stability of the generated pattern is the result of the autocatalytic property of the activators. Once positioned the activator would self-sustain itself through the production of more activator in the local area. However, if the patterning field is disturbed or changed during molecular pattern formation, the subsequently formed pattern would reorganise itself in accordance to

the changes to the patterning field. Although the activator-inhibitor model is capable of producing stable patterns, the model also omits the cellular components of biological systems and as such may not completely explain biological pattern formation alone.

With the relatively recent discoveries of a wide range of proteins which represent candidates for the functions described by the reaction-diffusion/ activator-inhibitor models, the models have become more widely accepted amongst developmental biologists studying biological pattern formation. The models have been used to explain the formation of biological patterns such as pigment patterns of fish and feathers, left-right body asymmetry and digit patterning (Asai *et al.*, 1999; Chen and Schier, 2002; Kondo and Asal, 1995; Nakamura *et al.*, 2006; Sheth *et al.*, 2012).

The reaction-diffusion/activator inhibitor model of pattern formation has been suggested to be the mechanism that is utilised in the formation of the feather micropattern (Jiang *et al.*, 1999; Jiang *et al.*, 2004; Michon *et al.*, 2008; Mou *et al.*, 2011; Noramly and Morgan, 1998). As described in section **1.3**, many molecules have been identified which function to promote or inhibit feather fate (activators and inhibitors respectively). Generally, WNTs and FGFs have been proposed to function as potential activators, whereas, BMPs have been shown to function mainly as inhibitors of feather fate based on experimental studies (reviewed by (Chen *et al.*, 2015)). Further studies showed that FGFs and BMPs were capable regulating each other's expression, forming possible activator-inhibitor pairs. FGF2 and FGF4 were shown to be capable of inducing the expression of *BMP2* and *BMP4* respectively (Jung *et al.*, 1998; Song *et al.*, 2004). On the other hand, BMP2 and BMP4 have been proposed to inhibit FGF signalling through their inhibitory effects on *FGFR1*, *FGFR2*, and *FGF4* expression (Jung *et al.*, 1998; Noramly and Morgan, 1998). The genes of the activators and inhibitors are both expressed within the forming feather primordia, rather than being expressed in separate distinct regions i.e. activators within the primordia and inhibitors in the interbud domains. This finding that local production of the activator and the inhibitor within the forming feather primordia is similar to the properties of the molecules described in reaction-diffusion based models. Molecular

perturbations studies have demonstrated that the range of feather primordium patterns generated through experimental manipulation can be explained using reaction-diffusion based modelling (Jiang *et al.*, 1999; Lin *et al.*, 2009; Michon *et al.*, 2008; Mou *et al.*, 2011; Noramly and Morgan, 1998). However, although possible activator-inhibitors pairs that may function in a reaction diffusion-like manner during feather primordium induction have been identified, an activator which self-activates (promotes its own production) has yet to be discovered. Also, whether the molecular activators and inhibitors show differential diffusivity *in vivo* and whether cellular interactions are involved in the generation of feather primordia has yet to be established.

1.4.2 Wolpert's Positional Information Model

One of the most well-known biological pattern generating models was proposed by Lewis Wolpert in the late 60's, commonly known as the French flag model (Wolpert, 1969). Although diffusion of a morphogen is the basis of this model, it differs significantly from reaction-diffusion based models described above. In the French flag model, a morphogen source is generated in one part of the developing structure. The morphogen diffuses from the initial site, spreading across the structure, forming a concentration gradient from high to low. Cells within the different regions of the structure would therefore be exposed to various concentrations of the morphogen which the cells use to determine their position within the structure and differentiate accordingly. In the French flag analogy, cells closest to the morphogen source, (and thus exposed to the highest concentration), develop into blue cells, cells exposed to intermediate concentrations of the morphogen would develop into white cells while cells farthest from the source would develop into red cells. In the simplest form, the French flag model only requires one morphogen gradient, although various other morphogen gradients, diffusing in different directions, can also be included. This would expose different cells throughout a structure to a cocktail of various combinations and concentration of morphogens which could theoretically generate a myriad of different cell types and patterns in a system. **(Figure 25)**

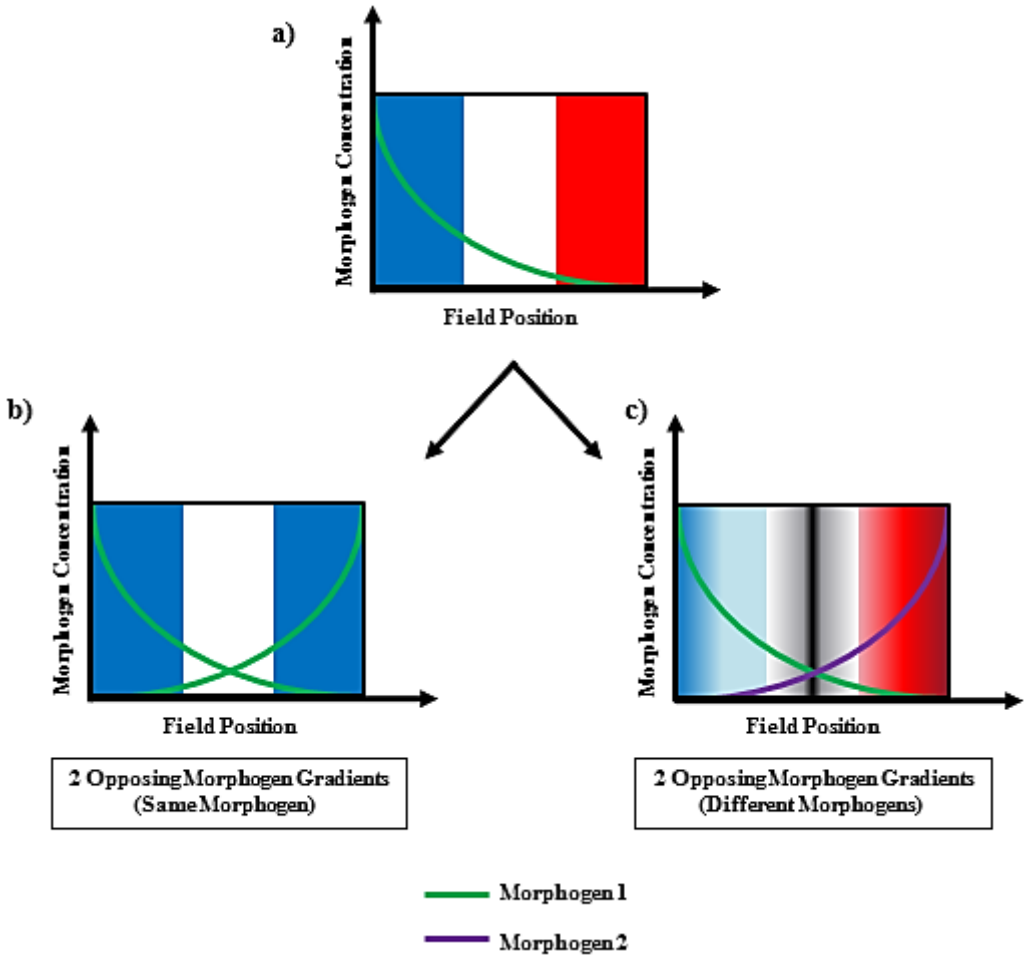

Figure 25. French flag model. a) A morphogen gradient dictates the identity of the cells based on the concentration of morphogens the cells are exposed to during development. In the basic French flag model, high morphogen concentration cause the formation of blue cells, medium concentrations, white cells, and low concentrations, red cells. **b)** Placing an opposing gradient of the same morphogen modifies the formed pattern. Due to the exposure of high concentration of the morphogen at both ends of the field, blue cells are formed, while in the middle white cells are still formed. **c)** If the opposing gradient is a different morphogen, then cells will differentiate based on the specific combination and concentration of morphogens exposed, resulting in a more varied pattern.

In real world biological systems, the model has most notably been applied to explain *Drosophila* embryogenesis. The bicoid protein in *Drosophila* regulates the anterior-posterior axis of the embryo by dictating the position of the head in the developing embryo (Driever and Nusslein-Volhard, 1988; Driever *et al.*, 1990). On the anterior end of developing *Drosophila* embryos, bicoid is produced which diffuses across the embryo, producing a morphogen gradient of high to low concentration, in an anterior-posterior direction. Bicoid is a transcription factor which regulates the activation of different sets of genes in cells, depending on the concentration of bicoid protein the cells are exposed to. In the simplest model, anterior regions exposed to the highest concentrations of bicoid are converted to head and thoracic segments while on the posterior end, where bicoid concentrations are lowest, the tail segment is formed. When bicoid protein was ectopically produced in the posterior end of the embryo, a dicephalic (two-headed) *Drosophila* embryo was produced, demonstrating that bicoid regulates the formation of the anterior structures of the *Drosophila* embryo (Driever *et al.*, 1990).

Wolpert's model can potentially be applied to the formation of the feather micropattern. The as of yet uncharacterised, morphogenetic wave which regulates the spatiotemporal sequence of primordium formation may be a morphogen gradient which originates from the midline. Based on the concentrations of the morphogen the cells are exposed to, the morphogen can function as a positional cue which dictate the timing and placement of individual feather primordia (Jiang *et al.*, 2004). However, patterns generated by the Wolpert model predetermines the position of each unit of the pattern via the morphogen gradient. It has been shown that in *ex vivo* chicken skin cultures, altering the position of the initial primary row of feather primordia, through experimental modulation, results in the complete reorganisation of subsequently formed primordia, indicating that the position of each primordium is not predetermined (Novel, 1973b). Subsequent studies have also demonstrated the self-organisational properties of the chicken skin through other methods such as reconstituted mesenchymal skin explant cultures (Jiang *et al.*, 1999). These studies suggest that the

Wolpert model of pattern formation is insufficient to describe the basis of feather primordium micropattern formation.

1.4.3 Oster's Mechanical Model

The models described thus far have primarily focused on how chemicals/morphogens can drive cellular organisation, based on positional cues provided by the molecular pre-pattern. However, these models are dependent on the initial formation of a molecular pre-pattern to generate the final structure and also omit cellular interactions that may affect the patterning process. In a model proposed by Oster *et al*, 1983 (Oster *et al.*, 1983), dermal cells in the ECM of developing structures alone can spontaneously induce the formation of periodically arranged cell aggregates without the need of chemical cues. Dermal cells form attachments to the ECM and when a cell migrates, it can generate traction forces that may distort the surrounding ECM. Distortions of the ECM may also come about from an increase in dermal cell density through cell proliferation, which may create strain on the surrounding ECM. In the initial state, the structure of the ECM is homogenous. The distortion of the ECM caused by cellular processes creates a gradient of high/low ECM concentration within the local area. Cells are presumed to preferentially bind to higher concentrations of ECM, thus, when the cells cause local distortions of the ECM (increasing ECM concentration locally), surrounding cells will migrate towards the area of increased ECM concentration. As more cells move, the ECM is further distorted, which attracts more cells to the local area from the surrounding region, resulting in the formation of a dermal cell aggregate locally **(Figure 26).**

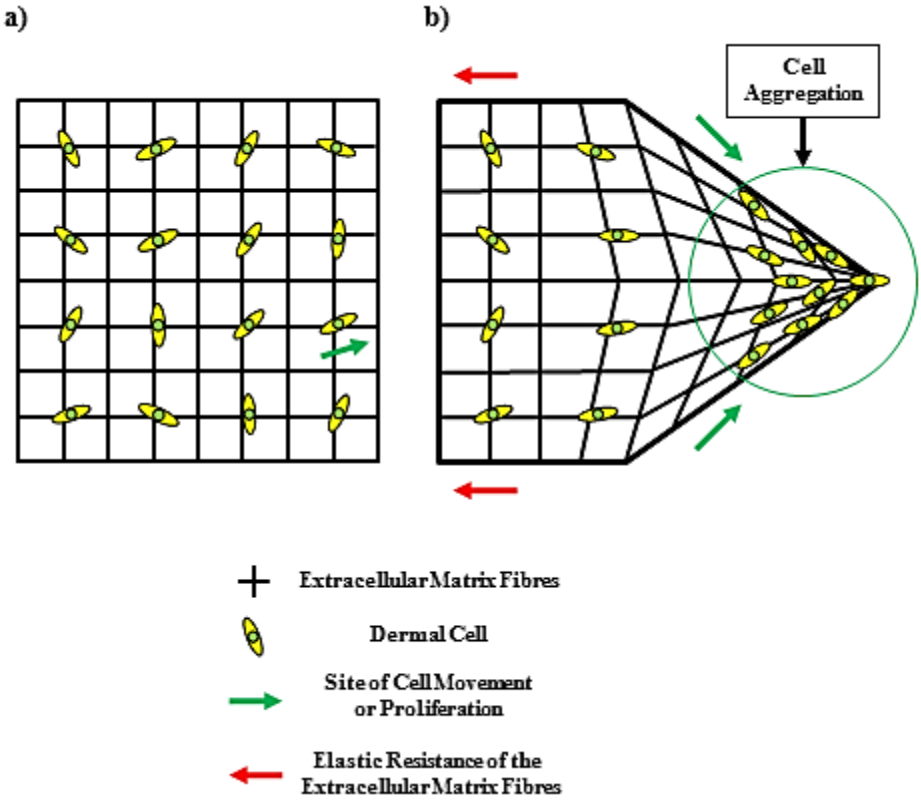

Figure 26. Mechanical Model. a) Dermal cells within an undistorted ECM prior to cell movement or proliferation. **b)** Distortion of the ECM by migrating or proliferating cells results in the formation of an ECM gradient. Dermal cells preferentially bind to higher concentrations of ECM and will migrate to regions of higher ECM concentrations. Elastic resistance of the ECM prevents the distortion of the ECM in regions outwith the site of cell aggregation.

Intuitively, one would predict from the model the formation of a single large dermal cell aggregate. However the model assumes the ECM is relatively elastic and, to some degree, can passively resist the stretching/distortion of the ECM caused by aggregating cells. In simple terms, the strain on the ECM caused by migrating cells is highest at the centre of the aggregating cell condensate which overcomes the elastic resistance of the ECM, thereby distorting it, forming an ECM concentration gradient. At a distance from the condensate centre, there would be fewer cells and so the traction forces generated in these regions would not overcome the elastic resistance of the

ECM, thereby regaining/ maintaining a homogenous ECM state outside of the forming cell condensate. In regions beyond the homogenous ECM, dermal cell concentrations are higher and thus can begin the formation of a separate dermal cell condensate at a distance from the initial condensate.

The model itself is analogous to the reaction-diffusion/ activator-inhibitor models. Instead of chemicals/ morphogens, local short range activation is the result of local recruitment of cells through distortion of the ECM by migrating cells while long range inhibition is exerted by passive elastic resistance of the ECM. Some interesting properties arise from the predicted model which differs from the molecular based models. Firstly, the dermis alone is capable of spontaneously generating a periodic pattern independently from the epidermis, when dermal cells create enough strain on the surrounding ECM through proliferation or migration. Secondly, if dermal cell density is high enough throughout the field, the induction of a dermal cell aggregate would result in the nucleation of aggregate formation, from the initial site of induction. That is, the initial aggregate would automatically cause a wave of dermal cell aggregate formation, spreading from the initial aggregate.

Previous studies have suggested several tissues/organs which may form from the mechanical model such as the somites, bone, and hair/feather primordium formation (Bard, 1990). However, subsequent studies have shown that in these systems, molecular signalling is integral to the process of their patterning (Abbott and Asmundson, 1957; Miura and Shiota, 2000; Mou *et al.*, 2006; Pourquié, 2003; Wells *et al.*, 2012). Currently, examples of vertebrate pattern formation which form from a purely mechanical or cellular patterning model has not been identified. It is plausible that the mechanical model of pattern formation may work in conjunction with molecular signalling to induce periodic pattern formation in tissues in *in vivo* systems.

1.5 Aims to be addressed

Various bird species display differences in the arrangement of their feathers (Clench, 1970; Nitzsch, 1867; Stettenheim, 2000), which arise during embryonic development. Using the chicken as a developmental model, many molecular candidates have been identified in having an important role in feather primordium induction. Previous studies have proposed that the periodic pattern of feather primordia arise from reaction-diffusion based mechanisms, however, an activator-inhibitor pair as defined by the Turing model has yet to be identified. Also, studies into the process of periodic pattern formation of feathers have primarily focused on chicken feather development, and thus, the mechanisms that govern pattern formation in other bird species have not been examined.

To uncover the developmental processes that underlie feather primordium formation, transgenic CAG-GFP chicken embryos will be used. The use of these transgenic chickens will allow the study of cell behaviour during feather primordium induction and formation in real time. Through modulation of culture conditions, the role of molecular signalling in feather primordium formation can be examined.

Specifically, the aims of this thesis are:

1. To study cell behaviour during feather primordium formation, and determine how FGF and BMP signalling may affect their behaviour.
2. To determine the role of EDA/EDAR signalling in the induction of feather primordium formation.
3. To determine how the basic pattern generating mechanism, defined in chickens, is modulated in a variety of flighted and non-flighted bird species.

MATERIALS AND METHODS

2. MATERIALS AND METHODS

2.1 Animal Methods and Techniques

2.1.1 Eggs, Egg Incubation and Embryology

Fertilised eggs were stored at 14°C prior incubation. Eggs were incubated vertically with the pointed end facing down at 37.8°C in a humidified incubator with no rotation throughout the incubation period. Embryos were extracted by opening the eggs at the widest pole and all extra embryonic membranes were removed. Once extracted the embryos were washed in 1X phosphate buffered saline (PBS) containing 1% penicillin-streptomycin (Invitrogen, Massachusetts, USA) and staged immediately. Embryos were staged based on Hamburger and Hamilton (1951) stages (See **Appendix I**).

Fertilised white leghorn chicken eggs were purchased from Henry Stewart & Co and incubated for a period of 7, 8, and 9 days representing HH 29, HH 31, and HH 33 respectively. The HH staging system will be used to describe the developmental stages of chicken embryos in experiments involving only chickens. In experiments comparing different avian species, number of days of incubation will be used instead to describe embryos. Embryos of the correct stage were either immediately fixed in 4% paraformaldehyde (PFA) in 1X PBS overnight at 4° or immediately dissected for *ex vivo* culture.

Fertilised transgenic green fluorescent protein (GFP) chicken eggs were obtained from the Roslin Institutes, Transgenic Chicken Facility based in the National Avian Research Facility (NARF). Eggs were incubated for 7 days representing HH 29. Transgenic embryos of the correct stage were immediately dissected for *ex vivo* culture.

Fertilised Khaki Campbell/Indian runner crossed ducks were obtained from a supplier in Gloucestershire, England. Eggs were incubated for 7 to 14 days, to obtain a range of embryonic stages for *in situ* hybridisation analysis or dissected for *ex vivo* culture.

Embryos of the correct stage were immediately fixed in 4% PFA in 1X PBS overnight at 4°C.

2.1.2 Ratite Egg Incubation

Eggs were incubated immediately upon delivery and incubated in a horizontal position at 36.4°C in a humidified incubator. Eggs were automatically rotated 90° periodically throughout the incubation period. Embryos were extracted by opening a 2 cm to 3 cm diameter hole on the side of the egg, above the air sac. The contents were carefully poured out and the embryo removed and washed in 1X PBS containing 1% penicillin-streptomycin. All extra embryonic membranes were removed while in 1X PBS.

Fertilised emu eggs (*Dromaius novaehollamdiae*) were purchased from various sources. Emu eggs were incubated for 15 to 21 days and extracted embryos were either immediately fixed in 4% PFA in 1X PBS overnight at 4°C or immediately dissected for *ex vivo* culture.

Fertilised rhea eggs (*Rhea pennata*) were purchased from Woodbine Farms in Northamptonshire. Extracted embryos were immediately fixed in 4% PFA in 1X PBS overnight at 4°C.

Fertilised ostrich eggs (*Struthio camelus*) were obtained from Woodbine Farms in Northamptonshire. Incubated eggs were rotated 180° every 2 hours during the day throughout the incubation period. Ostrich eggs were incubated for 13 to 18 days and extracted embryos were washed in PBS containing 1% penicillin-streptomycin. Embryos were immediately fixed in 4% PFA in 1X PBS overnight at 4°C.

2.1.3 *Ex vivo* Organ Culture - Skin Explants

Extracted embryos were harvested for *ex vivo* organ culture. After incubation, the embryos were extracted and washed in PBS containing 1% penicillin-streptomycin. Embryos were decapitated and transferred, ventral side down, on to a piece of blue paper roll. Dorsal skin was dissected by making small incisions with sprung scissors (Fine Science Tools, California, USA) around the embryo from the tail up to the neck

on both sides. The dissected embryo was transferred to fresh PBS containing 1% penicillin-streptomycin and the skin was removed using a pair of fine forceps (Fine Science Tools, California, USA) and transferred to a sterile nitrocellulose filter (Millipore, Massachusetts, USA, pore size 0.45 µm), dermis side in contact with the filter. Skin explants were placed on top of a stainless steel wire mesh and transferred to the centre well of a sterile centre well organ culture dish (Becton Dickinson/Falcon, Oxford, UK). 2 ml of Dulbecco's Modified Eagle's Medium (DMEM) containing 4500 mg/L L-glutamine, glucose and sodium bicarbonate (Sigma, Missouri, USA) supplemented with 2% foetal bovine serum (FBS) (Invitrogen, Massachusetts, USA) and 1% penicillin-streptomycin (referred to as standard culture medium) was added to the centre well. 2 ml of Milli-Q water was added to the outer well to maintain humidity. Explants were incubated in a 5% CO_2 atmosphere at 37°C in a Heracell^{TM}150 CO_2 incubator (DJB Labcare, Buckinghamshire, UK) and the medium changed was every 48 hours. Recombinant proteins or small molecule inhibitors were diluted in the standard culture medium at a range of doses to study changes in gene expression or morphology during patterning. Control cultures were prepared by supplementing culture medium with equal volumes of the reconstitution solution used to reconstitute the recombinant proteins or small molecule inhibitors (**Figure 27**).

Recombinant human (rh) proteins from the fibroblast growth factor (FGF) and bone morphogenetic protein (BMP) family were obtained from R&D systems, Abingdon, UK. rhFGF9 protein was reconstituted in 1X PBS containing 1% bovine serum albumin (BSA) at 100 µg/ml and applied to skin explant cultures at concentrations ranging from 250 ng/ml to 1 µg/ml. rhFGF20 protein was reconstituted in 1X PBS containing 1% bovine serum albumin (BSA) at 100 µg/ml and applied to skin explants at concentrations ranging from 250 ng/ml to 2 µg/ml.

The FGF receptor (FGFR) inhibitor, SU5402 (Sigma-Aldrich, Missouri, USA) (Sun *et al.*, 1999), was reconstituted at a concentration of 10 mM in dimethyl sulfoxide (DMSO) and applied to skin explant cultures at a range of concentrations from 2 µM to 15 µM.

Recombinant human proteins from the BMP family were obtained from R&D systems, Abingdon, UK. rhBMP4 was reconstituted in 4 mM hydrochloric acid (HCl) in 1X PBS containing 0.1% BSA and applied to skin explant cultures at concentrations ranging from 25 ng/ml to 1 µg/ml.

LDN193189 (Stemgent, Massachusetts, USA), an inhibitor of BMP type I receptors and Activin A receptor type I (Cuny *et al.*, 2008), was reconstituted at a concentration of 10 mM in DMSO and applied to skin explant cultures at a range of concentrations from 2 µM to 15 µM.

CHIR99021 (Axon Medchem, Netherlands), a glycogen synthase kinase 3 (GSK-3) inhibitor (Ring *et al.*, 2003), was reconstituted at a 10 mM concentration in DMSO and applied to skin explant cultures at a range of concentrations from 2 µM to 30 µM.

The ectodysplasin (EDA) pathway was stimulated through the addition of Fc-chEDA1, a recombinant protein containing the Fc domain of human immunoglobulin G1 (IgG1) fused to the tumour necrosis factor (TNF) domain of the chicken *EDA* A gene (*EDA1*). Fc-chEDA1was kindly donated to us by Pascal Schneider and was generated in a similar manner to the generation of the mouse Fc-EDA1 protein as described by Gaide and Schneider, 2003 (Gaide and Schneider, 2003). The protein was reconstituted at 1 mg/ml in 1X PBS and applied to skin cultures at a range of concentrations from 50 ng/ml to 2 µg/ml.

Anti-EDA monoclonal antibodies, Ecto-D2 (Kowalczyk-Quintas *et al.*, 2014), were applied to skin explant cultures to inhibit the EDA pathway. EctoD2 was reconstituted at a concentration of 2 mg/ml in 1X PBS and applied to skin explant cultures at concentrations ranging from 5 µg/ml to 10 µg/ml.

Methotrexate hydrate (Sigma-Aldrich, Missouri, USA), a dihydrofolate reductase inhibitor (Sasso *et al.*, 1994), was reconstituted in 1 M sodium chloride (NaOH) solution at a 5 mM concentration and applied to skin explant cultures at concentrations ranging from 50 nM to 5 µM.

Latrunculin A (Sigma-Aldrich, Missouri, USA), an inhibitor of actin polymerisation (Spector *et al.*, 1983), was used as a cell movement inhibitor. Latrunculin A was dissolved in DMSO at a stock concentration of 50 µg/ml and applied to skin explant cultures at concentrations ranging from 10 ng/ml to 150 ng/ml.

Skin explants were treated and cultured for 5 hours for quantitative reverse transcription polymerase chain reaction (qRT-PCR) and for 24 to 72 hours to study morphological changes over the course of the experiment. Three embryonic skins were treated per dose for qRT-PCR experiments and a minimum of two skins per dose were treated for morphological studies. After the required incubation time, skin explants were washed in PBS and either fixed in 4% PFA in 1X PBS at 4°C overnight or skins were transferred to TRI reagent (Sigma-Aldrich, Missouri, USA) and homogenised for RNA isolation.

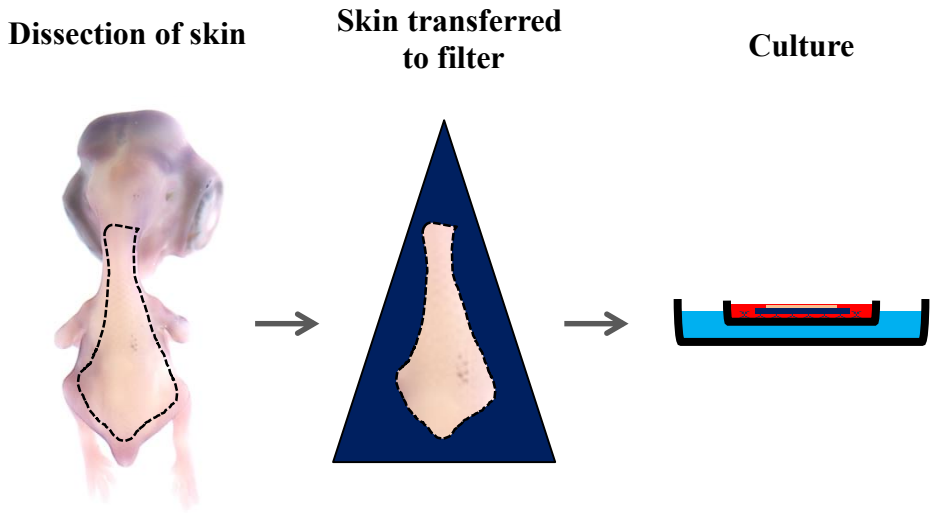

Figure 27. Preparation of chicken dorsal skin for ex vivo culture. Skin was dissected from the dorsal side of embryo (indicated by dotted lines), placed onto a nitrocellulose filter (dark blue triangle) and then cultured in a centre well culture dish. Prepared explants on filters were placed on top of a wire mesh in the centre well. Standard culture medium or supplemented culture medium was placed into the culture wells (red), covering the skin explant. Water was placed in the outer well to maintain humidity (blue).

2.1.4 Local Delivery of Proteins

Affi-Gel® Blue Gel beads (Bio-Rad, California, USA) were pre-treated proteins as followed. 10 µl of beads were washed in a 1.5 ml eppendorf containing 1 ml sterile 1X PBS for 15 minutes on ice. Beads were then centrifuged at 16,000 g for 10 minutes at 4°C and PBS removed. PBS wash was repeated once more for 15 minutes on ice before the beads were centrifuged again under the same conditions as before. PBS was removed and 10 µl of either rhFGF9 stock solution (100 µg/ml in 0.1% BSA in 1X PBS) or 100 µg/ml BSA in 1X PBS was added to the beads and rocked gently overnight at 4°C.

2 µl of beads were placed onto a nitrocellulose Millipore filter (pore size 0.45 µm) while in PBS. Dissected HH 29 white leghorn or GFP chicken dorsal skins were then manoeuvred and fixed on top of the beads, dermis side down.

White leghorn skin explants treated with beads were cultured for a maximum of 48 hours at 37°C in a 5% CO_2 incubator. At the end of the culture period, the explants were fixed in 4% PFA and stored at 4°C until use for *in situ* hybridisation or transferred to TRI reagent and homogenised for RNA isolation.

Bead treated GFP chicken skin explants were either used for *in situ* hybridisation or real time imaging experiments. Explants were cultured for a maximum of 48 hours at 37°C in a 5% CO_2 incubator. GFP chicken skin explants were imaged at the start of culture and then every 24 hours with a stereo microscope (Olympus SZX10) using cell^B (Olympus, UK) software under bright field or ultraviolet light. At the end of the culture period, the explants were fixed in 4% PFA and stored at 4°C until use for *in situ* hybridisation. For real time imaging, explants were imaged immediately for a period of 48 to 72 hours after preparation.

2.1.5 Real Time imaging of *ex vivo* Skin Explants

Real time imaging was performed using the Zeiss Live Cell Observer/ Deconvolution system with an incubated CO_2 stage using Zen2012 software (Zeiss, Oberkochen,

Germany). The incubation stage was maintained at 37°C and with a 5% CO_2 atmosphere throughout the course of the experiment. Prepared HH 29 GFP chicken dorsal skin explants were placed epidermal side down into individual wells of a 6-well dish containing 2 ml of standard culture medium or medium supplemented with recombinant proteins/small molecule inhibitors. Milli-Q water was placed into empty wells or spaces between the well to maintain humidity. The plate was placed onto the microscope stage and skins manoeuvred with a pipette tip to an anterior to posterior orientation. A sterile plastic weight was placed at the tip of the nitrocellulose filter paper, away from the skin. GFP signal was visualised under ultraviolet light (488 nm wavelength). Images were taken using with a 5X and 10X objectives at 10 minute intervals over a period of 48 to 72 hours.

2.1.6 Primary Row Removal

Three dissected HH 29 embryonic dorsal skins were transferred to a sterile nitrocellulose Millipore filter (pore size 0.45 µm), dermis side down. A scalpel blade was used to excise an area of skin corresponding to the site of the presumptive primary row of feather primordium formation at the midline of the dorsal tract. After primary row removal explants were placed on top of a stainless steel wire mesh and transferred to the centre well of a sterile centre well organ culture dish containing 2 ml of standard culture medium. Explants were cultured for a maximum of 48 hours at 37°C in a 5% CO_2 incubator, then fixed in 4% PFA in 1X PBS and stored at 4°C until required.

2.1.7 Stretching of Skin Explants

Dissected HH 33 embryonic dorsal skins were dissected and one corner of the skin placed on to a sterile nitrocellulose Millipore filter (pore size 0.45 µm) dermis side down using fine forceps. The skin was stretched to its maximum capacity flat against the Millipore filter by gently pulling and fixing each corner of skin to the filter with fine forceps. Explants were placed on top of a stainless steel wire mesh and transferred to the centre well of a sterile centre well organ culture dish containing 2 ml of standard culture medium. Explants were cultured for a maximum of 72 hours at 37°C in a 5%

CO_2 incubator and the medium changed every 48 hours. After incubation the explants were fixed in 4% PFA in 1X PBS and stored at 4°C until required.

2.1.8 Epidermal/Dermal Separation

Freshly dissected dorsal skins of HH 29 GFP transgenic chicken embryos and E14 emu embryos, were incubated in 2 mg/ml of dispase II protease (Sigma-Aldrich, Missouri, USA) in 1X PBS at 37°C for 10 minutes. Incubated skins were washed in 1% penicillin-streptomycin in 1X PBS and skin layers separated using fine forceps. Separated skin layers were transferred to TRI reagent and homogenised for RNA isolation. Explants were cultured in a 5% CO_2 atmosphere at 37°C for a maximum of 2 days and at the end of the culture period, the explants were fixed in 4% PFA in 1X PBS and stored at 4°C until required.

2.1.9 Epidermal/Dermal Recombination

Freshly dissected HH 29 stage GFP embryonic chicken or E14 emu dorsal skins were incubated in 2X magnesium (Mg^{2+}) and calcium (Ca^{2+}) free saline (see section **2.5** for recipe) containing 0.25% (w/v) ethylenediaminetetraacetic acid (EDTA) for 20 minutes at 37°C. Incubated skins were washed in 1% penicillin-streptomycin in 1X PBS and left to stand for 10 minutes before skin layers were separated using fine forceps. Recombinations were performed in 1X PBS containing 1% penicillin-streptomycin by placing the dermis layer from one embryo, ventral side down, onto a nitrolcellulose Millipore filter (pore size 0.45 µm) and stretching a correctly orientated epidermis layer from another embryo over the dermis. The combined skins were gently lifted out of the 1X PBS and placed into an individual well of a 6-well plate containing 500 µl of standard culture medium and incubated in a 5% CO_2 atmosphere at 37°C in a Heracell^{TM}150 CO_2 incubator (DJB Labcare, Buckinghamshire, UK) for 2 hours. Milli-Q water was placed into empty wells or spaces between the wells prior to incubation, to maintain humidity. After incubation 2 ml of pre-warmed standard culture medium was gently pipetted into the side of the well. Recombinants were cultured in a 5% CO_2 atmosphere at 37°C for a maximum of 6 days and medium

changed every 48 hours. Recombinants were imaged every 24 hours imaged with a stereo microscope (Olympus SZX10) using cell^B (Olympus, UK) software under bright field or ultraviolet light. At the end of the culture period, the recombinants were fixed in 4% PFA and stored at 4°C until use.

2.2 Nucleic Acids Techniques

2.2.1 RNA Isolation, DNase I Treatment of RNA and RNA Purification

RNA from *ex* vivo cultured embryonic chicken skins was isolated using TRI reagent. Tissues were washed in 1X PBS then placed into individual eppendorfs containing 100 µl of TRI reagent and homogenised using an electric pestle. The mixture was stored at -80°C overnight. The mixture was thawed at room temperature for 15 minutes, 10 µl of 1-bromo-3-chloropropane (Sigma-Aldrich, Missouri, USA) was added and the mixture was vortexed briefly. The mixture was left to stand at room temperature for 15 minutes and vortexed briefly before centrifuged at 16,000 g at 4°C for 15 minutes in a microcentrifuge (Biofuge® Fresco - microlitre rotor). The aqueous phase was transferred to a fresh eppendorf containing 50 µl of propan-2-ol, vortexed briefly and kept at -20°C for 10 minutes to precipitate the RNA. The mixture was centrifuged at 16,000 g at 4°C for 8 minutes, supernatant was discarded and the remaining RNA pellet was washed with 100 µl of 70% ethanol and centrifuged at 16,000 g at 4°C for 5 minutes. The supernatant was removed and the RNA pellet was air dried upside down for 30 minutes at room temperature and resuspended in 10 µl of Milli-Q water.

Isolated RNA was treated with RQ1 RNase- Free DNase (Promega, Madison, USA) by adding 2 U of RQ1 RNase-Free DNase along with RQ1 DNase 10X reaction buffer (400 mM Tris-HCL, 100 mM $MgSO_4$, 10 mM $CaCl_2$) diluted in Milli-Q water to a 1X working concentration and incubated at 37°C for 30 minutes.

RNA purification was performed following the RNA isolation protocol, as stated above, after addition of 100 µl of TRI reagent and 10µl of 1-bromo-3-chloropropane to the RQ1 RNase-Free DNase treated RNA sample. Samples were stored at -80°C until required.

2.2.2 Spectrophotometric Analysis for RNA and DNA Quality and Concentration

Freshly isolated or purified RNA or DNA was analysed neat in a spectrophotometer (NanoDrop® ND-1000). Absorbance at A_{260} was used to determine nucleic acid

concentration and ratio of absorbance at $A_{260/230}$ and $A_{260/280}$ was used to determine nucleic acid purity. Sample was considered pure if observed $A_{260/230}$ and $A_{260/280}$ values are between 2.0-2.2 and 1.8-2.1 respectively.

2.2.3 cDNA First Strand Synthesis

Superscript® III Reverse Transcriptase (RT) (Invitrogen, Massachusetts, USA) and random hexamers (Applied Biosystems, Massachusetts, USA) were used to synthesis cDNA from purified RNA obtained from cultured tissue. Reactions were performed by mixing 500 ng of purified RNA, 1 µl 5 µM random hexamers and 1 µl 10 mM dNTP mix to a final volume of 11µl with Milli-Q water and incubated at 65°C for 5 minutes in a thermocycler (MJ Research, Quebec, Canada, PTC-200). The reaction was transferred to ice for 5 minutes and made up to 20 µl by the addition of 4 µl of 5X first-strand buffer (Invitrogen, Massachusetts, USA), 1 µl of 0.1M DTT (Invitrogen, Massachusetts, USA), 1 µl of RNaseOUT™ recombinant ribonuclease inhibitor (Invitrogen, Massachusetts, USA) (corresponding to 40 U of RNaseOUT™) and 1 µl of Superscript® III RT (Invitrogen, Massachusetts, USA) (corresponding to 200 U of Superscript® III). The reaction was placed in the thermocycler under the cycling conditions: 25°C for 5 minutes, 50°C for 1 hour and 70°C for 15 minutes. RT negative and sample negative controls were performed for each experiment. Samples were stored in -20°C until use.

2.2.4 Quantitative RT-PCR

cDNA was thawed on ice for 20 minutes and diluted 1/10 in Milli-Q water for use as template for the reaction. Each reaction was performed in a final volume of 20 µl containing 3 µl of diluted cDNA template, 10 µl of SYBR Green Universal Master Mix - ROX (Roche, Basel, Switzerland), 1 µl of 10 µM stock from each primer (forward and reverse primers) and 5 µl of Milli-Q water. Reactions were performed in triplicate with at least three biological repeats to determine each data point. Amplification was performed in a Strategene MX3000P qPCR system (Agilent Technologies) for 40 cycles with the following cycling conditions: 95°C for 10

minutes, 40 cycles of 95°C for 15 seconds and 60°C for 30 seconds followed by 95°C for 1 minute, 60°C for 30 seconds, 95°C for 15 seconds and 25°C for 30 seconds. A serial dilution series from control cDNA was used to determine the relative expression levels of the gene of interest from a standard curve. Expression levels of genes of interest were normalised to those of *GAPDH*. Results were analysed using MxPro - Mx3000P software (Agilent Technologies)

2.2.5 Primer Sequences for Quantitative RT-PCR

GAPDH **S:** 5'- GACAACTTTGGCATTGTGGA-3'

GAPDH **AS:** 5'- GGCTGTGATGGCATGGAC-3'

FGF20 **S:** 5'- CCTCTTCGGTATCCTTGAATTCA-3'

FGF20 **AS:** 5'- TCAGAGCCATAGAGTTCTCCC-3'

BMP4 **S:** 5'- TGAGGAGCTTCCACCATGA-3'

BMP4 **AS:** 5'- TGCTGAGGTTGAAGACGAAG-3'

2.2.6 RT-PCR - Generation of Species Specific Riboprobes

Primers were designed based on ostrich, tinamou, duck, and chicken sequences using the full length cDNA sequence for chicken *EDA*, including 966 bp 3' UTR as a reference sequence for the generation of species specific *EDA* riboprobes for *in situ* hybridisation. Ostrich, tinamou, and duck *EDA* sequences were obtained by performing a nucleotide basic local alignment search tool (BLAST) search (BLASTn) using chicken cDNA sequence obtained from the Ensembl genome database as the query, searching against all known Aves through the use of the National Centre for Biotechnology Information database (NCBI). cDNA encoding 478 bp, which includes 355 bp of the ORF and 123 bp of the 3'UTR was generated for use as a template for the generation of species specific riboprobes. cDNA was generated by first strand synthesis (Section **2.2.3**) using mRNA isolated from ostrich and emu tissues and purified using the TRI-reagent protocol (Section **2.2.1**). 1 µl of the reverse

transcription reaction was used as a template for the PCR reaction. The template was mixed together with 3 µl of 10X PCR reaction buffer + $MgCl_2$ (Roche, Basel, Switzerland), 6 µl of GC rich buffer (Roche, Basel, Switzerland), 1 µl of 0.1 M DTT (Invitrogen Massachusetts, USA), 2 µl of 10 µM forward and reverse primers, 12.7 µl of Milli-Q water and 1 U of FastStart Taq DNA polymerase (Roche, Basel, Switzerland). Amplification was performed in a thermocycler under the following conditions: 95°C for 2 minutes, 40 cycles of 95°C for 15 seconds, 45°C for 15 seconds and 68°C for 15 seconds, followed by 68°C for 5 minutes. Samples were stored in -20°C until required. The following primers were used:

S: 5'-GTCTCGCATCACTATGAACC-3'

AS: 5'-GAATAAATAGCTCTGGATCA-3'

Struthio camelus (Ostrich) riboprobe - 478 bp

Dromaius novaehollamdiae (Emu) riboprobe - 478 bp

2.2.7 TOPO Cloning of RT-PCR Products - Cloning of Species Specific *EDA* (Emu & Ostrich)

Fresh RT-PCR products were inserted into the pCR4-TOPO cloning vector using the TOPO® TA Cloning® Kit for Sequencing (Invitrogen, Massachusetts, USA). The reaction was performed by mixing 1 µl of RT-PCR product with 1 µl of salt solution (Invitrogen, Massachusetts, USA), 1 µl of the TOPO® vector (Invitrogen) and 3 µl of Milli-Q water. The reaction was incubated at room temperature for 30 minutes and kept on ice until the product was transformed into *E. coli*.

2.2.8 *E. coli* Transformation

XL1- Blue Competent Cells (Stratagene, UK) were transformed by adding 1 µl of TOPO cloning reaction or plasmid provided, to 50 µl of competent cells and placed on to a shaker on ice for 30 minutes. Mixture was placed into a 42°C water bath for 30 seconds and transferred to ice for 2 minutes. 800 µl of lysogeny broth (LB) medium

was added to the cell and the suspension was shaken at 37°C for 1 hour. 200 µl of cell suspension were spread on to an LB agar plate containing ampicillin (100 µg/ml) and incubated over night at 37°C. Plates were kept at 4°C until use.

2.2.9 DNA Plasmid Isolation - Mini Preparation

5 ml of LB medium containing ampicillin (100 µg/ml) was inoculated with single colonies of transformed *E. coli* and placed in a shaking 37°C incubator overnight. After incubation the inoculated LB medium was centrifuged at 3200 g for 20 minutes at 4°C and supernatant discarded. DNA plasmid isolation was performed using the Wizard® *Plus* Minipreps DNA Purification System (Promega, Madison, USA). All of the following centrifugation steps were performed at room temperature. Bacterial pellets were resuspended in 250 µl of cell resuspension solution and transferred to 1.5 ml eppendorfs. 250 µl of cell lysis solution was added and incubated at room temperature for 5 minutes. 10 µl of alkaline protease solution was added to the mixture and left to stand for 5 minutes at room temperature. This was followed by the addition of 350 µl of neutralisation solution to the mixture. Mixture was centrifuged at 16,000 g for 10 minutes and the clear cell lysate was transferred to a spin column. The spin column was centrifuged at 16,000 g for 1 minute and the flow through discarded. 750 µl of column wash solution was added to the column and centrifuged at 16,000 g for 1 minute and the flow through was discarded. The column was washed again by the addition of 250 µl of column wash solution and centrifuged at 16,000 g for 2 minutes. Columns were transferred to a new collection tube and centrifuged once more at 16,000 g for 1 minute. To elute the DNA plasmid, 100 µl of nuclease free water was added to the column and transferred to a 1.5 ml eppendorf and centrifuged at 16,000 g for 1 minute. Isolated DNA plasmid was stored at -20°C until use. All pCR4-TOPO vector generated plasmids were validated by Sanger sequencing of the insert (Dundee DNA Sequencing and Services).

2.2.10 DNA Plasmid Isolation - Maxi Preparation

250 ml of LB medium containing ampicillin (100 µg/ml) was inoculated with single colonies of transformed *E. coli* and placed in a shaking 37°C incubator overnight. Following incubation, the inoculated LB medium was centrifuged aliquoted into 50 ml falcon tubes at 3200 g for 15 minutes at 4°C and the supernatant was discarded. DNA plasmid was isolated with the Plasmid Maxi Kit (Qiagen, Venlo, Netherlands). The bacterial pellets were resuspended in a total volume of 10 ml of buffer P1 and lysed with the addition of 10 ml of buffer P2 and left to stand at room temperature for 5 minutes. 10 ml of chilled buffer P3 was added to the mixture. Precipitate was removed through the use of a QIAfilter cartridge. The mixture was transferred to the cartridge and passed through to obtain a clear lysate. The cleared lysate was transferred and passed through an equilibrated QIAGEN-tip 500 (by passing through the QIAGEN-tip 500, 10 ml of buffer QBT). Flow through was discarded and the QIAGEN-tip 500 washed twice with 30 ml of buffer QC. The QIAGEN-tip 500 was transferred to a 50 ml falcon tube and DNA plasmid was eluted by the addition of 15 ml of buffer QF. The DNA plasmid was precipitated by adding 10.5 ml of propan-2-ol to the eluted DNA and centrifuged at 3200 g at 4°C for 1 hour. Supernatant was removed and the pellet was washed with 5 ml of 70% ethanol and centrifuged at 3200 g at 4°C for 1 hour. Ethanol was removed and the pellet was air dried at room temperature for 1 hour before being resuspended in 500 µl of 1X TE. Isolated DNA plasmid was stored at -20°C until use.

2.2.11 Restriction Digest of Isolated DNA Plasmid

Reactions were set up by diluting 4 µg-5 µg of the DNA plasmid in Milli Q water to a final volume of 42.5 µl to which 5 µl of 10X buffer (according to manufacturer's recommendations), 0.5 µl of 10 mg/ml BSA and 40 U of restriction enzyme was added. Reactions were incubated at 37°C overnight and then purified.

2.2.12 DNA purification

DNA purification was performed using the QIAquick Gel Extraction Kit (Qiagen, Venlo, Netherlands). All steps performed at room temperature unless stated otherwise and the spin column was rotated 180° after every centrifugation step. Three volumes of buffer QG and one volume of propan-2-ol were added to one volume of the DNA sample. The mixture was transferred to a QIAquick spin column and centrifuged at 16,000 g for 1 minute. Flow through was discarded and 500 µl of buffer QG was added to the column and centrifuged at 16,000 g for 1 minute. Flow through was discarded and 750 µl of buffer PE was added to the column and incubated at room temperature for 5 minutes. Column was centrifuged at 16,000 g for 1 minute and after discarding the flow through, the column was transferred to a new collection tube and centrifuged once more at 16,000 g for 1 minute. Buffer PE steps were repeated once more before the column was transferred to a 1.5 ml eppendorf tube and air-dried for 10 minutes at room temperature. DNA was eluted by adding of 30 µl of 1X TE to the spin column and centrifuged at 16,000 g for 1 minute. Purified DNA was stored at -20°C until use.

2.2.13 Agarose Gel Electrophoresis

1% (w/v) Ultrapure™ Agarose (Invitrogen, Massachusetts, USA) was dissolved in 1X TAE buffer and 0.3X final concentration of SYBR® Safe DNA Gel Stain (Invitrogen, Massachusetts, USA) was added. Samples mixed with 1/10 volume of 5X loading buffer (Bioline, London, UK) was loaded into the gel along with an appropriate DNA ladder based on the estimated size of products (HyperLadder™ 1 kb and HyperLadder™ 100 bp, Bioline, London, UK). Gels were run in 1X TAE buffer at 120V until bands were discernible. Gels were imaged in a Molecular Imager® Gel Doc™ XR System (Bio-Rad, California, USA) and images obtained using Quantity One® software (Bio-Rad, California, USA).

2.3 *In situ* Hybridisation

2.3.1 *In situ* Hybridisation - Digoxigenin Labelled Riboprobe Synthesis

DNA plasmids were used as templates for generating digoxigenin (DIG) labelled riboprobes for double or single *in situ* hybridisation reactions. Sense and antisense riboprobes were generated by linearising plasmids with restrictions enzymes and transcribed with T3, T7 or Sp6 RNA polymerase (Promega, Madison, USA). Plasmids were linearised as described in section **2.2.11**, and purified as described in section **2.2.12**.

1 µg of linear template DNA was diluted in Milli Q water to a final volume of 7 µl to which, 4 µl of 5X transcription buffer (Promega, Madison, USA), 4 µl of 0.1 M DTT (Promega, Madison, USA), 2 µl of RNaseOUT™ recombinant ribonuclease inhibitor (Invitrogen, Massachusetts, USA), 2 µl of Digoxigenin (DIG) RNA Labelling Mix (Roche, Basel, Switzerland) and 20 U of T3, T7 or SP6 RNA polymerase (Promega, Madison, USA) was added. The reaction was incubated at 37°C for 1 hour and centrifuged briefly. Another 20 U of RNA polymerase was added to the reaction and incubated at 37°C for 1 hour. Reactions were scaled up accordingly based on initial template DNA concentration. Reaction was briefly centrifuged and 2 U of RQ1 RNase-Free DNase to the reactions and incubated for a further 20 minutes at 37°C. To precipitate the labelled RNA, 75% ethanol containing 0.1 M lithium chloride was added to the reaction and stored at -20°C overnight. The RNA was centrifuged at 16,000 g at 4°C for 15 minutes. The supernatant was removed and the pellet was washed with 500 µl of 75% ethanol and centrifuged at 16,000 g at 4°C for 5 minutes. The ethanol was removed and the pellet was air dried at room temperature for 30-60 minutes. The pellet was resuspended in 20 µl of Milli Q water and stored at -80°C until use.

2.3.2 *In situ* Hybridisation - 2, 4-Dinitrophenyl Labelled Riboprobe Synthesis

A *β-Catenin* cDNA containing plasmid was used as a template for generating 2, 4-dinitrophenyl labelled riboprobes for double *in situ* hybridisation reactions. The

plasmid was linearised with NotI-HF restriction enzyme (New England Biolabs) and transcribed with T3 RNA polymerase (Promega, Madison, USA). Plasmids were linearised as described in (section **2.2.11**) and purified as described in (section **2.2.12**)

1 µg of linear template DNA was diluted in Milli-Q water to a final volume of 7 µl with 4 µl of 5X transcription buffer (Promega, Madison, USA), 4 µl of 0.1 M DTT (Promega, Madison, USA), 2 µl of 10 mM NTP mix (Sigma, Missouri, USA), 2 µl of RNaseOUT™ recombinant ribonuclease inhibitor (Invitrogen, Massachusetts, USA), and 20 U of T3 RNA polymerase. The reaction was incubated at 37°C for 1 hour and centrifuged briefly. Another 20 U of RNA polymerase was added to the reaction and incubated at 37°C for 1 hour. Reaction was briefly centrifuged and 2 U of RQ1 RNase-Free DNase to the reactions and incubated for a further 20 minutes at 37°C. RNA was precipitated as described in (Section **2.3.1**).

*Label*IT® DNP Labelling Kit (Mirus) was used to label the raw RNA with 2, 4-dinitrophenol (DNP). 5 µg of RNA was diluted in Milli-Q water to a final volume of 40 µl and mixed with 5 µl of 10X buffer A (Mirus) and 5 µl of the *Label* IT reagent (Mirus). The reaction was incubated at 37°C for 30 minutes and then briefly centrifuged at 16,000 g for 5 seconds. The reaction was incubated at 37°C for another 30 minutes. The DNP labelled RNA was purified using the Microspin Columns provided in the Kit. The columns were prepared by vortexing the column briefly, loosening the cap and removing the bottom closure. The column was placed into a 1.5 ml eppendorf and centrifuged at 735 g for 1 minute. The DNP labelled RNA sample was applied to the column which was then transferred to a fresh 1.5ml eppendorf and centrifuged at 735 g for 2 minutes. The column was discarded and the purified RNA was stored at -80°C until use.

2.3.3 Fixed Skin Explant and Embryo Preparation for *in situ* Hybridisation

Cultured skin explants and embryos fixed in 4% PFA in 1X PBS were washed three times in 1X PBST (1X PBS containing 0.1% Tween 20) treated with 0.01% diethylpyrocarbonate (DEPC) (Sigma-Aldrich, Dorset, UK) and dehydrated through increasing series of methanol dilutions, from 25% to 100%, in 1X PBS that had been

treated with 0.01% DEPC. Samples were then bleached in 5% hydrogen peroxide (Sigma-Aldrich, Missouri, USA) in methanol for 2 hours and then washed in 100% methanol twice. Samples were kept in 100% methanol and stored at -20°C until use.

2.3.4 Chicken Embryo Powder Preparation

HH 31 white leghorn chicken embryos were homogenised in a minimum volume of ice cold 1X PBS. 4 volumes of ice cold acetone was mixed with the homogenate at incubated on ice for 30 minutes. The mixture was centrifuged at 6000 g at 4°C for 10 minutes and the supernatant discarded. The pellet was washed with ice cold acetone and vortexed until the pellet was resuspended. The mixture was centrifuged at 6000 g at 4°C for 10 minutes and the supernatant discarded. The pellet was homogenised again and the left at room temperature to air dry. A minimal volume of acetone was added to the pellet and further homogenised before the mixture was centrifuged at 6000 g at 4°C for 10 minutes and the supernatant discarded. The pellet was air dried at room temperature and stored at 4°C until use.

2.3.5 Skin Explant and Embryo Washes for *in situ* Hybridisation

Skin explants and embryos stored in 100% methanol were washed in a descending series of methanol dilutions in 1X PBS treated with 0.01% DEPC and then washed three times in 0.01% DEPC treated 1X PBST . All wash steps were performed for 20 minutes at room temperature for skin explants. All embryos, regardless of stage, were washed for 1 hour, twice, at room temperature for each methanol wash step and for 30 minutes, three times, at room temperature for the final PBST washes.

2.3.6 Hybridisation of Riboprobe

Proteinase K treatment (20 µg/ml in 0.01% DEPC treated water) (Fisher BioReagents, New Hampshire, USA) was performed for 6 minutes and 30 seconds for skin explants and for 10-15 minutes for embryos depending on stage at room temperature. Samples were then washed for 10 minutes at room temperature, twice, in glycine (2 mg/ml in 0.01% DEPC treated 1X PBST). The samples were then washed twice in 0.01% DEPC

treated 1X PBST 20 minutes before fixation in 4% paraformaldehyde/0.2% glutaraldehyde in 1X PBS for 20 minutes at room temperature. Three 1X PBST washes for 30 minutes each were performed at room temperature post fixation and samples then pre-hybridised at 60°C in pre-heated hybridisation buffer in a hybridisation oven (Hybrigene - Techne). The samples were then incubated in fresh hybridisation buffer at 60°C for one hour in a hybridisation oven.

Fresh DIG labelled riboprobes (for single *in situ* hybridisation) or DNP labelled riboprobes (for double *in situ* hybridisation) were prepared by adding 1 ml of hybridisation buffer to the riboprobes and incubating at 80°C for 5 minutes. Denatured riboprobes were transferred to ice for 5 minutes and then added to 25 ml of hybridisation buffer and maintained at 60°C in a hybridisation oven until use.

Reused DIG or DNP labelled riboprobes were denatured at 80°C for 10 minutes and maintained at 60°C in a hybridisation oven until use.

Pre-hybridised skin explants or embryos were incubated in either, denatured DIG or DIG and DNP labelled riboprobes at 60°C in a hybridisation oven for 36 hours.

2.3.7 Post Hybridisation Wash, Blocking and Antibody Binding

Following hybridisation, the riboprobe solution was transferred to a 50 ml Falcon tube and stored at -20°C. Samples were washed three times in solution I for 30 minutes each at 60°C followed by three washes of solution III for 30 minutes each at 60°C in the hybridisation oven. Followed by three washes with 1X Tris-buffered saline containing 0.1% Tween 20 (TBST) at room temperature. Samples were blocked in 10% heat inactivated sheep serum (HISS) (Millipore, Massachusetts, USA) in 1X TBST containing 2 mM tetramisole hydrochloride (Sigma-Aldrich, Missouri, USA) for 2 hours at room temperature. Anti-digoxigenin-AP, Fab fragments (Roche, Basel, Switzerland) was pre-blocked in 1X TBST containing 1% HISS and 1% heat inactivated chicken embryo powder and diluted at 1/1000 dilution in 1% HISS in 1X TBST containing 2 mM tetramisole hydrochloride. Samples were then incubated in the pre-blocked antibody overnight at 4°C.

2.3.8 Post Antibody Wash & Colour Reaction

Antibody was decanted and stored at 4°C for up to a month. Samples were washed in 1X TBST containing 2 mM tetramisole hydrochloride three times for 10 minutes each at room temperature followed by 5 washes in the same buffer five times for one hour each. Samples were then stored in the buffer overnight at 4°C.

To develop the colour reaction, samples were washed in 1X alkaline phosphatase buffer (NTMT) containing 2 mM tetramisole hydrochloride three times for 10 minutes each at room temperature. This was followed by incubating the samples in developing solution (5-bromo-4-chloro-3-indolyl phosphate/nitroblue tetrazolium (Sigma*Fast*™ BCIP®/NBT tablet) dissolved in Milli-Q water) at room temperature in the dark until a satisfactory signal develops. Samples were washed in 1X PBST three times for 10 minutes each and then imaged with a stereo microscope (Olympus SZX10) using cell^B (Olympus, UK) software. For single *in situ* hybridisation reactions, after imaging the samples were re-fixed in 4% PFA and stored at 4°C.

2.3.9 Double *in situ* Hybridisation

For double *in situ* hybridisation reactions, after imaging, the samples were re-fixed in 4% PFA/0.2% glutaraldehyde in 1X PBST for 30 minutes at room temperature. After fixation, the samples were washed in 1X TBST containing 2 mM tetramisole hydrochloride three times for 30 minutes each at room temperature followed by a blocking in 10% HISS in 1X TBST containing 2 mM tetramisole hydrochloride for 2 hours at room temperature. Alkaline phosphatase anti-DNP antibody (Vector Laboratories, California, USA) was pre-blocked in 1X TBST containing 1% HISS and 1% heat inactivated chicken embryo powder and diluted at 1/1000 dilution in 1% HISS in 1X TBST containing 2 mM tetramisole hydrochloride. Samples were then incubated in the pre-blocked antibody overnight at 4°C.

2.3.10 Post Antibody Wash & Second Colour Reaction

Post antibody washes were performed under the same conditions as described in (Section **2.3.8**). The second colour reaction was developed by incubating the samples in the second developing solution (2.5 mg/ml of 5-bromo-4-chloro-3-indolyl-phosphate/2-(4-iodophenyl)-5-(4-nitrophenyl)-3phenyltetrazolium chloride (BCIP/ INT) stock solution (Roche, Basel, Switzerland) in 1X NTMT containing 2 mM tetramisole hydrochloride) at room temperature in the dark until a satisfactory signal develops. Samples were washed in 1X PBST three times for 10 minutes each and then imaged using the same equipment described in (Section **2.3.8**). After imaging the samples were re-fixed in 4% PFA and stored at 4°C.

2.3.11 Measurement of Pattern Generating Region Width

Measurement of the width of the patterning region of cultured HH 29 dorsal skin explants, as defined by *FGF20* expression was performed using Image-Pro® Plus software (Media Cybernetics Inc., Maryland UA). Width of *FGF20* expression on dorsal skin explants were measured on a minimum of three skin explants per treatment. Average width of *FGF20* expression in treated explants were normalised to those of control explants

2.4 Tissue Embedding and Histology

2.4.1 Paraffin Embedding and Sectioning

Cultured skin explants or whole embryos fixed in 4% PFA (including samples that have undergone *in situ* hybridisation) were washed in 1X PBS three times for 20 minutes each at room temperature.

For cultured skin explants, a section encompassing the entire dorsal tract and femoral tract was excised and covered with a nitrocellulose Millipore filter (pore size 0.45 µm) of equal size. The sample was then encased in Whatman® filter paper, labelled and the filter paper stapled together.

Embryos were prepared by removing the wings, hind limbs and any tissues above the shoulders with a scalpel blade.

Prepared samples were dehydrated through 70%, 90% and 100% ethanol for 2 hours each at room temperature followed by incubation in 1:1 (v/v) ethanol: chloroform (Sigma-Aldrich, Missouri, USA) until the samples lost buoyancy. Samples were then incubated in 100% chloroform overnight at room temperature. After incubation, the chloroform was replaced with molten paraffin and maintained at 60°C overnight in an oven. The samples were transferred to metallic moulds containing fresh molten paraffin, oriented, and allowed to set. Paraffin embedded samples were mounted on a Leica M26 microtome and 8 µm sections were cut across the dorsal tract. Sections were transferred to a heated 37°C water bath and collected on Superfrost™ microscope slides (Thermo Scientific, Massachusetts, USA). Sections were dried overnight on a heated 37°C slide drying bench (Electrothermal) and stored in slide boxes at room temperature until use.

2.4.2 Cryosectioning

Epidermal/dermal recombination skin explant cultures fixed in 4% PFA were transferred and stored in 15% sucrose in 0.12 M sodium phosphate buffer overnight at 4°C. The sucrose solution was removed from the explants and explants were trimmed

to size with a scalpel blade. Explants were then incubated in 15% sucrose/7.5% gelatine in 0.12 M sodium phosphate buffer at 37°C for 30 minutes. Explants were transferred to a mould, orientated, covered with 15% sucrose/7.5% gelatine solution and allowed to set at room temperature. The embedded skin explant was removed from the mould using a scalpel blade and fixed to a wooden cork with O.C.T. compound (VWR International, Pennsylvania, USA). The sample was then flash frozen in a plastic beaker containing isopentane which was cooled to -65°C on dry ice. Frozen blocks were stored at -80°C until use.

Blocks was fixed to a metal chuck, cork side down, with O.C.T. compound and placed on dry ice for 10 minutes to solidify. 10 µm thick sections were cut using a Bright OTF cryostat (A-M Systems, Livingston, UK) in a chamber and sample temperature of -24°C and -27°C respectively and collected on Superfrost™ microscope slides. Slides containing sections were stored at -80°C until use.

2.4.3 Haematoxylin and Eosin Staining of Paraffin Sections

Sections were stained with haematoxylin (Leica, Wetzlar, Germany) and eosin using the Leica Autostainer XL system using the following program. Sections were first de-waxed in three washes of xylene for 5 minutes each and then washed in 100% ethanol twice, once for 3 minutes and once for 2 minutes. This was followed by a wash in 95% ethanol for 2 minutes then soaked in water for 5 minutes. Sections were stained in filtered haematoxylin for 3 minutes and washed twice in water for 3 minutes each. After washing, the sections were soaked in Scott's tap water (Leica, Wetzlar, Germany) for 2 minutes, washed again in water for 2 minutes before being stained in eosin for 2 minutes. The stained sections were washed in water for 45 seconds and then dehydrated through a series of increasing ethanol dilutions from 70% to 100% for 30 seconds each, including a second wash of 100% ethanol for 1 minute. Finally the sections were washed in 1:1 (v/v) ethanol xylene for 1 minute followed by three washes of xylene for 1 minute each. Sections were mounted using D.P.X. mountant for histology (Sigma-Aldrich, Missouri, USA) and cover-slipped and allowed to cure

over night at room temperature. Sections were imaged using a Nikon Eclipse E600 microscope using Zen2012 (Blue) software (Zeiss, Oberkochen, Germany).

2.4. 4 4', 6-diamidino-2-phenylindole (DAPI) Staining of Cryosections

Sections stored in -80°C were warmed at room temperature for 5-10 minutes and then washed in pre-warmed 1X PBS at 37°C for 30 minutes to remove the gelatine. The sections were placed in a slide staining tray and covered in 1/1000 dilution of DAPI in 1X PBS for 3 minutes in the dark. After staining, sections were washed in 1X PBS twice for 10 minutes each. The sections were mounted in ProLong® Gold antifade reagent (Life Technologies) and cured overnight in the dark at 4°C. Sections were imaged with an inverted confocal microscope (Zeiss LSM 710) using the Zen2012 (Blue) software (Zeiss, Oberkochen Germany).

2.5 Solutions

1X Alkaline Phosphatase Buffer (NTMT)

0.1 M NaCl, 0.1 M Tris HCL (pH 9.5), 0.05 M magnesium chloride ($MgCl_2$), 0.01% (v/v) of Tween 20, 2 mM of tetramisole hydrochloride in Milli-Q water.

BCIP/INT Alkaline Phosphatase Substrate Developing Solution (*In situ* Hybridisation)

2-(4-iodophenyl)-5-(4-nitrophenyl)-3phenyltetrazolium chloride stock solution (Roche, Basel, Switzerland) was diluted in 1/133 in 1X NTMT and protected from light.

BCIP/NBT Alkaline Phosphatase Substrate Developing Solution (*In situ* Hybridisation)

One Sigma*Fast*™ BCIP®/ NBT tablet was dissolved in 10 ml of Milli-Q water and protected from light. This was scaled up accordingly depending on the final volume of colouring solution required.

Buffer P1 (Qiagen - Plasmid Maxi Kit)

50 mM Tris HCl (pH 8.0), 10 mM EDTA, and 100 µg/ml RNase A.

Buffer P2 (Qiagen - Plasmid Maxi Kit)

200 mM NaOH, and 1% (w/v) SDS.

Buffer P3 (Qiagen - Plasmid Maxi Kit)

3 M KCH_3COO (pH 5.5).

Buffer QBT (Qiagen - Plasmid Maxi Kit)

750 mM NaCl, 50 mM 3- morpholinopropanesulphonic acid (MOPS) (pH 7.0), 15% (v/v) isopropanol, and 0.15% (v/v) Triton® X-100.

Buffer QC (Qiagen - Plasmid Maxi Kit)

1 M NaCl, 50 mM MOPS (pH 7.0), and 15% (v/v) isopropanol.

Buffer QF (Qiagen - Plasmid Maxi Kit)

1.25 M NaCl, 50 mM Tris HCl (pH 8.5), and 15% (v/v) isopropanol.

10X Calcium-Magnesium Free Saline

1.37 M NaCl, 0.04 M of KCl, 4 mM of NaH_2PO_4, 1.8 mM of KH_2PO_4, 0.12 M of sodium bicarbonate ($NaHCO_3$) and 0.11 M of glucose in Milli-Q water. pH was adjusted to 7.5 using HCl.

Cell Lysis Solution (Promega - Wizard® *Plus* Minipreps DNA Purification System)

0.2M NaOH, and 1% (w/v) SDS.

Cell Resuspension Solution (Promega - Wizard® *Plus* Minipreps DNA Purification System)

50 mM Tris HCL (pH 7.5), 10 mM EDTA, and 100 µg/ml RNase A.

Column Wash Solution (Promega - Wizard® *Plus* Minipreps DNA Purification System)

60 mM KCH_3COO, 8.3 mM Tris HCl (pH 7.5), 0.04 mM EDTA (pH 8.0), and 60% (v/v) ethanol.

0.01% Diethylpyrocarbonate (DEPC) in 1X PBS

0.01% (v/v) of DEPC was added to 1X PBS. The mixture was vigorously shaken for a few minutes and incubated overnight and autoclaved.

DNA Ladder

HyperLadder™ 1 kb or HyperLadder™ 100 bp (Bioline, London, UK) was used throughout this project.

Heat Inactivated Sheep Serum (HISS)

Sheep serum (Millipore, Massachusetts, USA) was heated to 56°C for 30 minutes and stored at -20°C.

10% HISS/TBST Blocking Solution

1X TBST was mixed with 10% (v/v) of HISS and stored at -20°C.

Hybridisation Buffer

50% (v/v) of formamide (Sigma-Aldrich, Missouri, USA) 5X saline-sodium citrate (SSC) buffer (Sigma-Aldrich, Missouri, USA), 1% (w/v) sodium dodecyl sulphate (SDS), 50 µg/ml yeast RNA (Ambion® Life Technologies, Massachusetts, USA), 50 µg/ml heparin sulphate sodium salt (Sigma Aldrich, Missouri, USA) in Milli-Q water.

Lysogeny Broth (LB)

LB medium was prepared by mixing together 1% (w/v) Bacto™ - Tryptone (Becton Dickinson, New Jersey, USA), 0.5% (w/v) yeast extract, 1.5% sugars (Difco) and 125 mM NaCl in ddH_2O. pH was adjusted to 7.0 using 1 M NaOH then autoclaved at 15 psi for 20 minutes on liquid cycle. LB agar was prepared by adding 15 g/L of agar to LB medium before autoclaving.

Neutralisation Solution (pH 4.2) (Promega - Wizard® *Plus* Minipreps DNA Purification System)

4.09 M guanidine hydrochloride, 0.759 M KCH_3COO, and 2.12 M glacial acetate acid.

4% Paraformaldehyde (PFA)

4% (w/v) paraformaldehyde crystals in 0.01% DEPC treated 1X PBS. Stored at -20°C.

1X PBS Tween (PBST)

0.1% (v/v) of Tween 20 (Sigma-Aldrich, Missouri, USA) was mixed with 0.01% DEPC treated 1X PBS.

1% Penicillin-Streptomycin in 1X PBS

1% (v/v) penicillin-streptomycin (Invitrogen, Massachusetts, USA) was diluted in 1X PBS and stored at 4°C.

1X Phosphate Buffered Saline (PBS) pH 7.4

Oxoid^{TM} phosphate buffered saline tablet (Thermo Scientific, Massachusetts, USA) was dissolved in ddH_2O as per manufacturer's instructions and pH adjusted using 1 M HCl. Each tablet contains 8 g/L of sodium chloride (NaCl), 0.2 g/L of potassium chloride (KCl), 1.15 g/L of disodium hydrogen phosphate (NaH_2PO_4) and 0.2 g/L potassium dihydrogen phosphate (KH_2PO_4).

20X SSC Buffer

SSC Buffer 20X Concentrate (Sigma-Aldrich, Missouri, USA) contains, 3 M NaCl in 0.3 M sodium citrate buffer (pH 7.0) in ultrapure water.

0.24 M Sodium Phosphate Buffer (pH 7.2)

46 mM $NaH_2PO_4.H_2O$ and 0.225 M NaH_2PO_4 in Milli-Q water. pH was adjusted using HCl.

0.12 M Sodium Phosphate Buffer/15% Sucrose

15% (w/v) sucrose was dissolved in 0.12 M sodium phosphate buffer (0.24 M sodium phosphate buffer diluted 1:1 in Milli-Q water). The solution was stored at 4°C until use.

0.12 M Sodium Phosphate Buffer/15% Sucrose/7.5% Gelatin

Prepared 0.12 M sodium phosphate buffer/15% sucrose solution was supplemented with porcine skin type A gelatin (Sigma-Aldrich, Missouri, USA) to a final concentration of 7.5% (w/v). The gelatin was dissolved by heating the mixture to 37°C and stored at -20°C.

Solution 1 (*In situ* Hybridisation)

50% (v/v) of formamide, 5X SSC buffer, 1% (w/v) SDS in Milli-Q water.

Solution 3 (*In situ* Hybridisation)

50% (v/v) of formamide, 2X SSC buffer in Milli-Q water.

1X TBS Tween (TBST)

0.1% (v/v) of Tween 20 was dissolved in a 1/10 dilution of 10X TBS stock in Milli-Q water supplemented with tetramisole hydrochloride (Sigma-Aldrich, Missouri, USA) to a final concentration of 2 mM

50X Tris Acetate-EDTA (TAE) Buffer

2 M Tris base, 1 M of glacial acetic acid and 50 mM EDTA in ddH_2O.

10X Tris Buffered Saline (TBS)

1.37 M NaCl, 0.027 M of KCl, and 0.19 M of Tris-HCl in Milli-Q water and adjusted to pH 7.5 using NaOH.

Tris/EDTA (TE) Buffer (pH8)

10 mM Tris hydrochloride and 1 mM EDTA in ddH_2O.

RESULTS

3. RESULTS

3.1 Feather Primordium Formation during Embryonic Chicken Development

3.1.1 Observations of Cell Movement - Feather Pattern Development

The CAG-GFP transgenic chicken line (hereby referred to as GFP chicken) expresses cytoplasmic GFP, under the control of a ubiquitous promoter (McGrew *et al.*, 2008), providing a tool for tissue grafting, lineage tracing and cell tracking studies (Barraud *et al.*, 2010; Towers *et al.*, 2011; Zhao *et al.*, 2010). Through the use of the *ex vivo* skin explant culture system, the GFP chicken provides an opportunity to observe the process of feather primordium formation in real time and to observe how modulating various signalling pathways may impact the process.

Feather primordium induction in the dorsal tract was observed in real time in dorsal skin explants prepared from HH 29 GFP chicken embryos and cultured over a period of 60 hours. (**Video 1 & Figure 28a**). At time 0 h, the primary stripe is clearly visible in the middle of the explant as a region of intense GFP signal, indicating a high dermal cell density. Surrounding regions of the skin displayed a lower, homogenously distributed GFP signal. Over a period of 12 hours, the primary stripe separates into discrete cell condensates, forming the primary row of feather primordia. Individual feather primordia are observed as discrete regions of intense GFP signal (high cell density) separated by interbud domains displaying low GFP signals (low cell density). Once the primary row is established, new rows of primordia begin to form on either side of the primary row. This is observed as a gradual increase in GFP signal/cell density on either side of the primary row of feather primordia. Cells in skin regions outwith the feather primordium forming region remain homogenously distributed. As development of the explant continues, subsequent rows of primordia are formed across the entire field of view in a wave-like manner, at a rate of 8-10 hours per row. After 48 hours in culture, the initial primary row of feather primordia begins to differentiate, developing an anterior-posterior axis, as indicated by an increase in GFP signal on the posterior end of the feather primordia. The subsequent feather primordium rows gradually differentiate, beginning with the rows immediately adjacent to the primary

row of primordia. Meanwhile the feather primordia in the primary row begin their outward growth, forming the first row of feather buds.

At a higher magnification, the induction and formation of an individual feather primordium at the dorsal midline (where the initial row of primordia form) was observed in real time in HH 29 dorsal skin prepared from GFP chicken embryos (**Video 2 & Figure 28b**). This allowed me to observe cell behaviour prior to and during the process of feather primordium formation. In endogenous primordium formation, initially, cells are distributed homogenously and move around, undirected, across the field. After a period of 2 to 4 hours, cells begin to show directed movement towards the centre of the field of view, forming a cell condensate. Over the next 4 hours, cells in close proximity to the condensate move rapidly towards the condensate, enlarging it in the process until a maximum cell density is reached and the condensate stops increasing in size. Once the condensate has reached its maximum density, cells surrounding the condensate appear to not migrate towards or contribute to the condensate but display random movements similar to those observed in cells prior to the formation of the condensate.

The above observations suggest that during feather primordium formation, the induction of directed cell movement and cell aggregation is an integral part of the primordium forming process.

The use of the GFP chicken embryo to follow the process of feather primordium pattern formation allowed me to identify whether primordium patterning requires the formation of a molecular pre-pattern, to guide cell condensate formation, during skin development. The cellular pattern can be observed through the detection of the GFP signal, while the molecular pattern can be observed through the use of *in situ* hybridisation, to detect gene markers of feather primordium formation in the same skin sample. If the formation of a molecular pre-pattern is required for the formation of the feather pattern, then the appearance of a molecular pattern would precede the appearance of a cellular pattern. HH 29 GFP dorsal skin explants, were cultured for 24 hours and then fixed in paraformaldehyde after three rows of feather primordia

formed, and the beginnings of new primordium formation, lateral to the three defined rows, can be observed (**Figure 29**). The molecular periodic pattern of all the genes examined in this experiment, overlaps with the cellular periodic pattern. The focalisation of gene expression to within the forming/formed feather primordia or interbud domains, completely overlaps with the GFP signal. The results demonstrate that the formation of the feather primordia and the pattern of their arrangement do not arise from a molecular based pre-patterning system. The observed cellular rearrangements appear to occur simultaneously with changes in the molecular expression pattern.

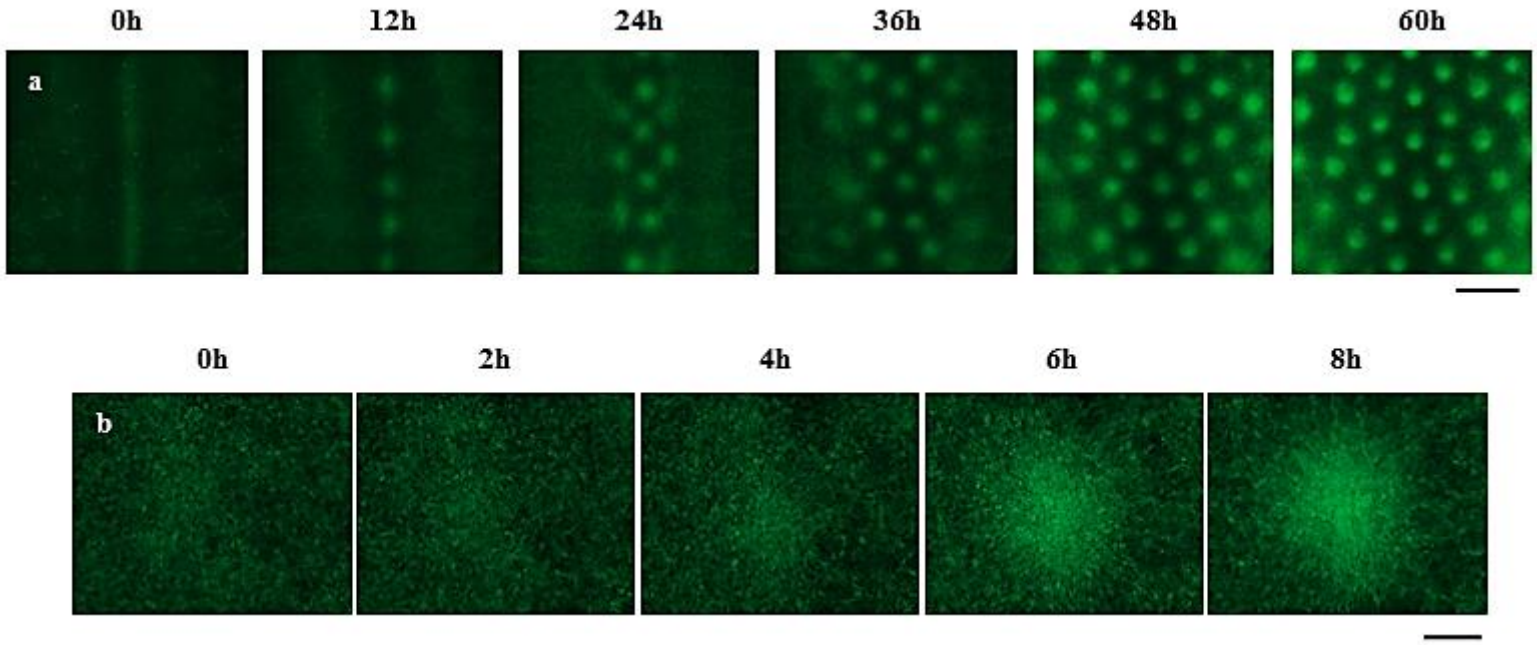

Figure 28. Feather primordium formation during embryonic chicken development ex vivo. a) Time series of feather primordium formation during dorsal tract development in a GFP chicken skin explant cultured for a period of 60 hours from HH stage 29. Intense GFP signal correlates with regions of high cell density (feather primordia). Explants positioned in an anterior-posterior orientation (top to bottom of the panel). **b)** Magnified view of a time series of feather primordium induction from the dorsal midline of an *ex vivo* HH 29 GFP chicken skin explant over a period of 8 hours. Scale bar **a)** - 500 µm **b)** - 100 µm.

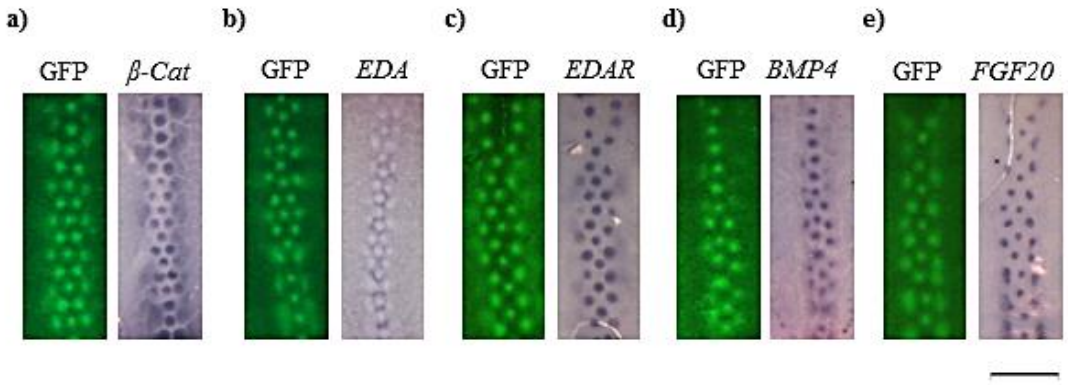

Figure 29. Primordium formation does not follow a molecular pre-pattern. Dorsal skin explants from GFP chicken embryos cultured for 24 hours and hybridised for **a)** *β-Catenin,* **b)** *EDA*, **c)** *EDAR*, **d)** *BMP4,* and **e)** *FGF20* expression. Regions of intense GFP signal correlates with areas of high cell density (primordia) which overlaps completely with the molecular markers of primordium formation. Scale bar - 1 mm.

3.1.2 *FGF20* Functions as a Chemoattractant in Embryonic Chicken Skin

The appearance of cell movement towards the forming endogenous cell condensate implies that chemotaxis plays an important role in the formation of cell aggregates, as suggested by Lin *et al* 2009 (Lin *et al.*, 2009).The importance of FGF protein family members in the induction of cell condensates in *ex vivo* skin culture has been known for many years (Jung *et al.*, 1998; Patel *et al.*, 1999; Song *et al.*, 1996; Song *et al.*, 2004). The recent identification of a defect in the *FGF20* gene underlying the scaleless trait (Wells *et al.*, 2012) further demonstrates the key role FGF signalling plays in feather primordium induction. Although the underlying defect in scaleless mutation has been identified, the function of endogenous *FGF20* in wild type feather forming skin has not yet been shown. Past studies have shown that recombinant FGF2 (Song *et al.*, 1996; Song *et al.*, 2004) and FGF4 proteins (Jung *et al.*, 1998; Patel *et al.*, 1999; Widelitz *et al.*, 1996) can induce the formation of or enlarge existing dermal cell condensates in either wild type or scaleless skin, however these FGFs belong to a different subfamily compared to that of FGF20, which is a member of the FGF9 subfamily (Itoh and Ornitz, 2004).

To address this, the effect of FGF20 on feather primordium induction in HH 29 GFP chicken skin explants was tested through the use of recombinant FGF9 protein. Recombinant human FGF20 (rhFGF20) protein does not display any signalling activity when tested on dorsal skin explant cultures. Explants treated with rhFGF20 do not display any phenotypic differences compared to control explants and the expression of downstream FGF signalling targets is unaffected by rhFGF20 treatment, as detected by qRT-PCR (data not shown). Instead, recombinant human FGF9 (rhFGF9) protein was used to indirectly mimic FGF20 activity because the two proteins are within the same subfamily of FGFs and may signal through the same set of FGFRs to exert their activity (Ornitz and Itoh, 2015).

In control explants cultured in the presence of BSA (bovine serum albumin) coated beads placed to the left of the dorsal midline, the endogenous process of primordium induction is unaffected by the presence of the bead (**Video 3 & Figure 30a**). Cells

move in an undirected manner across the field and around the bead, until the induction of endogenous cell condensate formation begins (indicated by arrows). Cells within close proximity to the condensate then begin to show directed movement towards the condensate. Thus the bead itself, and the BSA, do not attract cells or impairs endogenous primordium formation.

When a bead coated in rhFGF9 was placed on the dermis side of the explant in close proximity to the primary stripe and cultured, the formation of endogenous cell condensates is affected by the rhFGF9 coated bead (**Video 4 & Figure 30b**). At T0h the primary stripe visible as a region of high cell density. The cells around the bead respond to the presence of rhFGF9 and rapidly migrate towards the source of recombinant FGF protein, forming a cell aggregate around the bead. Over the duration of the culture, cells in direct contact with the bead swarm around the bead while cells at a distance from the bead migrate towards the source of rhFGF9 protein, enlarging the cell condensate in the process. The observation suggests that local sources of FGF proteins function as guidance cues to stimulate cell migration and aggregation around FGF sources.

The stimulation of cell migration towards rhFGF9 coated beads is dependent on the activation of FGF signalling (**Figure 31**). HH 29 GFP skin explants treated with BSA or rhFGF9 coated beads were cultured for 24 hours in either control medium or medium containing 15 µM of SU5402 (an inhibitor of FGF signalling). BSA bead treated explants cultured in control medium displayed a normal sequence of feather primordium formation which was unaffected by the presence of the bead (**Figure 31a**). Supplementing the culture medium with SU5402 inhibited the formation of endogenous feather primordia in BSA bead treated explants (**Figure 31b**). Explants treated with rhFGF9 coated beads in control medium were able to induce the formation of local cell aggregates around the beads (**Figure 31c**). However, when rhFGF9 bead treated explants were cultured in SU5402 supplemented medium, both the formation of endogenous feather primordia and the local induction of cell aggregation around the rhFGF9 sources were inhibited (**Figure 31d**). The results suggest that FGF signalling is required to induce cell migration towards sources of FGF protein.

In the above results I have demonstrated that the activation of the FGF signalling pathway by beads coated in rhFGF9 protein can stimulate cell migration and cell condensate formation around local sources of rhFGF9. However, when skin explants are cultured in rhFGF9 supplemented medium, endogenous feather primordium formation is completely inhibited (**Figure 32**). In untreated HH 29 control explants after 24 hours in culture, *in situ* hybridisation detection of *FGF20* expression (a marker of feather primordium formation), reveals that three rows of feather primordia have developed on the explant. In explants cultured in medium supplemented with 1 µg/ml rhFGF9, *FGF20* expression is not observed, indicating the absence of feather primordia in the treated explant. The observation suggests that stimulation of the FGF signalling pathway alone, cannot induce the formation of feather primordia. It appears that local sources of FGF proteins are required to induce the formation of discrete cell condensates. When FGF signalling is stimulated ubiquitously throughout the explant by rhFGF9 proteins in the culture medium, the absence of a local guidance cue prevents directed cell movement and clustering of cells.

These results show that FGF9 subfamily members have the ability, like other members of the FGF family, to induce chemotaxis of nearby cells and the formation of dermal cell condensates in skin explants in a manner analogous to endogenous condensate formation. However, induction of chemotaxis requires the local delivery of recombinant FGF proteins, rather than general stimulation of the FGF signalling pathway. This suggests that FGF proteins function as local guidance cues, to guide cells towards sources of FGF protein, during the formation the induction and formation of feather primordia.

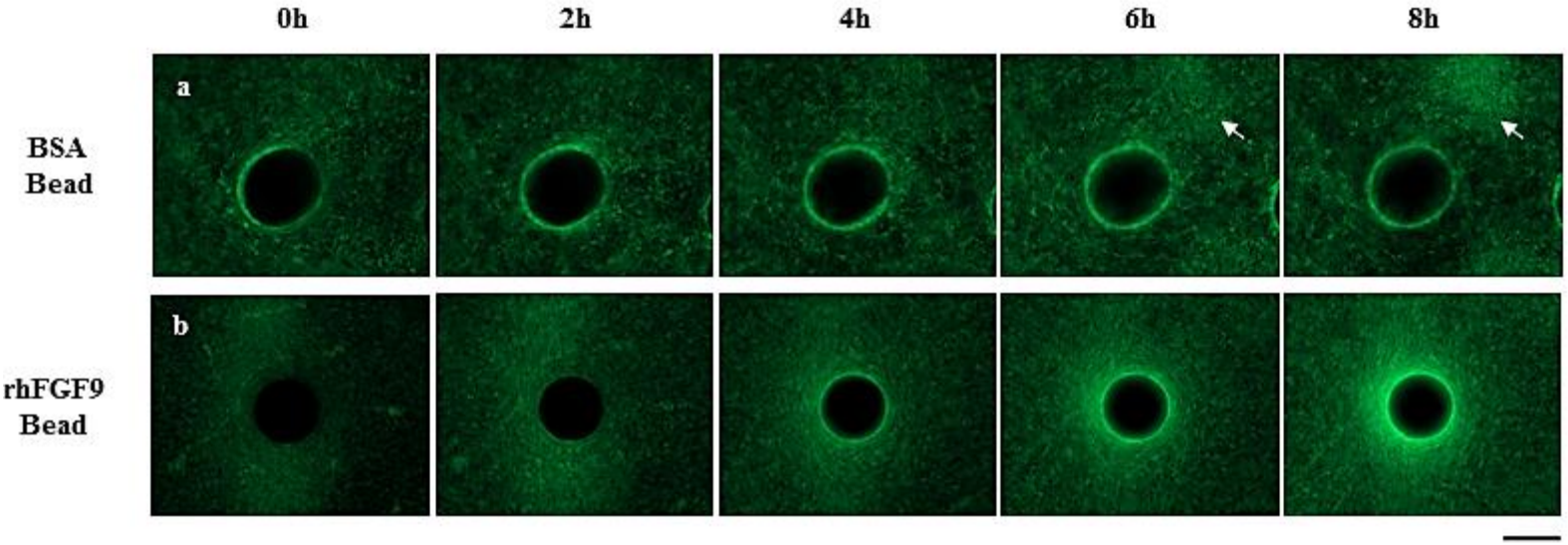

Figure 30. rhFGF9 induces cell aggregation. Time series of feather primordium induction from the dorsal midline of an *ex vivo* HH 29 GFP chicken skin explant over a period of 8 hours. Intense GFP signal correlates with regions of high cell density. **a)** BSA coated beads affect the normal process of primordium formation. Arrows indicate formation of an endogenous primordium. **b)** rhFGF9 coated bead stimulates cell aggregation towards the bead, forming a condensate around it. Scale bar - 100 µm.

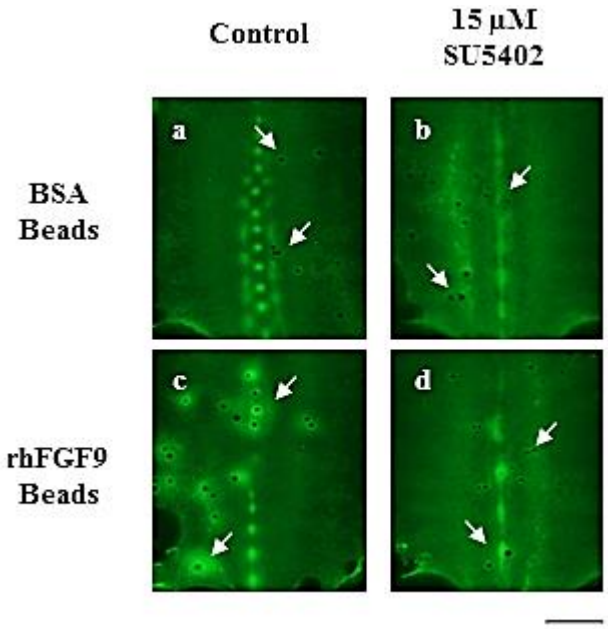

Figure 31. Blocking FGF signalling inhibits the formation of cell aggregates. a) HH 29 GFP skin explants cultured in the presence of BSA treated beads for 24 hours develop with no obvious effects. **b)** Application of 15 µM of SU5402 to BSA bead treated explants inhibit the formation of endogenous feather primordia. **c)** In the presence of rhFGF9 coated beads, cell migration towards sources of FGF protein is induced and cell aggregates form. **d)** Co-treatment of explants with both rhFGF9 coated beads and SU5402 inhibited the formation of cell migration towards the rhFGF9 beads. (White arrows indicate the position of beads) Scale bar - 1 mm.

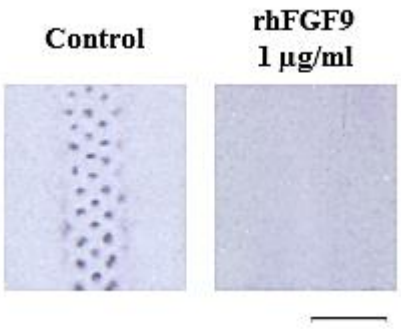

Figure 32. Local sources of FGF protein are required for the induction/formation of feather primordia. When HH 29 wild type skin explants were cultured in medium supplemented with 1 µg/ml of rhFGF9, the formation of endogenous feather primordia was completely inhibited, as detected by *FGF20* expression (a marker of feather primordium formation). Scale bar - 1 mm.

3.1.3 Cell Movement, Rather Than Cell Proliferation, is the Primary Driver Feather Primordium Formation

The induction of chemotaxis by rhFGF9 protein suggests that cell movement is an integral part of dermal cell condensate formation. The effect of inhibition of cell movement on endogenous and experimentally induced cell condensate formation via the treatment of skin explants with latrunculin A (an inhibitor of actin polymerisation) was therefore investigated (**Figure 33**). BSA coated beads did not affect the process of feather primordium formation of HH 29 dorsal skin explants after 24 hours in culture (**Figure 33a**). GFP skin explants treated with rhFGF9 beads displayed the formation of dermal cell aggregates as expected (**Figure 33b**). Inhibition of cell movement prevented the formation of endogenous primordia as well as the formation of cell aggregates around rhFGF9 coated beads (indicated by arrows), showing that an actin polymerisation dependent process is required for all movement of cells towards sources of FGF proteins (**Figure 33c**).

Cell movement appears to be required for the formation of feather primordia, however, whether cell proliferation may also have a role in the process has yet to be demonstrated. Cell proliferation was inhibited by culturing HH 29 dorsal skin explants prepared from wild type chicken embryos with the dihydrofolate reductase inhibitor, methotrexate (**Figure 34**). After 48 hours in culture, explants cultured in medium supplemented with 5 μM methotrexate were still capable of forming feather primordia, (as detected by *β-Catenin* expression through *in situ* hybridisation). However, the number of feather primordia formed in treated explants were reduced compared to control explants.

Taken together, the results suggest that cell movement, rather than cell proliferation plays a major role in the formation of feather primordia, but cell proliferation may regulate the number of feather primordia that are capable of forming on the skin.

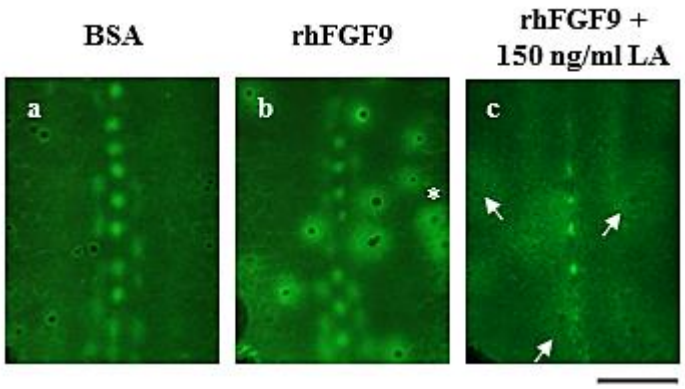

Figure 33. Blocking cell migration inhibits the formation of cell aggregates. a) HH 29 GFP skin explants cultured in the presence of BSA treated beads for 24 hours develop with no obvious effects. **b)** rhFGF9 coated beads stimulates cell aggregation around the source which can displace or inhibit the formation of native primordia in close proximity of the bead. Cell aggregates still form around beads outside of the patterning region (*). **c)** Addition of 150 ng/ml of latrunculin A to rhFGF9 coated bead treated skin inhibits the formation of endogenous primordia as well as cell aggregation around the beads (arrows). Scale bar - 1 mm.

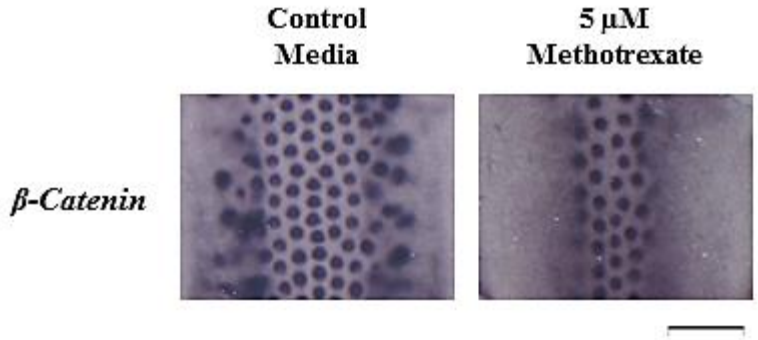

Figure 34. Blocking cell proliferation does not inhibit the formation of individual feather primordia. HH 29 WT skin explants cultured in medium supplemented with 5 µM of methotrexate reduces the number of formed primordia, but the formation of individual feather primordia is unaffected by the treatment . Scale bar - 1 mm.

3.1.4 FGF20 Functions as an Activator in Feather Primordium Induction

The reaction-diffusion model as proposed by Turing (Turing, 1952) and later refined by Gierer and Meinhardt (Gierer and Meinhardt, 1972) proposed a general mechanism to explain the autonomous pattern formation process in biological systems. In the formation of feather primordia, molecules such as FGFs and WNTs have been proposed as candidate activators during the induction of feather primordia based on their ability to promote feather primordium fate (Mandler and Neubuser, 2004; Noramly *et al.*, 1999; Song *et al.*, 1996; Song *et al.*, 2004; Wells *et al.*, 2012; Widelitz *et al.*, 2000). However, an activator as defined by Turing has yet to be to be discovered, that is, a molecule which can promote its own production and the production of its own inhibitor.

One of the main properties of an activator, as defined by Turing, is the ability to self-activate. Previous studies demonstrated that recombinant FGF proteins were capable of inducing the formation of dermal cell condensates but did not test the FGF's effect on its own production. To determine whether the FGF9 subfamily members of FGFs can stimulate their own expression, HH 29 GFP skin explants were cultured for 24 hours in the presence of rhFGF9 coated bead. Expression of *FGF20* was detected through *in situ* hybridisation (**Figure 35**). In control BSA bead treated skin explants, *FGF20* was detected only in the mature or developing feather primordia (**Figure 35a**). Upon application of rhFGF9 coated beads, ectopic expression of *FGF20* was detected in the region surrounding the bead suggesting a local self-activation process (black arrows) (**Figure 35b**). It should also be noted that, rhFGF9 coated beads are capable of disrupting the native patterning process and can displace endogenous primordium formation. Cells in the explant appear to preferentially move to the highest concentrations of FGF regardless of whether the original source of FGF proteins is endogenous or artificial.

Another property of an activator is the ability to induce the expression of its own inhibitor, forming a negative feedback loop. Previous studies showed that BMP protein family members have the ability to inhibit the induction of feather primordia (Jung *et*

al., 1998; Michon *et al.*, 2008; Noramly and Morgan, 1998; Patel *et al.*, 1999). BMP12, along with the selective expression of retinoic acid in the neck, inhibits the formation of feathers on the neck of a chicken displaying the naked neck trait (Mou *et al.*, 2011). BMPs therefore make ideal candidates as inhibitors in the Turing reaction-diffusion model. The effect of rhFGF9 treatment of HH 29 dorsal skin explants on *BMP4* expression was thus tested and analysed through qRT-PCR (**Figure 36**). After 5 hours, explants cultured in medium supplemented with 1 µg/ml rhFGF9 displayed comparable levels of *BMP4* expression to the those observed in control samples (n=3). The result suggests that rhFGF9 does not have a direct effect on *BMP4* expression.

Jung *et al*, 1998 and Song *et al*, 2004 previously demonstrated through *in situ* hybridisation the induction of *BMP* expression in dermal cell condensates induced by recombinant FGF proteins (Jung *et al.*, 1998; Song *et al.*, 2004). I therefore determined whether the dermal cell condensates induced by rhFGF9 coated beads would also express *BMP4* via *in situ* hybridisation analysis (**Figure 37**). HH 29 GFP dorsal skin explants were cultured for 24 hours in in the presence of either BSA or rhFGF9 coated beads. In control, BSA bead treated explants, *BMP4* expression is readily detectable in a similar expression pattern to that of *FGF20*, within the developing or developed feather primordia (**Figure 37a**). rhFGF9 beads induced the formation of dermal cell condensates and also the expression of *BMP4* around the bead, suggesting that rhFGF9 is capable of inducing *BMP4*, expression but indirectly through induction of cell condensation formation (**Figure 37c**).

BMP4 induction was only detected within the developing or developed dermal cell condensates, and so the effect on *BMP4* expression in cell movement inhibited, rhFGF9 bead treated explants was examined. Addition of 150 ng/ ml latrunculin A to culture medium inhibited the expression of *BMP4* in explants treated with control BSA beads, except at the dorsal midline where cell density is highest (**Figure 37b**). Explants co-treated with rhFGF9 beads and latrunculin A in the culture medium displayed a reduction in *BMP4* expression around the beads in comparison to the expression levels of *BMP4* in explants treated with only rhFGF9 beads (**Figure 37d**). Latrunculin A treatment itself does not affect *BMP4* expression levels, as revealed through qRT-PCR

analysis of HH 29 dorsal skin explants cultured in latrunculin A supplemented medium for 5 hours (n=3) (**Figure 38**). The qRT-PCR result indicates that the observed effect of inhibition of *BMP4* expression around the rhFGF9 coated bead in co-treated explants is not a direct effect of latrunculin A treatment itself. Taken together the results suggests cell aggregation is required for the induction of *BMP4* expression during feather primordium formation.

Thus far, the results presented suggest that FGF20 can potentially function as an activator during primordium induction due to rhFGF9's ability to induce the formation of cell condensates and also induce the expression of *FGF20* and *BMP4*. The requirement of cell aggregation in the induction of *BMP4* suggests that the mechanism behind primordium formation does not strictly follow a basic reaction-diffusion model as described by Turing. A model that includes a mixture of chemical and mechanical regulation may better explain *in vivo* feather primordium induction more accurately.

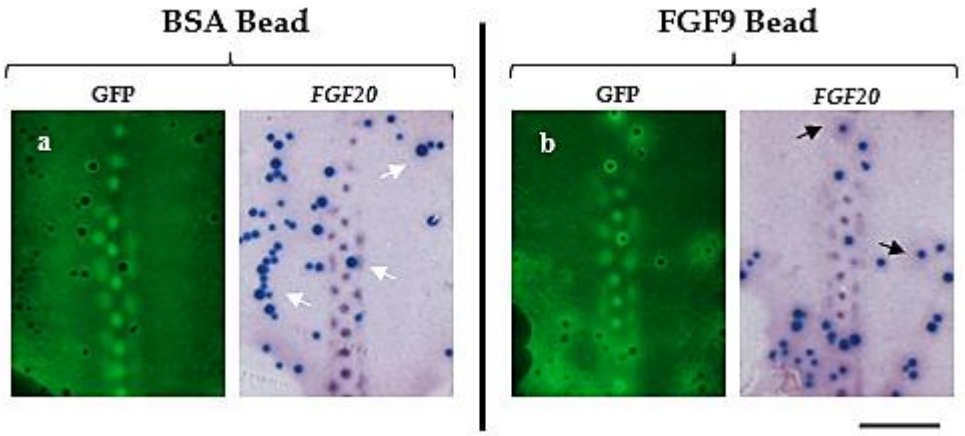

Figure 35. Local application of rhFGF9 stimulates cell movement towards the source and the expression of *FGF20*. a) Detection of *FGF20* transcripts in GFP skin explants cultured for 24 hours revealed localised expression of *FGF20* confined to developed and developing primordia and was unaffected by the presence of a BSA coated bead (white arrows). **b)** rhFGF9 coated beads induced the expression of *FGF20* in an area around the bead (black arrows). Scale bar - 1 mm.

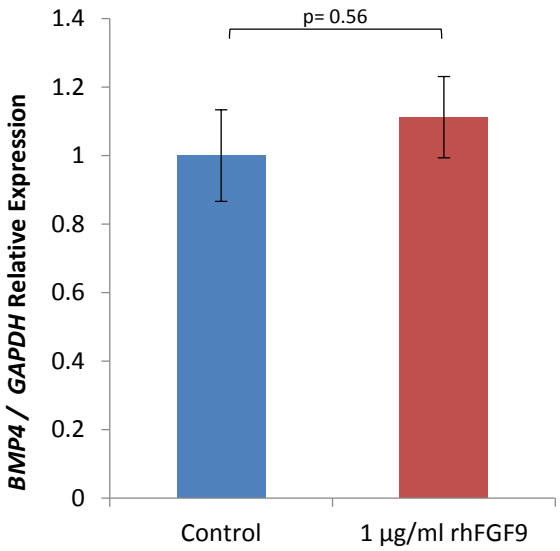

Figure 36. rhFGF9 does not directly induce *BMP4* expression in dorsal skin explants. Quantitative RT-PCR detecting *BMP4* in HH 29 skin explants cultured in the presence or absence of soluble rhFGF9 for 5 hours. These results indicate that, 1 µg/ml rhFGF9 does not have a direct effect on *BMP4* expression (n=3). Bars represent standard error of mean (SEM).

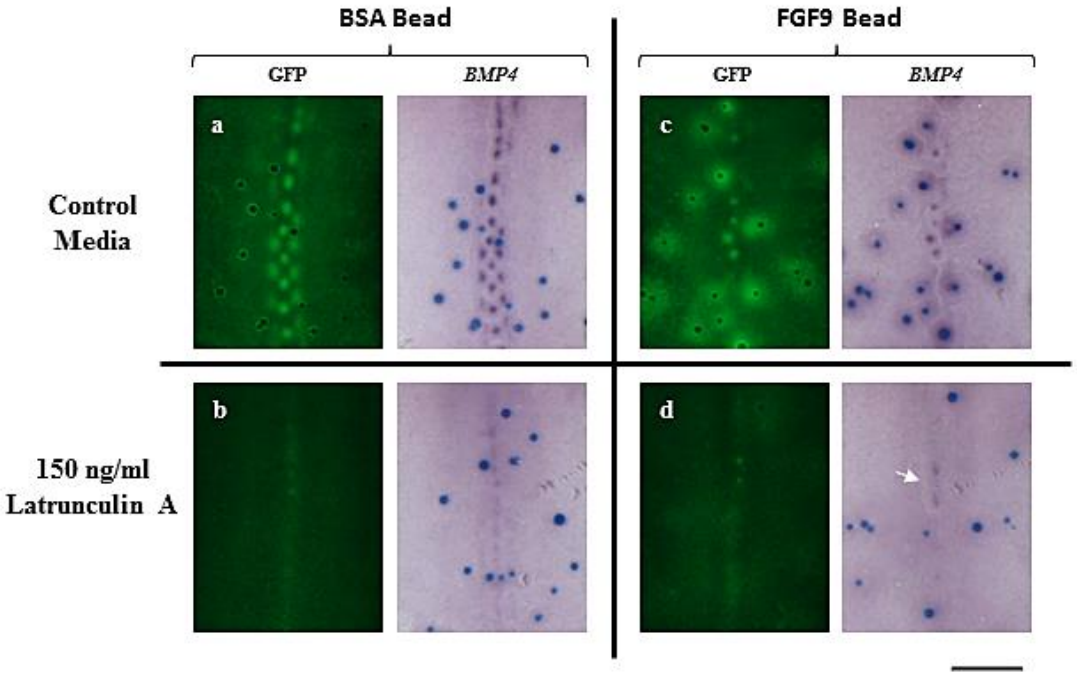

Figure 37. Activation of *BMP4* expression requires cell aggregation. Dorsal skin explants from HH 29 GFP chicken embryos cultured for 18 hours in the presence or absence of latrunculin A and hybridised with *BMP4* antisense probe. **a)** *BMP4* is only expressed in developing or developed feather primordia. **b)** *BMP4* is only expressed in the remnants of the dorsal midline where cell density is highest when cell movement is blocked. **c)** FGF9 coated beads stimulates the expression of *BMP4* in a local area around the bead. **d)** Inhibition of cell movement decreases the expression of *BMP4* around the FGF9 treated bead but *BMP4* remains detectable in remaining endogenous primordia (arrow). Scale bar - 1 mm.

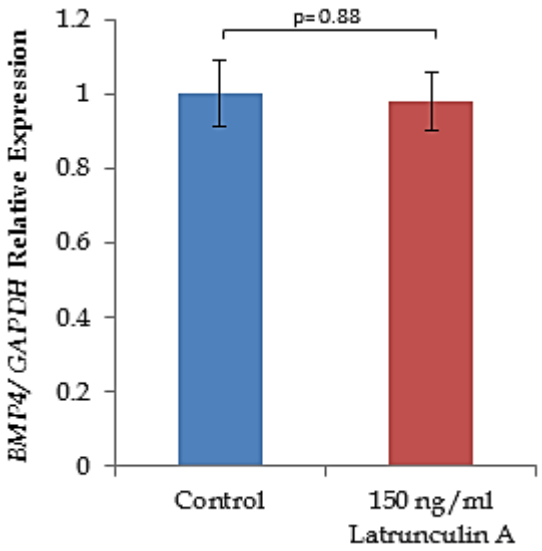

Figure 38. *BMP4* expression is unaffected by treatment of dorsal skin explants with Latrunculin A. Quantitative RT-PCR detecting *BMP4* in HH 29 skin explants cultured in the presence or absence of 150 ng/ml of latrunculin A for 5 hours showing latrunculin A does not have a direct effect on *BMP4* expression (n=3). Error bars represent SEM.

3.1.5 rhBMP4 Inhibits *FGF20* Transcription to Modulate Feather Primordium Stability

The inhibitory effects of BMPs on molecules involved in primordium induction and primordium formation have been well documented (Jung *et al.*, 1998; Mou *et al.*, 2011; Noramly and Morgan, 1998; Scaal *et al.*, 2002). However, these studies did not establish how the recombinant BMPs exerted their inhibitory effects on feather primordium formation. To address this gap in knowledge, I examined the effects of recombinant human BMP4 (rhBMP4) on primordium induction in GFP chicken skin explants.

The effects of treatment with rhBMP4 and LDN193189, an inhibitor of SMAD1/5/8 phosphorylation, to modulate BMP signalling were initially analysed on HH 29 dorsal skin explants to ascertain the experimental doses to be used in future experiments (**Figure 39**). In control explants, feather primordium formation can be visualised through *in situ* hybridisation for *FGF20* transcripts, which is expressed only in developed or developing feather primordia. As previously reported by Mou *et al* 2011, I show that addition of recombinant BMP protein, in this case rhBMP4, inhibits primordium formation in dorsal skins, with greater sensitivity to BMP signalling in rows lateral to the dorsal midline (**Figure 39a**). qRT-PCR analysis for *FGF20* expression in explants treated with 500 ng/ml of rhBMP4 for 5 hours revealed a near complete inhibition of *FGF20* expression in treated explants (n=6) (**Figure 39b**). The reduction of *FGF20* expression by rhBMP4 treatment may explain the inhibition of feather primordium formation in treated explants. Blocking BMP signalling in skin explants through treatment of explants with 10 μM LDN193189, lead to the formation of enlarged, fused primordia after 48 hours (**Figure 39c**). 5 hour treatment of skin explants with 10 μM LDN193189 resulted in an increase in *FGF20* expression, as detected through qRT-PCR (n=3) (**Figure 39d**). The results suggest that modulation of *FGF20* expression by BMPs may reduce the production of endogenous FGF20 protein and thereby regulate the ability of FGF20 to induce cell migration and aggregation.

The results so far demonstrate that BMPs have the ability to modulate FGF production via their inhibitory effects on *FGF* expression, but the effects of BMP proteins on primordia and cell migration have yet to be addressed. To determine if BMP's can affect cell migration or aggregation directly, rhBMP4 coated beads were applied to HH 29 GFP chicken skin explants and imaged over 36 hours. When BSA coated beads were applied to GFP explants, feather primordium induction and patterning was unaffected (**Video 5 & Figure 40a**). Application of rhBMP4 coated beads resulted in the destabilisation of endogenous feather primordia (**Video 6 & Figure 40b**).

Based on the above observations, the results can be interpreted as FGF20 being required for the induction of feather primordium formation and also the maintenance of feather primordium stability. The observed dismantling of the feather primordia may be due to the inhibition of FGF20 protein production via the inhibition of *FGF20* transcription by rhBMP4. To test whether FGF signalling is required to maintain the stability of formed primordia, the effects of inhibition of FGF signalling activity on HH 31 GFP dorsal skin explants was examined (**Video 7 & Figure 40c)**. At the beginning of culture, the BSA bead treated explants, cultured in 15 µM of SU5402, displayed three rows of fully formed feather primordia. Over the 36 hour period in culture, the formation of new feather primordium rows is not observed on the treated explant. Also, over the duration the culture period, the once distinct feather primordia gradually lose their stability. At the beginning of culture, the feather primordia are observed as discrete clusters of cell aggregates, however, the borders of each feather primordium is gradually less defined over the duration of culture. Taken together, the results indicate that FGF signalling is required for the induction of feather primordia and the maintenance of their stability. The inhibitory effects of BMP4 protein on feather primordium induction and maintenance may be due to the inhibition of *FGF20* transcription, ultimately preventing the production of FGF20 proteins.

Primordia in closest proximity to the rhBMP4 beads appeared to slowly dismantle and cells from the destabilised primordia began migrating towards the developing cell aggregates at the periphery of rhBMP4's active range. The cells from the original primordia are then repurposed in the formation and growth of new cell aggregates and

eventually form a ring of primordia around the rhBMP4 inhibitory zone. The breakup of endogenous primordia appears to be due to the loss of adherence between neighbouring cells within the primordia as opposed to active chemo-repellence by the rhBMP4 coated bead, as visualised in the video (**Video 6)**. If rhBMP4 does not function as a chemo-repellent, it would suggest that the formation of the inhibitory zone around the rhBMP4 coated beads is dependent on active FGF signalling outwith the rhBMP4s active range. To test if the formation of the inhibitory zone requires chemo-repellence by BMP signalling or chemo-attraction by FGF signalling, HH 31 dorsal skin explants, treated with rhBMP4 beads, were cultured in medium supplemented with 15 µM SU5402 (**Video 8 & Figure 40d**). As observed in treatments with BSA beads and SU5402, the feather primordia of rhBMP4 beads and SU5402 treated explants gradually lost their structure. However, the formation of the inhibitory zone around the rhBMP4 bead was greatly reduced when FGF signalling was inhibited. The result indicates that BMP4 protein does not function as a chemo-repellent factor during the formation of feather primordia. The result also indicate that the formation of the inhibitory zone around rhBMP4 sources is due to cell uptake, in FGF signalling active regions, outwith the active range of BMP signalling.

Based on the above results, it appears that BMP4 proteins function to inhibit *FGF20* transcription during feather primordium formation, which prevents the production of new FGF20 protein, and that active FGF signalling activity is required to maintain the stability of formed feather primordia. This would suggest that a sustained concentration of FGF20 protein is required to maintain the stability of cell aggregates. To determine whether sustained FGF20 protein levels can indeed induce the formation and stabilise cell aggregates, rhFGF9 coated beads were applied to HH 29 GFP skin explants and cultured with medium supplemented with 500 ng/ml of rhBMP4 for a period of 48 hours (**Video 9 & Figure 41**). The dose of rhBMP4 used, completely inhibits the formation of all endogenous primordia but cell migration and aggregation towards rhFGF9 sources is unaffected by the treatment.

Taken together, these results show that rhBMP4 can only affect the transcriptional regulation of *FGF20* and does not affect the chemo-attractant effect of FGF20

proteins, if present. The result also implies that after their induction and formation, if FGF20 self-activation is high enough, self-activation of FGF20 may overcome BMP4's inhibitory effects and will maintain the stability of the formed feather primordium, depending on the dose of BMP4 present.

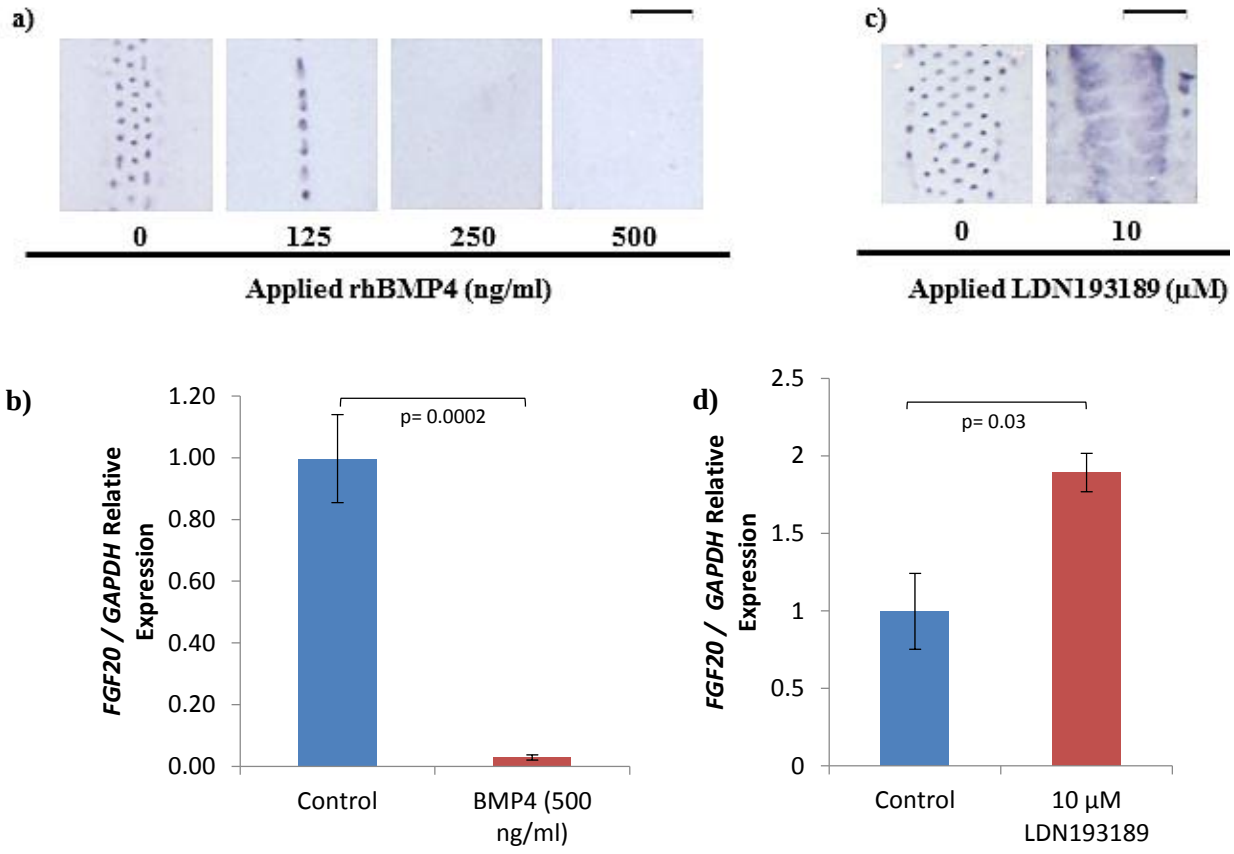

Figure 39. rhBMP4 inhibits pattern formation and expression of *FGF20*. a) rhBMP4 inhibits the formation of new primordium rows in a dose dependent manner over 24 hours, eventually inhibiting all endogenous primordium formation in HH 29 skin explants, as detected through *in situ* hybridisation for *FGF20* expression. **b)** qRT-PCR assessing *FGF20* expression levels in HH 29 skin explant cultured in the presence of 500 ng/ml rhBMP4 after 5 hours results in inhibition of *FGF20* expression compared to controls (n=6). **c)** Blocking endogenous BMP signalling with 10 µM of LDN193189 in HH 29 skin explants for 48 hours causes the formation of enlarged, fused primordia as detected by *FGF20 in situ* hybridisation. **d)** qRT-PCR assessing *FGF20* expression levels in HH 29 skin explant cultured in the presence of 10 µM of LDN193189 after 5 hours results in an increase of *FGF20* expression compared to controls (n=3). Error bars indicate SEM. Scale bar - 1 mm.

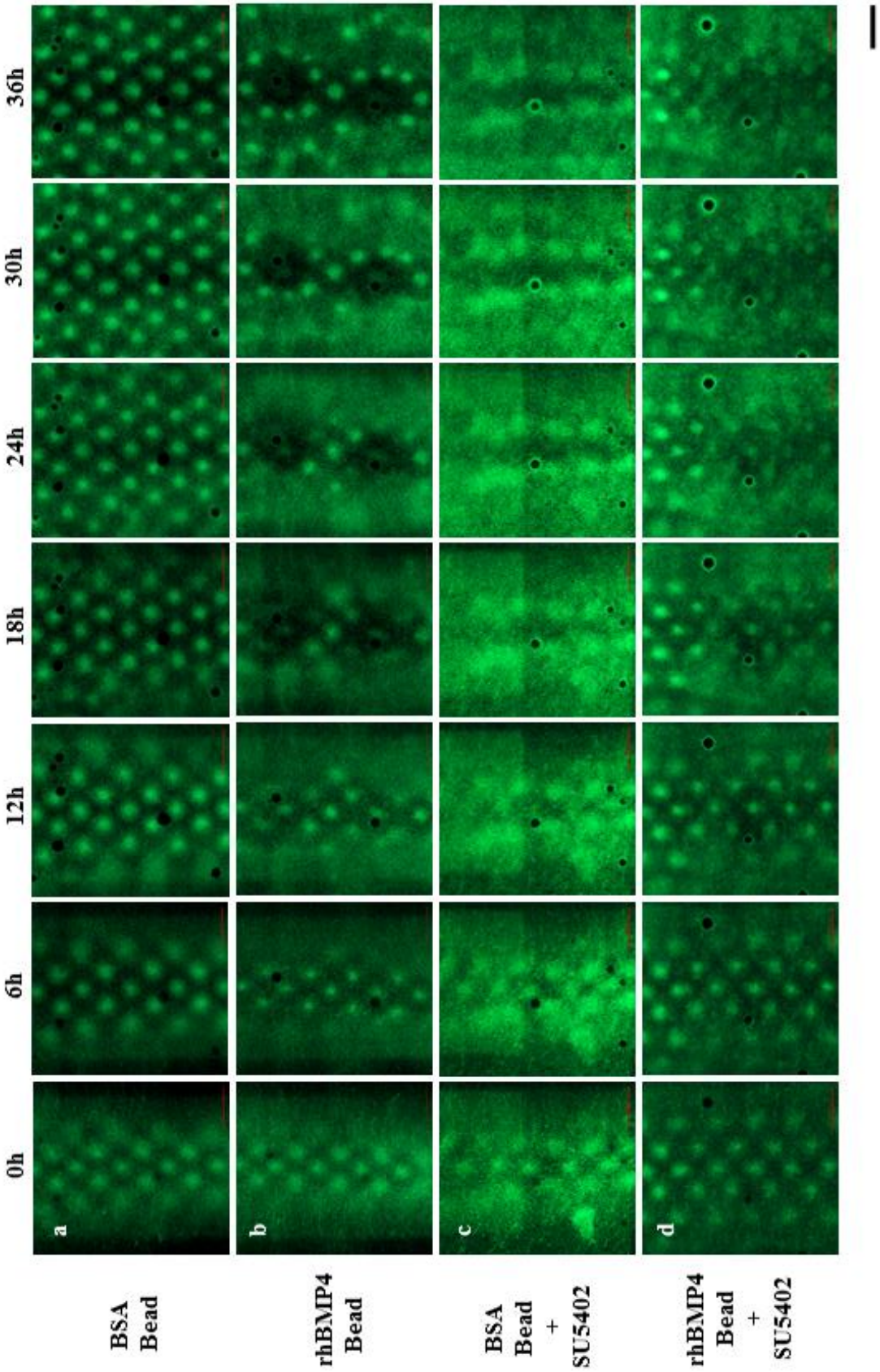
0h
6h
12h
18h
24h
30h
36h
a
b
c
d
BSA Bead
rhBMP4 Bead
BSA Bead + SU5402
rhBMP4 Bead + SU5402

Figure 40. Local application of rhBMP4 destabilises endogenous primordia through the inhibition of FGF signalling activity. a) HH 31 GFP skin explants cultured in the presence of BSA treated beads develop with no phenotypic effects. **b)** Application of rhBMP4 coated bead results in the destabilisation of existing primordia in close proximity to the bead and the formation of a zone of inhibition around the bead. Cells from destabilised primordia are repurposed for the formation of new cell aggregates. **c)** Application of 15 µM of SU5402 (an inhibitor of FGF signalling), to BSA bead treated skin results in the gradual break up of formed feather primordia. **d)** Co-treatment of explants with both rhBMP4 coated beads and 15 µM of SU5402 resulted in the eventual break up of endogenous feather primordia and also displayed a reduction in the appearance of the inhibitory zone around the rhBMP4 coated beads. Scale bar - 200 µm.

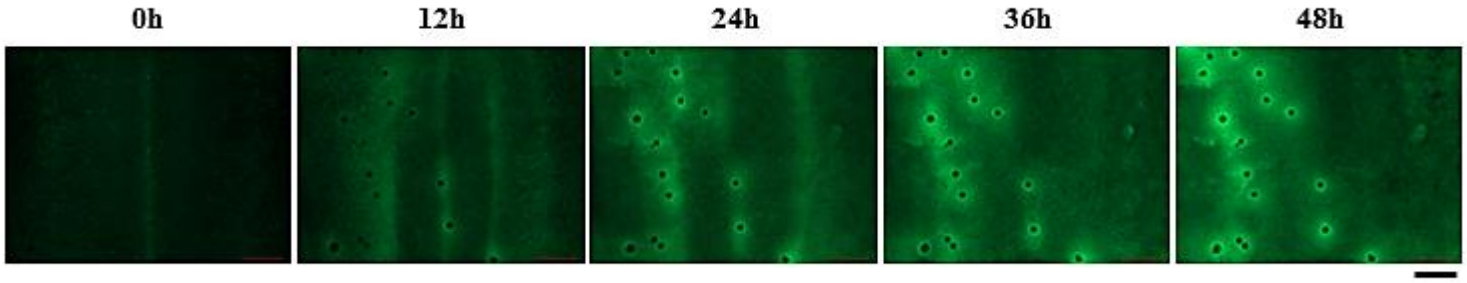

Figure 41. General application of rhBMP4 does not prevent cell migration to sources of rhFGF9. Supplementing culture medium with 500 ng/ml rhBMP4inhibits the formation of endogenous primordia in HH 29 GFP explants after 48 hours but rhFGF9 coated beads remain capable of inducing cell migration towards local sources of rhFGF9. Scale bar - 500 µm.

3.1.6 Function of Endogenous BMP signalling in Feather Primordium Formation

To understand the function of endogenous BMP signalling during the induction and formation of feather primordia, the effects of inhibiting BMP signalling on cultured GFP skin explants was analysed. 15 μM LDN193189 was applied to cultured HH 29 GFP skin explants and imaged over 36 hours. In control GFP explants, the normal sequence of events during feather primordium induction and patterning occurs (**Video 10 & Figure 42a**), as observed in section **3.1.1**. LDN193189 treated GFP explants, develop abnormally (**Video 11 & Figure 42b**). The breakup of the primary stripe is delayed, and enlargement of feather primordia and occasional fusions between neighbouring primordia can be observed. As development progresses, when new rows form in control explants, enlarged primordia in LDN193189 treated explants expand in size bilaterally and occasionally fuse with newer primordia that have formed lateral to the "primary row". The resulting final pattern in treated explants show clusters of floret shaped primordia as opposed to the distinct, hexagonally arranged primordia observed in control explants.

The data suggest that endogenous BMP signalling may limit the size of forming feather primordia by inhibiting cell aggregation in regions outside the active range of FGF signalling. In addition, they maintain primordium borders during their formation, without which, the forming primordia grow in an uncontrolled manner resulting in the formation of an abnormal primordium pattern. Interestingly, inhibiting BMP signalling does not affect the wave-like propagation of primordium induction. Although abnormal in appearance, the enlarged primordia expand in size laterally into areas corresponding to regions undergoing formation of new primordium rows in control explants, indicating that BMP signalling is not the limiting factor preventing the whole explant from patterning simultaneously.

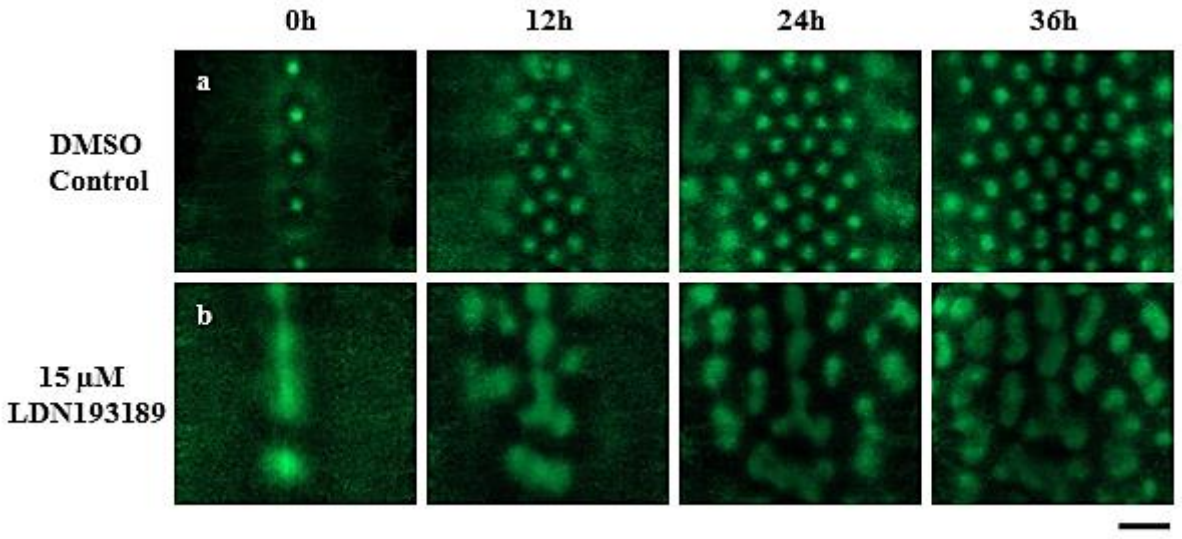

Figure 42. Inhibition of BMP signalling results in loss of primordium borders. a) Control GFP chicken dorsal skin explant after 36 hours in culture in the presence of DMSO. **b)** Explants cultured in the presence of 15 µM of LDN193189 exhibit larger primordia and occasional fusions between neighbouring primordia. Scale bar - 500 µm.

3.1.7 Mature Feather Primordia Inhibit the Formation of New Primordia in Interbud Domains.

Through tissue recombination experiments, previous studies observed a gradual decrease in the ability of the dorsal skin to induce feather primordium formation (Hughes *et al.*, 2011; Rawles, 1963). The ability of the dorsal skin to induce feather primordia is transient and peaks from E7 to E9. This indicates that only a small window of opportunity exists for the dorsal skin to induce the formation of feather primordia and that by E9, when the last of the feather primordium rows are laid out across the tract, the final feather primordium pattern may be set and unchangeable.

To examine whether the final periodic feather primordium pattern is unchangeable, dorsal skin explant displaying a full array of feather primordia were prepared from E9 chicken embryos, stretched and cultured for three days (**Figure 43**). Feather primordia were identified through *in situ* hybridisation analysis to detect sonic hedgehog (*SHH*) expression, a known marker of differentiating feather primordia (Ting-Berreth and Chuong, 1996). Control explants, cultured with minimal stretching, show outgrowth of existing feather primordia, with the formation of new, smaller feather primordia evident in the lateral areas of the dorsal tract only (black arrows). Stretched explants display outgrowth of existing feather primordia but also the presence of small, ectopic feather primordia within the interbud domains between existing feather primordia.

The results suggest that E9 skin has yet to lose its capacity to induce feather primordium formation, but also suggests that an inhibitory factor emanating from developing feather primordia (possibly BMPs), inhibit the formation of new feather primordia within the interbud domains of the dorsal skin. By increasing the size of the interbud region through mechanical stretching, the inhibitory effect from existing feather primordia is alleviated allowing the formation of a new ectopic feather primordia within the interbud domain.

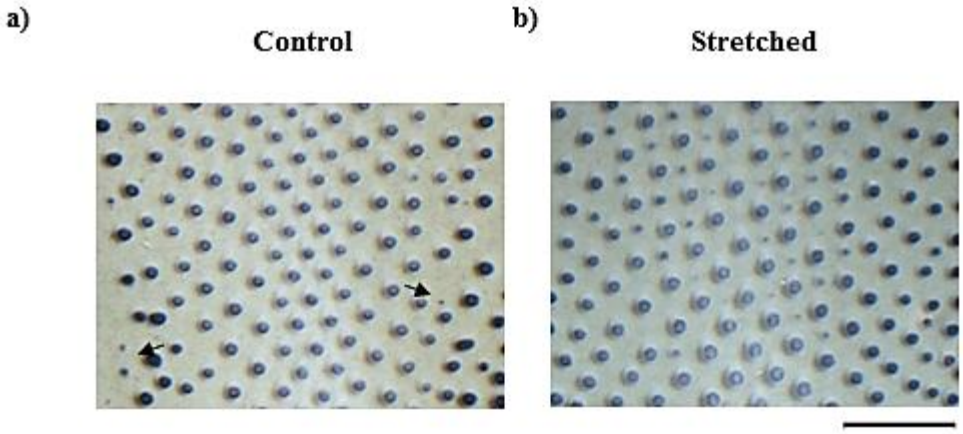

Figure 43. Existing feather primordia inhibit the insertion of ectopic feather primordia. Detection of *SHH* expression in skin explants cultured for 3 days from HH 34 when primordia are almost completely laid out in the dorsal tract. **a)** Control explants cultured with minimal stretching show normal outgrowth of feather primordia and induction of new primordia on the lateral edges of the dorsal tract (black arrows). **b)** When the explants are stretched, ectopic primordia develop between existing primordia. Scale bar - 1 mm.

3.2 Feather Primordium Periodic Pattern Formation and Pattern Fidelity

3.2.1 Mechanisms underlying the Wave-Like Propagation of Feather Primordium Formation

The chicken feather periodic pattern arises in a spatiotemporal sequence, resulting in the formation of a high fidelity, hexagonal pattern (Mayerson and Fallon, 1985) (as described in section **3.1.1**). Many models have been proposed to explain the sequential addition of new feather primordium rows during the formation of the primordium periodic pattern, but the prevailing observation describes the presence of a primordium inducing wave which spreads across the feather field, laying down successive rows of primordia in its wake (Davidson, 1983; Ede, 1972). Current studies have identified molecules involved in the induction or inhibition of primordium formation but the molecular or cellular basis behind the strict temporal and spatial patterning of feather primordia is currently unknown.

Due to FGF20's role in the induction of cell aggregation during the formation and propagation of feather primordia (as described in section **3.1**), the expression of *FGF*20 was examined. *In situ* hybridisation was performed on HH 29 dorsal skin explants after 24 and 48 hours in culture, to ascertain if *FGF20* expression followed the propagation of feather primordium induction during development and the possible involvement of FGF20 itself, in the propagation of feather primordium induction. At 24 hours, *FGF20* is only expressed within the midline region of the dorsal tract, in skin regions undergoing or that has undergone primordium induction but is excluded from the interbud regions (**Figure 44a**). After 48 hours, *FGF20* is expressed across the dorsal tract but restricted to the feather primordia only (**Figure 44b**). The more mature primordia located at the midline of the skin display polarised expression of *FGF20,* and expression is restricted to the anterior domain of the feather primordia. This observation suggests *FGF20* does follow and may itself induce the wave-like propagation of feather primordium formation.

To determine whether *FGF20* is involved in the propagation of primordium formation during embryonic development, rhFGF9 beads were applied to HH 29 GFP chicken

dorsal skin explants to stimulate the induction of dermal cell aggregate. Explants treated with BSA coated beads show no effects on the propagation of feather primordium formation (**Figure 45a**) Application of rhFGF9 coated beads to skin regions beyond the endogenous primordium forming region but within the presumptive dorsal tract (indicated by a *), are capable of inducing the formation of cell aggregates in these regions (**Figure 45b**). However, nucleation of pattern formation, spreading away from the ectopic cell aggregates does not occur, that is, the spreading, wave-like formation of primordium formation is not induced by the rhFGF9 coated bead. The result suggests that FGF20 is only involved in the formation of individual feather primordia but is not involved in the induction of the wave-like propagation of primordium formation.

This result suggests that the restricted, spatiotemporal induction of *FGF20* expression and therefore feather primordium formation via FGF signalling, across the feather tract during primordium induction is the underlying mechanism behind the wave-like propagation of feather primordium formation. However FGF signalling itself is not involved in the wave-like propagation of primordium formation but the process is regulated by a currently unknown mechanism.

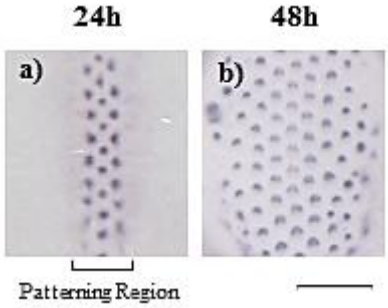

Figure 44. *FGF20* expression during propagation of feather primordium formation. *FGF20* expression was detected through *in situ* hybridisation on HH 29 dorsal skin explants after 24 hours and 48 hours in culture. **a)** *FGF20* expression only occurs in developing or developed primordia within region of skin undergoing primordium formation (patterning region marker). **b)** *FGF20* expression remains restricted to primordium domains. Scale bar - 1 mm.

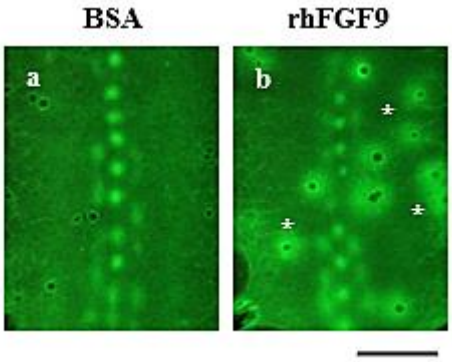

Figure 45. Nucleation of primordium formation is not induced by cell aggregation alone but requires the action of a propagating primordium induction wave. a) HH 29 GFP chicken dorsal skin explants cultured in the presence of BSA treated beads for 24 does not alter endogenous primordium formation. **b)** rhFGF9 coated beads applied at a distance from the primordium generating region still stimulates cell aggregation around the rhFGF9 source but nucleation of primordium induction is not observed. (*) indicates forming cell aggregates outside the endogenous primordium induction region. Scale bar - 1 mm.

3.2.2 Identification of Signalling Pathways Involved in Primordium Propagation

If restricted induction of *FGF20* expression is required for the wave-like propagation of primordium induction, then signalling pathways which can regulate *FGF20* expression may explain the wave propagation of primordium formation. Studies performed in developing mouse skin established that *FGF20* expression is a downstream target of the WNT/β-Catenin and EDA/EDAR signalling pathways (Huh *et al.*, 2013). To assess if the above pathways in chicken are capable of inducing *FGF20* expression, *FGF20* expression levels were analysed on skin explants by qRT-PCR analysis after stimulation of the WNT/β-Catenin and EDA/EDAR signalling pathways via the treatment of skin explants with small molecule inhibitors and recombinant proteins of the above pathways (**Figure 46**).

WNT/β-Catenin signalling in HH 29 dorsal skin explants was stimulated through the use of a selective inhibitor of glycogen synthase 3 beta (GSK3β), CHIR99021. HH 29 dorsal skin explants treated for 5 hours with CHIR99021 showed a 7-fold relative increase in *FGF20* expression compared to control explants (n=6) (**Figure 46a**). The results indicate that WNT/β-Catenin signalling is capable of inducing *FGF20* expression and could be involved in the wave-like propagation of primordium formation.

HH 29 skin explants cultured for 5 hours in media supplemented with 500 ng/ml of recombinant EDA protein (Fc-chEDA1), thereby stimulating the EDA/EDAR signalling pathway, also showed an increased in *FGF20* expression (n=6) (**Figure 46b**). Treated explants show a 3-fold relative increase in *FGF20* expression compared to control explants. The result suggests that in chicken dorsal skins, *FGF20* is also a downstream target of EDA/EDAR signalling.

The results indicate that stimulation of both WNT/β-Catenin and EDA/EDAR signalling can induce the expression of *FGF20* and that both WNT/β-Catenin and EDA/EDAR signalling pathways may be involved in the propagation of feather primordium formation in the dorsal tract of chicken embryos.

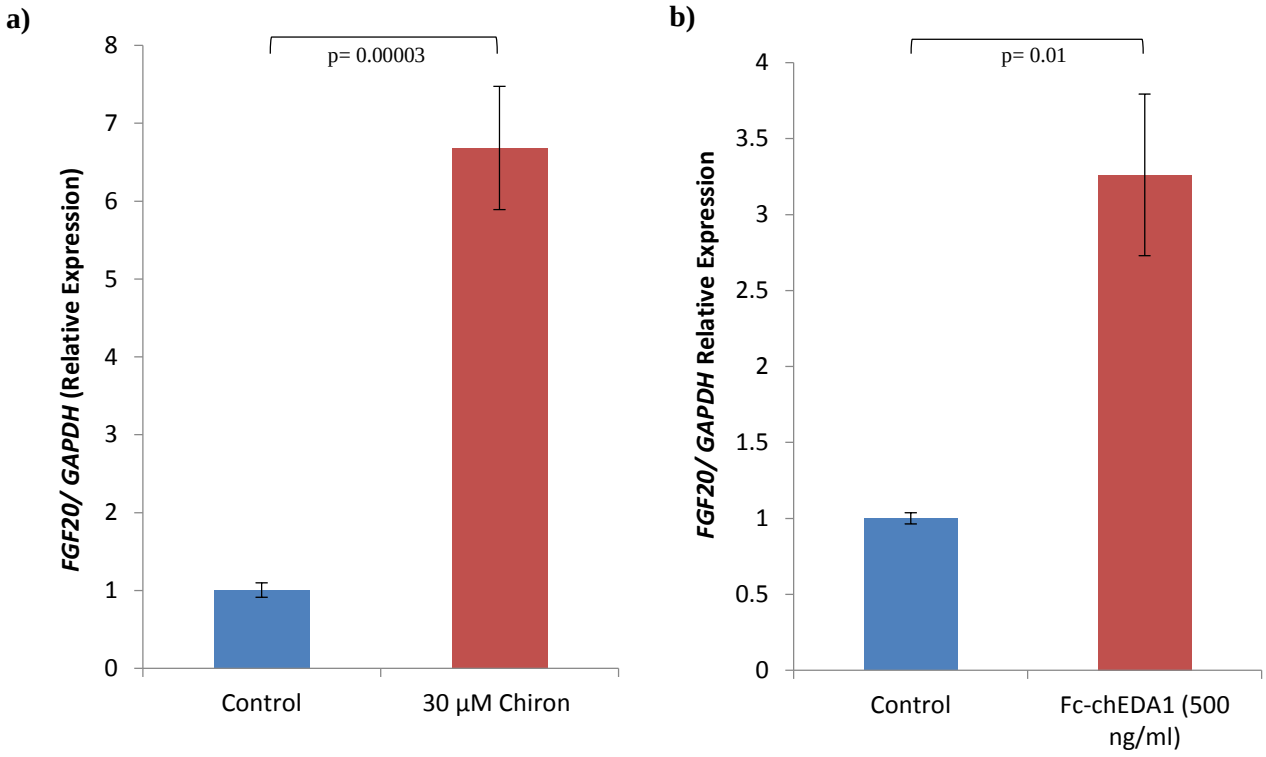

Figure 46. *FGF20* expression is induced by stimulation of WNT/β-Catenin and EDA/EDAR signalling pathways in chicken. qRT-PCR assessing *FGF20* expression levels in HH 29 skin explants after 5 hours in culture in medium supplemented with either **a)** 30 µM CHIR99021 (n=6) or **b)** 500 ng/ml Fc-chEDA1 compared to controls (n=6). Error bars indicate SEM.

3.2.3 *EDA*, a Molecular Candidate for the Feather Primordium Induction Wave

From my experimental results, both WNT/β-Catenin and EDA/EDAR signalling pathways are capable of inducing the expression of *FGF20*, and therefore are both candidate signalling pathways in the induction and propagation of feather primordium formation during chicken embryonic development. If either or both of the above pathways were involved in the propagation of primordium formation, the expression pattern or activity of components of the WNT/β-Catenin or EDA/EDAR pathways should precede the induction of feather primordium formation. To assess if either the WNT/β-Catenin or EDA/EDAR signalling pathway were involved in the propagation of primordium formation, the expression pattern of *β-Catenin*, *EDAR*, and *EDA* were compared and analysed through *in situ* hybridisation on HH 29 embryos prior to dissection and on cultured dorsal skin explants (**Figure 47 & Figure 48**).

The dorsal tract of HH 29 embryos displays diffuse *β-Catenin* expression, which is observed throughout the presumptive dorsal tract but also shows increased expression within the dorsal midline (**Figure 47a**). In HH 29 skin explants, after 24 hours in culture, *β-Catenin* expression is still observed throughout the dorsal tract with increased expression within the developing feather primordia but it is excluded from the interbud domains, displaying a "restrictive mode" of pattern expression (**Figure 48a**). By 48 hours in culture, the diffuse expression of *β-Catenin* within the dorsal tract is replaced by restricted expression of *β-Catenin* within feather primordia, separated by *β-Catenin* negative interbud domains, arranged periodically throughout the dorsal tract (**Figure 48b**). If *β-Catenin* expression controlled the observed propagation of primordium induction, then any skin region expressing *β-Catenin* would be expected to pattern immediately due to induction of *FGF20* expression by WNT/β-Catenin signalling. However, simultaneous primordium induction in *β-Catenin* expressing skin is not observed, indicating that WNT/β-catenin signalling is low or inactive throughout the tract prior to primordium induction/propagation and instead, another factor controls the wave-like propagation of feather primordium patterning. Previous studies suggest *β-Catenin* expression defines regions of skin competent to undergo primordium induction (Noramly *et al.*, 1999).

Analysis of *EDAR* expression revealed that the expression of *EDAR* follows a "restrictive mode" pattern of expression, overlapping with the observed *β-Catenin* expression pattern during the propagation of primordium formation. HH 29 embryo dorsal tracts initially display weak *EDAR* expression throughout the presumptive dorsal tract but higher expression within the developing dorsal midline (**Figure 47b**). As feather primordium formation is induced, *EDAR* expression is restricted to the developing feather primordia and excluded from interbud domains (**Figure 48c**). After 48 hours, *EDAR* expression can only be observed within feather primordia (**Figure 48d**). Similar to *β-Catenin*, *EDAR* may not be involved in the propagation of feather primordia because of the initially diffuse expression pattern of *EDAR* across the dorsal tract prior feather primordium induction, suggesting the involvement of another factor which drives the wave like propagation of feather primordium formation.

EDA is expressed in a "restrictive mode-like" expression pattern. Unlike *β-Catenin*, *EDA* is not initially expressed diffusely across the feather tract but is only expressed within the dorsal midline (**Figure 47c - Arrow**). In cultured skin explants, expression of *EDA* is restricted to the interbud regions surrounding the formed primordia, around the midline region of the dorsal tract. *EDA* expression is also observed ahead of the last primordia formed at that specific time point as a discrete stripe, around the width of one row of feather primordia (**Figure 48e**). After 48 hours, *EDA* expression has propagated across the entire dorsal tract but can only be detected within the interbud regions between developed primordia (**Figure 48f**). However, the propagation of *EDA* expression does not travel beyond the borders of the dorsal tract, as defined by *β-Catenin* expression.

From the above observations, *β-Catenin* and *EDAR* are poor candidates for the primordium induction wave due to their initial expression across the entire presumptive dorsal tract. *EDA* expression, on the other hand, not only overlaps with the wave-like propagation of feather primordium formation but can also detected ahead of the wave of primordium induction. Based on the *EDA* expression pattern during feather primordium pattern development and the ability of EDA/EDAR

signalling to induce *FGF20* expression, the results suggests that *EDA* is a candidate molecule which regulates the wave-like induction of feather primordium formation.

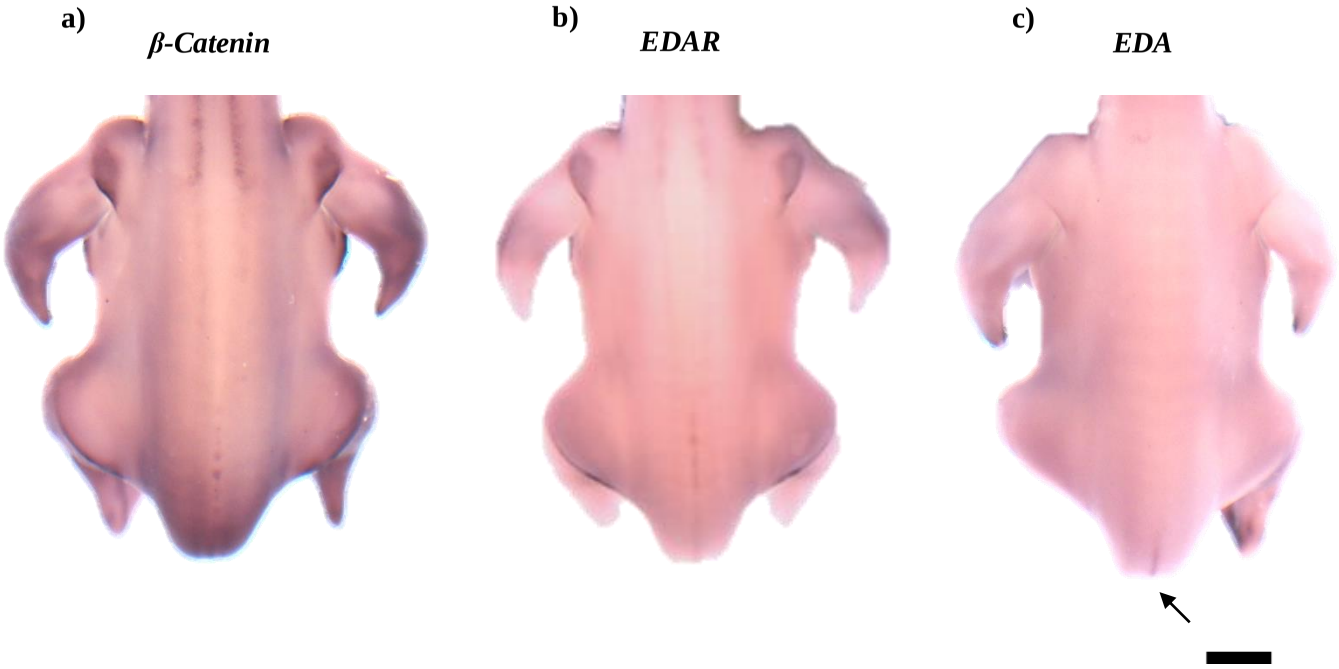

Figure 47. Comparison of expression of *β-Catenin*, *EDAR* and *EDA* embryonic dorsal tracts. *In situ* hybridisation performed on HH 29 chicken embryos **a)** *β-Catenin* is expressed across the entire dorsal tract and within the dorsal midline **b)** *EDAR* is also expressed weakly across the entire dorsal tract and within the dorsal midline. **c)** *EDA* expression can only be detected at the dorsal midline of the embryo at this stage (arrow). Scale bar - 1 mm.

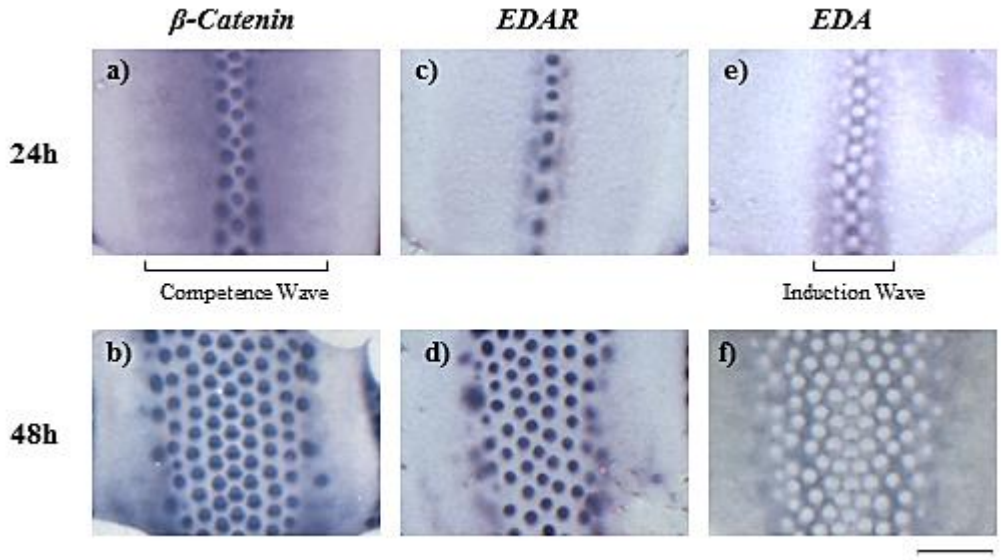

Figure 48. Comparison of expression of *β-Catenin*, *EDAR,* and *EDA* in cultured skin explants. *In situ* hybridisation performed on HH 29 dorsal skin explants after 24 hours and 48 hours in culture. **a), b)** *β-Catenin* is expressed across the entire dorsal tract after 24 in culture and follows the "restrictive mode" pattern of expression as feather primordia are induced (competence wave). **c), d)** *EDAR* expression also shows a "restrictive mode" pattern of expression, similar to *β-Catenin,* and can be detected throughout the presumptive dorsal tract, albeit at low levels of expression. ***e*), f)** *EDA* expression starts at the midline and travels bilaterally outwards during development, defining the regions that will undergo primordium formation (induction wave). Scale bar - 1 mm.

3.2.4 Application of Recombinant EDA Expands the Feather Primordium Generating Region

As stated above, restricted induction of *FGF20* expression across the feather tract appears to be the mechanism driving the wave-like propagation of feather primordium formation. The observed *EDA* expression pattern during primordium propagation and *FGF20* being a downstream target of EDA/EDAR signalling suggests the possible involvement of *EDA* in the wave-like primordium patterning process.

If spatiotemporally restricted expression of *EDA* defines the region of skin capable of primordium induction in the dorsal tract of chickens, then stimulation of the EDA/EDAR signalling pathway through application of Fc-chEDA1 to dorsal skin explant cultures would be expected to expand the region of skin undergoing primordium formation. To determine whether the restricted induction of *FGF20,* specifically, by the activation of the EDA/EDAR signalling pathway, defines the size of the primordium generating region in the dorsal tract, the effects of Fc-chEDA1 on the width of the primordium generating region was analysed.

HH 29 dorsal skin explants were treated with either LDN1963189 or FC-chEDA1 for 24 hours and the width of the primordium generating regions of treated explants were compared to those of control explants (**Figure 49a**). The width of the primordium generating region was defined through the visualisation of *FGF20* expression by *in situ* hybridisation.

LDN193189 applied to dorsal skin cultures was previously demonstrated to increase *FGF20* expression by blocking BMP signalling activity (**Figure 39d**). After 24 hours in culture, dorsal skin explants treated with 15 µM of LDN193189 displayed a stripe of *FGF20* expression, indicating the formation of fusions between developing primordia (**Figure 49b**). However, the LDN193189 treated skins do not show an increase in the width of the primordium generating region, compared to control explants (n=3) (**Figure 49d**). The result suggests alleviation of *FGF20* inhibition by BMP signalling results in an increase in *FGF20* expression, however, the effect is limited to within the endogenous primordium generating region where *FGF20*

expression is currently being induced. LDN193189 itself cannot induce the ectopic expression of *FGF20* throughout the dorsal tract. This indicates increasing *FGF20* expression alone does not result in the propagation of primordium formation, but primordium propagation occurs through the spread of a propagating factor that is capable of inducing *FGF20* expression, possibly *EDA*.

Skin explants cultured for 24 hours in the presence of 2 µg/ml Fc-chEDA1 show the formation of three to five rows of enlarged primordia and also the diffuse expression of *FGF20* beyond the developed primordia (**Figure 49c**). Measurements of the width of *FGF20* expression in Fc-chEDA1 treated explants show a two-fold increase in the width of the primordium generating region compared to the primordium generating region in control explants (n=3) (**Figure 49d**). The result suggest that the primordium generating region is defined by the expression of *EDA* and that the stimulation of the EDA/EDAR pathway, through the application of recombinant EDA protein, can modulate the size of the primordium generating region.

Taken together, these findings indicate that the induction of *FGF20* expression, by the propagation of *EDA* expression specifically, is involved in the induction and wave-like propagation of primordium formation during periodic pattern development. The restricted wave-like propagation of *EDA* expression defines the regions of skin within the tract where feather primordium formation can be induced and therefore regulates the propagation of primordium formation (induction wave).

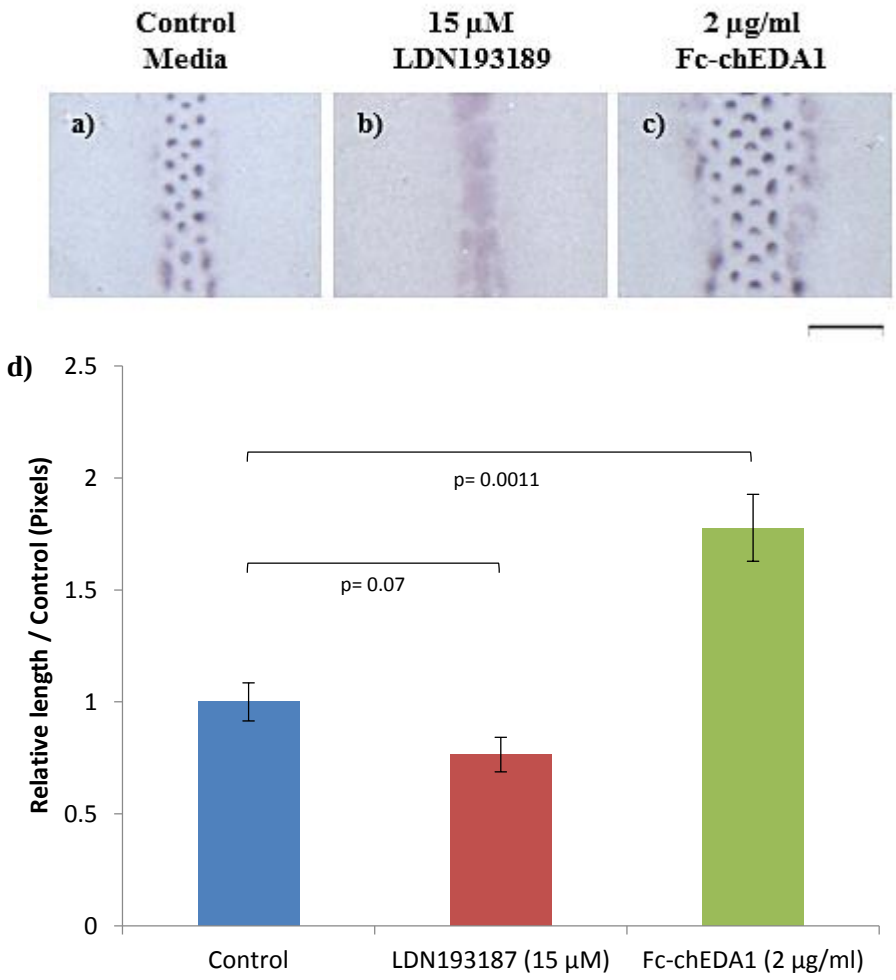

Figure 49. Stimulation of EDA/EDAR signalling increases the width of the feather primordium generating region. The skin region undergoing feather primordium induction as defined by *FGF20* expression after culture for 24 hours in **a)** control HH 29 chicken dorsal skin explants were compared to those of **b)** 15 µM LDN192189 or **c)** 2 µg/ml Fc-chEDA1 treated explants. **d)** Measurement of the width of region undergoing primordium induction as defined by *FGF20* expression (n=3). Error bars indicate SEM. Scale bar - 1 mm.

3.2.5 EDA/EDAR and WNT/β-Catenin Signalling Pathways Synergistically Induces *FGF20* Expression.

As observed in **Figures 47 & 48**, the propagation of *EDA* expression and therefore primordium induction appears to be limited to the tract regions as defined by *β-Catenin* expression, suggesting a possible link between the WNT/β-Catenin and EDA/EDAR signalling pathways. Previous studies showed that *FGF20* is a direct transcriptional target of WNT/β-Catenin signalling in engineered human epithelial cell lines and ovarian endometrioid adenocarcinomas (Chamorro *et al.*, 2005). Based on my experimental observation, that *FGF20* expression can be induced by both the WNT/β-Catenin and the EDA/EDAR signalling pathways in chicken (section **3.2.2**), it is conceivable that the two signalling pathways may cooperate together during primordium induction to synergistically stimulate *FGF20* expression in the developing dorsal tract.

To test whether synergy between WNT/β-Catenin and EDA/EDAR signalling pathways exists during the induction of *FGF20*, qRT-PCR analysis was performed on HH 29 skin explant cultures after 5 hour treatments with 20 µM CHIR99021, 50 ng/ml Fc-chEDA1 or a combination of the two (n = 9) (**Figure 50**).

Single treatments of either 20 µM CHIR99021 or 50 ng/ml Fc-chEDA1 resulted in a relatively modest increase of *FGF20* expression by approximately 1.5 to 2.5 fold respectively compared to untreated controls.

Explants treated with a combination of 20 µM CHIR99021 and 50 ng/ml Fc-chEDA1, for 5 hours showed a 5-fold relative increase in *FGF20* expression compared to controls. The increase in *FGF20* expression observed in the co-treated explants was greater than that of the combined relative increase of *FGF20* expression in single treatment.

The findings suggest that in dorsal skin explants, during feather primordium induction, WNT/β-Catenin and EDA/EDAR signalling pathways operate synergistically to induce the expression of *FGF20*.

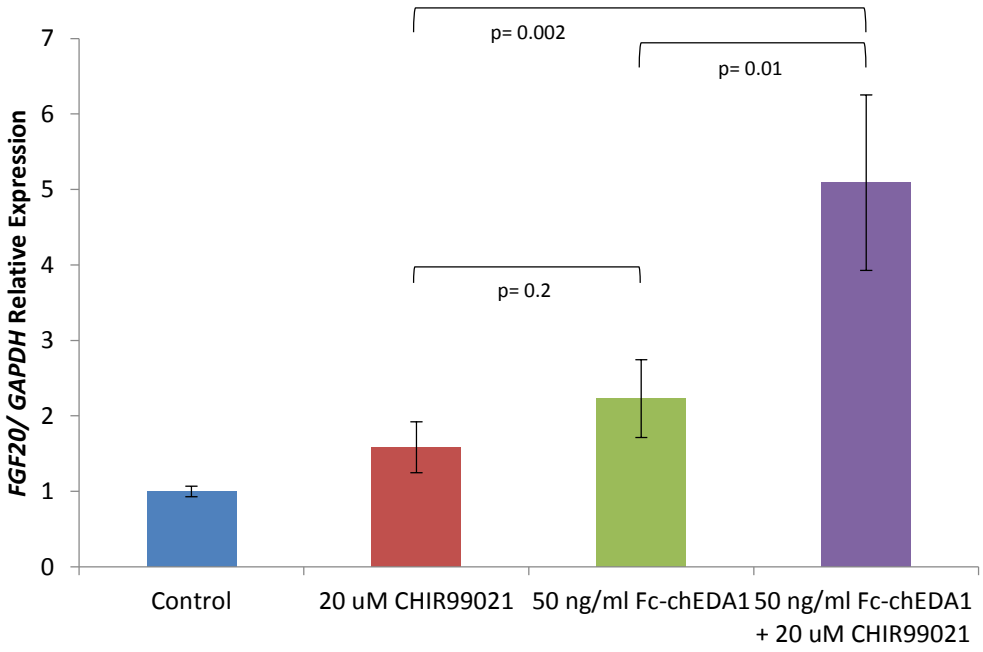

Figure 50. WNT/β-Catenin and EDA/EDAR signalling operate synergistically to induce FGF20 expression. qRT-PCR analysis of *FGF20* expression levels in HH 29 skin explant after culture for 5 hours in the presence of 20 µM CHIR99021, 50 ng/ml Fc-chEDA1 or a combination of the two. Individual treatments of either CHIR99021 or Fc-chEDA1 result in a 2-2.5 fold increase of *FGF20* expression compared to controls. Combination treatment result in an almost 5 fold increase in *FGF20* expression indicating synergy between the two pathways (n=9). Error bars indicate SEM.

3.2.6 Relationship between the Propagation of *EDA* Expression and Feather Primordium Pattern Fidelity

The identification of *EDA* as a permissive factor in the propagation of feather primordium induction indicates that the restricted expression of *EDA* might play a major role in the formation of the chicken periodic pattern. However, the relationship between sequential propagation of primordium induction and pattern fidelity has yet to be addressed.

If the spatiotemporal propagation of *EDA* is responsible for the formation of a high fidelity pattern, broadening of the initial region of skin expressing *EDA* prior to primordium induction should result in the simultaneous formation of an unorganised periodic pattern of low fidelity across the dorsal tract of the explant.

To test this theory, I developed a method to reversibly block primordium induction in dorsal skin explant cultures without affecting the competence of the explant to primordium induction or affecting *EDA* expression propagation during culture. As mentioned in **s**ection **3.1.3**, latrunculin A is an inhibitor of actin polymerisation and is capable of inhibiting primordium formation. From previous studies, the inhibitory effects of latrunculin A are known to be reversible, through the replacement of the culture medium (Coue *et al.*, 1987). Therefore, I analysed the effects of latrunculin A on *β-Catenin* expression (a known marker for epithelial competence to primordium induction (Noramly *et al.*, 1999)) and on the propagation of *EDA* expression through *in situ* hybridisation on HH 29 dorsal skin explant cultures treated with 150 ng/ml latrunculin A for 24 hours.

In control explants, after 24 hours in culture, three rows of primordia are formed on the explants (**Figure 51a**). *In situ* hybridisation analysis on the explants reveals the expression of *β-Catenin* follows the "restrictive mode" of pattern expression, while *EDA* propagation and restriction to within interbud domains is observable over the duration of the culture period. Latrunculin A treatment inhibits primordium induction throughout most of the skin explant, however, formation of the primary row of primordia at the dorsal midline of the tract can occasionally be observed in treated

explants (**Figure 51b**). *In situ* hybridisation shows that *β-Catenin* expression and propagation of *EDA* expression was not affected by the treatment, throughout the duration of the experiment. The results indicate that the maintenance of *β-Catenin* and propagation of *EDA* expression are not dependent on primordium formation or actin polymerisation processes.

To determine if temporally and spatially restricted propagation of *EDA* expression is responsible for a high fidelity periodic pattern of feather primordia, HH 29 dorsal skin explants were pre-treated with 150 ng/ml latrunculin A for 24 hours, to increase the area of *EDA* expression before primordium induction is induced. After the initial 24 hours the latrunculin A supplemented medium was replaced with control medium and cultured for a further 24 hours. Control explants were cultured in only control medium throughout the duration of the experiment, but the medium was also replaced after 24 hours in culture. After culture, the final pattern of feather primordia (as defined by *FGF20* expression) on skin explants pre-treated with latrunculin A were compared to those of control explants.

After 48 hours, the dorsal tract of control explants displayed a high fidelity pattern of hexagonally arranged feather primordia (**Figure 52a**). Whereas, explants pre-treated with 150 ng/ml latrunculin A for the first 24 hours, resulted in the formation of smaller feather primordia, arranged in an unorganised pattern (**Figure 52b**). The result suggest that the expansion of *EDA* expression prior to primordium induction, (therefore increasing the initial area of *FGF20* expression), results in the formation of a periodic pattern of feather primordium of reduced fidelity.

By broadening the initial area of skin expressing *EDA* before primordium induction, latrunculin A pre-treated explants would be expected to pattern simultaneously within the broadened region of *EDA* expression, after replacement of the culture medium. To examine whether simultaneous primordium induction occurred in explants pre-treated with latrunculin A, HH 29 GFP skin explants were pre-treated in 150 ng/ml latrunculin A supplemented medium for 24 hours and imaged over a period of 24 hours following replacement of supplemented medium with control medium, to visualise pattern

formation in real time. Control GFP dorsal skin explants developed a high fidelity, hexagonal pattern of primordia which arose sequentially through the addition of new primordium rows, over the duration of the experiment (**Video 12 & Figure 53a**). Explants pre-treated with latrunculin A show primordium induction was initially inhibited throughout the tract and cells were homogenously distributed across the field, with the exception of the dorsal midline (**Video 13 & Figure 53b**). Following the replacement of the culture medium with medium lacking latrunculin A, after 12 hours in culture it was observed that the formation of cell aggregates was induced almost simultaneously across the feather tract. The resultant pattern consists of small primordia arranged in an unorganised manner.

Thus, the formation of a high fidelity periodic pattern is attributed to the temporally and spatially restricted induction of *FGF20* expression by a travelling wave of *EDA* expression during feather primordium induction. The formation of an unorganised, low fidelity pattern is a consequence of the broadening of the region of skin expressing *EDA*, resulting in the loss of spatiotemporally restricted induction of *FGF20* expression.

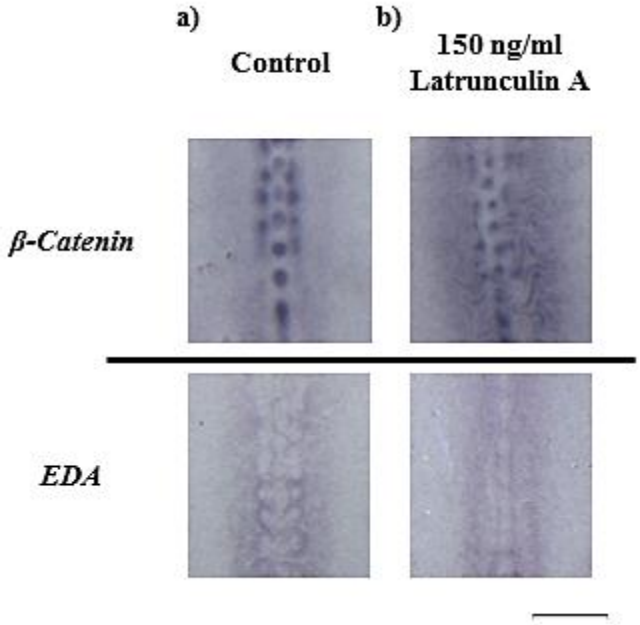

Figure 51. Inhibition of cell movement does not affect expression and propagation of the molecular waves. HH 29 dorsal skin explants cultured for 24 hours in **a)** control medium or **b)** in the presence of 150 ng/ml of latrunculin A. *In situ* hybridisation reveals latrunculin A treatment does not affect the maintenance of *β-Catenin* expression or the expression and propagation of *EDA*. Scale bar - 1 mm.

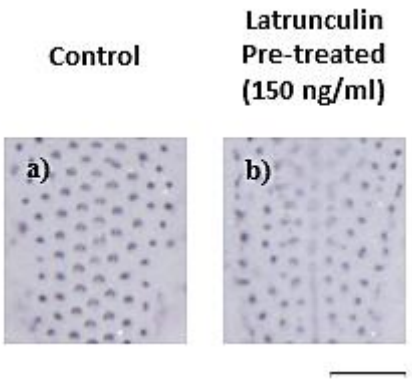

Figure 52. Gradual feather primordium induction by spatiotemporally restricted *EDA* expression propagation is required for a high fidelity periodic pattern of feather primordia. HH 29 dorsal skin explants cultured for a total period of 48 hours. **a)** Control explants display a hexagonal periodic pattern of high fidelity **b)** Explants pre-treated for 24 hours with 150 ng/ml of latrunculin A, followed by 24 hours incubation in control medium results in the formation a pattern of lower fidelity. Scale bar - 1 mm.

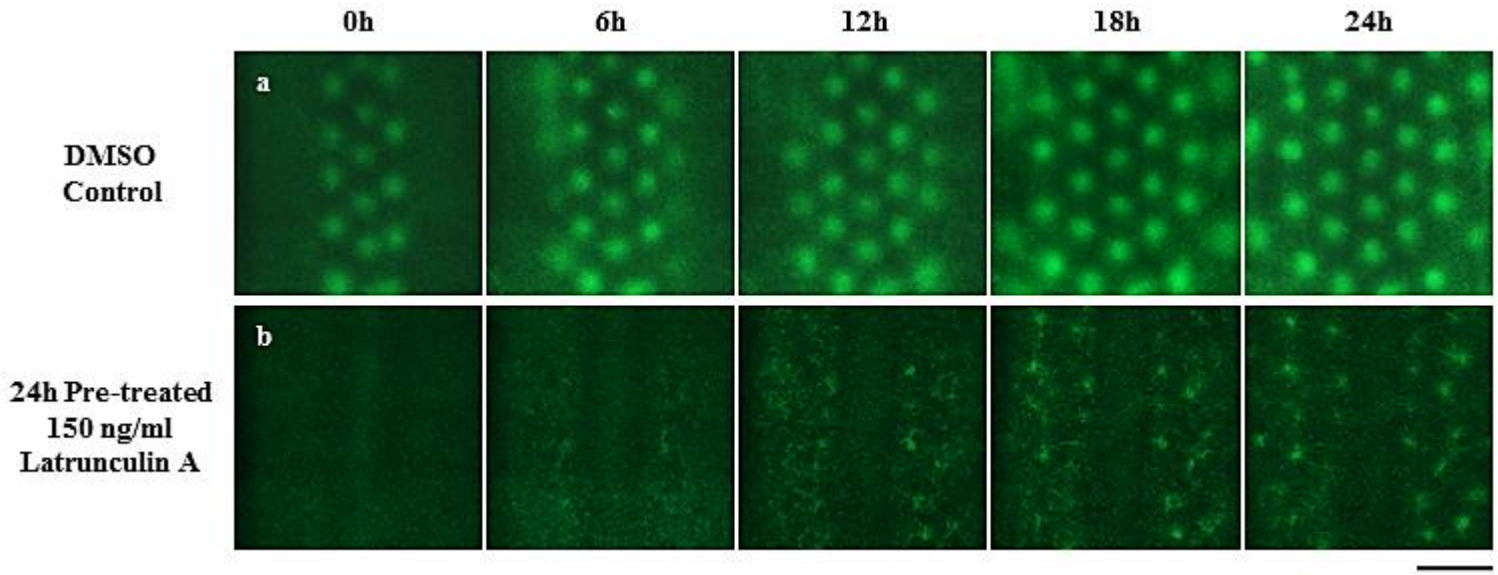

Figure 53. Disruption of feather primordium formation during wave propagation reduces pattern fidelity. HH 29 dorsal skin explants cultured in DMSO control medium for 24 hours after a 24 hour pre-treatment in 150 ng/ml latrunculin A supplemented medium or DMSO control medium. The sequence of pattern propagation is unaffected in DMSO control skin explants whereas the explants pre-treated with latrunculin A develops an unorganised pattern, simultaneously across the tract. Scale bar - 500 µm.

3.2.7 Dermal Cell Availability Limits the Effects of Primordium Induction by Recombinant EDA

If limited availability of EDA protein alone is responsible for the restricted propagation of the periodic pattern, due to the spatiotemporally restricted expression of *EDA*, then application of recombinant EDA protein to skin explant cultures would be expected to result in the expansion of the primordium generating region across the entire tract. However, I show that the application of Fc-chEDA1 to dorsal skin explants does not induce primordium formation throughout the entire width of the tract (**Figure 49**). Through treatment of skin explants with varying doses of Fc-chEDA1, I show that the effects of Fc-chEDA1 on the size of the primordium generating region is limited. HH 29 explants cultured for 24 hours after application of 500 ng/ml and 2 µg/ml of Fc-chEDA1, display enlarged primordia and a wider area of skin expressing *FGF20* transcripts compared to control explants, indicating that both treatments were able to expand the primordium generating regions (**Figure 54a**). However, measurements of the width of the patterning region, as defined by *FGF20* expression, show that the effects of Fc-chEDA1 treatment resulted in only a maximum of a 2-fold increase in the width of *FGF20* expression compared to control explants, regardless of the dose of Fc-chEDA1 tested (**Figure54b**). This result suggests another factor limits the region of skin capable of primordium induction.

Prior to the process of primordium induction, the density of the underlying dermis is not homogenous across the feather tract. In the dorsal tract of HH 29 chicken embryos, cell density is highest at the midline (arrow) but gradually decreases laterally from the midline (**Figure 55a**). At HH 31 the density of the dermis in regions of skin of a comparable area to HH 29 (black and red boxes) shows thickening of the dense dermis (**Figure 55b**). Based on previous studies and my own observations, the result suggests that dense dermis thickening propagates in a medial to lateral direction in the dorsal tract and that limited dermal cell availability in regions of skin lateral to the midline may prevent the induction of feather primordium formation by EDA/EDAR signalling.

As observed in **Figure 34**, cell proliferation does not affect the induction and formation of individual feather primordia, however, methotrexate treatment does affect the wave-like induction of feather primordium formation. Control explants displayed an almost complete array of feather primordia across the entire dorsal tract after culture, while treated explants only formed 5 rows of primordia. The observed reduction in the number of feather primordium rows in treated explants could be due to either, the inhibition of *EDA* expression propagation, or to the inhibition of dense dermis thickening. I performed *in situ* hybridisation on 48 hour cultures of HH 29 dorsal skin explants, treated with 5 μM methotrexate, to determine if *EDA* expression propagation was affected by the treatment (**Figure 56**). The result revealed that inhibition of cell proliferation by methotrexate treatment does not affect the propagation of *EDA* expression. The reduction of feather primordium rows in treated explants may be due to the inhibition of cell proliferation, preventing dense dermis thickening, which lowers the dermal cell density in the treated explants. This suggests that *EDA* expression and signalling may not be sufficient in inducing feather primordium formation when dermal cell density is too low.

To examine whether low dermal cell densities limited the effects of Fc-chEDA1 protein on the width of the feather primordium generating region, the lateral spread of dense dermis formation was inhibited in HH 29 dorsal skin explants through the removal of the dorsal midline prior to primordium induction and cultured for 48 hours. In control explants, dense dermis thickening is observed across almost the entirety of the tract, as observed through H & E staining of transverse sections of cultured explants (**Figure 57a**). Removal of the dorsal midline prior to primordium induction resulted in the inhibition of primordium wave-like propagation, forming only one row of primordia directly next to the site of excision (**Figure 57b & 57c**). *In situ* hybridisation revealed that expression of *β-Catenin* and propagation of *EDA* expression were unaffected by the procedure. The results indicate that the propagation of *EDA* expression is independent of the bilateral spread of dense dermis thickening and also that EDA/EDAR signalling alone is not capable of inducing feather

primordium formation if the underlying dermal cell density is not permissible to primordium induction.

Taken together, the findings indicate three main factors are required for the induction of feather primordium formation during embryonic chick development; 1) an epidermis competent to primordium induction (indicated by *β-Catenin* expression), 2) an inductive signal, to induce the process of primordium formation (EDA/EDAR signalling) and 3) the presence of an underlying dense dermis of sufficient cell density. The hexagonally arranged pattern of feather primordia arises through the spatiotemporally restricted propagation of the primordium induction signal (propagation of *EDA* expression specifically) and is the underlying process that results in the formation of a high fidelity pattern.

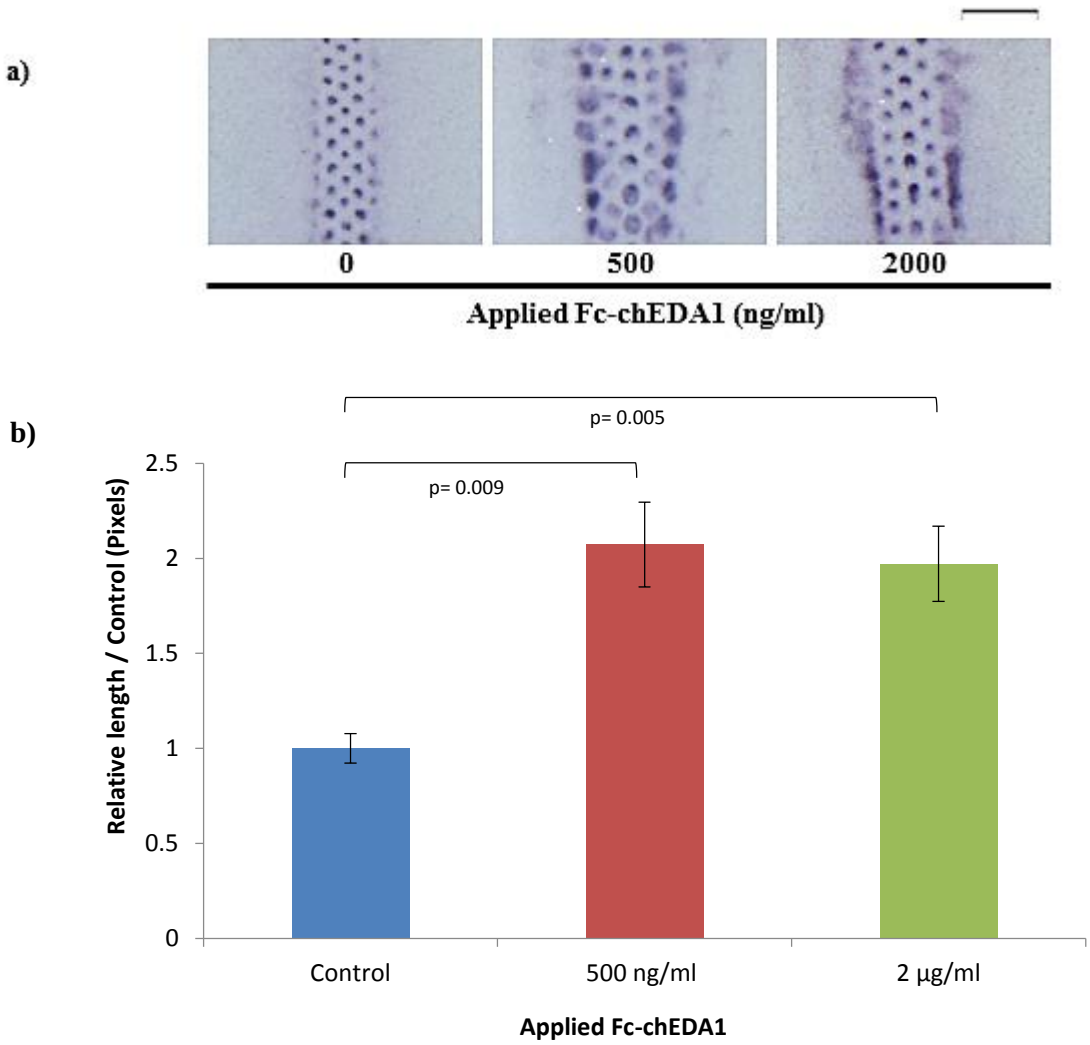

Figure 54. Stimulation of EDA/EDAR signalling does not induce feather formation across the entire dorsal tract. a) The area undergoing patterning, as defined by *FGF20* expression, in HH 29 chicken dorsal skin explants cultured for 24 hours in the presence of 500 ng/ml or 2000 ng/ml of Fc-chEDA1. **b)** Measurement of the width of patterning region as defined by *FGF20* expression (n=6). Error bars indicate SEM. Scale bar - 1 mm.

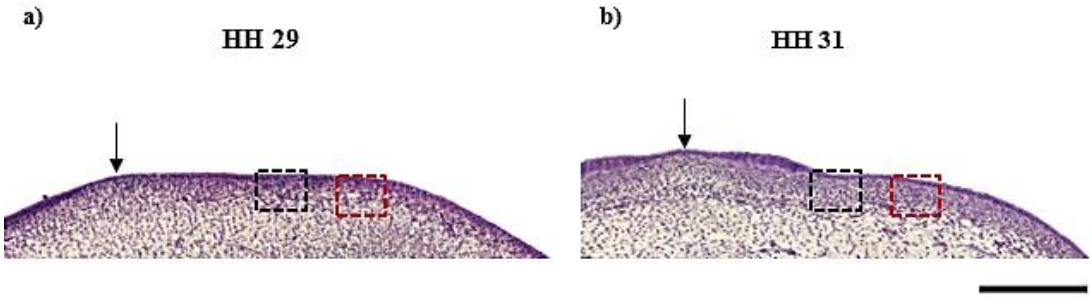

Figure 55. Comparison of dense dermis thickness between HH 29 and HH 31 chicken embryos. H & E staining of transverse sections from HH 29 and HH 31 chicken embryos. **a)** Before primordium induction (HH 29), dermal cell density gradually decreases laterally from the dorsal midline (compare nuclear density in black and red boxes). **b)** Over the course of development, dermal cell density increases across the dorsal tract. (Arrow indicates dorsal midline). Scale bar - 200 μm.

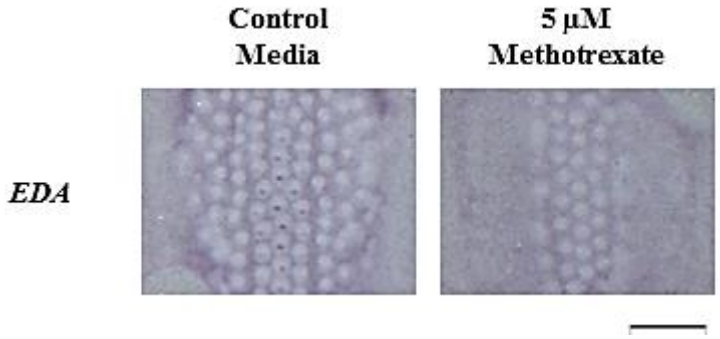

Figure 56. Cell proliferation is required for the wave-like propagation of feather primordium formation. HH 29 dorsal skin explants were cultured for 48 hours in medium supplemented with 5 µM methotrexate. Control explants display a full array of feather primordia after culture, as observed by detection of *EDA* expression through *in situ* hybridisation. Inhibition of cell proliferation in treated explants resulted in the formation of only five rows of feather primordia, however, *EDA* expression propagation is unaffected by the treatment. Scale bar - 1 mm.

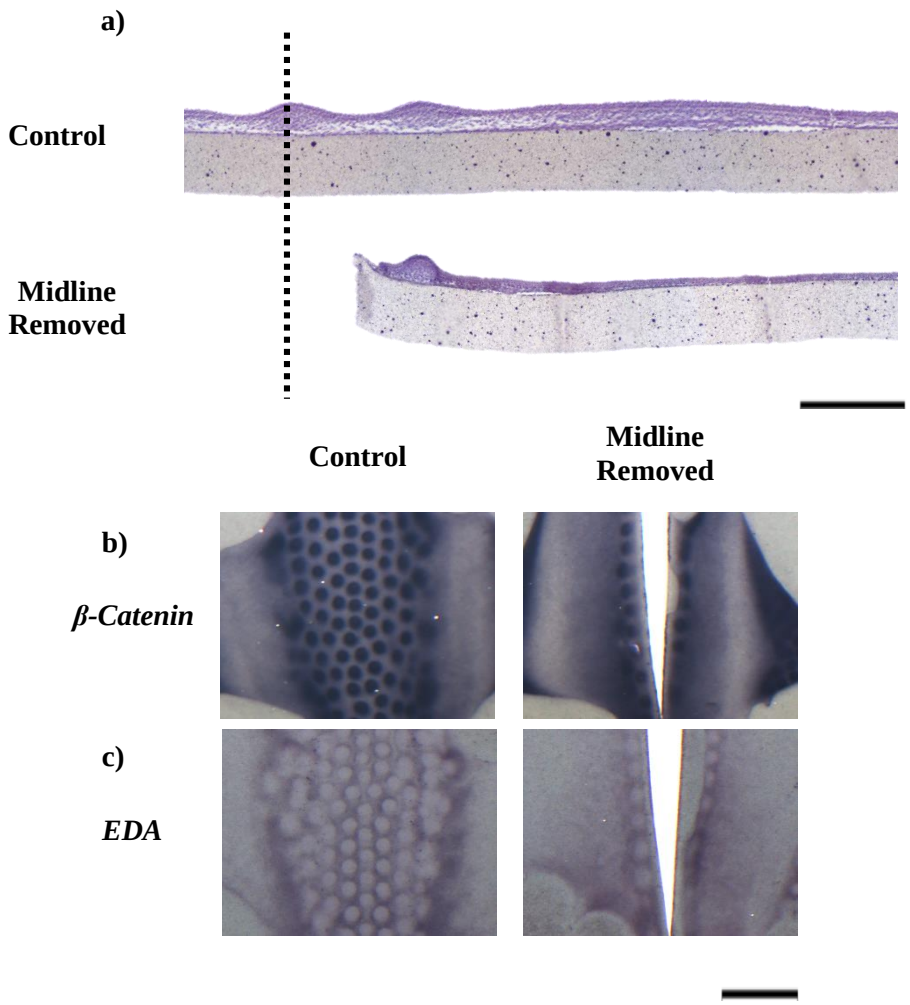

Figure 57. Excision of the dorsal midline inhibits dense dermis thickening but propagation of molecular waves is unaltered. The dorsal midline was excised from HH 29 dorsal skin explants and cultured for 48 hours, resulting in the inhibition of the wave-like propagation of primordium formation in excised explants. **a)** H & E staining of dorsal midline excised explants show reduced density of dermal cells lateral from the midline compared to controls (black line indicates position of the dorsal midline). *In situ* hybridisation reveals the expression of **b)** *β-Catenin* and **c)** propagation of *EDA* expression remains unaltered by the procedure. Scale bars **a) -** 200 µm **b-c**) - 1 mm.

3.2.8 Feather Primordium Formation can occur Independently of EDA/EDAR Signalling.

During mouse embryonic development, the formation of hair follicles occurs in several distinct phases. During the embryonic development of EDA-defective mouse mutants, Tabby, the formation of the primary hair follicles is prevented due to inactive EDA/EDAR signalling activity (Laurikkala *et al.*, 2002; Mou *et al.*, 2006). However, Tabby mice are still capable of generating secondary and tertiary hair follicles, which are smaller than primary hair follicles, suggesting that hair follicle formation can arise through an EDA/EDAR independent process.

To assess if EDA/EDAR signalling is essential for the formation of feather primordia, HH 29 dorsal skin explants were cultured in the presence of an anti-EDA1 antibody, Ecto-D2. After 24 hours in culture, three to five rows of feather primordia have developed on control explants, as observed through the detection of *β-Catenin* transcripts (**Figure 58a**). Three rows of feather primordia are formed when EDA/EDAR signalling was inhibited in explants treated with 10 µg/ml of Ecto-D2 (**Figure 58b**). However, the feather primordia that do form on the treated explants are smaller in size when compared to the primordia of control explants. After 48 hours in culture, control explants have developed a further four rows of feather primordia (**Figure 58c**). In treated explants, however, the wave-like propagation of feather primordium formation appears to have terminated after the formation of the first three rows of feather primordia (**Figure 58d**). The feather primordia that do form in the Ecto-D2 treated explants appear to be restricted to the medial regions of skin, where dermal cell density is highest. The reason why only three rows of feather primordia form on Ecto-D2 treated explants, may due to the absence of a dermis with a sufficient cell density in the skin regions lateral to the midline. The results indicate that the formation of feather primordia can occur through an EDA/EDAR independent mechanism but require a dermis of sufficient cell density to induce their formation. Detection of *EDA* transcripts, in the explants treated with Ecto-D2 for 48 hours, also reveals that the propagation of *EDA* expression does not require active EDA/EDAR signalling.

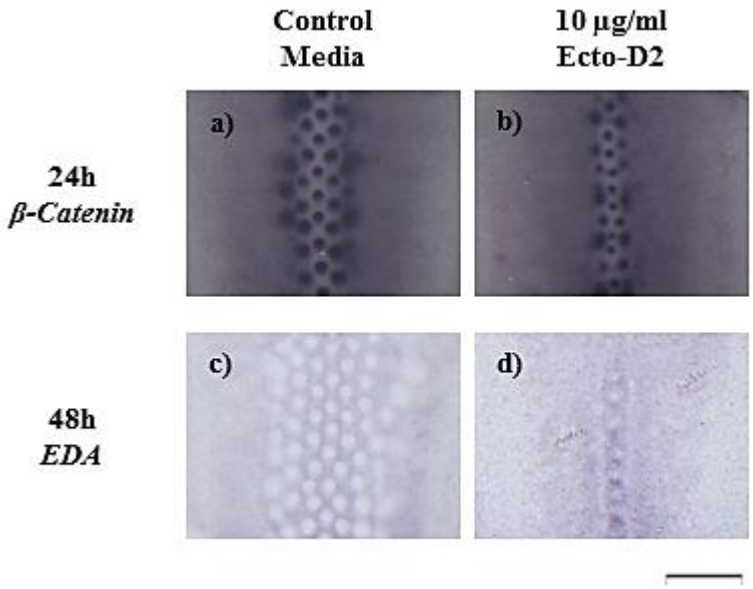

Figure 58. EDA/EDAR signalling is dispensable for the induction of individual feather primordia. a) HH 29 control explants cultured for 24 hours, developed three to five rows of feather primordia, as detected by *in situ* hybridisation of *β-Catenin* expression. **b)** When explants were cultured for 24 hours in medium supplemented with 10 µg/ml of Ecto-D2, three rows of feather primordia can be observed, but the formed primordia are smaller in size compared to control explants. The maintenance of *β-Catenin* expression was unaffected by the treatment. **c)** Control explants cultured for 48 hours, develop an extra four rows of feather primordia, and expression of *EDA* has propagated across the presumptive feather tract. **d)** After 48 hours in culture, explants treated with Ecto-D2 failed to develop extra rows of feather primordia, but *EDA* expression propagation was unaffected by the treatment. Scale bar - 1 mm.

3.3 Comparative Analysis of Feather Primordium Induction and Propagation.

Based on my current results, it appears that spatiotemporally restricted expression of *EDA* regulates the sequence of primordium induction and appears to be important for the development of a high fidelity periodic pattern of feather primordia during embryonic chicken development. However, different species of birds display different feather arrangement patterns (Clench, 1970; Nitzsch, 1867; Stettenheim, 2000) which may arise from a similar, but modified, pattern generating mechanism utilised in chicken skin development i.e. modifications to the spatiotemporally restricted expression of *EDA*. Developing dorsal tracts of different species of flighted and non-flighted birds were analysed through *in situ* hybridisation for *β-Catenin* and *EDA* expression, to determine whether the differences in the observed feather arrangement patterns of the different bird species, were the result of modifications to the basic patterning mechanism defined in chickens.

3.3.1 Guinea Fowl

Analysis of the expression of *β-Catenin* in the dorsal tract of guinea fowl during primordium development revealed that the expression pattern of *β-Catenin* in guinea fowl does not initially resemble those observed during early primordium induction in chick embryos. At E8, prior to the wave-like propagation of feather primordium induction, *β-Catenin* is strongly expressed within the primary stripe at the midline of the dorsal tract, similar to chickens and is also observed within the maturing somites. However, unlike chickens, *β-Catenin* is not initially expressed throughout the presumptive feather tract of embryonic guinea fowls (**Figure 59a**). *β-Catenin* still displays a "restrictive mode" of pattern expression, with focalisation of *β-Catenin* expression to within the feather primordia of the forming primary row, while inhibited in the interbud regions. From E9 onwards, *β-Catenin* expression begins to propagate bilaterally from the midline, laying down successive rows of feather primordia as *β-Catenin* expression travels across the dorsal tract (similar to the chicken *EDA* expression pattern) (**Figure 59b & 59c**). Once the tract is filled with feather primordia, *β-Catenin* expression can be only observed within the formed primordia and is

excluded from the interbud regions (**Figure 59d**). Mature feather buds show localised expression of *β-Catenin* towards the distal tip of the feather bud. The final primordium pattern, as indicated by *β-Catenin* expression, is hexagonal and appears to be of high fidelity.

The *EDA* expression pattern in developing guinea fowl embryos resembles those observed in skin periodic pattern formation in chickens. At E9 during primordium propagation, *EDA* is detected around the primary row of feather primordia, at the dorsal midline, restricted to the interbud domains but excluded from the primordia themselves (**Figure 60a**). By E10, *EDA* expression has propagated bilaterally from the midline and travelled a distance equal to approximately one primordium row but *EDA* expression remains within the interbud regions of the skin, surrounding the forming feather primordia (**Figure 60b**).

A double *in situ* hybridisation was performed on the same embryos used to detect *EDA* expression to compare the *β-Catenin* expression pattern with those of the *EDA* expression pattern during primordium propagation. Interestingly, *EDA* expression remains one to two primordium rows behind the propagating feather primordia in guinea fowls (as detected by *β-Catenin* expression), whereas in chickens, *EDA* expression remains one primordium row ahead of feather primordium propagation. In E9 guinea fowls, while diffuse expression of *EDA* can be observed around the primary row of feather primordia only, *β-Catenin* expression is detected within three rows of primordia (**Figure 60c**). At E10, *β-Catenin* is expressed within five rows of feather primordia and also partially extends laterally into the presumptive dorsal tract but *EDA* expression lags behind showing expression within the interbud regions of the first three rows of feather primordia (**Figure 60d**). The observation indicates that *β-Catenin* expression propagation occurs faster than that of *EDA* expression propagation during the wave-like induction of feather primordium formation in guinea fowls.

The observed expression pattern of *β-Catenin* during guinea fowl development suggests that *β-Catenin* expression in guinea fowl, may be involved in the wave-like propagation of feather primordia, since the observed *EDA* expression pattern does not

directly correlate with primordium induction. The observed *β-Catenin* expression pattern in guinea fowl also suggests that *β-Catenin* expression in birds does not necessarily dictate the location and size of the presumptive feather bearing tracts as suggested by previous studies based on chicken experiments (Noramly *et al.*, 1999). In chicken, *β-Catenin* is initially expressed across the entire width of the presumptive feather tracts prior to primordium induction, and does not display wave-like propagation as observed in guinea fowls. The guinea fowl results indicate that, *β-Catenin* expression also represents regions of skin that are competent to primordium induction but that *β-Catenin* expressing regions are not strictly defined but are capable of expansion during embryonic development, creating new regions of skin capable of primordium induction.

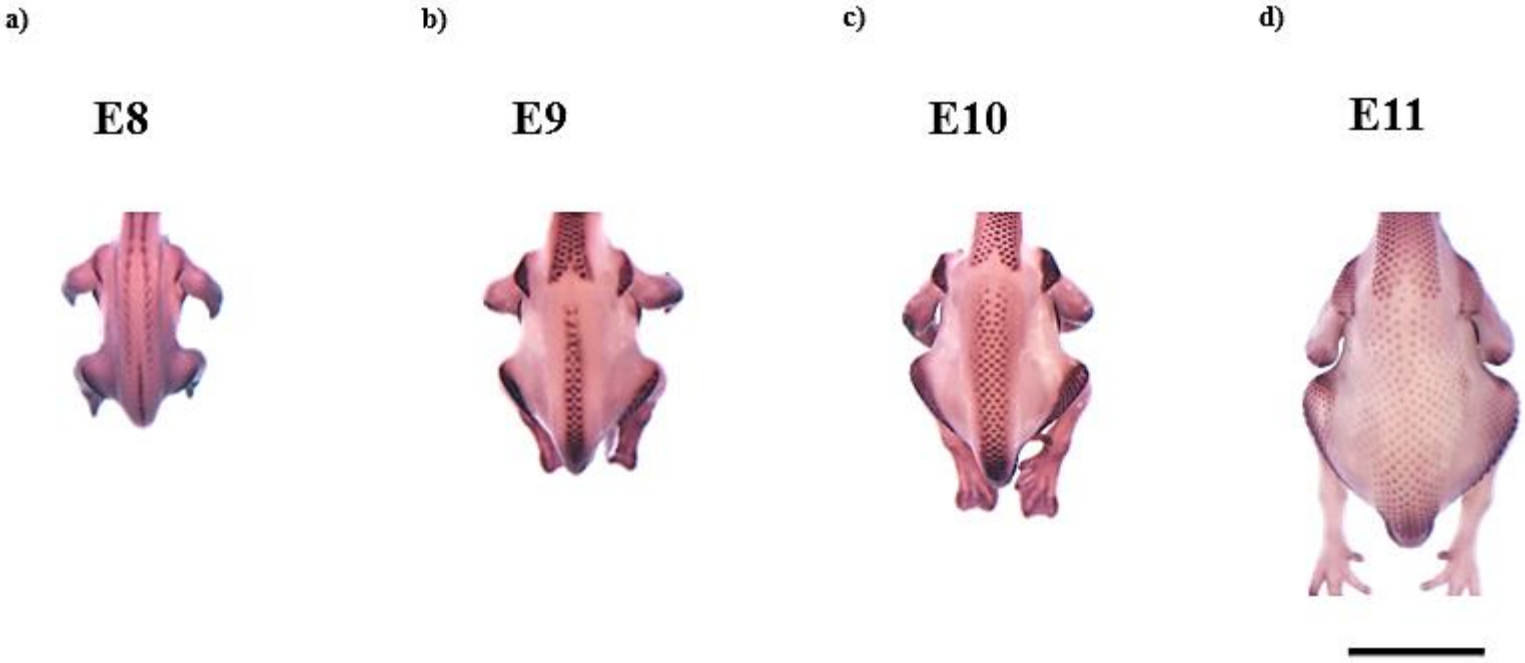

Figure 59. Primordium formation and *β-Catenin* expression in the developing guinea fowl embryo. a) Within the presumptive dorsal tract, before primordium induction, *β-catenin* is expressed within the somites of E8 guinea fowl embryos and is also observed within the primary stripe at the dorsal midline of the tract. **b)** At E9, propagation of *β-Catenin* expression is observed and is restricted to the developing feather primordia as primordia form. **c)** Over the course of propagation of feather primordium formation, *β-Catenin* expression continues to spread across the presumptive dorsal tract. *β-Catenin* expression remains restricted to within the feather primordia. **d)** At E11, guinea fowl embryos display a hexagonally arranged periodic pattern of feather primordia. Mature feather buds display polarised expression of *β-Catenin* localised to the distal tip of the feather bud. Scale bar - 5 mm.

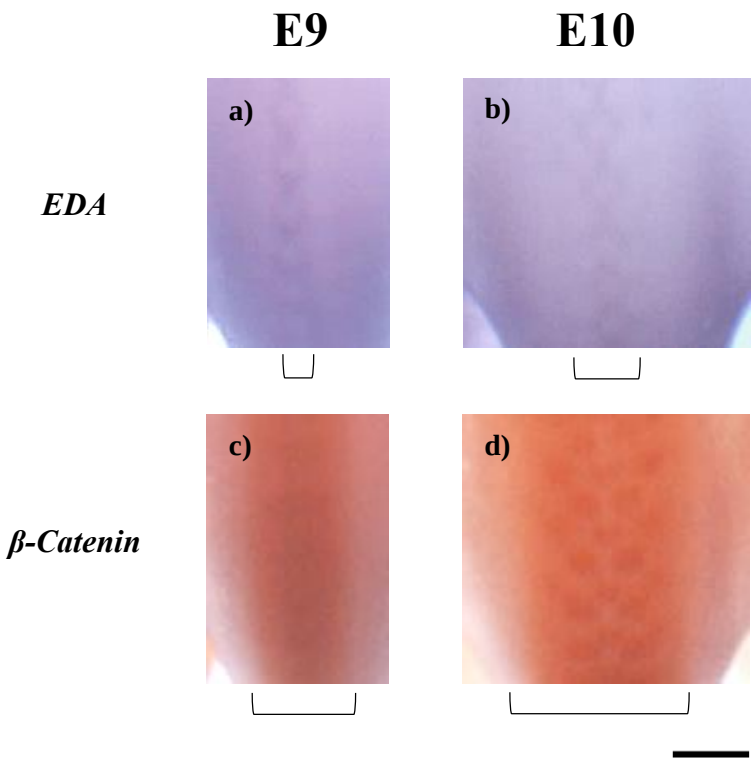

Figure 60. Comparison of *β-Catenin* and *EDA* expression in the developing dorsal tracts of guinea fowl embryos. Detection of *EDA* (purple staining) and *β-Catenin* (orange staining) expression of the dorsal tract of E9 and E10 guinea fowl embryos. **a)** Within the presumptive dorsal tract of E9 guinea fowl embryos, *EDA* expression is restricted to the interbud regions of the midline primary row of forming feather primordia. **b)** By E10, *EDA* expression propagation is observed, but lags behind the wave of feather primordium propagation by one row on either side of the midline. **c)** *β-Catenin* detection on E9 guinea fowl embryos shows the *β-Catenin* expression pattern at this stage is broader than that of *EDA* expression (approximately the width of three primordium rows) **d)** At E10, *β-Catenin* expression propagation remains ahead of *EDA* expression by one to two primordium rows. Brackets indicate width of detected gene expression. Scale bar - 500 µm

3.3.2 Duck

Before primordium induction, at E8, *β-Catenin* is expressed strongly throughout the presumptive dorsal tract but is excluded from a triangular region of skin that widens in a posterior-anterior direction, resulting in the formation of a characteristic "V" shaped *β-Catenin* expressing region in the dorsal tract of developing duck embryos (**Figure 61a**). Primordium formation is initially induced on the inner side of the two arms of the "V", as observed through the restriction of *β-Catenin* expression to within the forming primordia while excluded from the interbud regions (**Figure 61b**). Primordium formation and *β-Catenin* expression gradually propagates bilaterally from the initial site of induction, until the entirety of the skin is covered in feather primordia (**Figure 61c**). When propagation of feather primordium induction has ceased, feather primordia are arranged in a hexagonal pattern in the dorsal tract and *β-Catenin* expression is localised to the feather primordia but is excluded from interbud domains (**Figure 61d**). At E10, an expanded region of *β-Catenin* expression from neighbouring feather tracts (the femoral and lateral tracts) can be seen migrating towards the dorsal tract. The expanded *β-Catenin* expression eventually merges with the dorsal tract until the apteric regions are no longer visible. New rows of feather primordia are added in the wake of the propagating wave of "ectopic" *β-Catenin* expression.

EDA expression was not detected clearly on whole duck embryos. *EDA* expression during the induction of feather primordia was instead visualised on cultured skin explants prepared from E8 duck embryos prior to primordium induction. After one day in culture, expression of *EDA* is observed strongly as a "V" shaped stripe, corresponding to the site of initial feather primordium induction. Diffuse expression of *EDA* is detectable, lateral to the stripe of *EDA* expression (**Figure 62a**). Expression of *EDA* propagates across the dorsal tract in a bilateral direction from the initial site of induction of *EDA* expression, promoting the formation of new feather primordia in its wake (**Figure 62b**). As *EDA* expression propagates, it is restricted to the interbud domains. Eventually, *EDA* expression is observed throughout the entire dorsal tract, between feather primordia and within the anterior end of the maturing feather bud (**Figure 62c**).

Unlike the species examined thus far, ducks undergo a secondary wave or feather primordium induction during embryonic development, which form independently of *EDA* expression (**Figure 63**). The feather primordia in the second wave are much smaller in comparison to the first wave of feather primordia and their formation is only induced after the formation of the first wave of feather primordia has ended.

At E10, *β-Catenin* expression is restricted to within the feather primordia only (**Figure 63a**). At E11, *β-Catenin* expression reappears diffusely between the existing primordia. The reappearance of *β-Catenin* expression begins at or close to the dorsal midline where the most mature feather primordia reside, before spreading laterally across the skin. The secondary wave of *β-Catenin* expression remains within the interbud domains its propagation, similar to the previously observed *EDA* expression pattern (**Figure 63b**). From E12 onwards, the diffuse *β-Catenin* expression between primordia focalises to form discrete spots of *β-Catenin* expression (**Figure 63c**). The spots of *β-Catenin* expression eventually give rise to individual feather primordia (indicated by *SHH* expression within the feather primordia (**Figure 63g**)). Whereas, *EDA* expression, at E10 is detected throughout the dorsal tract in the interbud spaces but gradually disappears from these regions and is later focalised to the anterior end of the first wave of mature feather bud (**Figure 63d-63f**). The secondary feather primordia are organised in a low fidelity pattern, compared to the arrangement of the first wave of feather primordia and appear to be induced in any region of skin not occupied by the first wave of feather primordia.

The results reveal that the mechanisms underlying the formation of the two waves of feather primordia in ducks are individually distinct from one another which results in the formation of two different types of feather primordia during the embryonic development of ducks. During the first wave of feather primordium induction, *EDA* expression and propagation is required for the sequential formation of large primordia, arranged in a high fidelity periodic pattern. Secondary feather primordia, on the other hand, arise through an *EDA* independent process, forming much smaller feather primordia.

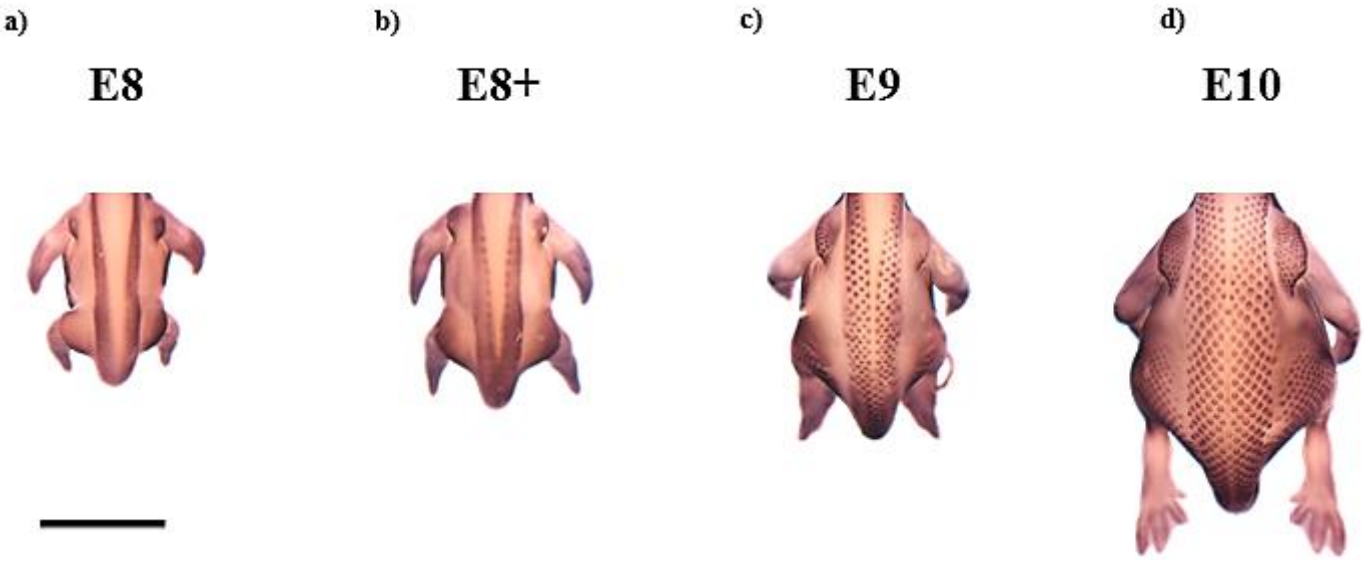

Figure 61. Primordium formation and *β-Catenin* expression in the developing duck embryo. a) At E8, before primordium induction, *β-Catenin* is expressed in a large "V-shaped" region on the dorsal side of the embryo. Between the "arms" of *β-Catenin* expression, expression of *β-Catenin* is not observed. **b)** Feather primordia are initially induced on the inner arms of the "V-shaped" *β-catenin* positive region, and at the dorsal midline, towards the caudal end of the tract. *β-Catenin* expression, follows the "restrictive mode" pattern of expression. **c)** At E9, feather primordium formation has propagated laterally to cover the initially *β-Catenin* positive region with feather primordia, and also medially to "fill" in the initially *β-Catenin* negative region of skin. **d)** At E10, ducks display a highly organised, hexagonal periodic pattern of feather primordia. *β-Catenin* expression from lateral and femoral feather tracts appear to migrate from their initial site of expression, eventually covering the apteric regions and merging with the dorsal tract Scale bar - 5 mm.

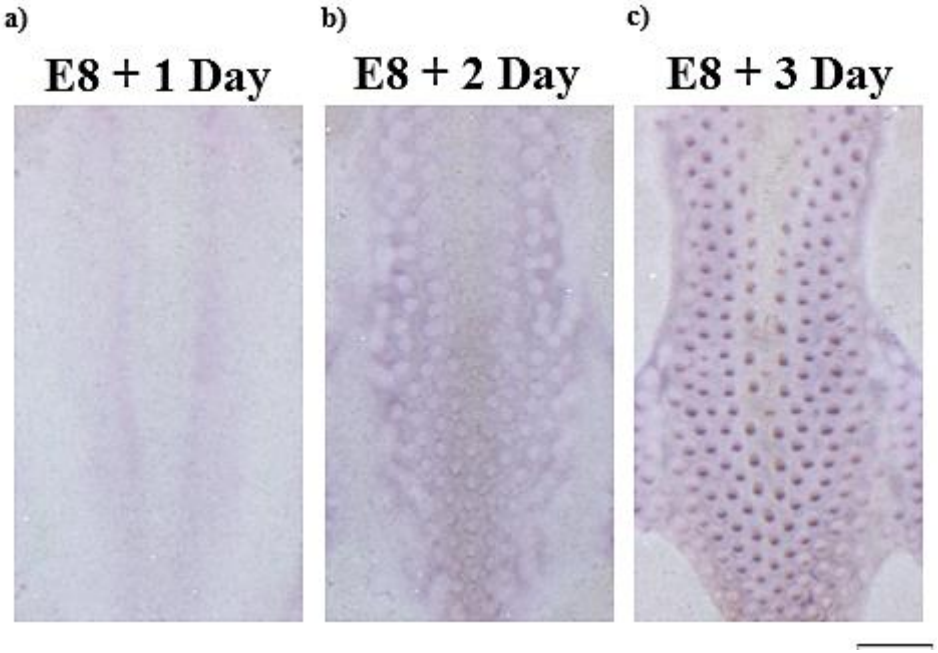

Figure 62. Primordium formation and *EDA* expression in the developing duck embryo. Detection of *EDA* expression on cultured duck dorsal skin explants. **a)** *EDA* expression is observed in a "V-shaped" pattern (similar to *β-Catenin* expression in duck). Initially, *EDA* expression is induced on the inner arms of the "V" and later propagates bilaterally, preceding the induction of feather primordium formation, eventually covering the dorsal tract of the embryo. Highest levels of *EDA* expression is initially detected at the site of the primary row of feather primordium induction, on the inner arms of the "V". **b)** Similar to the chicken and guinea fowl embryos, *EDA* expression is restricted to within the interbud regions, as feather primordium formation is induced across the tract **c)** After 3 days in culture, *EDA* expression has covered most of the skin explants, remaining mostly within the interbud regions. Mature feather primordia display *EDA* expression on the posterior end of the primordia. Scale bar - 1 mm.

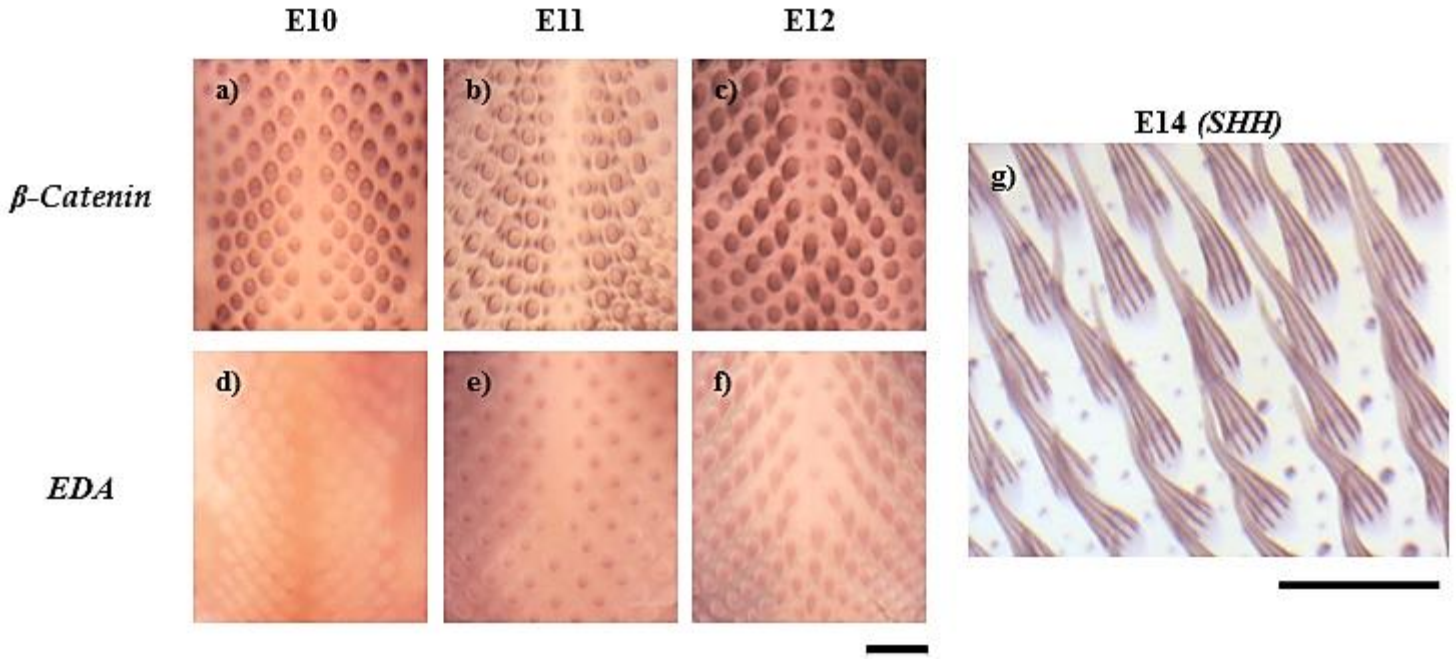

Figure 63. Ducks undergo a secondary wave of feather primordium induction which form independently of *EDA* expression. Detection of *β-Catenin* and *EDA* expression through *in situ* hybridisation during the secondary wave of feather primordium induction. **a)** *β-Catenin* expression is only observed within the maturing feather primordia in E10 embryos. **b)** At E11, diffuse expression of *β-Catenin* is induced in the interbud spaces in the medial regions of the tract initially which gradually propagates laterally. **c)** By E12, the initially diffuse expression of *β-Catenin* between the initial wave of feather primordia has focalised into discrete primordia. **d)** *EDA* expression is restricted to the interbud domains of E10 dorsal tracts. **e)** As *β-Catenin* expression is induced in the interbud regions, *EDA* expression gradually disappears from the interbud spaces but increases within the maturing first wave of feather primordia. **f)** By E12, *EDA* expression cannot be detected in the interbud spaces. **g)** Detection of *SHH* expression on an E14 duck embryo. *SHH* expression is detected as stripes within the first wave of feather buds and on the distal tips of the secondary primordia, which indicate that the smaller spots are indeed feather primordia. Scale bar - 1mm.

3.3.3 Ostrich

During the early stages of feather development (around E13), the *β-Catenin* expression pattern observed in ostriches is similar to that found in the embryonic chicken dorsal tracts. *β-Catenin* is initially expressed diffusely throughout the presumptive feather tracts. Expression of *β-Catenin* broadens in the dorsal region between the wings and the legs, covering part of the lateral regions on either side of the embryo (**Figure 64a**). At E14, primordium induction (as indicated by restricted expression of *β-Catenin*), does not begin at the dorsal midline as in chickens, but in regions lateral to the midline (**Figure 64b**). *β-Catenin* expression is restricted to developing or developed primordia and is excluded from interbud regions. Primordium formation propagates inwards, towards the midline of the dorsal tract, eventually covering the entire tract with feather primordia (except for a stripe of skin devoid of feather primordia in the middle of the embryo). During the inward wave-like primordium propagation, primordium insertion between existing primordia can be observed. *β-Catenin* expression occasionally reappears and focalises between existing feather primordia, forming new feather primordia between them (**Figure 64c**). The constant insertion of new primordia between existing ones, prior to feather outgrowth, results in the formation of a periodic pattern of low fidelity, consisting of primordia of different age and size across the tract (**Figure 64d**). As primordia mature and differentiate, *β-Catenin* is restricted to the distal tip of growing feather buds.

Unlike the flighted species examined thus far, ostriches do not display spatiotemporal restricted expression of *EDA* during periodic pattern formation. At E13, before the induction of primordium formation, *EDA* is expressed throughout the presumptive dorsal tract and excluded from the apteric regions (**Figure 65a**). As embryonic development progresses, feather induction occurs in regions devoid or expressing low levels of *EDA*, while *EDA* expressing regions remain unchanged within the tracts and does not show restriction of expression to within the interbud spaces during primordium induction (**Figure 65b**). At E16, *EDA* expression is observed in the dorsal region of the embryo, forming a band of *EDA* expressing skin but is not observed anywhere else on the dorsal side of the embryo outwith the band (**Figure 65c**).

Compared to chicken and other flighted Ave species, the final primordium pattern observed in ostriches is relatively unorganised and of a low fidelity. During embryonic development, spatiotemporal wave-like induction of feather primordia from the midline of the tract does not occur. Instead, induction of feather primordia is initiated from the lateral regions of the tract, which then spreads towards the midline, the inverse of primordium induction process observed in flighted species of Aves. Also unlike flighted species, during feather primordium induction in ostrich, *EDA* expression is initially observed across the entire presumptive dorsal tract before any visible evidence of primordium induction has begun. This suggests that the low fidelity feather primordium periodic pattern observed in ostriches could be associated with the lack of restricted spatiotemporal propagation of *EDA* expression. However, as observed in experimental manipulations of chicken skin explant cultures (see section **3.2.6**), expansion of the *EDA* expression domain prior to feather primordium induction results in the simultaneous induction of feather primordium formation within the tract. This is not observed in the ostrich embryos and primordium induction around the dorsal midline of the tract is delayed. This suggests the possibility that a lack of a permissive factor within the dorsal tracts of ostriches prevents the simultaneous induction of feather primordia across the tract, despite the presence of overlapping expression of *β-Catenin* and *EDA*.

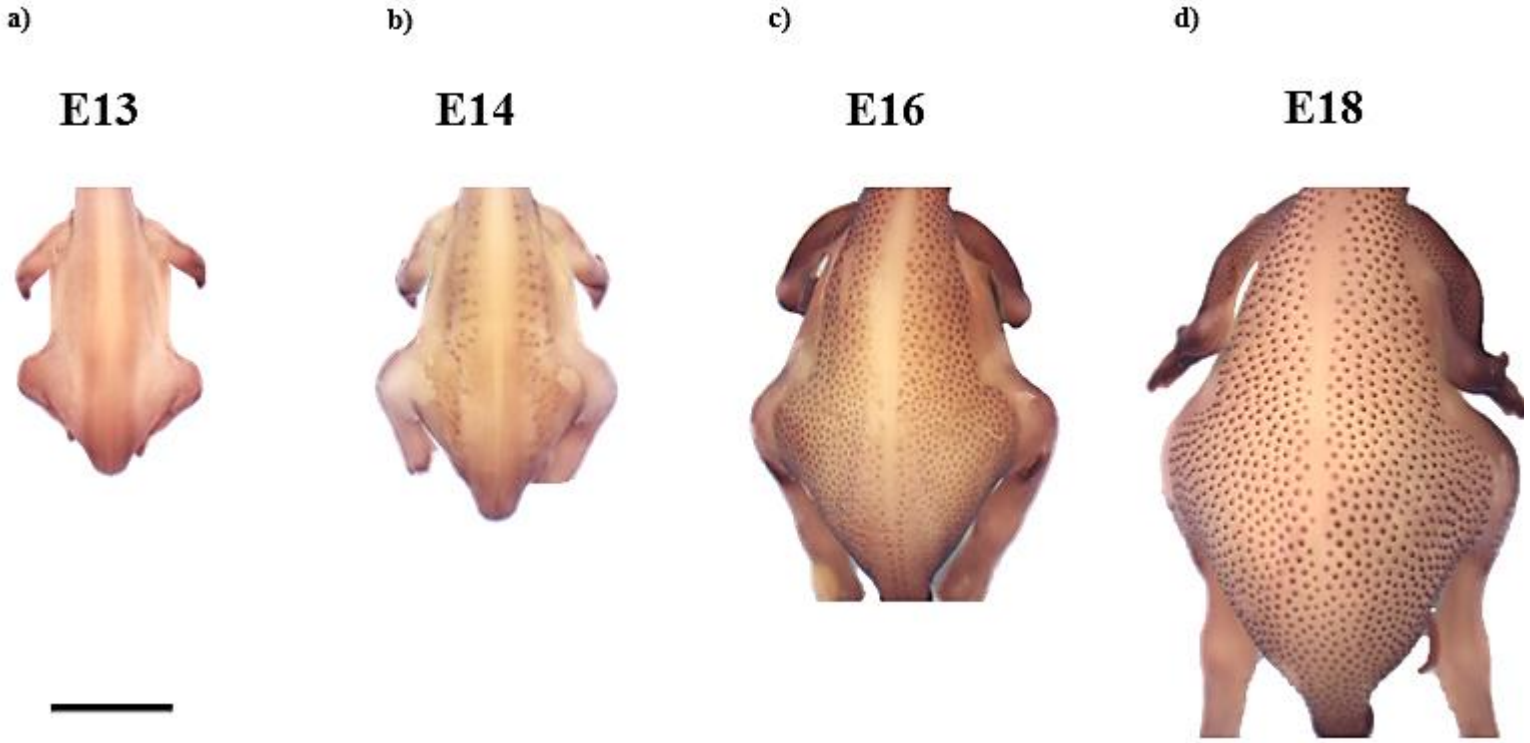

Figure 64. Primordium formation and *β-Catenin* expression in the developing ostrich embryo. a) Before primordium induction, diffuse expression of *β-Catenin* can be observed in the presumptive feather tracts and excluded from the apteric regions. **b)** As primordium formation is induced, *β-Catenin* is restricted to the developing feather primordia which form laterally from the midline region of the tract **c)** At E16, primordium formation has spread from the lateral regions of the dorsal tract towards the midline of the tract. *β-Catenin* expression remains restricted to developing and developed primordia. **d)** At E18, ostrich embryos display an unorganised low fidelity periodic pattern or feather primordia. Scale bar - 5 mm.

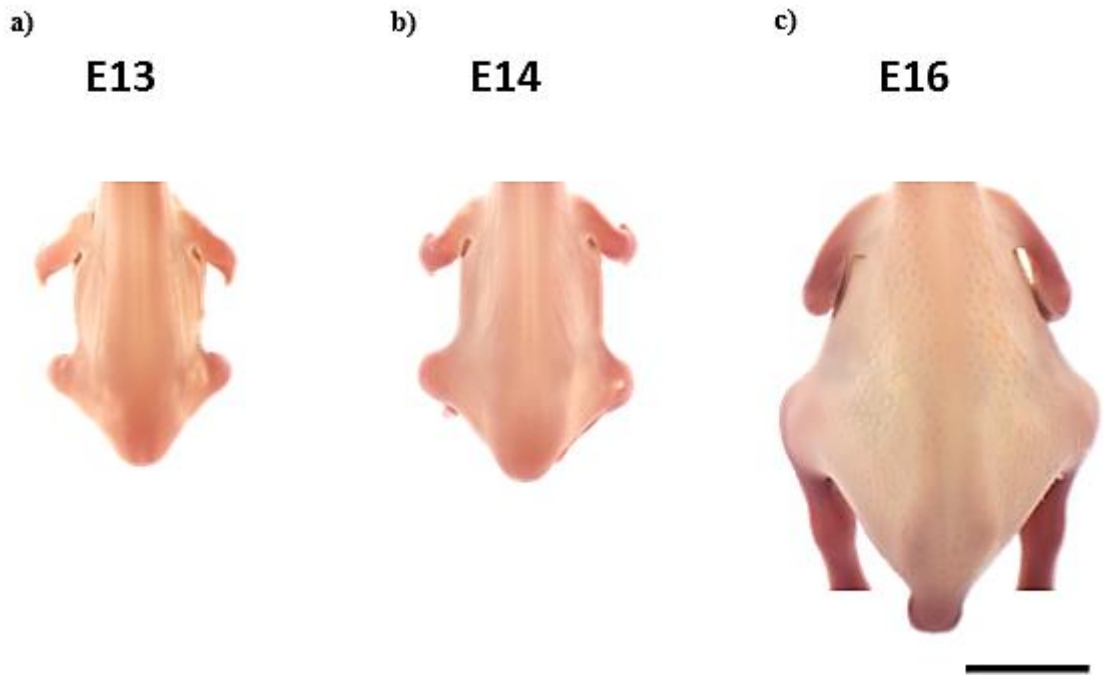

Figure 65. *EDA* expression in the developing ostrich embryo dorsal tract. Before primordium induction *EDA* is expressed across the entire presumptive dorsal tract and remains within the tract throughout embryonic development, overlapping the initial *β-Catenin* expression pattern. *EDA* expression is excluded from both primordia and interbud regions during primordium induction and formation. Scale bar - 5 mm.

3.3.4 Emu

At E15, the presence of a presumptive dorsal tract is indicated by the homogenous detection of *β-Catenin* transcripts within the dorsal side of the embryos, separated by *β-Catenin* negative "apteric" regions (**Figure 66a**). Primordium induction is initiated on the lateral regions and in the posterior end of the dorsal tract of emu embryos, indicted by the observed "restrictive mode" of pattern expression of *β-Catenin* (**Figure 66b**). The process of primordium induction appears to be different in the dorsal tract, compared to that of the lateral regions. On the lateral regions, large stripes of strongly *β-Catenin* positive regions, separated by *β-Catenin* negative regions, form on the outside of the presumptive dorsal tract. The stripes of *β-Catenin* separate during embryonic development, forming individual feather primordia. Whereas, within the posterior region of the dorsal tract, feather primordia are observed to form as discrete spots, expressing high levels of *β-Catenin* separated by *β-Catenin* negative interbud domains. Primordium induction gradually propagates inwards towards the midline of the tract from the lateral regions and the posterior end of the dorsal tract, until the entire dorsal area, including the apteric regions of the embryo, are covered in feather primordia (**Figure 66c**). From E19 onwards, new primordia are inserted in the interbud regions as the embryo grows in size. By E21, almost the entire body of the embryo is covered in an unorganised pattern of tightly packed primordia of various sizes (**Figure 66d**).

EDA expression is initially observed throughout the presumptive dorsal tract in emus before the induction of primordium formation, following a similar expression pattern to *EDA* as observed during ostrich development. *EDA* is not shown to be expressed in a spatiotemporally restricted manner in the stages analysed. Even at E14, *EDA* expression is already clearly visible throughout the presumptive feather tract, indicating spatiotemporal expression of *EDA* does not occur during emu embryonic development (**Figure 67a**). Over the course of development, *EDA* expression remains within the confines of the dorsal tract (**Figure 67b**). At E18, when primordium induction has been initiated in the posterior end of the dorsal tract and the lateral regions of the embryo, the *EDA* expression pattern within the dorsal tract remains the

same as previous stages and *EDA* expression is not observed in the interbud regions between existing or developing primordia. The *EDA* expression pattern during the development of emus is analogous to that observed during the development of ostrich embryos (**Figure 67c**).

Similar to ostriches, the final periodic pattern of feather primordia observed in emu embryos is of low fidelity. The process of periodic pattern formation in emu skin follows similar parallels to ostrich skin patterning. In emus, induction of feather primordia initially occurs in a lateral to medial direction during primordium induction. Also expression of *EDA* is observed throughout the presumptive dorsal tract of emu embryos prior to the onset of primordium induction. It is possible that the loss of pattern fidelity within the dorsal tract of both ostriches and emus is the results of similar modifications to the basic feather primordium induction process used in feather primordium development in flighted species.

Another similarity between the ostriches and emus is that the induction of feather primordia within the dorsal midline of the tract is also delayed, despite the presence of both *β-Catenin* and *EDA* expression throughout the presumptive dorsal tract prior to primordium induction. This suggests a permissive factor may be missing in the dorsal tracts of both species, which delays the onset of feather primordium induction around the dorsal midline of the tracts.

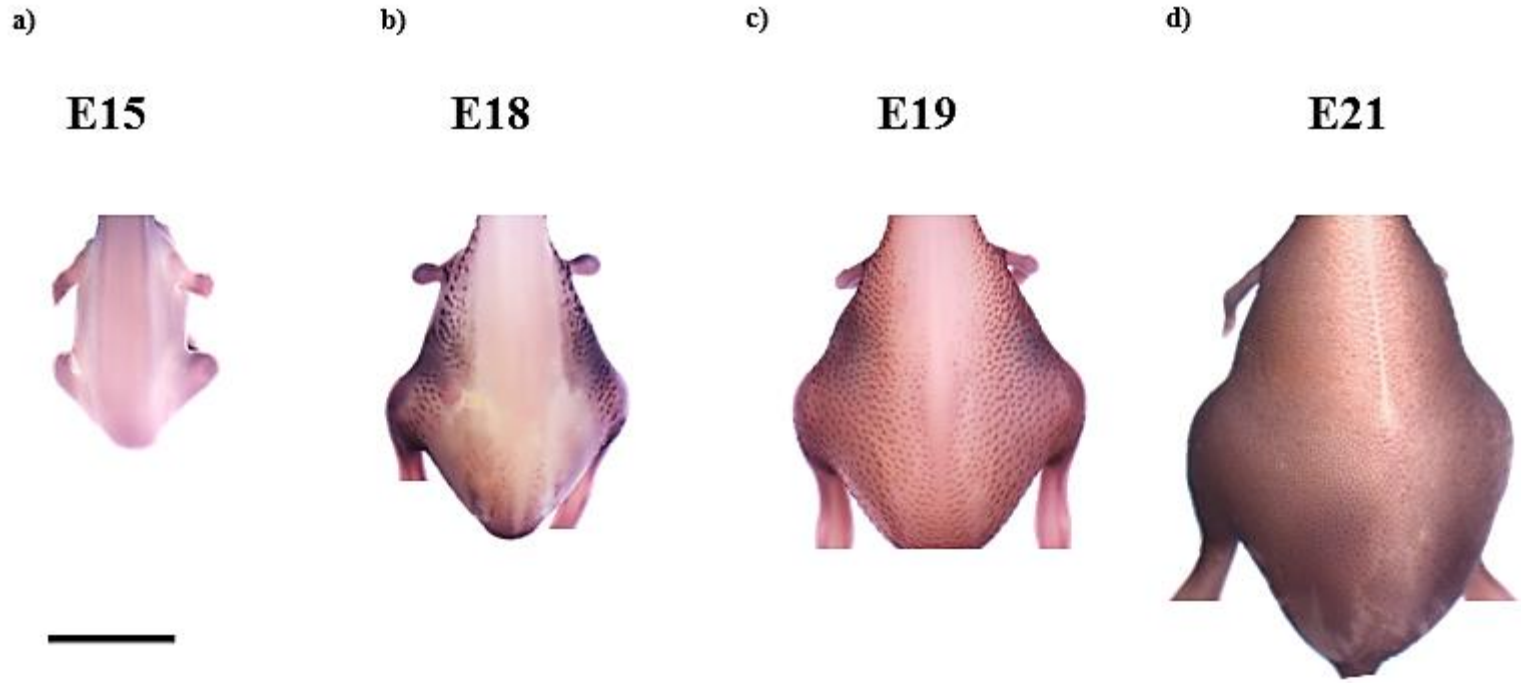

Figure 66. Primordium formation and *β-Catenin* expression in the developing emu embryo. a) Before primordium induction, *β-Catenin* is initially expressed in the presumptive feather tracts and excluded from the apteric regions. **b)** Feather primordia are induced lateral to, and outside, the dorsal tract and *β-Catenin* expression is increased within the developing feather primordia. **c)** Over the course of development primordium formation spreads from the lateral regions to within the presumptive dorsal tract. *β-Catenin* expression remains within feather primordia. **d)** At E21, emu embryos display an unorganised low fidelity periodic pattern or feather primordia which completely cover the skin, even within the apteric regions. *β-Catenin* is expressed within feather primordia but is excluded from interbud regions. Scale bar - 5 mm.

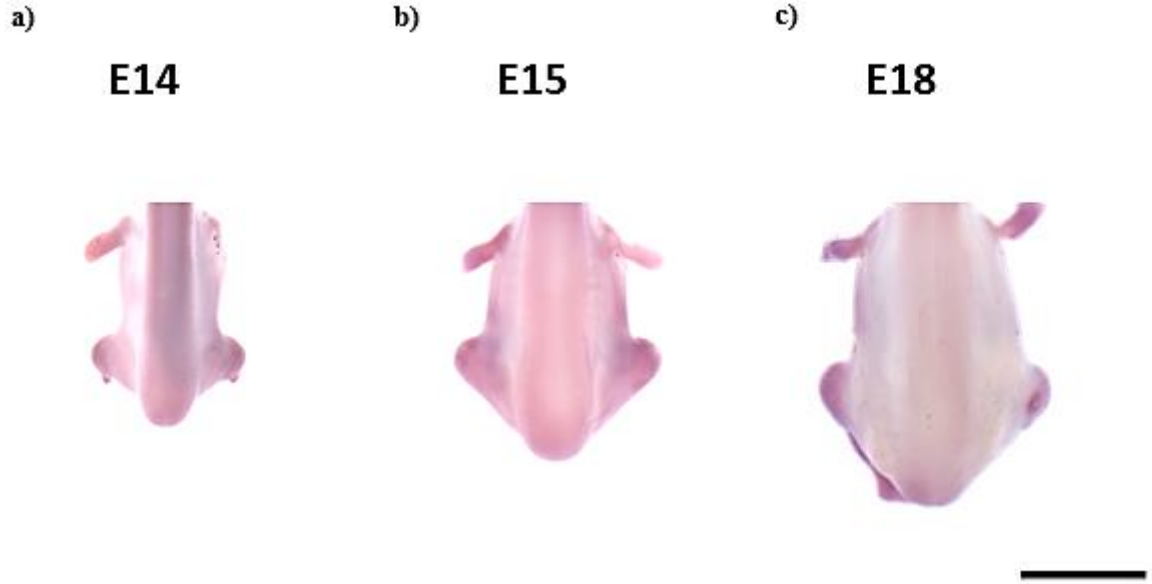

Figure 67. *EDA* expression in the developing emu embryo dorsal tract. Emu embryos do not show gradual wave-like propagation of *EDA* expression. *EDA* is expressed across the entire presumptive feather tract throughout embryonic development, overlapping the initial *β-Catenin* expression pattern and *EDA* does not show restrictive expression to either primordium or interbud domains during primordium induction and formation. Scale bar - 5 mm.

3.4 Determination of the Mechanisms Underlying Ostrich and Emu Dorsal Tract Pattern Formation

3.4.1 Dorsal Tract Epidermis of Emus can Induce Feather Primordium Formation if a Dermis of Sufficient Cell Density is Present

Despite the observed presence of *EDA* expression across the dorsal tract in emus, prior to feather primordium induction, simultaneous primordium induction across the dorsal tract does not occur. The above observation indicates that either; 1) the absence of an epidermis competent to primordium induction or 2) a dermis of sufficient cell density is lacking within the presumptive dorsal tract of the developing embryos, which is preventing the simultaneous induction of feather primordia across the entire tract. If the dorsal tract epidermis of emu embryos was competent to induce primordium formation at a developmental stage prior to endogenous primordium induction, *ex vivo* recombination of E14 emu dorsal tract epidermis onto a permissive dermis of high cell density, should produce a skin capable of inducing the formation of feather primordia.

To evaluate whether the primary defect underlying the delayed induction of feather primordium formation within the midline region of the dorsal tract of emu embryos is of epidermal or dermal origin, hetero-specific epidermal-dermal recombination was performed. Epidermis and dermis of dorsal tract skins prepared from HH 29 GFP chicken and E14 emu embryos were separated and then recombined. The following epidermal-dermal recombinations between GFP chicken and emu embryos were performed and analysed; GFP chicken epidermis with GFP chicken dermis, GFP chicken epidermis with emu dermis and emu epidermis with GFP chicken dermis and cultured for 96 hours. The use of GFP chicken embryos in the recombination experiment provides a simple method to distinguish the origin of cells in the two recombined skin layers (**Figure 68**).

Control recombination between GFP chicken epidermis and GFP chicken dermis resulted in the formation of a periodically patterned array of feather primordia of similar sizes after a period of 96 hours in cultures (**Figure 68a**). Primordium formation is visible after 24 hours and feather bud outgrowth is observed following a further 72

hours in culture. This result demonstrates that the competence of feather primordium induction and formation in both the epidermis and dermis of GFP chicken embryos is unaffected by the epidermal-dermal separation and recombination procedure.

Primordium induction was not observed in cultures of recombinants consisting of GFP chicken epidermis and emu dermis throughout the duration of culture (**Figure 68b**). No morphological changes were observed within the recombined explant throughout the 96 hour period in culture, suggesting that E14 emu dermis is not permissive to primordium induction, despite the presence of an overlying epidermis competent to primordium induction.

The reciprocal recombination between emu epidermis and dermis from GFP chicken embryos resulted in feather primordium induction on the emu epidermis. The rescued feather primordia arise and differentiate in a similar sequence to that observed in control recombinations (**Figure 68c**). After 24 hours in culture, the induction of cell aggregation and feather primordium formation is observed and over the duration of culture, new feather primordia are induced and feather bud outgrowth can also be seen. After 96 hours in culture, the explant displays feather buds of unequal size and shapes, arranged in an unorganised pattern.

Histological examination of all recombinants after 96 hours by detection of GFP in sections counter-stained with DAPI, was performed to reveal any possible cross contamination of cells between the epidermis and dermis in the hetero-specific recombinants. In control GFP chicken epidermis and GFP chicken dermis recombinants, co-localisation of GFP and DAPI signal can be detected throughout both skin layers (**Figure 69a**). In hetero-specific recombinants, between GFP chicken and emu skin layers, GFP signal is restricted to either the epidermal or dermal layer of the recombinant (**Figure 69b & 69c respectively**), indicating that the skin layer originated from the GFP chicken embryo. Thus, feather primordium formation observed in the recombinants consisting of emu epidermis recombined with GFP chicken dermis was induced solely by the emu epidermis during culture and not the result of cross

contamination of cells from GFP chicken epidermis during the separation/recombination procedure.

Although morphologically similar to endogenous feather primordia observed in control chicken to chicken recombinations, whether the molecular identity of the emu epidermis/chicken dermis induced primordia are similar to control primordia has not been addressed. *In situ* hybridisation was performed on emu epidermis/GFP chicken dermis recombinants after 24 hours in culture to determine if the induced feather primordia in the recombinants displayed molecular characteristics similar to those observed during endogenous primordium induction in chicken (**Figure 70**). The *in situ* hybridisation analysis revealed that in the emu epidermis/GFP chicken dermis recombinants, the *β-catenin* expression pattern in the forming feather primordia follows a "restrictive mode" pattern of expression. The recombinants initially displayed diffuse expression of *β-Catenin* across the tract, followed by restriction and focalisation of *β-Catenin* expression to within the forming feather primordia and excluded from interbud regions. The result show that primordia induced by the emu epidermis follows a similar pattern of *β-Catenin* expression to those observed during endogenous chicken primordium induction (see section **3.2.3**).

The results demonstrate that E14 emu dorsal tract epidermis retains the ability to induce the formation of feather primordia, suggesting that delayed feather primordium induction within the emu dorsal tract is associated with a defect within the dermis of developing emu embryos.

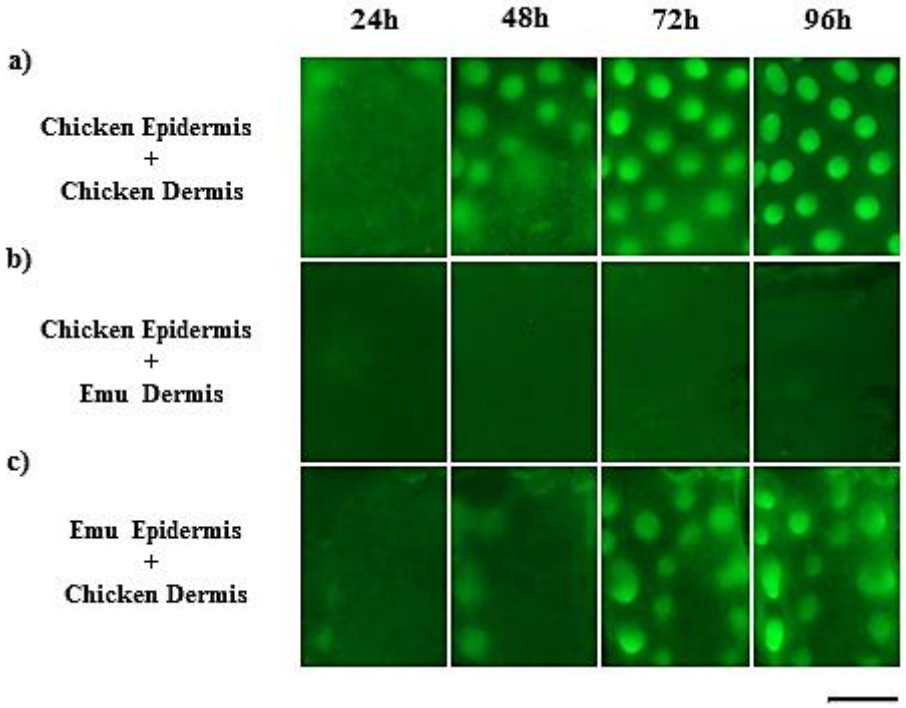

Figure 68. Hetero-specific epidermal/dermal recombination rescues feather primordium formation in emu dorsal tract epidermis. Separated epidermis and dermis from HH 29 GFP chicken and E14 emu dorsal skins were recombined and cultured for a period of 96 hours. **a)** GFP chicken/GFP chicken control recombination show feather primordium induction is unaffected by the procedure. **b)** Recombination between GFP chicken epidermis and emu dermis does not result in primordium induction throughout the duration of culture. **c)** Feather primordium induction is rescued in explants of emu epidermis recombined with GFP chicken dermis, demonstrating that the underlying patterning defect in the emu dorsal tract is of dermal origin. Scale bar - 500 µm.

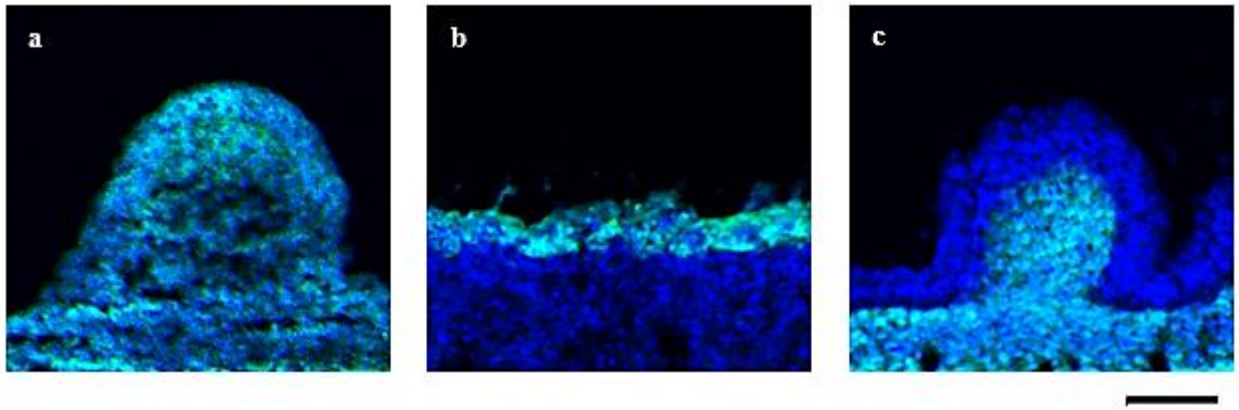

Figure 69. No cross contamination of epidermal or dermal cell was observed in the recombinants. Cryosections of recombined skin explants after 96 hours in culture revealed there was no cross contamination between the skin layers as detected by DAPI staining. **a)** Co-localisation of GFP and DAPI signal can be detected throughout the control GFP chicken epidermis/GFP chicken dermis recombinant. **b)** Detection of GFP signal is restricted to the epidermal layer of the GFP chicken epidermis. While the dermal layer, which originated from an emu embryo displayed no GFP signal, indicating that the epidermis and dermis of the recombinant originated purely from the GFP chicken and emu embryo respectively. **c)** Emu epidermis and GFP chicken dermis recombinant show GFP localisation specifically in the dermis of the recombinant Scale bar - 50 µm.

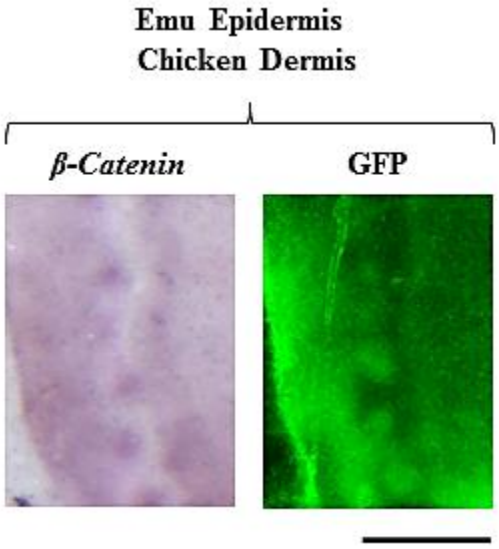

Figure 70. *β-Catenin* expression in emu epidermis induced primordia display a "restrictive mode" pattern of expression. *In situ* hybridisation reveals *β-Catenin* transcripts are expressed in the "restrictive mode" pattern of expression in the forming primordia of the recombined emu epidermis and chicken GFP dermis, after 24 hours in culture. Scale bar - 1 mm.

3.4.2 Feather Primordium Induction in the Medial Regions of the Dorsal Tract of Emus and Ostriches is Initiated through the inward Propagation of Dense Dermis Formation from the Lateral Regions to the Midline

The dermal cell density in the presumptive dorsal tracts of emu and ostrich embryos were analysed to determine whether failure of dense dermis formation in the medial regions of the dorsal tracts was associated with the delayed induction of primordium formation, despite the observable expression of *EDA* transcripts across the *β-Catenin* expressing dorsal tract (**Figure 71 & Figure 72**).

Histological examination of transverse sections of developing chicken and emu dorsal tracts, though H & E staining, revealed key differences in the initial distribution of dense dermis across the dorsal tracts of both species, prior to the onset of feather primordium induction. In chickens, at E6.5, a dense layer of cells in the underlying dermis was detected in the medial regions of the dorsal tract (**Figure 71a**). Skin regions lateral to the dorsal midline displayed a gradual decrease of dermal cell density in a medial to lateral direction (**Figure 71b**). In emu dorsal tracts, the initial location of dense dermis thickening was reversed compared to the initial dense dermis distribution observed in the chicken dorsal tract. In E15 emu embryos, the dorsal midline exhibited a low dermal cell density (**Figure 71c**), while the lateral regions showed a layer of dense dermis of comparable thickness to E6.5 chicken midline dense dermis (**Figure 71d**). Later, at E18, dermal thickening can be observed around the dorsal midline of the tract (**Figure 71e**), but dermal cell density has yet to reach a comparable dermal thickness to E6.5 chicken midline dermis. Regions lateral to the dorsal midline showed a continued increase in dermal cell density in E18 emu embryos (**Figure 71f**).

Transverse sections of the developing ostrich dorsal tracts revealed that prior to feather primordium induction, regions of skin displaying the highest dermal cell densities were located at the lateral regions of the embryo, while more medial regions of skin displayed a lower dermal cell density, similar to the developing emu embryos (**Figure 72**). As ostrich embryos develop, the underlying dermis across the dorsal tract thickens but retains the gradient of high to low dermal cell density in a lateral to medial

direction. The observation indicates that the propagation of dense dermis thickening observed in ostriches, is analogous to that of the developing emu dense dermis thickening during skin development.

The above observations suggests that, despite the presence of *EDA* expression across the tract, delayed feather primordium induction within the medial regions of the dorsal tracts of ostrich and emu embryos may be associated with the loss of a dermis of sufficient dermal cell density. The loss of dense dermis formation within the medial regions of the dorsal tracts of ostrich and emu embryos may also be responsible for the lateral to medial wave-like propagation of feather primordium induction, rather than a medial to lateral direction as observed in flighted species of Aves. Dense dermis formation from lateral regions may gradually fill the medial regions of the dorsal tract to compensate for the loss of dense dermis formation at the midline of ostrich and emu dorsal tracts.

Taken together, the findings indicate that in emus, and possibly ostriches, delayed feather primordium induction within the medial regions of the dorsal tract is caused, not by loss of competence of the dorsal epidermis but is associated with the failure of dense dermis formation and propagation from the dorsal midline. Instead, the medial regions of the dorsal tract of emus and ostriches relies on the spread of dense dermis from lateral regions of the embryo towards the dorsal tract before induction of feather primordium formation can be initiated.

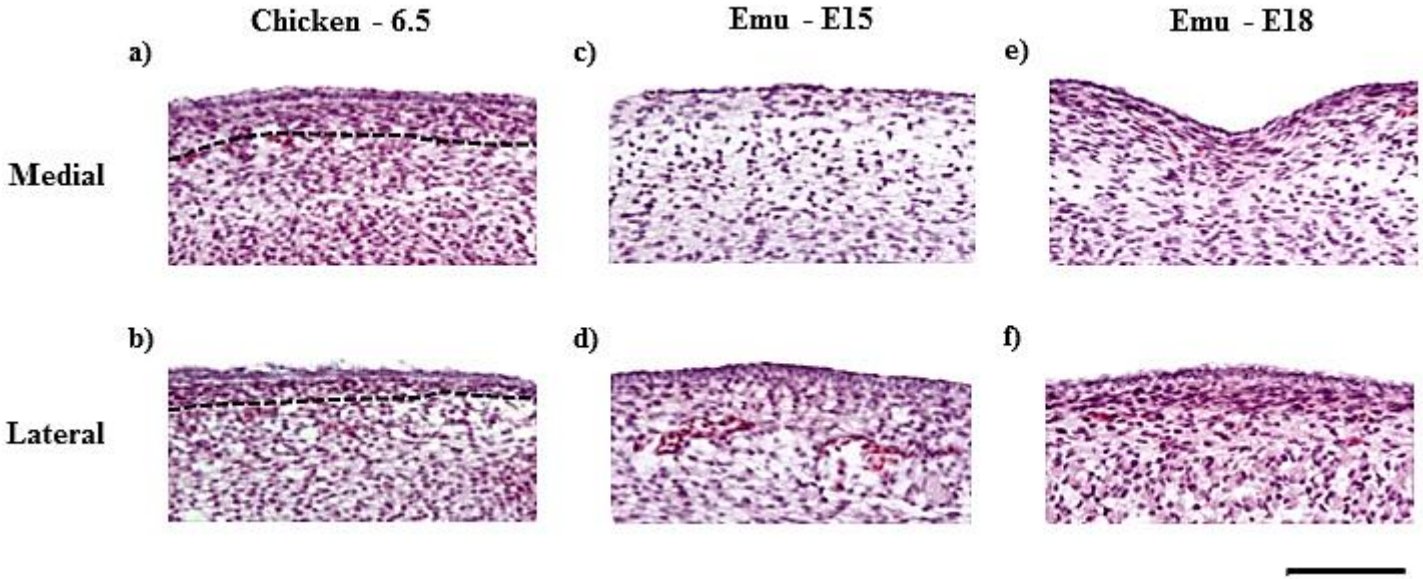

Figure 71. Comparison of dermis thickness between E6.5 chicken and E15/E18 emu embryos. H & E staining of transverse sections from E6.5 chicken, E15 emu and E18 emu embryos. **a)** Prior to feather primordium induction, at the dorsal midline, E6.5 chicken shows a high density of dermal cells whereas **b)** the regions lateral to the dorsal tract shows a lower dermal cell density. **c)** In E15 emu skin, dense dermis appears to not have formed yet at the dorsal midline, instead, **d)** dense dermis forms from the lateral regions of the embryo initially. **e)** At E18, dermal cell density has increased at both the dorsal midline and **f)** lateral regions in emu embryos. Dotted lines outline dense dermis thickness. Scale bar - 100 μm.

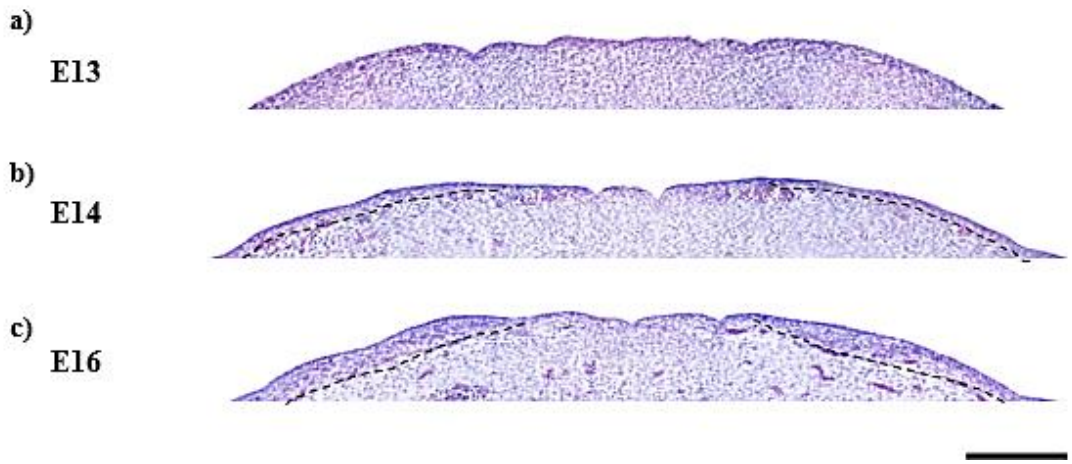

Figure 72. Dense dermis thickening occurs in a lateral to medial direction in the developing ostrich dorsal tract. H & E staining of transverse sections from E13, E14, and E16 ostrich embryos. **a)** At E13, prior to primordium induction, the underlying dermal cell density is low across the dorsal tract. **b)** At E14, cell density of the dermis on the lateral regions of the tract begins to thicken, while regions of skin more medial show little to no change in dermal cell thickness. **c)** At E16, the lateral regions show an increased density of dermal cells, and dermal thickening has propagated towards the medial regions of the skin, but dermal cell density at the midline remains low. Dotted lines outline dense dermis thickness. Scale bar - 200 μm.

DISCUSSION

4. DISCUSSION

Using the chicken embryo as my primary developmental model, the research presented in this thesis identifies the regulatory relationships between the molecular signals involved in feather primordium induction. The research also identifies how these molecular signals regulate cellular behaviour to induce the formation of periodically arranged feather primordia.

The periodic pattern of feather primordia in chicken arises in a strict spatiotemporal sequence. New rows of feather primordia are added sequentially, lateral to the previous row, in a wave-like manner across the dorsal tract during embryonic development. The initial aim of this research was to study cell behaviour during feather primordium induction. From the real-time imaging experiments, I observed that the induction of cell movement and aggregation are key processes in the formation of feather primordia. I then searched for a molecule that could induce cell migration, in a reaction-diffusion like manner, to promote feather primordium formation. Based on previous studies, the potential ability of *FGF20* to promote its own expression and the expression of its inhibitor, *BMP4*, during feather primordium induction was tested. Through these studies, I observed that spatiotemporally restricted induction of *FGF20* expression was required to produce the wave-like propagation of feather primordium formation. I identified a molecular candidate, *EDA*, which could potentially function as the inductive signal that sweeps across the skin to stimulate *FGF20* expression, initiating the process of feather primordium formation, and so I attempted to discern the mechanisms driving primordium wave propagation. Additionally, using the knowledge gained from these studies in chicken, I describe the process of periodic patterning of feather primordia in several other species of Aves.

This discussion will focus on the role of each of the molecular or cellular components involved in feather primordium induction and periodic patterning of feather primordia. How the "basic" molecular and cellular toolkit involved in feather primordium formation can be modified to produce the various periodic patterns of feather primordia observed in different species of Aves, will also be discussed.

4.1 The Process of Primordium Induction

4.1.1 Real-Time Tracking of Cell Behaviour During Feather Patterning

Previous studies relied primarily on *in situ* hybridisation or immunohistological analysis of markers involved in feather primordium formation to examine the process of their formation (Chuong and Edelman, 1985; Drew *et al.*, 2007; Jiang *et al.*, 2004; Lin *et al.*, 2009). However, these methods require the fixation of samples which provide only a single snapshot in time of the primordium formation process, losing valuable information. The use of the CAG-GFP transgenic chickens (GFP chicken) (McGrew *et al.*, 2008) in the study of feather primordium induction and patterning provides a powerful tool to dissect the molecular and cellular processes underlying primordium induction. By utilising the GFP transgenic chicken in the *ex vivo* culture system, I developed a method which, for the first time, allowed the process of individual feather primordium induction and the wave-like propagation of primordium formation to be observed in real time on a single skin explant.

Studying feather primordium induction in real time using skin explants prepared from GFP chicken embryos revealed centripetal migration of cells towards a chemotactic source during the formation of individual feather primordia. The rapid local accumulation of dermal cells over an 8 hour period, within the initially induced dermal cell aggregate implies directed cell movement may be the primary driver of feather primordium formation, due to the speed at which the aggregate formed. The process of feather primordium formation shows parallels to the formation of hair follicles in mouse (Ahtiainen *et al.*, 2014). Ahtiainen *et al*, 2014 showed in embryonic mouse explants, that cell proliferation in the epidermis played a minor role in the formation the epidermal placodes (precursors of hair follicles), and that directed cell migration was required during the formation of primary hair follicles. Similar to their results, I demonstrated that the effect of inhibiting actin polymerisation in developing chicken skin explants results in the inhibition of cell aggregation in both the epidermis and dermis. The observation suggests the possibility that hair follicle and feather primordium formation may follow similar processes, though my studies focused more

on the behaviour of the dermal cells of the skin, rather than the epidermal cells focused on by Ahtiainen *et al,* 2014 (Ahtiainen *et al.*, 2014).

Previous studies, utilising [3H] thymidine incorporation, showed cell proliferation to be almost completely absent from recently formed feather primordia, until outgrowth of the feather primordia begins and cell proliferation resumes (Jiang and Chuong, 1992; Michon *et al.*, 2008; Wessells, 1965). The same result was observed in artificially induced dermal cell condensates using recombinant FGF2 treated beads (Song *et al.*, 2004). Cells within the aggregate, within the immediate vicinity of the bead show no bromodeoxyuridine (BrdU) uptake (a synthetic analogue of thymidine), whereas cells outwith the active range of the recombinant FGF2 showed staining for BrdU. These results indicate that during the process of feather primordium formation, cell proliferation ceases. Cell proliferation was not detected within the forming feather primordia but was detected in the interbud regions of the skin. Uptake of [3H] thymidine or BrdU was observed in the interbud domains, showing that within the interbud domains, cell proliferation remains active (Jiang and Chuong, 1992; Song *et al.*, 2004; Wessells, 1965). These studies suggests that cell proliferation has little effect on the formation of individual primordia.

In agreement with previous studies, I show that cell proliferation plays a minimal role in the formation of individual feather primordia. Addition of a cell proliferation inhibitor, methotrexate (Sasso *et al.*, 1994; Yamasaki *et al.*, 2003), to dorsal skin explant cultures, reduced the number of feather primordia formed on the explant but did not inhibit the formation of individual feather primordia. The result suggest that cell proliferation is not required for the formation of dermal cell aggregates, but may regulate the number of feather primordia that can form on the skin, likely through the modulation of dermal cell numbers. Whether cell proliferation is required for the wave-like propagation of feather primordium formation, is to be determined.

Previous studies have proposed that the formation of feather primordia and their arrangement arises through a reaction-diffusion based mechanism (Gierer and Meinhardt, 1972; Jiang *et al.*, 1999; Jiang *et al.*, 2004; Maini *et al.*, 2006; Murray *et*

al., 1983; Nagorcka, 1986; Turing, 1952). The reaction-diffusion model of pattern formation, originally proposed by Turing (Turing, 1952), explains the chemical basis of pattern formation. Biological patterns generated by this model require the formation of a molecular pre-pattern, which functions as a blueprint to guide the cellular patterning process. The use of the GFP transgenic embryos allowed me to track the changes in cellular arrangements during feather primordium induction and formation. During primordium induction and formation, dermal cells within a local area are stimulated to migrate and aggregate, forming dermal cell condensates. Using *in situ* hybridisation analysis, to analyse the expression pattern of various genes associated with primordium induction and formation, I was able to correlate the molecular expression changes with the process of dermal cell condensate formation. The process of dermal cell aggregation, as detected through GFP, directly overlaps with changes in the gene expression pattern during feather primordium formation. Gene expression changes are not observed outwith the regions of skin undergoing dermal cell condensate formation. The observation shows that the formation of feather primordia and their pattern of arrangement, do not arise from a predefined molecular pre-pattern. The results indicate that the formation of the molecular and cellular patterns occur concurrently, suggesting a purely chemical based patterning model cannot fully explain the process of feather primordium formation or their patterning.

4.1.2 Molecular Components of Reaction-Diffusion Based Patterning: Roles of FGF20 in Appendage Induction

Studies that identified the causative mutations underlying feathering defects in various breeds of chickens have been invaluable for the identification and study of the endogenous inductive signalling pathways involved in the formation of feather primordia (Mou *et al.*, 2011; Wells *et al.*, 2012). Wells *et al*. 2012, identified a nonsense mutation within the *FGF20* gene in the scaleless chicken line which is associated with the near complete loss of feather follicle formation. During embryonic development, scaleless chickens do not develop epidermal placodes or dermal condensates (Song *et al.*, 1996). In *FGF20* knock-out mice, primary hair follicle formation fails. The failure of primary hair follicle formation results from the absence

of dermal cell condensate induction (Huh *et al.*, 2013), suggesting that *FGF20* may serve an evolutionarily conserved role in the induction and formation of dermal cell condensates. However, sections of E14.5 *FGF20* knock-out mouse embryos revealed that the initial process of primary hair follicle formation, (the induction of epidermal placodes), is unaffected by loss the of *FGF20* function. The result indicates that the process of epidermal placode induction differs between chicken and mouse. In mouse, epidermal placodes can form independently of *FGF20* activity, while the scaleless chicken breed lack visible epidermal placodes throughout embryonic development.

The importance of FGF proteins in the induction of dermal cell condensates has been well studied, and has been suggested to function as activators in a reaction-diffusion like manner during feather primordium formation based on their effects on promoting feather primordium fate (Jung *et al.*, 1998; Mandler and Neubuser, 2004; Patel *et al.*, 1999; Song *et al.*, 1996; Song *et al.*, 2004; Tao *et al.*, 2002; Viallet *et al.*, 1998). These studies implicated the role of various FGF protein family members in the formation of dermal cell condensates. The similar effects of FGF signalling on epidermal appendage formation observed in these studies is possibly due to the broad receptor binding specificities of the FGF family of proteins (Ornitz and Itoh, 2015) and that FGF20 specifically is the endogenous inducing factor in the formation of dermal condensates in both mouse and chickens.

Although FGF20 has been implicated in the formation of dermal cell condensates during development of feather primordia in chicken, the effect of recombinant FGF20 protein (rFGF20) could not be tested in the *ex vivo* culture system. Delivery of rhFGF20 protein via a bead or directly into the culture medium resulted in no visible effects on the treated skin explants. Also, qRT-PCR analysis of treated explants revealed no upregulation of direct target genes of FGF signalling, such as ETV5 (data not shown). This is likely due to inactivity of the rhFGF20 protein, due to either 1) homodimerisation of the protein, which has been shown to be inhibitory (Kalinina *et al.*, 2009) or 2) instability of rhFGF20 proteins under culture conditions (Buchtova *et al.*, 2015).

Due to this limitation, I opted to use recombinant human FGF9 protein (rhFGF9) to indirectly study the effects of FGF20 signalling activity on developing dorsal skin explant cultures. FGF9 protein is within the same subfamily of FGF proteins as FGF20 and has previously been shown to function redundantly to FGF20 in the maintenance of stemness of isolated nephron progenitor cells from mouse kidneys *in vitro* (Barak *et al.*, 2012; Itoh and Ornitz, 2004). From my own experiments, bead-mediated delivery of rhFGF9 protein on dorsal skin explants resulted in the induction of directed cell movement towards the bead, initiating the process of dermal cell aggregate formation. The results indicated that the rhFGF9 protein is functionally active and stable under the basic culture conditions used in this study and could be used as proxy to study the function of FGF20 protein activity in feather primordium formation.

4.1.3 Molecular Components of Reaction-Diffusion Based Patterning: FGF20 as an Activator

The reaction-diffusion model of pattern formation, originally proposed by Turing (Turing, 1952), has previously been suggested to be the underlying mechanism which gives rise to the periodic arrangement of feather primordia during chicken skin development (Jiang *et al.*, 1999; Jiang *et al.*, 2004; Lin *et al.*, 2006; Michon *et al.*, 2008; Mou *et al.*, 2011; Noramly and Morgan, 1998). It has been demonstrated that FGF signalling can induce the expression of *BMP2* and *BMP4*, which are known inhibitors of FGF signalling (Jung *et al.*, 1998; Song *et al.*, 2004). However, another important aspect of an activator as defined by Turing has yet to be established in FGF signalling during primordium induction, that is, self-activation. Previous studies focused on the induction and expression of genetic markers of primordium formation, demonstrating that the artificially induced feather primordia show similar gene expression profiles to endogenous feather primordia (Jung *et al.*, 1998; Patel *et al.*, 1999; Song *et al.*, 2004; Viallet *et al.*, 1998). Through *in situ* hybridisation, I showed that application of rhFGF9 coated beads to developing GFP dorsal skin explants resulted in the induction of *FGF20* expression around the bead, corresponding to the regions of induced cell aggregation. The loss of feather primordium induction in the scaleless chicken line (loss of FGF20 function) and the ability of rhFGF9 protein to

induce cell aggregation and the expression of *FGF20* during feather primordium formation solidifies the position of FGF20 as a candidate activator in the Turing reaction-diffusion model of feather primordium formation.

During feather primordium formation, cells move towards FGF protein sources of higher concentrations. I demonstrated through bead-mediated delivery of rhFGF9 proteins to skin explants, that rhFGF9 was able to induce cell migration and aggregation of dermal cells outside the endogenous patterning region (where no *FGF20* was expressed). rhFGF9 coated beads were also able to disrupt the endogenous primordium formation process within the endogenous patterning region (where endogenous *FGF* was expressed). Through the use of an inhibitor of FGF signalling, I showed that the effects of the rhFGF9 coated beads were mediated directly through the stimulation of the FGF signalling pathway. SU5402 treatment of skin explants inhibited the formation of both the endogenous cell condensates and the rhFGF9 induced dermal cell condensates. However, I further demonstrated that local stimulation of FGF signalling is required for the formation of dermal cell condensates, rather than general stimulation of FGF signalling activity. When skin explants were cultured in medium supplemented with rhFGF9, formation of endogenous feather primordia was completely inhibited. FGF proteins appear to function as local guidance factors, directing cell migration towards FGF sources. Through supplementing the culture medium with rhFGF9, FGF signalling would be activated generally across the entire skin, and thus cannot function as a guidance factor to direct cell aggregation. Cells within the treated explants are unable to sense/follow an FGF gradient, to direct their movement, due to the presence of ubiquitous stimulation of FGF signalling and thus, the formation of cell aggregates is prevented. In a previous study, Widelitz *et al,* 1996 (Widelitz *et al.*, 1996) showed that explants cultured in medium supplemented with rhFGF2 or rhFGF4 protein resulted in the formation of enlarged and occasionally fused feather primordia. However, these experiments were performed on skin explants prepared from HH 31 chicken embryos which have existing feather primordia prior to the treatment. Their results indicate that FGF signalling can alter the development and differentiation of existing feather primordia.

Despite the observed preferential migration of cells towards higher sources of FGF protein, an inhibitory zone forms around the rhFGF9 coated bead, where no primordium induction occurs. As mentioned above, FGF signalling has been demonstrated to induce the expression of its own inhibitors, *BMP2/4*, within the induced cell condensates (Jung *et al.*, 1998; Song *et al.*, 2004). In a reaction diffusion-model, the active range of the inhibitor is greater than that of the activator. The formation of the inhibitory zone around the rhFGF9 induced condensate could be the result of long-range inhibition of *FGF20* expression by BMP proteins, which is produced by the cell condensate. Another possibility is that due to the uptake of surrounding cells by the growing condensate, the depletion of cells in the regions surrounding the condensate prevents the induction of new feather primordia. Because the cell density within the region outside of the condensate has been reduced, primordium formation cannot occur and primordium formation can only resume in regions with a permissible cell density at a distance from the bead. The two possibilities could be distinguished by adding rhFGF9 beads to dorsal skin explants cultured in medium supplemented with a BMP signalling inhibitor, LDN193189. If the BMP signalling activity is required for the formation of the inhibitory zone around the rhFGF9 coated bead, application of LDN193189 would prevent the formation or decrease the size of the inhibitory zone. Whereas, the size of the inhibitory zone would be unaffected by the LDN193189 treatment, if limited dermal cell numbers alone was the cause of inhibitory zone formation.

Apart from functioning as a local guidance cue for cell migration during primordium induction, I further demonstrate that FGF20 induced signalling is also required for the maintenance of primordium stability. Inhibition of FGF signalling, through the application of SU5402 to HH 31 dorsal skin explants, resulted in the inhibition of the formation of primordium rows, lateral to existing rows, and also the destabilisation of the existing primordia. Cells within the destabilised primordia appear to lose their adherence to one another and disperse homogenously after inhibition of FGF signalling. The results are analogous to those obtained by Lin *et al*, 2009 (Lin *et al.*, 2009). Lin *et al*, demonstrated that blocking ERK activity (an effector protein of FGF

signalling), through the use of a molecular inhibitor U0126, resulted in the destabilisation of the existing primordia, turning once discrete primordia into a large fused stripe. However, ERK is utilised as a downstream signalling effector protein of the MAPK/ERK pathway which can be stimulated by other proteins apart from FGF, such as EGF, and so, one cannot attribute their observations directly to the loss of FGF signalling.

4.1.4 Molecular Components of Reaction-Diffusion Based Patterning: Regulation of BMP4 by FGF20

The induction of an inhibitor to FGF signalling by recombinant FGF proteins had been previously demonstrated. Jung, *et al* 1998 and Song *et al* 2004 showed that recombinant FGF4 can induce *BMP4* expression and recombinant FGF2 can induce *BMP2* expression respectively (Jung *et al.*, 1998; Song *et al.*, 2004). Consistent with these results, I demonstrate that rhFGF9 is also capable of inducing *BMP4* expression within the induced cell condensates of bead treated GFP explants. Interestingly, qRT-PCR analysis of HH 29 dorsal skin explants, cultured in medium supplemented with 1 µg/ml of rhFGF9 for 5 hours does not induce an increase of *BMP4* expression, indicating that rhFGF9 does not directly induce the expression of *BMP4* in treated explants, independently of cell movement and aggregation.

As observed through *in situ* hybridisation analysis of *BMP4* expression, in rhFGF9 bead treated skin explants, *BMP4* expression is only observed within endogenous feather primordia or the artificially induced cell condensates. Therefore, the effect of inhibiting cell condensate formation on *BMP4* expression of rhFGF9 bead treated skin explants was tested. Co-treatment of rhFGF9 coated beads and latrunculin A resulted in the loss of endogenous primordium formation and the near complete inhibition of *BMP4* expression around the bead, suggesting that the induction of *BMP4* expression by rhFGF9 coated beads was an indirect result of cell condensate formation and not a direct effect of the local increase in FGF signalling itself. This implies the possibility that cell to cell interaction during cell aggregation may itself play a role in *BMP4* induction. How cell aggregation in the forming feather primordia are able to induce

BMP4 expression has not been examined in this study, but the behaviour observed in developing feather primordia may follow similar parallels to the "community effect" as described and modelled in *Xenopus* studies (Gurdon, 1988; Saka *et al.*, 2011). In their model, the community effect occurs when an induction signal induces the formation of a cell aggregate and when a sufficient cell density is reached, genes induced/expressed within the cell aggregate are amplified. The community effect itself appears to be required to establish and maintain the collective identity of the cells within an aggregate through direct cell to cell interactions. Whether the induction of *FGF20* expression by rhFGF9 also requires the formation of a dermal cell aggregate, similar to induction of *BMP4* expression, has not been addressed in this current study.

A consequence of the observation of cell aggregation inducing *BMP4* expression in this study, is that increasing cell density within a local area of the skin alone would theoretically induce the expression of *BMP4*, independently of a condensate inducing signal. Hypothetically, the gradual thickening of the underlying dense dermis at the midline of the dorsal tract may autonomously induce the expression of *BMP4* and possibly induce the formation of a periodic pattern, independent of local guidance through FGF signalling. This could explain how in the scaleless mutant chicken line, the primary row of primordia in both the spinal and femoral tracts is still able to form despite the loss of endogenous FGF20 signalling activity (Sawyer and Abbott, 1972). The primary stripes found on each feather bearing tract display a much higher cell density than the surrounding skin regions and may spontaneously form a periodic pattern of feather primordia based on this direct BMP induction hypothesis or possibly through purely mechanical based mechanisms as proposed by Oster *et al*, 1983 (Oster *et al.*, 1983). In the model proposed by Oster *et al*, the dermis is capable of forming a periodic pattern independently of the epidermis through interactions between cells and the extracellular matrix. Local cell aggregation or proliferation would distort the surrounding ECM, resulting in the spontaneous nucleation of pattern formation from the initial site of high cell density i.e. the primary stripe, without the need of a molecular induction signal.

4.1.5 Molecular Components of Reaction-Diffusion Based Patterning: BMPs as Inhibitors

Previous studies implicated BMPs as inhibitors in the reaction-diffusion model, from the observed inhibition of feather primordium formation after stimulation of BMP signalling in developing embryonic chicken skin (Houghton *et al.*, 2005; Jung *et al.*, 1998; Mou *et al.*, 2011; Noramly and Morgan, 1998). Mou *et al*, 2011 showed that elevated expression of *BMP12* coupled with restricted expression of retinoic acid in the neck, results in the complete loss of feathering in the neck of the naked neck chicken line (Mou *et al.*, 2011). Although a causative gain of function mutation associated with *BMP12* resulted in the inhibition of feather formation, rhBMP4 protein was used throughout this study to test the effects of modulating BMP signalling during primordium formation. In the above study Mou *et al*, demonstrated that the effect of rhBMP4 treatment on chicken explant cultures was analogous to the effects observed after recombinant BMP12 treatment, suggesting that the two proteins may stimulate similar signalling responses.

Consistent with previous studies (Jung *et al.*, 1998; Mou *et al.*, 2011), when I supplement culture medium with rhBMP4, inhibition of primordium formation and a reduction of *FGF20* expression, in a dose dependent manner was observed. Michon *et al*, 2008 suggested that BMP's inhibitory action is the result of the possible antagonistic roles of distinct BMP proteins that may function as either chemo-attractants or inhibitors of cell migration during feather primordium formation(Michon *et al.*, 2008). BMP2 and BMP4 (which are both part of the same sub-family of BMP proteins (Sakou, 1998)) were suggested to function as inhibitors of cell migration. Contrary to their observations, my results indicate that BMP4 does not affect cell migration during feather primordium formation. Application of rhBMP4 to the culture medium, at a dose which completely inhibits endogenous primordium formation, to rhFGF9 bead treated explants does not affect the migration and aggregation of cells around the rhFGF9 bead. The result indicates, that BMP signalling does not affect FGF signalling directly and that inhibition of primordium formation by BMPs is the result of inhibition of *FGF20* transcription, preventing the production of new FGF20 protein.

As long as a local source of FGF protein is present, cells will move towards the source regardless of increased BMP signalling activity.

Similar to Mou *et al*, 2011 (Mou *et al.*, 2011), differential sensitivity to inhibition of primordium formation within the dorsal tract was observed in rhBMP4 treated explants. Feather primordium formation was inhibited in a dose dependent manner, with the greatest sensitivity to inhibition restricted to the lateral regions of the dorsal tract (**Figure 73**). In agreement with Mou *et al*, the lateral skin sensitivity to BMP inhibition is possibly the result of the later formation of primordia in those regions. From my previous result, stimulation of cell aggregation around local sources of rhFGF9 is unaffected by the presence of rhBMP4 in the culture medium. From this result, I propose a mechanism underlying the sensitivity to inhibition of primordium formation in the lateral regions. Dorsal skin explants used in this study were prepared from HH 29 chicken embryos, where *FGF20* expression is already induced at the dorsal midline of the tract. As stated above, if FGF20 protein is present, induction of cell aggregation will occur and may induce the self-activation of *FGF20* expression. If self-activation of FGF20 signalling activity remains higher than the inhibitory effect of BMP4 signalling activity, then the primordium already formed will remain stable. This hypothesis may explain why the primary row of feather primordia are always inhibited last when explants are treated with increasing doses of rhBMP4 proteins. Due to the later induction of *FGF20* expression in the lateral regions of the skin, inhibition of *FGF20* transcription by BMP signalling will result in the lateral regions of skins to never be exposed to endogenous FGF20 proteins and this cannot induce primordium formation.

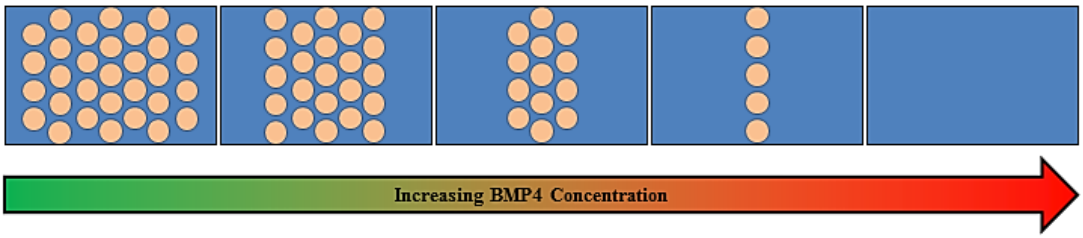

Figure 73. Diagrammatic representation of skin explants treated with increasing doses of rhBM4. Explant on the far left is an untreated control. Explants to the right of the control are diagrammatic representations of increasing rhBMP4 concentrations in the culture medium. As rhBMP4 concentrations increase, skin explants display a reduction in the number of primordium rows, beginning with the rows in the most lateral regions of the explant. At a high enough dose of rhBMP4 the formation of all feather primordia is inhibited.

Application of rhBMP4 coated beads in close proximity to developed feather primordia in HH 31 GFP skin explants results in the breakup of the feather primordia and the formation of a zone of inhibition surrounding the bead. This result suggests that the stability of a primordium is dependent on the level of FGF signalling activity within the primordium, rather than through an intrinsic adhesiveness of the cells within the primordium, as previously suggested by Jiang *et al*, 1999 (Jiang *et al.*, 1999). From this observation, I propose that even after the formation of a feather primordium, a continual supply of FGF protein is required to maintain the stability of the primordium. Live imaging of feather patterning shows that cells within the destabilised feather primordia appear to migrate away from the rhBMP4 coated bead, forming an inhibitory zone around the bead, similar to treatments with rhFGF9 beads. It is possible that within the destabilised feather primordia, FGF20 protein production has halted due to the inhibition of *FGF20* transcription by the local increase of BMP signalling. As shown in section **3.1.4**, cells within feather primordia will preferentially migrate towards higher concentrations of FGF protein sources. The formation of the inhibitory zone around the rhBMP4 coated bead may be the result of attraction and migration of the cells from the destabilised feather primordia, by FGF protein sources outwith the

active range of BMP signalling. Another possibility is that local application of rhBMP4 results in the chemo-repellence of cells within the direct vicinity of the bead, however, I show that rhBMP4 does not function as a chemo-repellence factor during the formation of feather primordia. Co-treatment of skin explants with SU5402 to inhibit FGF signalling and local application of rhBMP4 beads reveal that the formation of the zone of inhibition is an FGF dependent process. When FGF signalling is inhibited, the movement of cells from the destabilised primordia, adjacent to the rhBMP4 bead, is reduced. The results suggest that the formation of the inhibitory zone around rhBMP4 beads is due to the uptake of cells by FGF signalling, outwith the zone of inhibition around the bead, rather than a direct chemo-repellent effect of BMP signalling.

4.1.6 Molecular Components of Reaction-Diffusion Based Patterning: Role of Endogenous BMPs in Appendage Formation

To date, the function of exogenous effects of recombinant BMPs during feather primordium formation have been dissected, but studies into the function of endogenous BMP signalling in the formation of feather primordia are limited (Noji *et al.*, 1993; Sakou, 1998). Using retroviral vectors that induced the expression of a BMP signalling inhibitor, *Noggin* or the over-expression of *BMP2* or *BMP4* to modulate BMP signalling, Noramly *et al*, 1998 demonstrated that endogenous BMP signalling is required to maintain the shape and limit the growth of induced feather primordia (Noramly and Morgan, 1998). They also show that BMP signalling inhibits feather primordium fate and propose a model that suggests BMP signalling mediates lateral inhibition of feather primordium formation to maintain the spacing between feather primordia. The results presented in this study are consistent with their findings. I demonstrate that treatment of skin explants with a BMP signalling inhibitor, LDN193189, resulted in the formation of enlarged primordia and fusions between neighbouring feather primordia. The loss of BMP signalling resulted in unrestricted growth of dermal condensates during primordium formation and loss of lateral inhibition between neighbouring feather primordia. Noramly and Morgan *et al*, 1998 (Noramly and Morgan, 1998) hypothesised that BMPs regulate the growth of feather

primordia through modulation of FGF signalling via their effect on the *FGF receptor 1* (*FGFR-1*). They observed that increasing BMP signalling resulted in the loss of *FGFR-1* expression within the developing feather tracts. As I demonstrated, BMP signalling rapidly inhibits the transcription of *FGF20* suggesting that the inhibition of primordium induction is through suppression of FGF20 protein production rather than *FGFR-1* expression. *FGFR-1* is normally expressed in the dermis of growing cell condensates induced by FGF signalling (Noji *et al.*, 1993; Song *et al.*, 2004), suggesting that the observed loss of *FGFR-1* expression is indirectly the result of loss of primordium formation. The observation also suggests that the induction of *FGFR-1* expression within the cell condensate may be the mechanism which maintains the attraction of cells to the local sources of FGF protein, and if FGF protein production is halted, these cells may automatically seek new sources of FGF protein.

Real time observation of developing GFP dorsal skin explants treated with LDN193189 revealed that BMP signalling is not involved in the induction of the propagation of feather primordium formation, but BMP signalling only affects the process of individual primordium formation. When BMP signalling was inhibited, induced primordia show unrestricted growth resulting in fusions between neighbouring primordia. However the wave-like propagation of the enlarged primordia follow the normal propagation of primordium formation as observed in control explants. Additionally, no ectopic induction of primordium formation outwith the endogenous primordium generating region was observed.

Dorsal skin explants treated with LDN193189 show elevated expression of *FGF20* expression due to alleviation of BMP inhibition, indicating that the observed enlargement of primordia and fusions may be the result of increased FGF signalling within the forming primordia. As demonstrated in section **3.1.3**, ectopic induction of local FGF signalling, through bead-mediated delivery of rhFGF9 protein induces the formation of ectopic dermal cell condensates in skin regions outwith the endogenous primordium forming region. The lack of ectopic feather primordium formation in skin regions, beyond the endogenous primordium forming region in LDN193189 treated explants, suggests that propagation of *FGF20* expression is not restricted by BMP

signalling, and that BMP signalling only inhibits the expression of *FGF20* in skin regions capable of inducing *FGF20* expression at that time.

4.1.7 Regulation of the Molecular Components of Reaction-Diffusion Based Patterning: A Model

Based on previous published work and my own observations in this study, I developed a model of molecular and cellular interactions which seeks to explain the process of individual feather primordium formation (**Figure 74**). FGF20 and its inhibitor BMP4 are specifically involved in the induction of feather primordium formation and are not involved in primordium wave propagation. Induction of epidermal *FGF20* expression results in the formation of cell aggregates through stimulation of cell migration towards sources of FGF20 protein. Local self-activation of *FGF20* expression maintains the growth of the forming feather primordia and continued supply of FGF20 protein maintains the stability of the feather primordia through cell accumulation. As the cell density within the dermal cell condensate increases, a cell density threshold is reached and *BMP4* expression is induced within the condensate. Long-range BMP4 signalling activity then modulates FGF signalling through inhibition of *FGF20* expression which limits the growth of the developing feather primordia and maintains the spacing between neighbouring primordia through lateral inhibition, preventing the formation of fusions. The reaction-diffusion theory predicts that BMP4 protein should have a higher active range (possibly through passive diffusion) than that of FGF20, so that local levels of BMP4 protein within the feather primordium are never sufficient to completely inhibit *FGF20* transcription due to the higher diffusion rate of BMP proteins. This would allow for local self-activation of FGF signalling within the feather primordium and therefore the stability of the feather primordium is maintained.

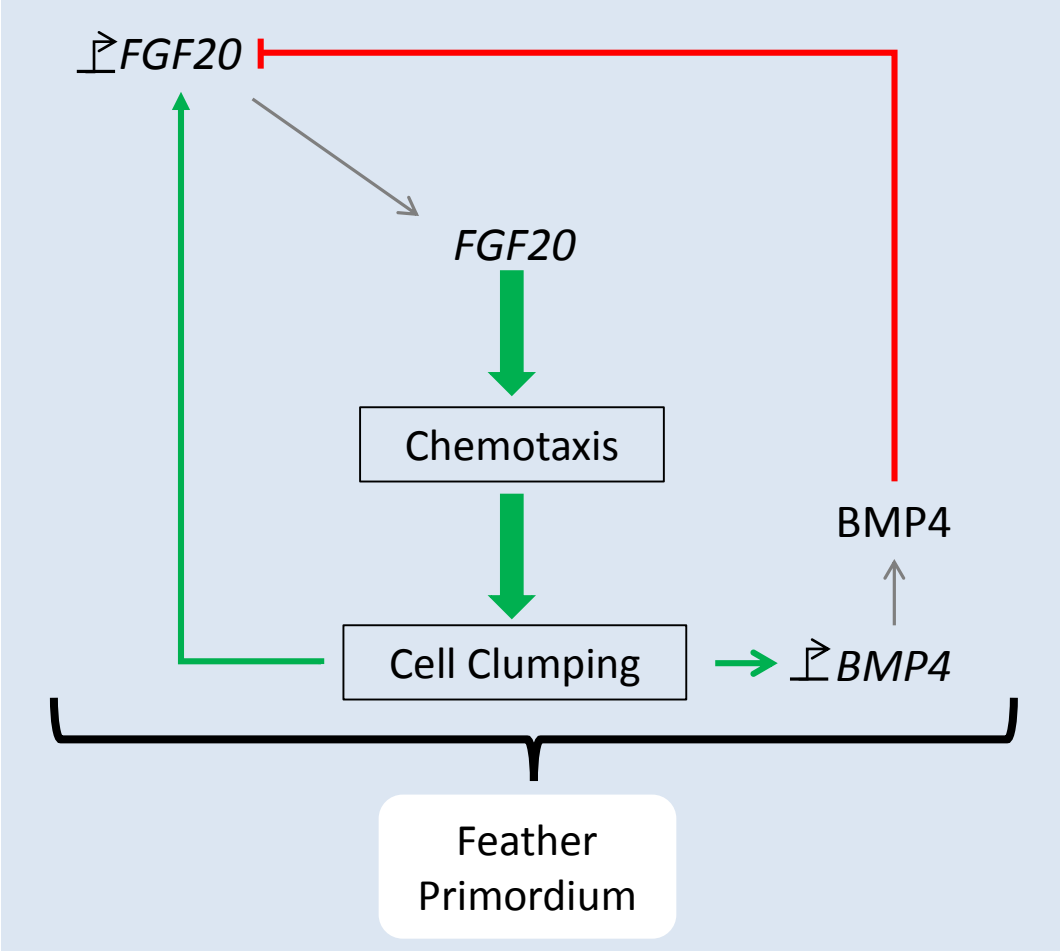

Figure 74. Schematic of the molecular and cellular processes involved in feather induction. In skin regions competent to feather primordium induction, *FGF20* expression is induced and stimulates cell migration towards the source of FGF20 protein forming local cell aggregates. As cell aggregates expand in size, *FGF20* is induced locally, a process that results in self-activation of *FGF20* expression and stimulation of chemotaxis. When the growing cell aggregate reaches a threshold of dermal cell density, *BMP4* expression is induced within the aggregate which inhibits *FGF20* transcription. In this way FGF20 and BMP4 can form an activator-inhibitor pair. Through a reaction-diffusion based process, the short-range self-activation and long-range negative feedback between the activator and inhibitor, regulates the growth of the forming feather primordium and prevents fusions between neighbouring feather primordia through lateral inhibition. Green arrows indicate stimulation, lines indicate inhibition, grey arrows indicate translation of mRNA to protein and boxes indicate cellular processes.

However, not addressed experimentally in this thesis, is that during feather primordium induction and formation, differential diffusivity of the activator (FGF20) and the inhibitor (BMP4) drives the formation of the observed periodic pattern of feather primordia. Reaction-diffusion based models postulate that pattern formation arises through local short-range self-activation and long-range inhibition (Gierer and Meinhardt, 1972). Miura, 2007 showed that the diffusion co-efficient of FGF10 protein is much lower than that of BMP4 within matrigel (Miura, 2007), an artificial extracellular matrix (ECM) mimic (Hughes *et al.*, 2010; Kleinman and Martin, 2005). Miura proposed that the differences in diffusion constants between FGF10 and BMP4 are due to their differences in heparin sulphate proteoglycan binding (HSPG) which is present in the matrigel and in the ECM. FGF proteins have previously been shown to bind HSPG in cell culture (Fannon *et al.*, 2000), and the slower diffusion of FGF proteins could be due to their binding to HSPG in the ECM. To study the diffusion rates of FGF20 and BMP4 protein, active fusions of fluorescent proteins to FGF20 and BMP4 could be generated and analysed on dorsal chicken skin explants through methods, such as fluorescence recovery after photo-bleaching (FRAP) to determine diffusion rates of each protein. Similar methods were described in the analysis of diffusion rates of TGF-β protein family members in zebrafish embryos and drosophila larval wing disk (Muller *et al.*, 2012; Zhou *et al.*, 2012). Parameterisation of the key molecules involved in the generation of feather primordia may further refine the understanding of reaction-diffusion based models of feather primordium formation.

The induction of *BMP4* expression within forming cell aggregates highlights another possible area of further study. The results indicated a possible "community effect", as described by (Gurdon, 1988; Saka *et al.*, 2011), due to the requirement of cell aggregation to induce the expression of *BMP4* during feather primordium formation. Song *et al,* 2004 demonstrated, using rhFGF2 coated beads, that molecules such as *BMP2* and *FGFR1* are also expressed within artificially induced dermal cell condensates, but whether these genes are induced by FGF signalling or by the forming condensate was not examined in the study (Song *et al.*, 2004). It is possible that the forming dermal cell aggregates may express genes unique to the aggregate which

regulate the growth and stabilise the formation of the feather primordia. The possible induction of *FGFR1* expression by the dermal cell aggregate for example, may further reinforce the cohesiveness of the cells within the aggregate towards local sources of FGF proteins. Identification of novel genes specifically induced in the cell aggregate may further refine my current model of feather primordium formation. This could be done by combining methods such as 3D spheroid culture systems and micro-array analysis to study the gene expression profiles of the dermal cell condensates, as described by Higgins *et* al 2013 (Higgins *et al.*, 2013). In this study, gene expression profiles of intact human dermal papillae, 2D cultures of human dermal papilla cells and 3D spheroid cultures of human dermal papilla cells were reported to vary depending on the method of which of the sample was prepared from prior to analysis. When compared, dermal papilla cells cultured in compact 3D spheroids were more similar in their genetic profiles to intact dermal papillae than those of cells cultured under conventional 2D culture conditions. Their results suggest that the formation and maintenance of a dermal cell condensate may have regulatory effects on the gene expression profiles of the cells within the condensate. The genes expressed may maintain the collective identity of the cells within the condensate. Based on their results and from my own observations, it plausible that the formation of dermal cell condensates, during feather primordium induction, can induce the expression of *BMP4* or other genes.

Throughout this section I have described that FGF20 and BMP4 proteins may function as an activator-inhibitor pair during the induction and formation of individual feather primordia, based on the regulatory relationship between the two molecules observed in this study. I have shown that FGF20 is able to stimulate its own expression, through an auto-catalytic process, and also the expression of its own inhibitor, *BMP4*, fulfilling the key aspects of an activator-inhibitor pair in a reaction-diffusion based patterning system.

4.2 Wave-Like Propagation of Primordium Formation

4.2.1 Models of Sequential Wave-Like Addition of Primordium Rows

Feather follicles are arranged in a periodic pattern of high fidelity and arise through a strict spatiotemporal sequence during embryonic development, resulting in the formation of a hexagonally arranged array of feather follicles within feather bearing tracts. It has been proposed that the hexagonally arranged feather follicles serve a streamlining function to reduce drag during flight (Homberger and de Silva, 2000; Lucas and Stettenheim, 1972; Pennycuick *et al.*, 1996), but the mechanism underlying the spatiotemporal addition of new feather rows during tract development is relatively understudied.

Reaction-diffusion models are able to recreate the observed hexagonal array of feather primordia that form on the tracts of developing chicken embryos (Gierer and Meinhardt, 1972; Jiang *et al.*, 1999; Jiang *et al.*, 2004; Maini *et al.*, 2006; Murray *et al.*, 1983; Nagorcka, 1986; Oster *et al.*, 1983; Turing, 1952). However, these models only demonstrate simultaneous pattern formation of the entire tract but fail to explain the mechanism underlying the sequential propagation of feather primordium formation across the feather tract. Reaction-diffusion based models are likely to be oversimplified when considering real biological systems, in part because they only describe the molecular basis of pattern formation and omit the involvement of cellular processes. Based on real-time imaging data and the lack of a molecular pre-pattern apparent in the CAG-GFP skin, such a molecular-based mechanism cannot fully explain the process of primordium patterning in chicken skin. These models also assume that the initial distribution of activators and inhibitors is homogenous across the field prior to patterning but do not explain the origin of production of the activators and inhibitors. The models also rely heavily on diffusion-based instability to create periodic patterns without taking into account how the cellular processes may affect the distribution and diffusion of the activators and inhibitors.

Mechano-chemical models of pattern formation, as proposed by Oster and Murray alone, cannot fully explain the process of the wave-like propagation of feather

primordia (Murray *et al.*, 1983; Oster *et al.*, 1983). As mentioned previously, mechano-chemical models predict that dermal cells alone are capable of undergoing pattern formation independently of inductive signals from the epidermis. The model also proposes that when an aggregate forms, that nucleation of primordium formation would occur and spread across the field. The final pattern arises through the spreading of primordium formation using the previous primordia as a template to align themselves. Previous studies using the scaleless chicken line, along with my own observations, contradict this model of feather primordium pattern formation. In the scaleless chicken line, the primary defect behind the failure of primordium formation was found to be epidermal and subsequent studies identified that this was due loss of FGF20 protein function, indicating the need for an epidermal signal to guide the formation of dermal cell condensates (Sengel and Abbott, 1963; Wells *et al.*, 2012).

As described in the results presented in this thesis, both the activator and inhibitor, *FGF20* and *BMP4* respectively, are not initially expressed across the feather field prior to pattern formation. *FGF20* appears to be induced by an upstream signal while *BMP4* expression is induced by the formation of cell aggregates, suggesting that a purely reaction-diffusion based model is insufficient in explaining the formation of individual feather primordia and their sequential wave-like induction.

Experimental observation of the wave-like propagation of feather primordium formation in the dorsal tract of chickens suggests the existence of an unknown feather primordium inducing factor, which propagates bilaterally from the midline, inducing the formation of new feather primordia in its wake (Davidson, 1983; Ede, 1972; Patel *et al.*, 1999). Jiang *et al*, 1999 revealed that cells within the underlying dermis are all equally able to participate in the formation of feather primordia or take on interbud fates. This suggests the sequential propagation of feather primordium formation occurs through the action of a primordium inducing factor rather than the organisation of cells with pre-specified fates (Jiang *et al.*, 1999).

Patel *et al*, 1999 showed that within the dorsal tract, the feather primordium inducing factor originated from the midline and hypothesised, through *in situ* hybridisation

analysis, that propagation of *Follistatin* expression, an inhibitor of BMP signalling (Fainsod *et al.*, 1997; Hemmati-Brivanlou *et al.*, 1994), regulated the wave-like propagation of feather primordium induction. Patel *et al*, proposed that alleviating the inhibitory effect of BMP's, allowed the wave-like propagation of feather primordium formation. The initial expression of *Follistatin* as presented by Patel *et al* shows broad expression of *Follistatin* across the dorsal tract prior to the induction of feather primordia, and as demonstrated by my own experimental work, alleviation of inhibition by BMP signalling activity does not result in the expansion of the endogenous primordium forming region. My results instead indicate that spatiotemporally restricted wave-like induction of *FGF20* expression by a spreading inductive signal, originating from the dorsal midline of the tract, is the mechanism underlying the wave-like propagation of feather primordium induction/formation. Artificial induction of cell aggregation around sources of rhFGF9, through bead-mediated delivery, in skin regions outside the endogenous feather primordium generating region does not result in nucleation of pattern formation from the bead. That is, cell aggregation alone does not stimulate the wave-like propagation of feather primordium formation, outwith the primordium generating skin region. The wave-like propagation of the inductive signal, thus, the propagation of *FGF20* expression, regulates the sequential formation of new primordium rows across the tract. The requirement of spatiotemporal induction of FGF signalling in the wave-like propagation of feather primordium formation remained unobserved in previous studies. This was possibly due to the analysis of treated explants after primordium wave propagation had terminated at the end of the tract and endogenous feather primordia had already surrounded the bead induced dermal cell aggregate (Jung *et al.*, 1998; Patel *et al.*, 1999).

4.2.2 EDA is the Molecular Component of the Propagating Morphogenetic Wave

Based on my observations of the *EDA* expression pattern during the wave-like propagation of primordium formation, the effects of recombinant EDA protein on *FGF20* expression, and the width of the primordium generating region, I propose that

EDA is the factor that regulates the spatiotemporally restricted wave-like induction of *FGF20* expression.

In situ hybridisation analysis of *EDAR* expression in the dorsal tract during feather primordium induction shows that its expression pattern overlaps with the observed *β-Catenin* expression pattern, following the "restrictive mode" of pattern expression as described by(Jiang *et al.*, 1999). *EDAR* expression is induced through WNT/β-Catenin signalling, while *EDA* is induced by another as of yet unknown factor (Houghton *et al.*, 2005). In my study, inducing WNT/β-Catenin activity through the use of an inhibitor of GSK3β activity, increased the expression of *EDAR* in treated explants, as detected through qPCR analysis (data not shown). This may suggest that the initial expression pattern of *β-Catenin* across the presumptive dorsal tract primes the epidermis for EDA/EDAR signalling in preparation for the EDA ligand, through the induction of *EDAR* expression across the tract.

Molecules expressed in the "restrictive mode" are initially expressed homogenously throughout the presumptive tract while "*de novo*" molecules are expressed only after a primordium has been established. The *EDA* expression pattern in chicken does not follow the described "restrictive" or "*de novo*" mode of pattern expression during propagation of primordium formation. We term the observed expression pattern of *EDA* as the "induction" mode/wave. Initially *EDA* is spatiotemporally restricted with the initial expression observed only at the dorsal midline of the tract, prior to bilateral propagation. As *EDA* expression propagates across the tract, new feather primordia are induced and expression of *EDA* is restricted to the interbud regions.

Application of Fc-chEDA1 to HH 29 skin explants results in the rapid induction of *FGF20* expression and causes the expansion of the endogenous primordium forming region, as defined by *FGF20* expression. This demonstrates that the limited availability of EDA protein during primordium induction in the dorsal tract restricts primordium formation. In the scaleless chicken line, *EDAR* expression and *EDA* expression/propagation is unaffected by the loss of primordium formation (Drew *et al.*, 2007). In the dorsal tract, *EDA* expression still propagates bilaterally from the

initial primary stripe located at the dorsal midline of the tract. This indicates that propagation of *EDA* expression is independent of primordium formation and is upstream of the primordium induction process.

In my model, I propose that propagation of feather primordium formation is the result of the restricted induction and expression of *FGF20* by the travelling *EDA* wave from the dorsal midline (**Figure 75**). Previous studies associated the EDA/EDAR signalling pathway with the induction of feather primordium formation in chicken but did not associate EDA/EDAR signalling with the wave-like propagation of primordium formation due to the local effects of their treatments, which only affected a limited region of the tract (Drew *et al.*, 2007; Houghton *et al.*, 2005). Loss of EDA/EDAR signalling in both humans and mice results in the loss or abnormal formation of epidermal appendages, such as hair and teeth (Charles *et al.*, 2009; Gaide and Schneider, 2003; Headon and Overbeek, 1999; Kere *et al.*, 1996; Laurikkala *et al.*, 2002; Thesleff and Mikkola, 2002; Wisniewski *et al.*, 2002). Mutations affecting the EDA/EDAR signalling pathway have been identified in rats, dogs, and cows, and all show similar abnormalities in epidermal appendage formation suggesting an evolutionarily conserved role for EDA/EDAR signalling in the development of epidermal appendages in mammalian species (Casal *et al.*, 2005; Drogemuller *et al.*, 2001; Kuramoto *et al.*, 2011). The abnormal or loss of scales and teeth formation in various fish models have also been attributed to mutations within the *EDAR* or *EDA* gene implying that the function of EDA/EDAR signalling in epidermal appendage development may have developed early on during the evolution of vertebrates (Atukorala *et al.*, 2010; Harris *et al.*, 2008; Kondo *et al.*, 2001). Surprisingly, as of yet, no known mutation in the EDA/EDAR signalling pathway in Aves has been identified so the role of endogenous EDA/EDAR signalling during feather primordium formation has largely remained unknown.

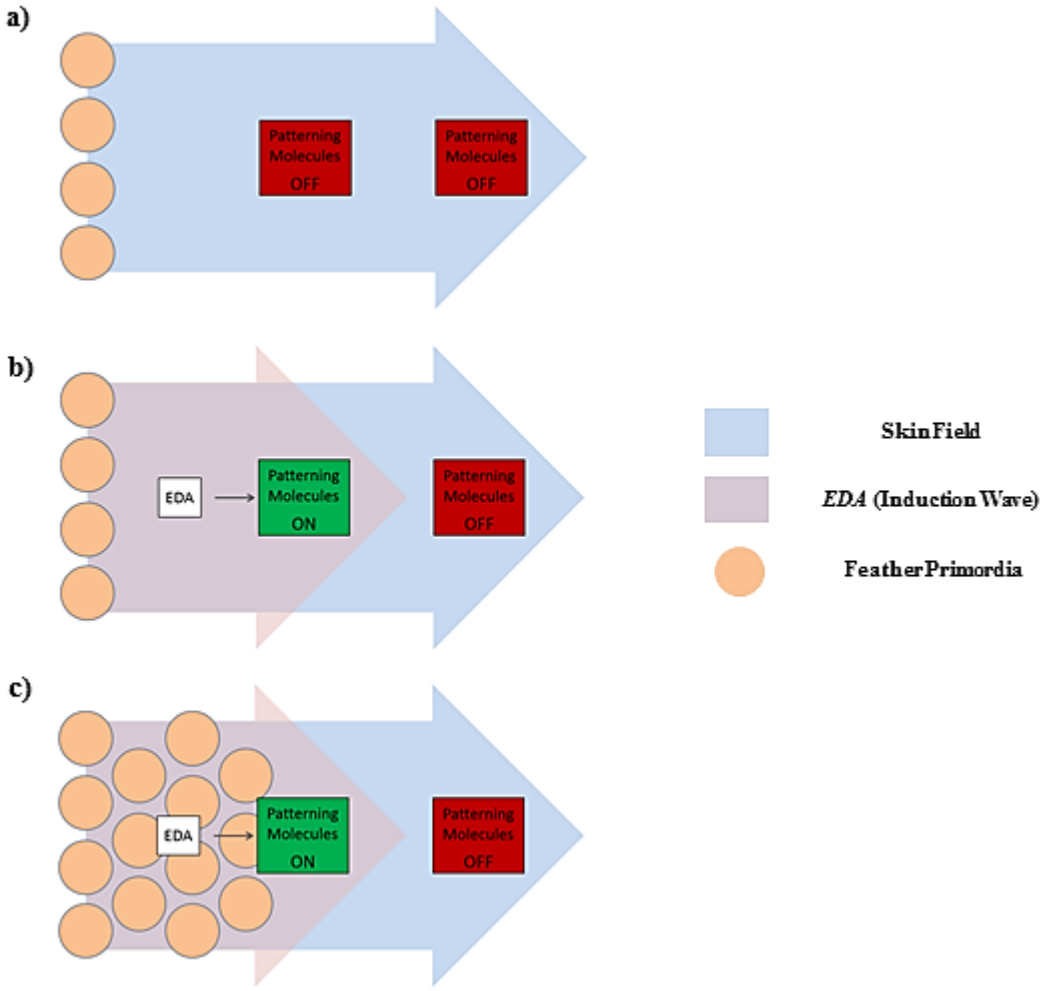

Figure 75. Schematic of the processes involved in the sequential wave-like induction of feather primordia. The primordia on left of each diagram represents the midline of the dorsal tract. a) Prior to the induction of EDA expression, the skin field lateral to the midline does not express pattern formation molecules, FGF20 and BMP4. b) As EDA expression propagates across the skin field, the expression of the pattern formation molecules is induced, c) resulting in the formation of feather primordia.

FGF20 has previously been shown to be a direct downstream target of the WNT/β-Catenin signalling pathway in studies of human epithelial cell lines and developing mouse skin (Chamorro *et al.*, 2005; Huh *et al.*, 2013). The importance of β-Catenin as

a competence factor in hair/feather primordium induction and formation has been well characterised in previous studies (Huelsken *et al.*, 2001; Noramly *et al.*, 1999; Widelitz *et al.*, 1999; Widelitz *et al.*, 2000), but the initial expression of *β-Catenin* across the presumptive dorsal tract prior to primordium induction suggests that the activity of WNT/β-Catenin signalling alone is not sufficient to induce *FGF20* expression. If WNT/β-Catenin signalling was the only *FGF20* inducing factor, then induction of feather primordium formation within the *β-Catenin* positive skin regions should occur simultaneously. However, this is not observed. I demonstrate that β-catenin is not just a competence factor, but operates synergistically with the EDA/EDAR signalling pathway to promote the induction of *FGF20* expression. Co-treating skin explants with a minimal dose of both CHIR99021 and Fc-chEDA1 results in a large increase in *FGF20* expression in co-treated skins, greater than the moderate increase of *FGF20* expression observed in the single treatments with either one of the signal modulators. The synergy observed probably occurs due to the ability of both WNT/β-Catenin and EDA/EDAR signalling pathways to induce *FGF20* expression independently. WNT/β-Catenin can induce the expression of *FGF20* directly but also perhaps indirectly, through the induction of *EDAR* expression, allowing for EDA/EDAR signalling to occur in the presence of EDA ligand as *EDA* expression propagates across the *β-Catenin*/*EDAR* expressing feather tract.

4.2.3 Spatiotemporal Propagation of *EDA* Expression Regulates the Hexagonality of the Feather Primordium Pattern.

In mouse embryos, *EDA* expression is observed homogenously throughout the skin field prior to primordium induction (Laurikkala *et al.*, 2002). In the developing mouse embryo, during hair primordium induction, hair primordia form almost simultaneously across the skin but the resulting arrangement of hair primordia show a low fidelity periodic pattern. Using the chicken embryo as a model, I reveal that the spatiotemporal propagation of *EDA* expression is required for the formation of a periodically arranged array of feather primordia of high fidelity. Expanding the width of *EDA* expressing skin prior to primordium induction, through the reversible inhibition of cell movement results in the almost simultaneous induction of primordia across the tract. These

primordia are smaller and show a disorganised pattern compared to untreated skin explants.

Based on their reconstituted mesenchymal explant experiments, Jiang *et al,* 1999 (Jiang *et al.,* 1999) proposed that an optimal packing density of the feather primordia is the underlying mechanism behind the hexagonal arrangement of feather primordia in chicken. However, I propose a different mechanism which underlies the formation of a reproducible hexagonal primordium pattern (**Figure 76**). Through the restricted expression of *EDA* at the midline of the dorsal tract, primordium formation is forced to form in a single row. As *EDA* expression gradually propagates from the midline laterally, more space is created to allow the insertion of new rows, but because the size of the primordium generating region is still limited by restricted *EDA* expression, new primordia are forced to form and align themselves using the previous row of primordia as a template. The initial formation of a primary row of primordia at the dorsal midline may allow the formation of a reproducible feather pattern on both sides of the dorsal tract of individual chickens and also a reproducible feather pattern between different individual chickens. Without the midline row of placodes, the orientation of the pattern may be altered, varying the patterns of primordium arrangements between individual chickens.

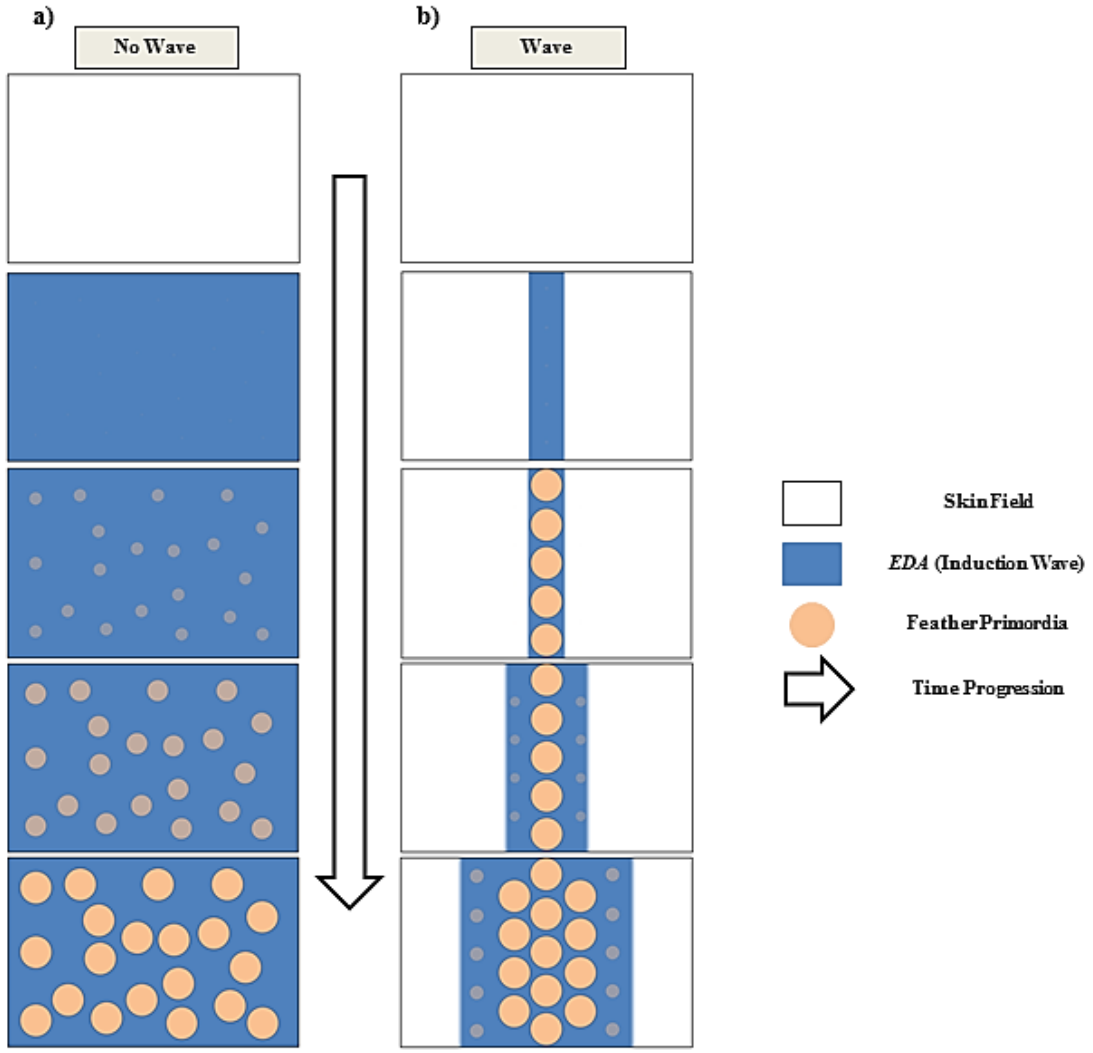

Figure 76. Spatiotemporal induction of feather primordium induction is required for the formation of a hexagonally arranged feather pattern. a) When EDA is expressed ubiquitously throughout the skin field, primordia form wherever there is space, resulting in the formation of a randomly arranged pattern of primordia. b) Spatiotemporally restricted expression of EDA restricts the region of skin capable of undergoing primordium formation, forcing the primordia to align in a single row. As EDA expression propagates bilaterally, the region of skin capable of primordium formation widens, allowing the formation of new rows of primordia. The new rows of feather primordia use the previous row as a template to align themselves, resulting in the formation of a hexagonally arranged pattern of primordia.

Jiang *et al*, 1999 using the reconstituted mesenchymal explant culture method, demonstrated that a periodically arranged hexagonal pattern of feather primordia can be formed without the presence of a wave of propagation or a primary row of feather primordia (Jiang *et al.*, 1999). The method involved the reconstitution of disassociated mesenchymal cells prepared from HH 30 dorsal skin and plated at different densities, overlain with an intact epidermis from the dorsal tract before culture. Explants seeded with high number of dermal cells show simultaneous formation of primordia of equal size across the entire tract and were arranged in a hexagonal pattern due to optimal packing density of feather primordia. The observed simultaneous primordium induction in the reconstituted mesenchymal explant culture may be the result of prior propagation of *EDA* expression across the separated epidermis prior to placement of the epidermis on to top of the reconstituted mesenchymal cells. *EDA* expression is observed in both the epidermis and dermis (Drew *et al.*, 2007; Houghton *et al.*, 2005) but early expression of *EDA*, prior to primordium induction, is exclusive to the epidermis while dermal *EDA* expression is only induced after primordium formation (Houghton *et al.*, 2005), indicating that the *EDA* induction wave propagates through the epidermis to induce primordium formation. The localisation of expression and propagation of the inductive signal, *EDA*, to the epidermis rather than the dermis may be an important feature of the feather primordium induction process. Over time the cell density of the underlying dermis of the dorsal tract increases in a medial to lateral direction (Mayerson and Fallon, 1985). If *EDA* was induced and propagated through the dermis, the concentration and activity of the inductive signal would change over time and may alter the activity of the inductive signal due to the gradual thickening of the dense dermis. Whereas cell density within the epidermis remains relatively stable during embryonic development so concentrations of the inductive signal would remain constant as *EDA* expression propagates through the epidermis. How *EDA* expression itself is restricted and regulated is currently unknown and has not been investigated in the current study.

The hexagonal pattern of feather primordia observed in the reconstituted mesenchymal explant culture by Jiang *et al* 1999, was only observed when explants were seeded

with a high density of dermal cells prior to culture. Explants with initially lower cell density resulted in the absence or formation of lower numbers of primordia of varying sizes, arranged in a disorganised manner (Jiang *et al.*, 1999). Their results indicate the need for a threshold of dermal cell density in the formation of feather primordia.

4.2.4 Primordium Induction by EDA/EDAR Signalling Requires a Dermis of Permissive Cell Density.

During chicken development, dermal cell density within the tract is not homogenous but displays the highest density of dermal cells at the dorsal midline which gradually decreases in a medial to lateral direction. Over the course of embryonic development, the dermis thickens across the tract in a medial to lateral direction (Mayerson and Fallon, 1985). I show that when Fc-chEDA1 was applied to developing skin explants, regardless of the concentrations tested, only a maximum of a two-fold increase in the width of the primordium forming region, as defined by *FGF20* expression, was observed. The results suggested that the effects of Fc-chEDA1 on primordium induction are limited. Outside the expanded region of *FGF20* expression, dermal cell density may not be sufficient to permit primordium formation. Inhibition of dense dermis thickening across the dorsal tract of HH 29 skin explants, through excision of the dorsal midline prior to *EDA* propagation, inhibits the wave-like propagation of feather primordium formation. *In situ* hybridisation analysis of midline excised explants revealed that *β-Catenin* expression and *EDA* expression/propagation remain largely unaffected by the procedure. However, only one or two rows of primordia ever form, lateral to the excision site where dermal density is highest. Taken together, the results suggest that even when the molecular components of feather induction are intact, feather primordium induction cannot take place when the cellular components are lacking. The results also indicate that the induction and propagation of *EDA* expression is independent of dense dermis formation.

Inhibition of cell proliferation in dorsal skin explant cultures, through the use of methotrexate, also reduced the number of feather primordium rows, suggesting that cell proliferation may be required for the formation and spread of dense dermis.

However, in this current study, I have yet to establish that dense dermis formation has failed in the methotrexate treated explants. Methotrexate treatment does not affect the expression of either *β-Catenin* or *EDA,* or completely inhibit primordium formation, which is restricted to the medial regions of the skin, indicating that the molecular components are functioning in the treated explants. The formation of primordia in the treated explants, to within the medial regions of the tract suggests the possibility that the spread of dense dermis is prevented by the inhibition of cell proliferation.

4.2.5 Primordium Induction by EDA/EDAR Signalling Requires a Dermis of Permissive Cell Density.

In summary, the work discussed in this section highlights that periodic pattern formation of feather primordia in chicken is a highly dynamic process involving the interplay between both molecular and cellular regulation to induce feather primordium formation and the wave-like propagation of feather primordium induction. The results presented in this thesis, indicate that three factors are required for the induction of primordium formation in developing chicken skins; 1) An epidermis competent to primordium induction (as indicated by the expression of *β-Catenin*), 2) expression of *EDA*, overlapping with the competent epidermis, to synergistically induce the expression of *FGF20* with *β-Catenin* and 3) a dermis of a dermal cell which is permissible to primordium induction and able to induce *BMP4* expression (and possibly other genes) in the event of the formation of cell condensates.

Propagation of *EDA* expression specifically, is required for the formation of a hexagonally arranged periodic pattern of feather primordia. Absence or dysregulation any of these factors during development results in the inhibition of primordium induction or the formation of an abnormal periodic feather primordium pattern of lowered fidelity.

The above results also suggest that the primary inductive signals that induce feather primordium formation are located within the epidermis rather than the dermis as suggested by previous studies (Dhouailly, 1973; 1975; 1977; Higgins *et al.*, 2013). The previous studies observed, through epidermal-dermal recombination experiments, that

the dermis was capable of inducing the formation of epidermal placodes on the overlying recombined epidermis. However, these experiments relied on the use of a dermis with existing dermal cell condensates, prior to the recombination procedure. As demonstrated in my own study, dermal cell condensates express genes that are unique to the condensate which may signal to and influence epidermal cell behaviour. In essence, the previous studies showed that dermal cell condensates can induce the formation of epidermal placodes, but they fail to show that a naive dermis can induce appendage formation. From my own observations, all the primary inductive signals, *β-Catenin*, *EDA,* and *FGF20* are all expressed within the epidermis and are induced independently of dense dermis formation. The dermal layer appears to be a latent player in the formation of feather primordia and only appears to function after the initial epidermal signal induces the formation of dermal cell aggregates, when a minimum dermal cell density is reached. The induced dermal cell aggregates in turn, induce *BMP4* expression to regulate the growth of the forming feather primordia through long-range inhibition of *FGF20* expression and possibly mediates lateral inhibition between feather primordia. The underlying mechanisms that induce the observed expression patterns of *β-Catenin* and *EDA* expression prior to the induction of feather primordium formation are currently unknown and has not been investigated in this current study but opens up an interesting area for further research in the study of feather pattern formation.

In mouse, hair formation occurs in waves and loss of EDA/EDAR signalling results in only the absence of guard hairs, which form in the first wave of hair primordium induction (Headon and Overbeek, 1999; Headon *et al.*, 2001; Mou *et al.*, 2006). Secondary and tertiary hair formation is unaffected by the loss of EDA/EDAR signalling, indicating hair primordium induction can occur independently of EDA/EDAR signalling. I demonstrated in chicken that recombinant EDA can induce the formation of feather primordia through its ability to stimulate *FGF20* expression. Downstream signalling of the EDA/EDAR pathway requires the activation of NF-κB (Doffinger *et al.*, 2001; Kumar *et al.*, 2001). Inhibition of NF-κB activity results in the complete inhibition of primordium induction (Drew, 2006), demonstrating the

importance of EDA/EDAR signalling during feather primordium induction in chicken. However, NF-κB is a downstream signalling effector molecule of several other TNF signalling pathways other than EDA/EDAR signalling and that the inhibition of feather primordium induction described by Drew *et al,* may be the result of non-specific effects of the treatment. Using a function blocking antibody that specifically targets EDA proteins, Ecto-D2, I show that feather primordia can arise through an EDA/EDAR signalling independent mechanism. However, primordium formation is only observed within the medial regions of the dorsal tract in treated explants, where dermal cell density is initially highest. The observation suggests two possible functions of endogenous EDA/EDAR signalling; 1) EDA/EDAR signalling is required for dermal cell proliferation, or 2) EDA/EDAR signalling may lower the threshold of dermal cells required for primordium induction.

The effect of Ecto-D2 treatment on dorsal skin explant patterning is similar to those observed in the methotrexate treated explants, suggesting the possibility that Ecto-D2 may function analogously to methotrexate. However, as demonstrated in the midline removal experiments, *EDA* expression is observed across the dorsal tract after the excision of the midline, but dermal thickening is not observed in these manipulated explants after culture. This suggests that EDA/EDAR signalling may be active in the skin regions lateral to the excision site and is not involved in promoting cell proliferation.

The other possibility is that the synergistic induction of *FGF20* expression, by both EDA/EDAR and WNT/β-Catenin signalling, may lower the threshold of dermal cell density required to induce the formation of feather primordia. The enhanced FGF signalling may exert a stronger chemotactic response from the cells of the dermis, resulting in the formation of larger feather primordia, while also requiring less dermal cells to form (**Figure 77**). In this model, feather primordium formation can occur independently of EDA/EDAR signalling, possibly through WNT/β-Catenin induction of *FGF20* expression, but requires a high dermal cell density to initiate primordium formation. Endogenous EDA/EDAR signalling lowers the threshold of dermal cell density required to induce primordium formation, through the synergistic induction of

FGF20 expression by both EDA/EDAR and WNT/β-Catenin signalling. Enhancing EDA/EDAR signalling (and therefore *FGF20* expression), through the application of Fc-chEDA1, further lowers the threshold of dermal cell density required to a minimal level, but below this minimal threshold, primordium induction cannot occur. This may explain why the effects of Fc-chEDA1 does not induce the formation of feather primordia ubiquitously across the tract. If dermal cell density is below a critical level, regardless of the level of *FGF20* induction by EDA/EDAR and WNT/β-Catenin signalling, primordium formation does not occur.

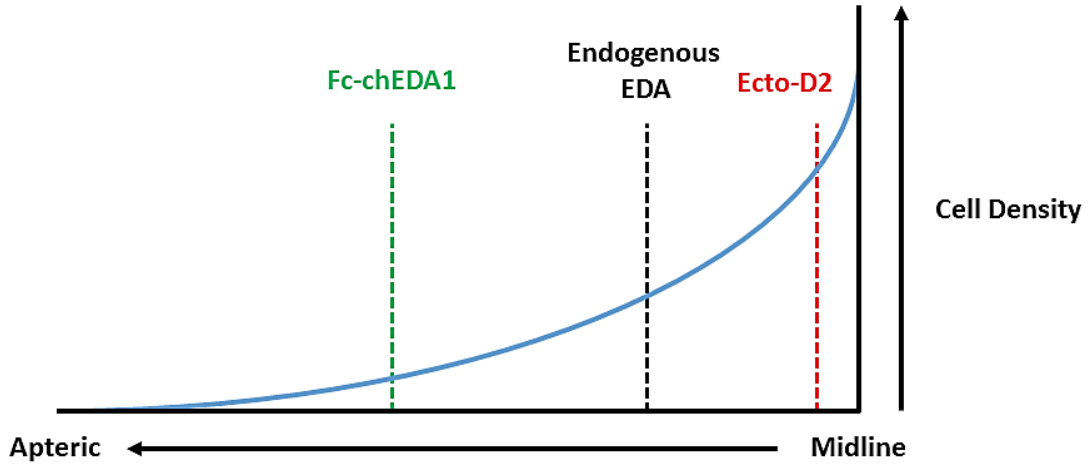

Figure 77. Schematic of the effects of EDA/EDAR signalling on feather primordium induction. The graph represents dermal cell density across the dorsal tract from the midline. Dermal cell density increases in an apteric to midline direction (Blue curve). Dotted lines represent the location in the tract which primordium induction can occur. Red dotted line - Ecto-D2 treatment (reduced or absence of EDA/EDAR signalling), black dotted line - endogenous EDA/EDAR signalling, and green dotted line - Fc-chEDA1 treatment (enhanced EDA/EDAR signalling). Intersection between the dotted lines and the cell density curve indicate the limit of pattern induction under different conditions of EDA/EDAR signalling.

4.2.6 Testing of the Proposed Model for Feather Patterning by Simulation

In collaboration with Dr Kevin Painter, we developed a mathematical model for periodic pattern formation in chickens based on the molecular and cellular interactions observed in this study (**Appendix II**). The model consists of a basic reaction-diffusion mechanism, as described in section **1.4.1**, but also includes the regulation of molecular components via dermal cell interactions. The model itself follows four basic rules derived from my experimental observations: 1) a travelling molecular wave stimulates the activation of the epidermis (*EDA*), 2) activation of the epidermis stimulates the production of a chemoattractant (*FGF*), which induces dermal cell migration and the formation of dermal cell condensates, 3) production of the chemoattractant (*FGF*) is maintained by the dermal cell condensate, and 4) the dermal cell condensates also produces the inhibitor of the chemoattractant (*BMP*). Due to the lack of experimental data, some parameters such as the speed of the travelling wave and diffusion rates of the activators and inhibitors were assigned values that simply permit periodic patterning. A more detailed version of the rules and parameters used in the simulations can be found in **Appendix II**.

Using these basic set of rules, two *in silico* experiments were performed to assess; 1) whether the basic model can simulate feather primordium pattern formation in a manner similar to that observed during the development of embryonic chickens and 2) if the travelling molecular wave of epidermal activation is required for the formation of a hexagonal periodic pattern of high fidelity (**Appendix II**).

In the first *in silico* experiment, the resulting simulation matches the experimentally observed sequence of periodic pattern formation observed during feather primordium patterning. The result demonstrates that the basic model is capable of generating experimentally observed periodic patterns (**Figure 80**).

In the second experiment, activating the epithelium across the entire patterning field prior to pattern formation results in the formation of dermal cell aggregates of various shapes and sizes, arranged in pattern of lowered fidelity. This result shows similar parallels to my own experimental observations (**Figure 81**). Expanding the region of

EDA expressing skin, that is, the induction wave prior to feather primordium induction results in a decrease of pattern fidelity. Based on experimental evidence and *in silico* simulations, a travelling wave of activation is required for the formation of a periodic pattern of high fidelity. However, in **Figure 81**, the *in silico* simulation shows the formation of a wide range of shapes and sizes of dermal cell aggregates, which are not observed experimentally. This suggest that the model in principle, is capable of generating periodic patterns observed in biological experiments, but requires refinement via future experimental work to fully replicate the current biologically obtained experimental data. Further testing of the current model may highlight missing molecular or cellular interactions which could be tested experimentally, to produce a more accurate model of periodic pattern formation.

4.3 Comparative Analysis of Primordium Formation and Pattern Analysis between Chicken and Different Ave Species

As described in the introduction, in the chicken, feathers form in distinct feather bearing tracts, separated by non-feather bearing apteric regions (Lucas and Stettenheim, 1972). This basic topology of tracts and apteric regions is maintained in different species of Aves but the size and shape of the tracts or apteric regions can vary greatly between species, especially between dorsal tracts (Clench, 1970; Nitzsch, 1867; Stettenheim, 2000). The observed differences have been hypothesised to be related to environmental or behavioural adaptations of the different species such as flying, gliding, swimming etc. (Homberger and de Silva, 2000).

In this study, the periodic pattern of feather primordia in the dorsal tracts of several species of flighted or non-flighted Aves was examined and compared to those of chicken. The study revealed that the process of periodic patterning of feather primordia varied between species. However, in general the arrangement of feather primordia in flighted species was of a higher fidelity than those of non-flighted species. Using the knowledge gained from my studies in the chicken embryo, it appears that the observed differences in the periodic pattern of feather primordia in the dorsal tracts of various Ave species can be related to the modulation of the *β-Catenin* and *EDA* expression pattern and also to the initial distribution of dense dermis during embryonic development.

4.3.1 Guinea Fowl

The dorsal tract of guinea fowls display a periodically arranged hexagonal pattern of feather primordia which, from my observations, arises in a manner analogous to that of chicken primordium pattern formation. In the presumptive dorsal tract of guinea fowl embryos, both *β-Catenin* and *EDA* are initially expressed at the dorsal midline of the dorsal tract. The expression of both genes then propagates bilaterally from the midline, laying down new feather primordium rows in their wake. Propagation of *β-Catenin* expression remains ahead of both *EDA* expression and primordium induction, while the propagation of *EDA* expression remains slightly behind primordium

induction. The observation suggests that propagation of *β-Catenin* in guinea fowl may be directly involved in the propagation of feather primordium formation. However, *in situ* hybridisation analysis revealed that *β-Catenin* expression expands much faster than the induction of feather primordia, indicating that an unknown factor is limiting the induction of feather primordia in the expanded *β-Catenin* expression skin region. *EDA* expression is observed to be constantly around one or two primordium rows behind the last row of primordia formed, during the wave-like propagation of primordium formation. This indicates that in guinea fowl, propagation of *EDA* expression may not be the main component driving the wave-like propagation of primordium formation. However, in both mouse and chicken, EDA protein has been shown to exist in a diffusible form (Drew *et al.*, 2007; Schneider *et al.*, 2001). It is possible that EDA protein may be diffusing ahead of the *EDA* expressing skin regions to initiate feather primordium induction within the *β-Catenin* expressing regions of developing guinea fowl embryos. Existence of EDA proteins outwith the site of *EDA* expression could be observed through the use of immunohistological detection using EDA specific antibodies.

As observed in chicken during periodic pattern formation of feather primordia, propagation of *EDA* expression alone is able to explain the formation of a high fidelity hexagonal pattern of primordia. In guinea fowl, the propagation of both *β-Catenin* and *EDA* expression may further enforce the formation of a high fidelity pattern across the tract, or that propagation of *β-Catenin* expression itself may be the norm in flighted species of Aves. Both chickens and guinea fowl belong to the order of Galliformes but chickens have been selectively bred for meat and egg production, rather than survival in the wild, for a longer period than guinea fowl, and the lack of positive selection for flight ability may have resulted in the loss of *β-Catenin* propagation in chicken. Examination of *β-Catenin* expression in other flighted Ave species would resolve this question.

4.3.2 Duck

Adult duck dorsal tract skin displays a high fidelity, hexagonally arranged periodic pattern of large contour feathers, interspersed with smaller down feathers. The presence of two different types of feathers on dorsal tract is unique among the bird species studied in this thesis. From my observations, the two feather types arise through different mechanisms, during embryonic development. However, the basic mechanism of the sequential wave-like propagation of feather primordia during dorsal tract patterning is similar to those observed in the other two flighted species studied in this thesis, albeit modified, to produce the final duck feather pattern. Expression of *β-Catenin* during duck embryo development is very dynamic. Initially, as in chicken, *β-Catenin* expression is observed throughout the defined feather tracts and excluded from the apteric regions. As the embryo develops, *β-Catenin* expression within the femoral tracts expands across the body of the duck eventually merging with neighbouring tracts, resulting in feather primordium induction throughout the body of the duck. How this occurs was not investigated in this study. *EDA* expression appears to serve similar functions to those observed in chicken. Propagation of *EDA* expression is followed by the induction of feather primordium formation but propagation of *EDA* expression does not originate from a single stripe from the midline of the dorsal tract. *EDA* expression is initially observed within the inner arms of the V-shaped region of *β-Catenin* expression and propagates bilaterally on both sides of the embryo. This observation indicates that initial site of *EDA* expression induction is restricted to the boundaries dictated by *β-Catenin* expression. This is observed in all the species examined in this study, *EDA* expression is never observed outwith the skin regions displaying *β-Catenin* expression.

Interestingly, after the formation first wave of feather primordia, *β-Catenin* expression reappears in the interbud spaces between existing feather primordia while *EDA* expression gradually disappears from the interbud regions. The ectopic expression of *β-Catenin* eventually focalises forming new, smaller feather primordia. This observation indicates that in ducks there are two waves of feather primordium formation, the first wave requires *EDA* expression while the second wave forms

independently of *EDA* expression. In newly hatched ducks, there exist two main types of feathers on the body, the pennaceous feathers (have a rachis) and the plumulaceous down feathers in between (Harris *et al.*, 2002). The pennaceous feathers are the ones formed in the first wave of feather induction during embryonic development whereas the plumulaceous feathers form in the second wave. This suggests possible functions for EDA/EDAR signalling during duck embryonic development: 1) propagation of *EDA* expression itself is required for the formation of a high fidelity primordium pattern, and 2) the activity of EDA protein may be involved in the formation of larger primordia, possibly through the synergistic induction of *FGF20* expression with WNT/β-Catenin signalling (as observed in chicken). The synergistic induction of *FGF20* expression results in increased cell migration to the primordium. In primordia that form independently of *EDA* expression, the primordia are much smaller in size and are organised in an irregular pattern.

The mechanism for the activation of *β-Catenin* expression between existing feather primordia is unknown. In chickens, the induction of new feather primordia between pre-existing primordia does not occur *in ovo*, but in *ex vivo* culture conditions when the interbud spaces between pre-existing primordia is increased through mechanical stretching, formation of primordia is induced in the interbud spaces. This suggests, that in chicken, an inhibitory factor that inhibits *β-Catenin* expression in the interbud regions is produced by the existing feather primordia, which diffuses into the interbud space to inhibit primordium formation. In duck embryos, the second wave of feather primordia only form once the primary wave of feather primordium formation is almost complete and is never observed prior to this. *β-Catenin* expression initially appears in the interbud spaces between the most mature feather primordia located at the dorsal midline and spreads across the tract. This suggests that in ducks, as feather primordia mature, production of the diffusible inhibitor by the primary wave of feather primordia is either reduced or halted. It is also possible that an inhibitor of the inhibitory factor is produced in the mature feather primordia, which alleviates inhibition of *β-Catenin* expression in the interbud spaces.

4.3.3 Flightless Ratites

Recent genetic studies determined that ostriches and emus descended from a common flighted ancestor, and that both the ostriches and emus lost the ability to fly independently (Baker *et al.*, 2014; Mitchell *et al.*, 2014). Interestingly, both species display a low fidelity periodic pattern of feather primordia, and through this study I showed that the observed periodic patterns of feather primordia arise through very similar mechanisms in both the ostriches and emus, despite having both developing flightlessness independently of each other.

Initially, *β-Catenin* expression in both species is observed throughout the presumptive feather tracts and excluded from the "apteric" regions, similar to chicken, however, *EDA* expression is also observed throughout the *β-Catenin* defined tract prior to primordium induction in both ostriches and emus. Propagation of *EDA* expression is not observed in both ostriches and emus at the developmental stages examined in this study. The final arrangement of feather primordia in both the ostrich and emu show a low fidelity periodic pattern and based on my experiments using the chicken embryo, it was initially hypothesised that the loss of spatiotemporally restricted expression of *EDA* expression was the cause low fidelity primordium pattern in ostriches and emus. In *ex vivo* chicken experiments, the expansion of *EDA* expression prior to feather primordium induction resulted simultaneous primordium induction across the tract. Closer examination of embryos at intermediate stages of feather primordium induction revealed that in both species, feather primordium induction within the medial regions of the dorsal tract was delayed or inhibited despite the presence of overlapping expression of *β-Catenin* and *EDA* across the presumptive tract. Also, in the non-flighted species, the wave-like propagation of feather primordium induction occurs in a lateral-medial direction rather than medial-lateral direction, as observed during feather primordium induction in flighted Ave species. This indicated the possibility that a permissive factor required for feather primordium induction within the medial regions of the dorsal tract of ostrich and emu embryos was lacking. Through hetero-specific epidermal-dermal recombination experiments, I showed that the epidermis from the emu dorsal tract was competent to primordium induction and that the primary

defect behind the delayed primordium formation within the medial regions of the dorsal tract was of dermal origin. Previous studies suggested that the epithelial expression of *β-Catenin* was associated with competence of the skin to feather primordium induction, but how *β-Catenin* expression is established is unknown (Widelitz *et al.*, 1999; Widelitz *et al.*, 2000). Based on the results from this study, in ostrich and emu feather primordium development, I show that the formation of a *β-Catenin* expressing epidermis which is competent to primordium induction is independent of the formation of the dense dermis.

4.3.4 The Impact of Variation in Dermal Cell Density on Feather Pattern Fidelity

Transverse sections of the dorsal tracts of emu embryos revealed that the initial lack of a dermis of sufficient cell density was the underlying cause that delayed primordium induction in the medial regions of the dorsal tract, despite the presence of a competent epidermis. The result may also be applicable to the delayed induction of feather primordia within ostrich dorsal tracts. As mentioned in the introduction, in chicken the origins of the dense dermis varies between different feather tracts. The dorsal dermis originates from the dermomyotome and *WNT11* function has been shown to be essential for the proper formation of the dense dermis in the medial regions of the dorsal tract (Mauger, 1972b; Morosan-Puopolo *et al.*, 2014; Olivera-Martinez *et al.*, 2000; Olivera-Martinez *et al.*, 2002). Loss of function of *WNT11* results in the inhibition of cell migration of dermogenic progenitors from the dermomyotome and the loss of dense dermis formation. Within the dorsal tract of ostrich and emu embryos, it was observed that dense dermis thickening spreads in a lateral to medial direction. This sequence of dense dermis formation is analogous to the formation of the dense dermis in mouse. At E13 developing mouse embryos also initiate dermal thickening on the lateral regions of the embryo, with gradual thickening in a lateral to dorsal direction, prior to the induction of hair primordia (Dhouailly *et al.*, 2004; Li *et al.*, 1995). This suggests that dense dermis formation within the medial regions of the dorsal tract of ostriches and emus has been lost, possibly through loss of migration of dermal cell progenitors from the dermomyotome (**Figure 78**). This could be the result of loss or inhibition of *WNT11* activity within the dermomyotome of developing

ostriches and emus. *Dermo-1* expression is one of the earliest indicators of dense dermis formation in avian skin and has been shown to be involved in the formation of the dense dermis in chicken skin *(Hornik et al., 2005; Scaal et al., 2001). In situ* hybridisation analysis to examine the *Dermo-1* expression pattern in both ostrich and emu embryos should reveal whether dense dermis initiation in the dorsal tract, prior to feather primordium induction, has indeed been lost in these species.

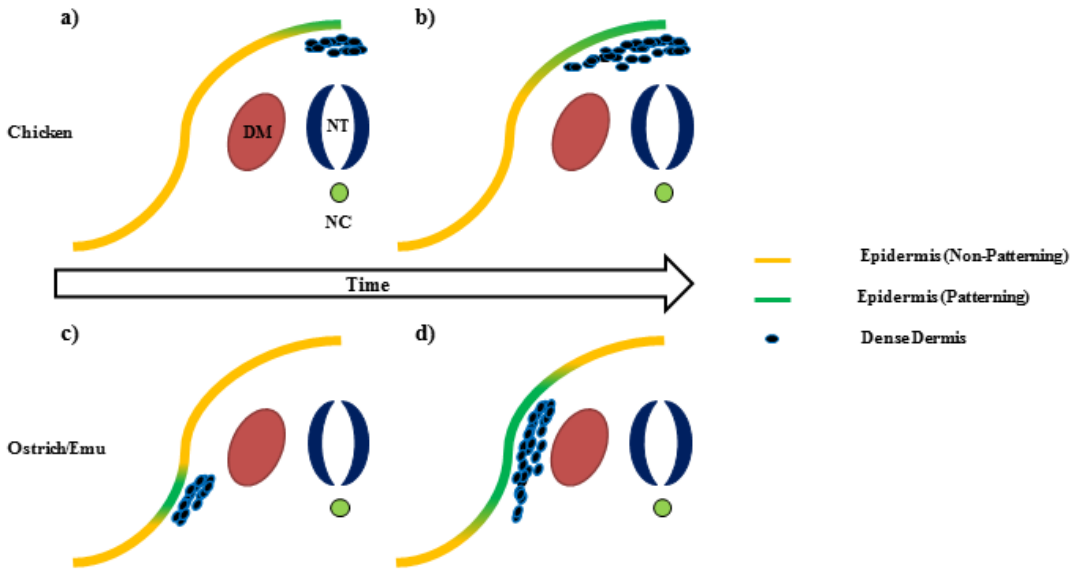

Figure 78. Diagrammatic comparison of dense dermis formation and skin patterning between chickens and the flightless ratites, ostrich and emus. a-b) In chicken, dense dermis formation (blue circles) begins at the dorsal midline, above the neural tube (NT), and spreads laterally from the midline. **c-d)** In ostriches and emus, dense dermis formation begins on skin regions lateral from the dorsal midline, and migrates towards the midline during embryonic development. (Regions of skin displaying a dermal cell density sufficient for primordium induction is highlighted in green while skin regions with too low a dermal cell density to promote primordium formation are yellow). DM - dermomyotome, NC - notochord.

In chicken, the lateral and ventral dense dermis originates from the somatopleure and experiments performed by Sengel *et al*, 1990 demonstrated that removal of part of the

spinal/dorsal tract resulted in the migration of femoral tract dermis into the dorsal tract region. (Dhouailly *et al.*, 2004; Fliniaux *et al.*, 2004b; Sengel, 1990). This suggests that during feather tract formation, lateral inhibition may be the mechanism that separates the different tract regions, resulting in the formation of the apteric regions. If a feather tract is partially removed, lateral inhibition by the removed tract is prevented and thus surrounding tracts can "invade" the space that the removed tract would normally occupy. This may explain the lateral-medial propagation of dense dermis formation observed in the dorsal tracts of developing ostrich and emu embryos. Dense dermis from lateral skin regions may be migrating towards medial regions of the dorsal tract to compensate for the loss of dermomyotome derived dense dermis within the dorsal tract of ostrich and emu embryos.

4.3.5 Comparative Analysis of Primordium Formation and Pattern Analysis between Chicken and Different Ave Species: Summary

Overall, by studying the expression pattern of *β-Catenin* and *EDA* and through the analysis of dense dermis distribution during the process of feather primordium induction and periodic pattern formation in both flighted and non-flighted Ave species, I was able to observe how the above factors were modulated to produce the different periodic patterns of feather primordia.

β-Catenin is one of the earliest genes expressed within the feather tracts of all the Ave species examined. In HH 29 chicken embryos, moderate levels of *β-Catenin* expression is observed across each of the presumptive feather tracts prior to feather primordium induction and appears to indicate skin regions that are competent to feather formation, while skin regions lacking *β-Catenin* expression define the apteric regions (Jiang *et al.*, 1999; Widelitz *et al.*, 2000). As the embryo grows the feather tracts expand in size and *β-Catenin* expression expands accordingly but *β-Catenin* expression remains within the defined boundaries of the presumptive feather tracts, separated by the apteric regions. The observed expression pattern of *β-Catenin* in all the species examined in this project indicate that the appearance of *β-Catenin* does not define the size and shape of the feather. Instead this study has revealed that skin regions

displaying expression of *β-Catenin* changes over time and that *β-Catenin* expression defines epithelial competence to feather primordium induction specifically, rather than the skin as a whole. Dermal competence requires the formation of a dermis of sufficient cell density which appears to be regulated independently from the induction of epithelial competence.

The expression of pattern *EDA* and initial location of dense dermis formation, on the other hand, show the biggest differences in non-flighted species of Aves compared to those of flighted species. In flighted species, *EDA* expression propagates laterally from the initial site of expression, preceding the induction of feather primordia and eventually covers the presumptive tract, laying down new primordium rows in its wake, resulting in the formation of hexagonally arranged feather primordia. Whereas in non-flighted species, *EDA* expression does not show propagation of expression within the dorsal tract but initially overlaps with the *β-Catenin* expression pattern. Along with the lack of *EDA* expression propagation, delayed formation of dense dermis within the medial regions of the dorsal tract results in the formation of a low fidelity periodic pattern of feather primordia. This suggests that there may be a correlation with propagation of *EDA* expression and dermomyotome derived dermis with the ability to fly. Whether the ostriches and emus lost dense dermis formation within the medial regions of the dorsal tract prior to the loss of *EDA* expression propagation is unknown and also whether these losses resulted in flightlessness or was a consequence of the loss of flight cannot be ascertained from this current study.

The induction and formation of hair, feather and scale primordia share many common developmental signalling pathways, as discussed above (for a more detailed review see (Biggs and Mikkola, 2014)) These include, WNT/β-Catenin, EDA/EDAR, FGFs, SHH, BMPs among many other signalling pathways. Both mammals and birds are believed to have evolved from a common basal amniote ancestor and later diverged into two distinct groups. Mammals belong to the synapsid lineage while birds and reptiles belong to the diapsid lineage. The sequential wave-like propagation of primordium formation has thus far, only been observed within avian species and so the evolutionary origin of the wave-like propagation is an interesting area for future

study. The evolutionary origins of birds and flight have been of great scientific interest. Since the discovery of *Archaeopteryx*, an ancient bird-like species displaying both reptilian and avian characteristics (teeth and feathers), the question of whether birds descended from dinosaurs was hotly debated. With the recent discoveries of a vast array of dinosaur fossils displaying feather-like structures on their skin, the theory that birds are descendants of the dinosaur lineage is now widely accepted (Hu *et al.*, 2009b; Li *et al.*, 2012; Qiang *et al.*, 1998; Xu *et al.*, 2001; Xu *et al.*, 2003; Xu *et al.*, 2004; Xu and Zhang, 2005; Xu *et al.*, 2012). All extinct dinosaurs belong to the archosaur group of the diapsid lineage and currently, the only living members of the archosaur group are birds and crocodiles. Currently, very few studies into the development of the scale pattern in crocodiles have been performed. Milinkovitch *et al*, 2013 demonstrated that head scales on the head of crocodiles do not form as individual units, such as in the formation of hair and feathers, but arise through cracking, caused by mechanical stress during the growth of the embryo (Milinkovitch *et al.*, 2013). The patterning process of scales between the head and body of crocodile appear to arise differently. While the periodic pattern of head scales appears to be random in size and shape, periodic pattern of crocodilian scales on the dorsal and ventral sides of individual crocodiles appear to be of relatively high fidelity, in square arrangements. Interestingly, Milinkovitch *et al*, 2013 also performed an *in situ* hybridisation of *SHH* expression on a developing corn snake embryo which revealed a highly hexagonal arrangements of scale primordia. It would be interesting to determine if crocodiles, and possibly snakes, develop scale primordia in a sequential wave-like induction process during embryonic development to establish if primordium wave propagation in avian species is an evolutionarily derived mechanism of primordium patterning.

APPENDICES

Appendix I

Embryological Stages of the Developing Chicken

The following section will describe the morphological landmarks that were used to identify the developmental stages of chicken embryos used in this study. Staging of the embryos was based on the chicken staging system developed by Hamburger and Hamilton 1951 (Hamburger and Hamilton, 1952). However, due to slight variations in the timing of feather primordium appearance between individual embryos of the same stage (based on multiple landmarks), the appearance of the primordia took precedence over the other anatomical landmarks described by Hamburger and Hamilton during the staging process. Images were adapted from Hamburger and Hamilton 1951 (Hamburger and Hamilton, 1952), note that the images are not scaled proportionally.

Stage 29 (E6.5)

Feather Primordia - Distinct feather are not visible on any of the presumptive feather tracts. In the dorsal tract, a primary stripe of high dermal cell density is visible at the caudal midline of the tract.

Beak - No visible egg tooth.

Wings - Wing is bent at the elbow. Grooves are visible between the first, second and third digits. The second digit itself, is visibly longer than the other two digits.

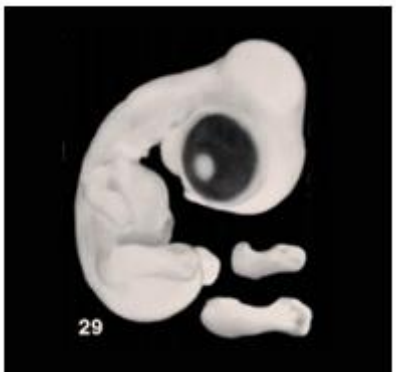

Stage 31 (E7.5)

Feather Primordia - In the dorsal tract, three fully formed rows are visible, with the emergence of forming rows on either side of the last fully formed rows.

Beak - Egg tooth is clearly distinct and the upper mandible protrudes noticeably.

Wings - Distinct webbing between the first and second digits.

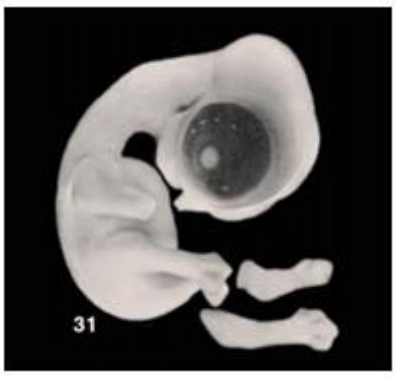

Stage 33 (E8.5)

Feather Primordia - In the dorsal tract, the entire tract is almost covered in primordia. Around eleven to thirteen fully formed rows are visible. Outgrowth of the medial rows can be observed.

Wings - Webbing between the radius and first digit becomes visible while webbing between individual digits show regression.

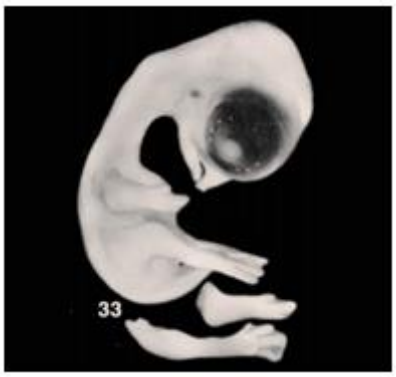

Appendix II

Mathematical Model for Chemotaxis-Mediated Feather Patterning.

A schematic showing the principal components of the mathematical model is given in **Figure 79**. (Note: the following description and figures were prepared by Dr Kevin Painter of Heriot-Watt University)

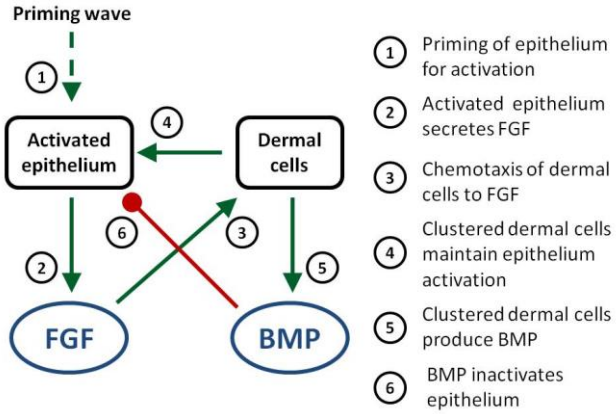

Figure 79. Schematic of the mathematical model. Cellular components shown in curved black boxes, molecular components shown in elliptic blue boxes. Promoting actions shown with green arrows, inhibiting actions shown with red dots.

Our mathematical model considers the evolution over space and time of four key variables: dermal cell density, $c(x,y,t)$; the activated state of the epithelium, $a(x,y,t)$; FGF concentration, $f(x,y,t)$; and, BMP concentration, $b(x,y,t)$. In addition, we consider an imposed "priming wave", $w(x,y,t)$, that allows the epithelium to become activated and hence primes the skin for patterning. Here, t represents time and (x,y) defines the spatial position in a two-dimensional rectangular slice of embryonic skin, where x represents the anterior-posterior coordinate and y the medial-lateral coordinate. We note that for reasons of model simplicity we have not attempted an *explicit* description of tissue depth. However, a degree of depth representation is implicitly given by the variables: the overlying epithelium is represented by its activation state, while dermal cells reside in the underlying mesenchyme.

Mathematically, our model is given by a system of partial-differential equations of reaction-diffusion-advection type with equations given in the following "word" form:

$$Rate\ of\ variable\ change\ = Change\ due\ to\ movement + Change\ due\ to\ production/loss.$$

Priming wave

An initial wave is assumed to spread through the tissue in medial to lateral fashion, priming the skin for patterning. Currently, we do not model the specific molecular regulation of this process: this represents a challenge more appropriate for future modelling. Rather, we impose a functional form for $w(x, y, t)$ as follows:

$$w(x, y, t) = (1 + \tanh(\omega_1 t - \omega_2 y))/2.$$

The above generates a "travelling-wave" type profile that progressively shifts the skin between an unprimed ($w = 0$) and primed ($w = 1$) state, beginning at the medial-most region and spreading laterally with speed ω_1/ω_2. Note that currently we assume any spread along the x-axis (anterior-posterior) is negligible.

Cell populations

The dynamics of the dermal cells, $c(x, y, t)$, are given as follows:

$$c_t = D_c \nabla^2 c - \nabla \cdot (c\chi(c, f)\nabla f).$$

The right hand side terms both derive from cellular movement: the first specifies a diffusion-type term, representing an undirected (random) component to dermal cell movement (with associated random motility coefficient D_c); the second term describes positive chemotaxis of dermal cells up FGF gradients (Process 3 in **Figure 79**). The function $\chi(c, f)$ is the chemotactic sensitivity: here we choose $\chi(c, f) = \alpha e^{-c}$, where α defines the chemotactic strength coefficient and the e^{-c} component limits "overcrowding": it assumes chemotactic movement is reduced as the cells become increasingly aggregated. Note that for simplicity we do not explicitly consider dermal cell proliferation: rather, we suppose the density of dermal cells by the time each row forms is (approximately) the same and absorb their proliferation into the initial

conditions. Specifically, we set $c(x, y, 0) = c_0 + \xi(x, y)$: c_0 determines the local density of cells by the time each new row of buds is about to form, while $\xi(x, y)$ defines a small addition of environmental noise.

We do not model the epithelial cell population *per se*, rather we consider its overall activity state, defined by $a(x, y, t)$. In terms of the model, this activity defines the local proportion of epithelium cells that are secreting FGF. Specifically, we assume:

$$a_t = k_{on}(w, c) \cdot (1 - a) - k_{off}(b, c) \cdot a \, .$$

Note that $a(x, y, t)$ varies between 0 (inactivated) and 1 (activated). The two terms on the right hand side respectively describe activation and inactivation, with rates $k_{on}(w, c)$ and $k_{off}(b, c)$. For these two functions we assume:

$$k_{on}(w, c) = w \cdot (k_1 + k_2 c) \, ; \qquad k_{off}(b) = k_3 \cdot b \cdot H(c_a - c).$$

Activation depends on the priming wave (Process 1 in **Figure 79**) and is further enhanced by dermal cells (Process 4). The second term deactivates the epithelium at a rate depending on the concentration of BMP (Process 6), although we assume this is only possible if the dermal cell density is below some critical ``clustering density'', c_a: i.e. the presence of a cluster maintains the activity in the overlying epithelium. Here, $k_{1,2,3}$ are constant parameters, while $H(\cdot)$ denotes the unit Heaviside function. Initially we assume the skin is in a fully inactive state ($a(x, y, 0) = 0$).

We assume the molecular components FGF and BMP are secreted as diffusible ligands, with dynamics of the following form:

$$f_t = D_f \nabla^2 f + k_{FGF} a - \delta_f f$$

$$b_t = D_b \nabla^2 b + h(c) c - \delta_b b$$

The terms on the right hand side represent molecular diffusion (with diffusion coefficients $D_{f,b}$), secretion/production and decay (with decay rates $\delta_{f,b}$), respectively. The production term for FGF derives from secretion by the activated epithelium, at a constant rate k_{FGF} (process 2 in **Figure 79**). BMP is produced by the dermal cells

(process 5), although we assume that this occurs at a rate that increases with their degree of clustering. Specifically, we consider the Hill function

$$h(c) = k_{BMP}\frac{c^l}{c_a^l + c^l},$$

where k_{BMP} is the maximum production rate, c_a is the clustering density and l is the Hill coefficient. Initially we assume neither molecular component is present and set ($f(x, y, 0) = f(x, y, 0) = 0$).

Simulation 1 - Epithelial Activation by a Travelling-Wave

"Time 0"

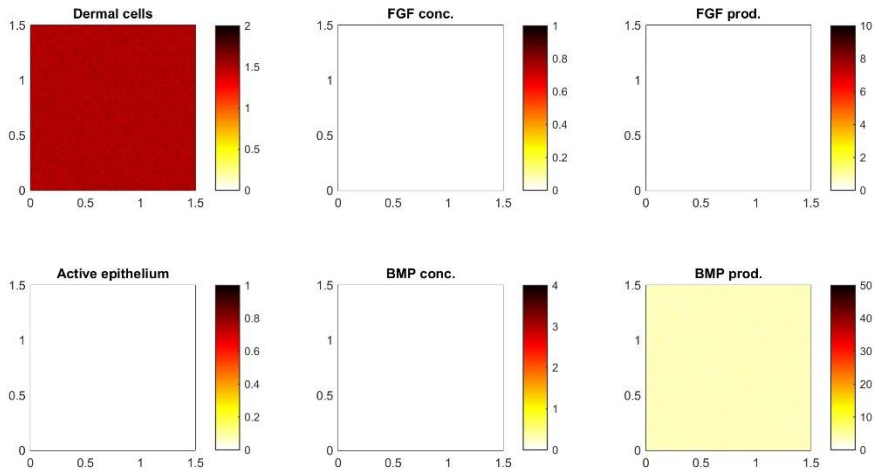

"Time 1"

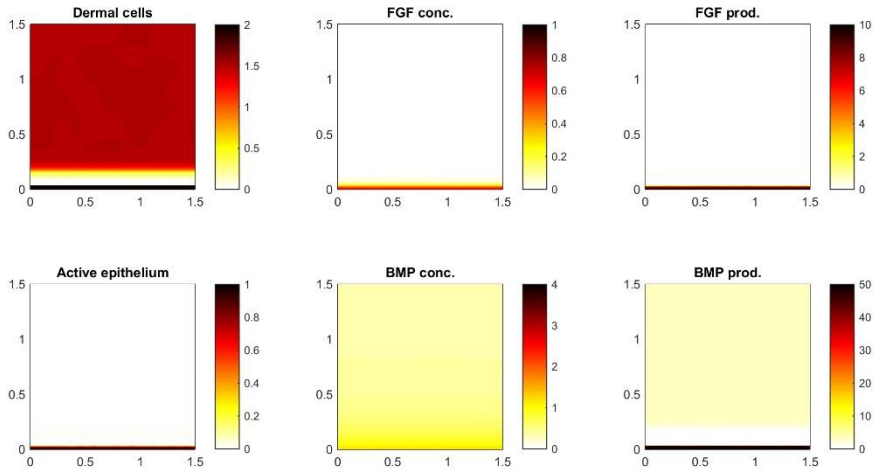

"Time 2"

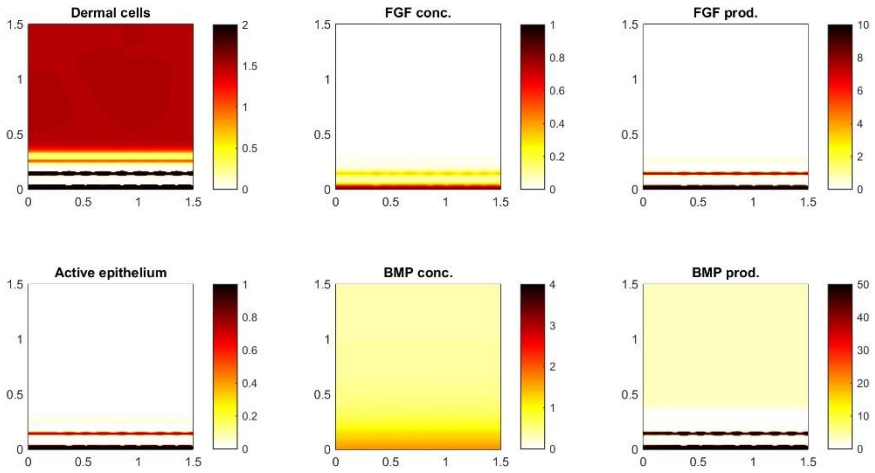
Dermal cells
FGF conc.
FGF prod.
Active epithelium
BMP conc.
BMP prod.

"Time 3"

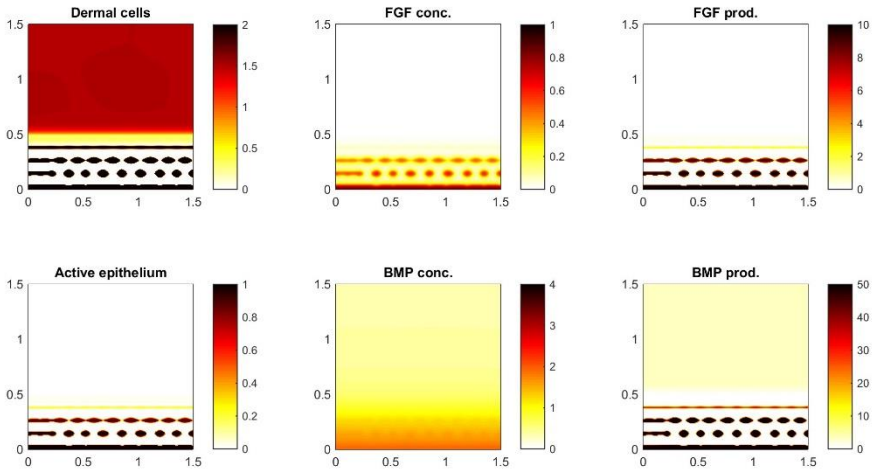
Dermal cells
FGF conc.
FGF prod.
Active epithelium
BMP conc.
BMP prod.

"Time 4"

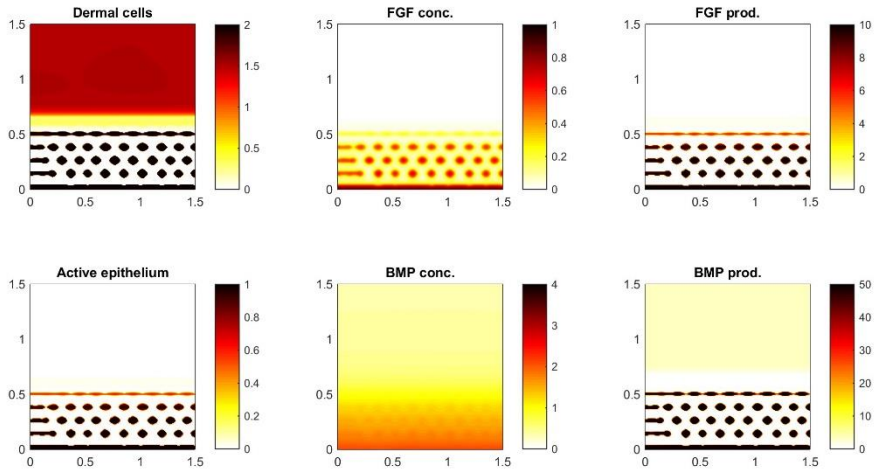

Figure 80. *In silico* periodic pattern formation via a travelling wave of activation. The travelling molecular wave, indicated by the gradual movement of epidermal activation (bottom left panel), induces the sequential formation of periodically arranged rows of dermal cell condensates (top left panel) as the wave travels across the patterning field. As the travelling wave moves across the homogenous field of dermal cells, the epithelium is activated and stimulates the production of the chemoattractant, FGF, resulting in the local increase of FGF concentration (top right and top middle panel respectively). The presence of FGF stimulates dermal cell migration and aggregation. As dermal cell density increases, the production of BMP by the dermal cells increase accordingly and diffuses from the aggregate (bottom right and bottom middle panel). The dermal cell condensate also maintains the local activation of the epithelium. FGFs and BMPs interact via a reaction-diffusion mechanism resulting in the formation of periodically arranged spots of dermal cell condensates. The resulting pattern is hexagonal and shows a high level of fidelity.

Simulation 2 - Ubiquitous Epithelial Activation

"Time 0"

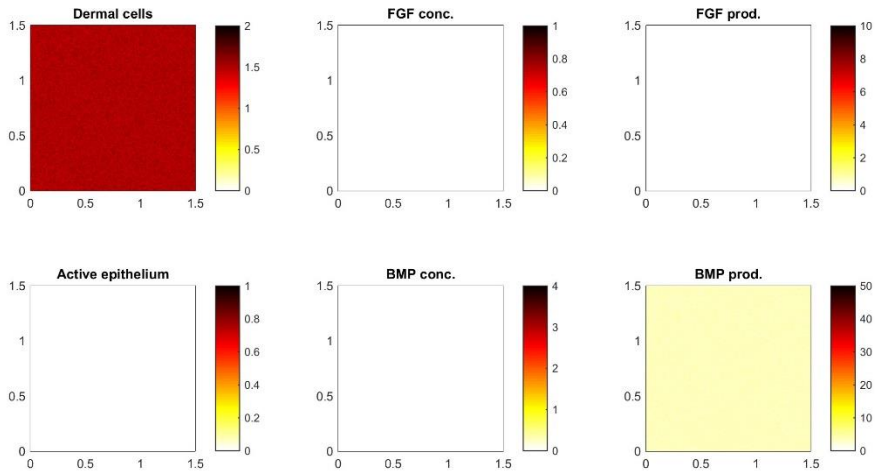

"Time 1"

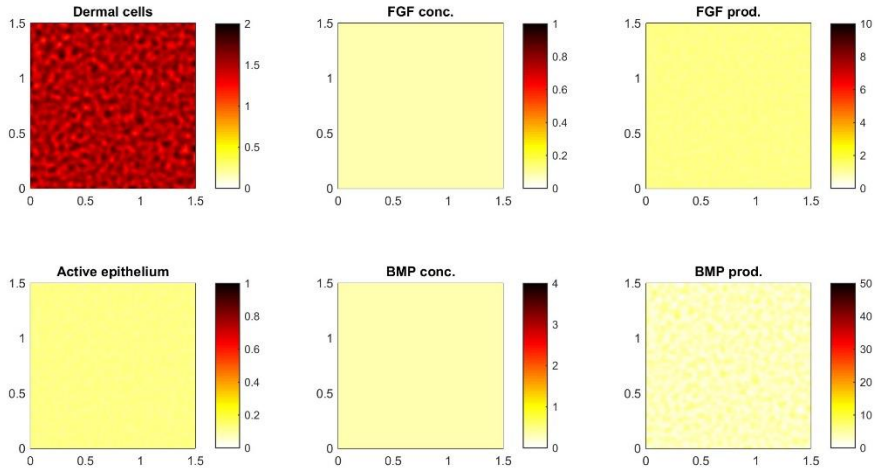

“Time 2”

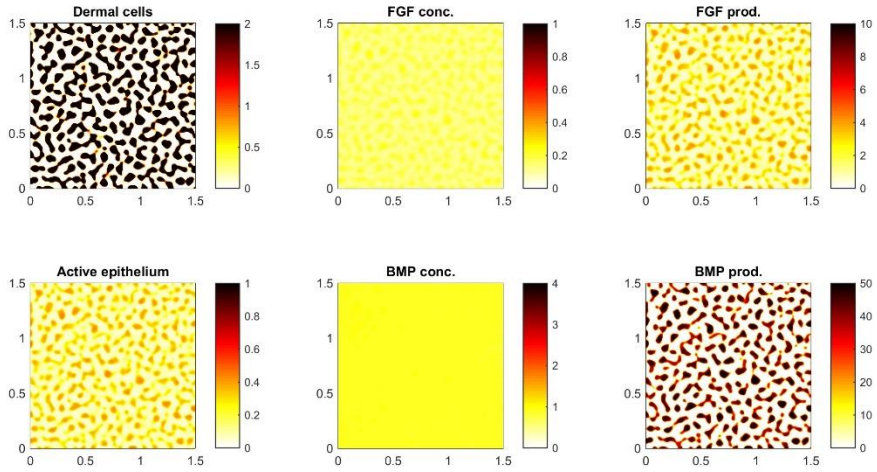
Dermal cells
FGF conc.
FGF prod.
Active epithelium
BMP conc.
BMP prod.

“Time 3”

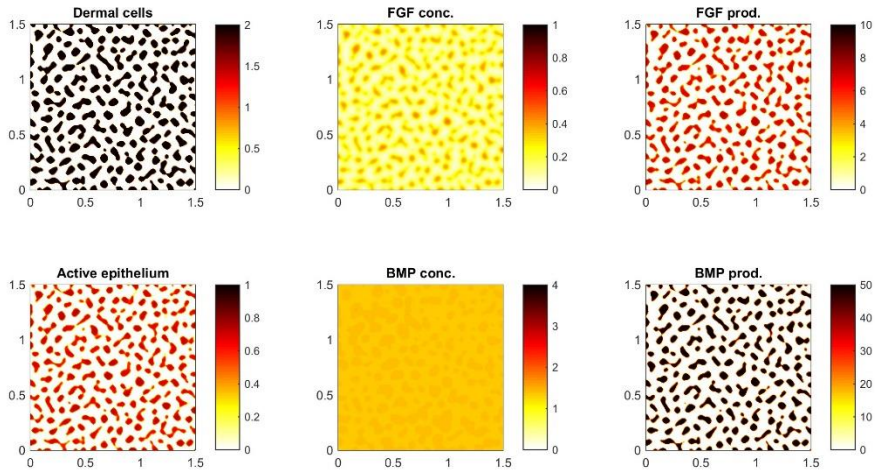
Dermal cells
FGF conc.
FGF prod.
Active epithelium
BMP conc.
BMP prod.

”Time 4”

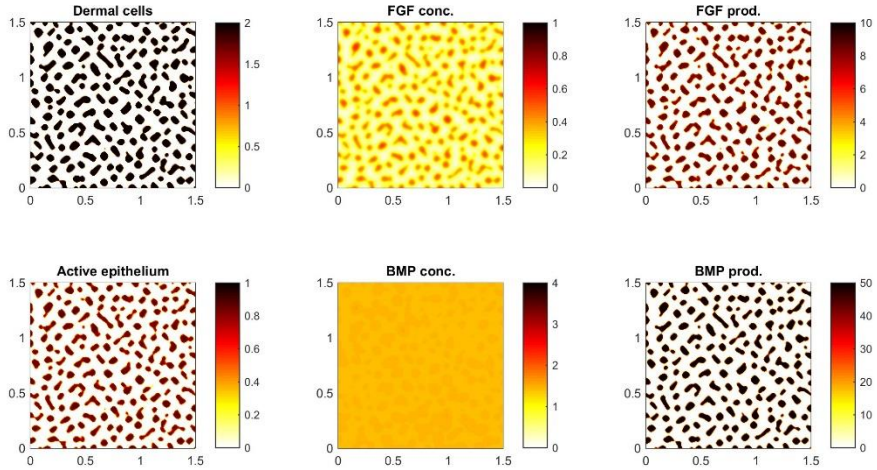

Figure 81. *In silico* periodic pattern formation via a fully activated epithelium. The travelling wave of activation is replaced with a fully activated epithelium in this simulation. All other rules and parameters remain unchanged. When the epithelium is fully activated across the patterning field, the resulting final pattern is drastically altered, hexagonality of the pattern is lost. Dermal cell aggregates initially form stripes but eventually separate, forming dermal cell condensates of various shapes and sizes, arranged in a low fidelity pattern.

BIBLOGRAPHY

Abbott UK, Asmundson VS (1957). Scaleless, an Inherited Ectodermal Defect in the Domestic Fowl *Journal of Heredity* 48(2)*:*63-70.

Abbott UK (1965). Selection for Feather Number in Scaleless Chickens. *Poultry science* 5(44)*:*1347-1429.

Aberle H, Bauer A, Stappert J, Kispert A, Kemler R (1997). beta-catenin is a target for the ubiquitin-proteasome pathway. *The EMBO journal* 16(13)*:*3797-3804.

Ahtiainen L, Lefebvre S, Lindfors PH, Renvoise E, Shirokova V, Vartiainen MK *et al.* (2014). Directional cell migration, but not proliferation, drives hair placode morphogenesis. *Developmental cell* 28(5)*:*588-602.

Andl T, Ahn K, Kairo A, Chu EY, Wine-Lee L, Reddy ST *et al.* (2004). Epithelial Bmpr1a regulates differentiation and proliferation in postnatal hair follicles and is essential for tooth development. *Development (Cambridge, England)* 131(10)*:*2257-2268.

Asai R, Taguchi E, Kume Y, Saito M, Kondo S (1999). Zebrafish leopard gene as a component of the putative reaction-diffusion system. *Mechanisms of development* 89(1-2)*:*87-92.

Atit R, Conlon RA, Niswander L (2003). EGF signaling patterns the feather array by promoting the interbud fate. *Developmental cell* 4(2)*:*231-240.

Atukorala AD, Inohaya K, Baba O, Tabata MJ, Ratnayake RA, Abduweli D *et al.* (2010). Scale and tooth phenotypes in medaka with a mutated ectodysplasin-A receptor: implications for the evolutionary origin of oral and pharyngeal teeth. *Archives of histology and cytology* 73(3)*:*139-148.

Baden HP, Maderson PF (1970). Morphological and biophysical identification of fibrous proteins in the amniote epidermis. *The Journal of experimental zoology* 174(2)*:*225-232.

Baden HP, Lee LD (1978). Fibrous protein of human epidermis. *The Journal of investigative dermatology* 71(2)*:*148-151.

Bafico A, Liu G, Yaniv A, Gazit A, Aaronson SA (2001). Novel mechanism of Wnt signalling inhibition mediated by Dickkopf-1 interaction with LRP6/Arrow. *Nature cell biology* 3(7)*:*683-686.

Baker AJ, Haddrath O, McPherson JD, Cloutier A (2014). Genomic support for a moa-tinamou clade and adaptive morphological convergence in flightless ratites. *Molecular biology and evolution* 31(7)*:*1686-1696.

Barak H, Huh SH, Chen S, Jeanpierre C, Martinovic J, Parisot M *et al.* (2012). FGF9 and FGF20 maintain the stemness of nephron progenitors in mice and man. *Developmental cell* 22(6)*:*1191-1207.

Bard J, Lauder I (1974). How well does Turing's theory of morphogenesis work? *Journal of Theoretical Biology* 45(2)*:*501-531.

Bard JBL (1990). Traction and the formation of mesenchymal condensations in vivo. *BioEssays* 12(8)*:*389-395.

Barraud P, Seferiadis AA, Tyson LD, Zwart MF, Szabo-Rogers HL, Ruhrberg C *et al.* (2010). Neural crest origin of olfactory ensheathing glia. *Proceedings of the National Academy of Sciences of the United States of America* 107(49)*:*21040-21045.

Bayes M, Hartung AJ, Ezer S, Pispa J, Thesleff I, Srivastava AK *et al.* (1998). The anhidrotic ectodermal dysplasia gene (EDA) undergoes alternative splicing and encodes ectodysplasin-A with deletion mutations in collagenous repeats. *Human molecular genetics* 7(11)*:*1661-1669.

Bell E, Thathachari YT (1963). Development of feather keratin during embryogenesis of the chick. *The Journal of cell biology* 16(215-223.

Bellot F, Crumley G, Kaplow JM, Schlessinger J, Jaye M, Dionne CA (1991). Ligand-induced transphosphorylation between different FGF receptors. *The EMBO journal* 10(10)*:*2849-2854.

Bereiter-Hahn J, Matoltsy AG, Richards KS (1984). Biology of the integument: Springer-Verlag.

Biggs LC, Mikkola ML (2014). Early inductive events in ectodermal appendage morphogenesis. *Seminars in Cell & Developmental Biology* 25–26(11-21.

Boch J, Scholze H, Schornack S, Landgraf A, Hahn S, Kay S *et al.* (2009). Breaking the code of DNA binding specificity of TAL-type III effectors. *Science (New York, NY)* 326(5959)*:*1509-1512.

Boneko VM, Merker HJ (1988). Development and Morphology of the Periderm of Mouse Embryos (Days 9-12 of Gestation). *Acta Anat* 133(4)*:*325-336.

Botchkarev VA, Botchkareva NV, Sharov AA, Funa K, Huber O, Gilchrest BA (2002). Modulation of BMP Signaling by Noggin is Required for Induction of the Secondary (Nontylotrich) Hair Follicles. 118(1)*:*3-10.

Botchkarev VA (2003). Bone Morphogenetic Proteins and Their Antagonists in Skin and Hair Follicle Biology[ast]. *J Investig Dermatol* 120(1)*:*36-47.

Brackenbury R, Rutishauser U, Edelman GM (1981). Distinct calcium-independent and calcium-dependent adhesion systems of chicken embryo cells. *Proceedings of the National Academy of Sciences of the United States of America* 78(1)*:*387-391.

Brusatte Stephen L, Lloyd Graeme T, Wang Steve C, Norell Mark A (2014). Gradual Assembly of Avian Body Plan Culminated in Rapid Rates of Evolution across the Dinosaur-Bird Transition. *Current Biology* 24(20)*:*2386-2392.

Brush AH (2000). Evolving a Protofeather and Feather Diversity. *American Zoologist* 40(4)*:*631-639.

Buchtova M, Chaloupkova R, Zakrzewska M, Vesela I, Cela P, Barathova J *et al.* (2015). Instability restricts signaling of multiple fibroblast growth factors. *Cellular and molecular life sciences : CMLS* 72(12)*:*2445-2459.

Bunow B, Kernevez J-P, Joly G, Thomas D (1980). Pattern formation by reaction-diffusion instabilities: Application to morphogenesis in Drosophila. *Journal of Theoretical Biology* 84(4)*:*629-649.

Cadi R, Dhouailly D, Sengel P (1983). Use of retinoic acid for the analysis of dermal-epidermal interactions in the tarsometatarsal skin of the chick embryo. *Developmental biology* 100(2)*:*489-495.

Capecchi MR (2005). Gene targeting in mice: functional analysis of the mammalian genome for the twenty-first century. *Nature reviews Genetics* 6(6)*:*507-512.

Casal ML, Scheidt JL, Rhodes JL, Henthorn PS, Werner P (2005). Mutation identification in a canine model of X-linked ectodermal dysplasia. *Mammalian genome : official journal of the International Mammalian Genome Society* 16(7)*:*524-531.

Casas L, Szűcs R, Vij S, Goh CH, Kathiresan P, Németh S *et al.* (2013). Disappearing Scales in Carps: Re-Visiting Kirpichnikov's Model on the Genetics of Scale Pattern Formation. *PloS one* 8(12)*:*e83327.

Chamorro MN, Schwartz DR, Vonica A, Brivanlou AH, Cho KR, Varmus HE (2005). FGF-20 and DKK1 are transcriptional targets of beta-catenin and FGF-20 is implicated in cancer and development. *The EMBO journal* 24(1)*:*73-84.

Chang C-H, Jiang T-X, Lin C-M, Burrus LW, Chuong C-M, Widelitz R (2004a). Distinct Wnt members regulate the hierarchical morphogenesis of skin regions (spinal tract) and individual feathers. *Mechanisms of development* 121(2)*:*157-171.

Chang CH, Jiang TX, Lin CM, Burrus LW, Chuong CM, Widelitz R (2004b). Distinct Wnt members regulate the hierarchical morphogenesis of skin regions (spinal tract) and individual feathers. *Mechanisms of development* 121(2)*:*157-171.

Charles C, Pantalacci S, Tafforeau P, Headon D, Laudet V, Viriot L (2009). Distinct impacts of Eda and Edar loss of function on the mouse dentition. *PloS one* 4(4)*:*e4985.

Chen CF, Foley J, Tang PC, Li A, Jiang TX, Wu P *et al.* (2015). Development, regeneration, and evolution of feathers. *Annual review of animal biosciences* 3(169-195.

Chen CW, Jung HS, Jiang TX, Chuong CM (1997). Asymmetric expression of Notch/Delta/Serrate is associated with the anterior-posterior axis of feather buds. *Developmental biology* 188(1)*:*181-187.

Chen J, Chuong CM (2012). Patterning skin by planar cell polarity: the multi-talented hair designer. *Exp Dermatol* 21(2)*:*81-85.

Chen Y, Schier AF (2002). Lefty proteins are long-range inhibitors of Squint-mediated Nodal signaling. *Current Biology* 12(24)*:*2124-2128.

Chodankar R, Chang CH, Yue Z, Jiang TX, Suksaweang S, Burrus L *et al.* (2003). Shift of localized growth zones contributes to skin appendage morphogenesis: role of the Wnt/beta-catenin pathway. *The Journal of investigative dermatology* 120(1)*:*20-26.

Choi HJ, Huber AH, Weis WI (2006). Thermodynamics of beta-catenin-ligand interactions: the roles of the N- and C-terminal tails in modulating binding affinity. *The Journal of biological chemistry* 281(2)*:*1027-1038.

Chuong CM, Edelman GM (1985). Expression of cell-adhesion molecules in embryonic induction. I. Morphogenesis of nestling feathers. *The Journal of cell biology* 101(3)*:*1009-1026.

Chuong CM, Widelitz RB, Ting-Berreth S, Jiang TX (1996). Early events during avian skin appendage regeneration: dependence on epithelial-mesenchymal interaction and order of molecular reappearance. *The Journal of investigative dermatology* 107(4)*:*639-646.

Chuong CM, Chodankar R, Widelitz RB, Jiang TX (2000). Evo-devo of feathers and scales: building complex epithelial appendages. *Current opinion in genetics & development* 10(4)*:*449-456.

Clench MH (1970). Variability in body pterylosis, with special reference to genus *Passer*. *The Auk* 87)*:*650-691.

Connor MJ (1988). Oxidation of retinol to retinoic acid as a requirement for biological activity in mouse epidermis. *Cancer research* 48(24 Pt 1)*:*7038-7040.

Coue M, Brenner SL, Spector I, Korn ED (1987). Inhibition of actin polymerization by latrunculin A. *FEBS letters* 213(2)*:*316-318.

Couly G, Le Douarin NM (1988). The fate map of the cephalic neural primordium at the presomitic to the 3-somite stage in the avian embryo. *Development (Cambridge, England)* 103 Suppl(101-113.

Crowe R, Henrique D, Ish-Horowicz D, Niswander L (1998). A new role for Notch and Delta in cell fate decisions: patterning the feather array. *Development (Cambridge, England)* 125(4)*:*767-775.

Crowe R, Niswander L (1998). Disruption of scale development by Delta-1 misexpression. *Developmental biology* 195(1)*:*70-74.

Cruywagen GC, Maini PK, Murray JD (1992). Sequential pattern formation in a model for skin morphogenesis. *IMA journal of mathematics applied in medicine and biology* 9(4)*:*227-248.

Cuny GD, Yu PB, Laha JK, Xing X, Liu JF, Lai CS *et al.* (2008). Structure-activity relationship study of bone morphogenetic protein (BMP) signaling inhibitors. *Bioorganic & medicinal chemistry letters* 18(15)*:*4388-4392.

Davidson D (1983). The mechanism of feather pattern development in the chick. 1. The time of determination of feather position. *Journal of embryology and experimental morphology* 74(245-259.

Delfini MC, Dubrulle J, Malapert P, Chal J, Pourquie O (2005). Control of the segmentation process by graded MAPK/ERK activation in the chick embryo. *Proceedings of the National Academy of Sciences of the United States of America* 102(32)*:*11343-11348.

Delfini MC, De La Celle M, Gros J, Serralbo O, Marics I, Seux M *et al.* (2009). The timing of emergence of muscle progenitors is controlled by an FGF/ERK/SNAIL1 pathway. *Developmental biology* 333(2)*:*229-237.

Dhouailly D (1973). Dermo-epidermal interactions between birds and mammals: differentiation of cutaneous appendages. *Journal of embryology and experimental morphology* 30(3)*:*587-603.

Dhouailly D (1975). Formation of cutaneous appendages in dermo-epidermal recombinations between reptiles, birds and mammals. *Wilhelm Roux' Archiv* 177(4)*:*323-340.

Dhouailly D (1977). Dermo-epidermal interactions during morphogenesis of cutaneous appendages in amniotes. *Front Matrix Biol* 4(86-121.

Dhouailly D (1978). Feather-forming capacities of the avian extra-embryonic somatopleure. *Journal of embryology and experimental morphology* 43(1)*:*279-287.

Dhouailly D, Hardy MH (1978). Retinoic acid causes the development of feathers in the scale-forming integument of the chick embryo. *Wilhelm Roux' Archiv* 185(2)*:*195-200.

Dhouailly D, Rogers GE, Sengel P (1978). The specification of feather and scale protein synthesis in epidermal-dermal recombinations. *Developmental biology* 65(1)*:*58-68.

Dhouailly D (1984). Specification of feather and scale patterns. *Pattern Formation New York: Macmillan:*581-601.

Dhouailly D, Prin F, Kanzler B, Viallet JP (1998). Variations of cutaneous appendages: regional specification and cross-species signals. *Molecular basis of epithelial appendage morphogenesis* 1(45-56.

Dhouailly D, Olivera-Martinez I, Fliniaux I, Missier S, Viallet JP, Thelu J (2004). Skin field formation: morphogenetic events. *The International journal of developmental biology* 48(2-3)*:*85-91.

Dhouailly D (2009). A new scenario for the evolutionary origin of hair, feather, and avian scales. *Journal of anatomy* 214(4)*:*587-606.

Doffinger R, Smahi A, Bessia C, Geissmann F, Feinberg J, Durandy A *et al.* (2001). X-linked anhidrotic ectodermal dysplasia with immunodeficiency is caused by impaired NF-kappaB signaling. *Nature genetics* 27(3)*:*277-285.

Drew CF (2006). Role of the Edar subfamily in feather placode inititation and patterning. In: DD Headon and S University of Manchester. School of Life editors. Manchester: Manchester : University of Manchester.

Drew CF, Lin CM, Jiang TX, Blunt G, Mou C, Chuong CM *et al.* (2007). The Edar subfamily in feather placode formation. *Developmental biology* 305(1)*:*232-245.

Driever W, Nusslein-Volhard C (1988). A gradient of bicoid protein in Drosophila embryos. *Cell* 54(1)*:*83-93.

Driever W, Siegel V, Nusslein-Volhard C (1990). Autonomous determination of anterior structures in the early Drosophila embryo by the bicoid morphogen. *Development (Cambridge, England)* 109(4)*:*811-820.

Drogemuller C, Distl O, Leeb T (2001). Partial deletion of the bovine ED1 gene causes anhidrotic ectodermal dysplasia in cattle. *Genome research* 11(10)*:*1699-1705.

Dudley AT, Lyons KM, Robertson EJ (1995). A requirement for bone morphogenetic protein-7 during development of the mammalian kidney and eye. *Genes & development* 9(22)*:*2795-2807.

Dwyer NK (1971). Chick scale morphogenesis: Early events in the formation of overall shank pattern and individual scale shape.

Ede DA (1972). Cell behaviour and embryonic development. *The International journal of neuroscience* 3(4)*:*165-174.

Elias PM, Menon GK (1991). Structural and lipid biochemical correlates of the epidermal permeability barrier. *Advances in lipid research* 24(1-26.

Fainsod A, Deissler K, Yelin R, Marom K, Epstein M, Pillemer G *et al.* (1997). The dorsalizing and neural inducing gene follistatin is an antagonist of BMP-4. *Mechanisms of development* 63(1)*:*39-50.

Fannon M, Forsten KE, Nugent MA (2000). Potentiation and Inhibition of bFGF Binding by Heparin: A Model for Regulation of Cellular Response†. *Biochemistry* 39(6)*:*1434-1445.

Fisher CE, Michael L, Barnett MW, Davies JA (2001). Erk MAP kinase regulates branching morphogenesis in the developing mouse kidney. *Development (Cambridge, England)* 128(21)*:*4329-4338.

Fliniaux I, Viallet JP, Dhouailly D (2004a). Signaling dynamics of feather tract formation from the chick somatopleure. *Development (Cambridge, England)* 131(16)*:*3955-3966.

Fliniaux I, Viallet JP, Dhouailly D (2004b). Ventral vs. dorsal chick dermal progenitor specification. *The International journal of developmental biology* 48(2-3)*:*103-106.

Freinkel RK (1972). Lipogenesis in epidermal differentiation of embryonic chicken skin. *The Journal of investigative dermatology* 59(4)*:*332-338.

Fuchs E, Green H (1980). Changes in keratin gene expression during terminal differentiation of the keratinocyte. *Cell* 19(4)*:*1033-1042.

Fuchs E, Marchuk D (1983). Type I and type II keratins have evolved from lower eukaryotes to form the epidermal intermediate filaments in mammalian skin. *Proceedings of the National Academy of Sciences of the United States of America* 80(19)*:*5857-5861.

Fuchs E (2007). Scratching the surface of skin development. *Nature* 445(7130)*:*834-842.

Gaide O, Schneider P (2003). Permanent correction of an inherited ectodermal dysplasia with recombinant EDA. *Nature medicine* 9(5)*:*614-618.

Gaur U, Aggarwal BB (2003). Regulation of proliferation, survival and apoptosis by members of the TNF superfamily. *Biochemical pharmacology* 66(8)*:*1403-1408.

Gierer A, Meinhardt H (1972). A theory of biological pattern formation. *Kybernetik* 12(1)*:*30-39.

Glazier JA, Zhang Y, Swat M, Zaitlen B, Schnell S (2008). Coordinated Action of N-CAM, N-cadherin, EphA4, and ephrinB2 Translates Genetic Prepatterns into Structure during Somitogenesis in Chick. Current topics in developmental biology, pp. 205-247.

Gordon MD, Nusse R (2006). Wnt signaling: multiple pathways, multiple receptors, and multiple transcription factors. *The Journal of biological chemistry* 281(32)*:*22429-22433.

Greenwold MJ, Sawyer RH (2010). Genomic organization and molecular phylogenies of the beta (beta) keratin multigene family in the chicken (Gallus gallus) and zebra finch (Taeniopygia guttata): implications for feather evolution. *BMC evolutionary biology* 10(148.

Greenwold MJ, Sawyer RH (2011). Linking the molecular evolution of avian beta (beta) keratins to the evolution of feathers. *Journal of experimental zoology Part B, Molecular and developmental evolution* 316(8)*:*609-616.

Greenwold MJ, Sawyer RH (2013). Molecular evolution and expression of archosaurian beta-keratins: diversification and expansion of archosaurian beta-keratins and the origin of feather beta-keratins. *Journal of experimental zoology Part B, Molecular and developmental evolution* 320(6)*:*393-405.

Greenwold MJ, Bao W, Jarvis ED, Hu H, Li C, Gilbert MT *et al.* (2014). Dynamic evolution of the alpha (alpha) and beta (beta) keratins has accompanied integument diversification and the adaptation of birds into novel lifestyles. *BMC evolutionary biology* 14(249.

Gurdon JB (1988). A community effect in animal development. *Nature* 336(6201)*:*772-774.

Haake AR, König G, Sawyer RH (1984). Avian feather development: Relationships between morphogenesis and keratinization. *Developmental biology* 106(2)*:*406-413.

Haara O, Harjunmaa E, Lindfors PH, Huh SH, Fliniaux I, Aberg T *et al.* (2012). Ectodysplasin regulates activator-inhibitor balance in murine tooth development through Fgf20 signaling. *Development (Cambridge, England)* 139(17)*:*3189-3199.

Hamburger V, Hamilton HL (1952). A series of normal stages in the development of the chick embryo. *Developmental Dynamics* 195(4)*:*231-272.

Hamilton HL (1952). Lillie's Development of the Chick.

Han G, Chiappe LM, Ji S-A, Habib M, Turner AH, Chinsamy A *et al.* (2014). A new raptorial dinosaur with exceptionally long feathering provides insights into dromaeosaurid flight performance. *Nature communications* 5(

Harris MP, Fallon JF, Prum RO (2002). Shh-Bmp2 signaling module and the evolutionary origin and diversification of feathers. *The Journal of experimental zoology* 294(2)*:*160-176.

Harris MP, Linkhart BL, Fallon JF (2004). Bmp7 mediates early signaling events during induction of chick epidermal organs. *Developmental Dynamics* 231(1)*:*22-32.

Harris MP, Rohner N, Schwarz H, Perathoner S, Konstantinidis P, Nusslein-Volhard C (2008). Zebrafish eda and edar mutants reveal conserved and ancestral roles of ectodysplasin signaling in vertebrates. *PLoS genetics* 4(10)*:*e1000206.

Hart KC, Robertson SC, Kanemitsu MY, Meyer AN, Tynan JA, Donoghue DJ (2000). Transformation and Stat activation by derivatives of FGFR1, FGFR3, and FGFR4. *Oncogene* 19(29)*:*3309-3320.

Hartsough MT, Mulder KM (1995). Transforming growth factor beta activation of p44mapk in proliferating cultures of epithelial cells. *The Journal of biological chemistry* 270(13)*:*7117-7124.

Hatzfeld M, Franke WW (1985). Pair formation and promiscuity of cytokeratins: formation in vitro of heterotypic complexes and intermediate-sized filaments by homologous and heterologous recombinations of purified polypeptides. *The Journal of cell biology* 101(5 Pt 1)*:*1826-1841.

Headon DJ, Overbeek PA (1999). Involvement of a novel Tnf receptor homologue in hair follicle induction. *Nature genetics* 22(4)*:*370-374.

Headon DJ, Emmal SA, Ferguson BM, Tucker AS, Justice MJ, Sharpe PT *et al.* (2001). Gene defect in ectodermal dysplasia implicates a death domain adapter in development. *Nature* 414(6866)*:*913-916.

Hemmati-Brivanlou A, Kelly OG, Melton DA (1994). Follistatin, an antagonist of activin, is expressed in the Spemann organizer and displays direct neuralizing activity. *Cell* 77(2)*:*283-295.

Higgins CA, Chen JC, Cerise JE, Jahoda CA, Christiano AM (2013). Microenvironmental reprogramming by three-dimensional culture enables dermal papilla cells to induce de novo human hair-follicle growth. *Proceedings of the National Academy of Sciences of the United States of America* 110(49)*:*19679-19688.

Hocevar BA, Brown TL, Howe PH (1999). TGF-beta induces fibronectin synthesis through a c-Jun N-terminal kinase-dependent, Smad4-independent pathway. *The EMBO journal* 18(5)*:*1345-1356.

Homberger DG, de Silva KN (2000). Functional Microanatomy of the Feather-Bearing Integument: Implications for the Evolution of Birds and Avian Flight. *American Zoologist* 40(4)*:*553-574.

Hornik C, Krishan K, Yusuf F, Scaal M, Brand-Saberi B (2005). cDermo-1 misexpression induces dense dermis, feathers, and scales. *Developmental biology* 277(1)*:*42-50.

Houghton L, Lindon C, Morgan BA (2005). The ectodysplasin pathway in feather tract development. *Development (Cambridge, England)* 132(5)*:*863-872.

Hu D, Hou L, Zhang L, Xu X (2009a). A pre-Archaeopteryx troodontid theropod from China with long feathers on the metatarsus. *Nature* 461(7264)*:*640-643.

Hu D, Hou L, Zhang L, Xu X (2009b). A pre-Archaeopteryx troodontid theropod from China with long feathers on the metatarsus. *Nature* 461(7264)*:*640-643.

Huelsken J, Vogel R, Erdmann B, Cotsarelis G, Birchmeier W (2001). beta-Catenin controls hair follicle morphogenesis and stem cell differentiation in the skin. *Cell* 105(4)*:*533-545.

Hughes CS, Postovit LM, Lajoie GA (2010). Matrigel: A complex protein mixture required for optimal growth of cell culture. *PROTEOMICS* 10(9)*:*1886-1890.

Hughes MW, Wu P, Jiang TX, Lin SJ, Dong CY, Li A *et al.* (2011). In search of the Golden Fleece: unraveling principles of morphogenesis by studying the integrative biology of skin appendages. *Integrative biology : quantitative biosciences from nano to macro* 3(4)*:*388-407.

Huh SH, Narhi K, Lindfors PH, Haara O, Yang L, Ornitz DM *et al.* (2013). Fgf20 governs formation of primary and secondary dermal condensations in developing hair follicles. *Genes & development* 27(4)*:*450-458.

Huttenlocher A, Sandborg RR, Horwitz AF (1995). Adhesion in cell migration. *Current opinion in cell biology* 7(5)*:*697-706.

Israel A (2000). The IKK complex: an integrator of all signals that activate NF-kappaB? *Trends in cell biology* 10(4)*:*129-133.

Israel DI, Nove J, Kerns KM, Kaufman RJ, Rosen V, Cox KA *et al.* (1996). Heterodimeric bone morphogenetic proteins show enhanced activity in vitro and in vivo. *Growth factors (Chur, Switzerland)* 13(3-4)*:*291-300.

Itoh N, Ornitz DM (2004). Evolution of the Fgf and Fgfr gene families. *Trends in genetics : TIG* 20(11)*:*563-569.

Itoh N (2010). Hormone-like (endocrine) Fgfs: their evolutionary history and roles in development, metabolism, and disease. *Cell and tissue research* 342(1)*:*1-11.

Jiang TX, Chuong CM (1992). Mechanism of skin morphogenesis. I. Analyses with antibodies to adhesion molecules tenascin, N-CAM, and integrin. *Developmental biology* 150(1)*:*82-98.

Jiang TX, Jung HS, Widelitz RB, Chuong CM (1999). Self-organization of periodic patterns by dissociated feather mesenchymal cells and the regulation of size, number and spacing of primordia. *Development (Cambridge, England)* 126(22)*:*4997-5009.

Jiang TX, Widelitz RB, Shen WM, Will P, Wu DY, Lin CM *et al.* (2004). Integument pattern formation involves genetic and epigenetic controls: feather arrays simulated by digital hormone models. *The International journal of developmental biology* 48(2-3)*:*117-135.

Jinek M, Chylinski K, Fonfara I, Hauer M, Doudna JA, Charpentier E (2012). A Programmable Dual-RNA–Guided DNA Endonuclease in Adaptive Bacterial Immunity. *Science (New York, NY)* 337(6096)*:*816-821.

Johansson JA, Headon DJ (2014). Regionalisation of the skin. *Seminars in Cell & Developmental Biology* 25–26(3-10.

Johnson DE, Williams LT (1993). Structural and functional diversity in the FGF receptor multigene family. *Advances in cancer research* 60(1-41.

Jung H, Chuong C (1998). Periodic pattern formation of the feathers. *Molecular basis of epithelial appendage morphogenesis(CM Chuong, ed) RG Landes, Georgetown, Tx:*359-369.

Jung HS, Francis-West PH, Widelitz RB, Jiang TX, Ting-Berreth S, Tickle C *et al.* (1998). Local inhibitory action of BMPs and their relationships with activators in feather formation: implications for periodic patterning. *Developmental biology* 196(1)*:*11-23.

Kalinina J, Byron SA, Makarenkova HP, Olsen SK, Eliseenkova AV, Larochelle WJ *et al.* (2009). Homodimerization controls the fibroblast growth factor 9 subfamily's receptor binding and heparan sulfate-dependent diffusion in the extracellular matrix. *Molecular and cellular biology* 29(17)*:*4663-4678.

Kere J, Srivastava AK, Montonen O, Zonana J, Thomas N, Ferguson B *et al.* (1996). X-linked anhidrotic (hypohidrotic) ectodermal dysplasia is caused by mutation in a novel transmembrane protein. *Nature genetics* 13(4)*:*409-416.

Kleinman HK, Martin GR (2005). Matrigel: Basement membrane matrix with biological activity. *Seminars in Cancer Biology* 15(5)*:*378-386.

Kohn AD, Moon RT (2005). Wnt and calcium signaling: β-Catenin-independent pathways. *Cell Calcium* 38(3–4)*:*439-446.

Komiya Y, Habas R (2008). Wnt signal transduction pathways. *Organogenesis* 4(2)*:*68-75.

Kondo S, Asal R (1995). A reaction-diffusion wave on the skin of the marine angelfish Pomacanthus. *Nature* 376(6543)*:*765-768.

Kondo S, Kuwahara Y, Kondo M, Naruse K, Mitani H, Wakamatsu Y *et al.* (2001). The medaka rs-3 locus required for scale development encodes ectodysplasin-A receptor. *Current biology : CB* 11(15)*:*1202-1206.

Kouhara H, Hadari YR, Spivak-Kroizman T, Schilling J, Bar-Sagi D, Lax I *et al.* (1997). A lipid-anchored Grb2-binding protein that links FGF-receptor activation to the Ras/MAPK signaling pathway. *Cell* 89(5)*:*693-702.

Kowalczyk-Quintas C, Willen L, Dang AT, Sarrasin H, Tardivel A, Hermes K *et al.* (2014). Generation and characterization of function-blocking anti-ectodysplasin A (EDA) monoclonal antibodies that induce ectodermal dysplasia. *The Journal of biological chemistry* 289(7)*:*4273-4285.

Kuhl M, Sheldahl LC, Park M, Miller JR, Moon RT (2000). The Wnt/Ca2+ pathway A new vertebrate Wnt signaling pathway takes shape. *Trends in Genetics* 16(7)*:*279-283.

Kumar A, Eby MT, Sinha S, Jasmin A, Chaudhary PM (2001). The ectodermal dysplasia receptor activates the nuclear factor-kappaB, JNK, and cell death pathways and binds to ectodysplasin A. *The Journal of biological chemistry* 276(4)*:*2668-2677.

Kuramoto T, Yokoe M, Hashimoto R, Hiai H, Serikawa T (2011). A rat model of hypohidrotic ectodermal dysplasia carries a missense mutation in the Edaradd gene. *BMC genetics* 12(91.

Laurikkala J, Pispa J, Jung HS, Nieminen P, Mikkola M, Wang X *et al.* (2002). Regulation of hair follicle development by the TNF signal ectodysplasin and its receptor Edar. *Development (Cambridge, England)* 129(10)*:*2541-2553.

Lechler T, Fuchs E (2005). Asymmetric cell divisions promote stratification and differentiation of mammalian skin. *Nature* 437(7056)*:*275-280.

Li L, Cserjesi P, Olson EN (1995). Dermo-1: A Novel Twist-Related bHLH Protein Expressed in the Developing Dermis. *Developmental biology* 172(1)*:*280-292.

Li Q, Gao K-Q, Meng Q, Clarke JA, Shawkey MD, D'Alba L *et al.* (2012). Reconstruction of Microraptor and the Evolution of Iridescent Plumage. *Science (New York, NY)* 335(6073)*:*1215-1219.

Li YI, Kong L, Ponting CP, Haerty W (2013). Rapid evolution of Beta-keratin genes contribute to phenotypic differences that distinguish turtles and birds from other reptiles. *Genome biology and evolution* 5(5)*:*923-933.

Lin CM, Jiang TX, Widelitz RB, Chuong CM (2006). Molecular signaling in feather morphogenesis. *Current opinion in cell biology* 18(6)*:*730-741.

Lin CM, Jiang TX, Baker RE, Maini PK, Widelitz RB, Chuong CM (2009). Spots and stripes: pleomorphic patterning of stem cells via p-ERK-dependent cell chemotaxis shown by feather morphogenesis and mathematical simulation. *Developmental biology* 334(2)*:*369-382.

Linask KK, Ludwig C, Han MD, Liu X, Radice GL, Knudsen KA (1998). N-cadherin/catenin-mediated morphoregulation of somite formation. *Developmental biology* 202(1)*:*85-102.

Logan CY, Nusse R (2004). The Wnt signaling pathway in development and disease. *Annual review of cell and developmental biology* 20(781-810.

Lü J, Brusatte SL (2015). A large, short-armed, winged dromaeosaurid (Dinosauria: Theropoda) from the Early Cretaceous of China and its implications for feather evolution. *Sci Rep* 5(

Lucas AM, Stettenheim PR (1972). Avian anatomy: Integument Washington D.C: [U.S. Department of Agriculture in cooperation with Michigan Agricultural Experiment Station].

Luo G, Hofmann C, Bronckers AL, Sohocki M, Bradley A, Karsenty G (1995). BMP-7 is an inducer of nephrogenesis, and is also required for eye development and skeletal patterning. *Genes & development* 9(22)*:*2808-2820.

MacDonald BT, Tamai K, He X (2009). Wnt/β-Catenin Signaling: Components, Mechanisms, and Diseases. *Developmental cell* 17(1)*:*9-26.

Maderson PFA (1972). When? Why? And how? Some speculations on the evolution of the vertebrate integument. *American Zoologist* 12(159–171.

Maini PK, Baker RE, Chuong CM (2006). Developmental biology. The Turing model comes of molecular age. *Science (New York, NY)* 314(5804)*:*1397-1398.

Malbon CC, Wang HY, Moon RT (2001). Wnt signaling and heterotrimeric G-proteins: Strange bedfellows or a classic romance? *Biochemical and biophysical research communications* 287(3)*:*589-593.

Mandler M, Neubuser A (2004). FGF signaling is required for initiation of feather placode development. *Development (Cambridge, England)* 131(14)*:*3333-3343.

Massague J (2000). How cells read TGF-beta signals. *Nature reviews Molecular cell biology* 1(3)*:*169-178.

Massague J (2003). Integration of Smad and MAPK pathways: a link and a linker revisited. *Genes & development* 17(24)*:*2993-2997.

Matoltsy AG (1969). Keratinization of the avian epidermis: an ultrastructural study of the newborn chick skin. *Journal of ultrastructure research* 29(5)*:*438-458.

Matsubayashi Y, Ebisuya M, Honjoh S, Nishida E (2004). ERK activation propagates in epithelial cell sheets and regulates their migration during wound healing. *Current biology : CB* 14(8)*:*731-735.

Mauger A (1972a). [The role of somitic mesoderm in the development of dorsal plumage in chick embryos. II. Regionalization of the plumage-forming mesoderm]. *Journal of embryology and experimental morphology* 28(2)*:*343-366.

Mauger A (1972b). [The role of somitic mesoderm in the development of dorsal plumage in chick embryos. I. Origin, regulative capacity and determination of the plumage-forming mesoderm]. *Journal of embryology and experimental morphology* 28(2)*:*313-341.

Mayer JA, Chuong CM, Widelitz R (2004). Rooster feathering, androgenic alopecia, and hormone-dependent tumor growth: what is in common? *Differentiation; research in biological diversity* 72(9-10)*:*474-488.

Mayerson PL, Fallon JF (1985). The spatial pattern and temporal sequence in which feather germs arise in the white Leghorn chick embryo. *Developmental biology* 109(2)*:*259-267.

McCormick F (1993). How receptors turn Ras on. *Nature* 363(6424)*:*15-16.

McGrew MJ, Sherman A, Lillico SG, Ellard FM, Radcliffe PA, Gilhooley HJ *et al.* (2008). Localised axial progenitor cell populations in the avian tail bud are not committed to a posterior Hox identity. *Development (Cambridge, England)* 135(13)*:*2289-2299.

Mcloughlin C (1961). Importance of Mesenchymal Factors in Differentiation of Chick Epidermis .2. Modification of Epidermal Differentiation by Contact with Different Type of Mesenchyme. *Journal of embryology and experimental morphology* 9(3)*:*385-&.

Menon GK, Maderson PF, Drewes RC, Baptista LF, Price LF, Elias PM (1996). Ultrastructural organization of avian stratum corneum lipids as the basis for facultative cutaneous waterproofing. *Journal of morphology* 227(1)*:*1-13.

Menon GK, Menon J (2000). Avian Epidermal Lipids: Functional Considerations and Relationship to Feathering. *American Zoologist* 40(4)*:*540-552.

Merat P (1986). Potential usefulness of the Na (naked neck) gene in poultry production. *World's Poultry Science Journal* 42(02)*:*124-142.

Michon F, Charveron M, Dhouailly D (2007). Dermal condensation formation in the chick embryo: requirement for integrin engagement and subsequent stabilization by a possible notch/integrin interaction. *Developmental dynamics : an official publication of the American Association of Anatomists* 236(3)*:*755-768.

Michon F, Forest L, Collomb E, Demongeot J, Dhouailly D (2008). BMP2 and BMP7 play antagonistic roles in feather induction. *Development (Cambridge, England)* 135(16)*:*2797-2805.

Mikels AJ, Nusse R (2006). Purified Wnt5a protein activates or inhibits beta-catenin-TCF signaling depending on receptor context. *PLoS biology* 4(4)*:*e115.

Miki T, Bottaro DP, Fleming TP, Smith CL, Burgess WH, Chan AM *et al.* (1992). Determination of ligand-binding specificity by alternative splicing: two distinct growth factor receptors encoded by a single gene. *Proceedings of the National Academy of Sciences of the United States of America* 89(1)*:*246-250.

Mikkola ML, Pispa J, Pekkanen M, Paulin L, Nieminen P, Kere J *et al.* (1999). Ectodysplasin, a protein required for epithelial morphogenesis, is a novel TNF homologue and promotes cell-matrix adhesion. *Mechanisms of development* 88(2)*:*133-146.

Milinkovitch MC, Manukyan L, Debry A, Di-Poi N, Martin S, Singh D *et al.* (2013). Crocodile head scales are not developmental units but emerge from physical cracking. *Science (New York, NY)* 339(6115)*:*78-81.

Miller JC, Tan S, Qiao G, Barlow KA, Wang J, Xia DF *et al.* (2011). A TALE nuclease architecture for efficient genome editing. *Nature biotechnology* 29(2)*:*143-148.

Mitchell KJ, Llamas B, Soubrier J, Rawlence NJ, Worthy TH, Wood J *et al.* (2014). Ancient DNA reveals elephant birds and kiwi are sister taxa and clarifies ratite bird evolution. *Science (New York, NY)* 344(6186)*:*898-900.

Miura T, Shiota K (2000). TGFβ2 acts as an "Activator" molecule in reaction-diffusion model and is involved in cell sorting phenomenon in mouse limb micromass culture. *Developmental Dynamics* 217(3)*:*241-249.

Miura T (2007). Modulation of activator diffusion by extracellular matrix in Turing system (Workshops on "Pattern Formation Problems in Dissipative Systems" and "Mathematical Modeling and Analysis for Nonlinear Phenomena"). *RIMS Kokyuroku Bessatsu* 3(165-176.

Mohammadi M, Dionne CA, Li W, Li N, Spivak T, Honegger AM *et al.* (1992). Point mutation in FGF receptor eliminates phosphatidylinositol hydrolysis without affecting mitogenesis. *Nature* 358(6388)*:*681-684.

Morgan BA, Orkin RW, Noramly S, Perez A (1998). Stage-specific effects of sonic hedgehog expression in the epidermis. *Developmental biology* 201(1)*:*1-12.

Morlon A, Munnich A, Smahi A (2005). TAB2, TRAF6 and TAK1 are involved in NF-kappaB activation induced by the TNF-receptor, Edar and its adaptator Edaradd. *Human molecular genetics* 14(23)*:*3751-3757.

Morosan-Puopolo G, Balakrishnan-Renuka A, Yusuf F, Chen J, Dai F, Zoidl G *et al.* (2014). Wnt11 Is Required for Oriented Migration of Dermogenic Progenitor Cells from the Dorsomedial Lip of the Avian Dermomyotome. *PloS one* 9(3)*:*e92679.

Mou C, Jackson B, Schneider P, Overbeek PA, Headon DJ (2006). Generation of the primary hair follicle pattern. *Proceedings of the National Academy of Sciences of the United States of America* 103(24)*:*9075-9080.

Mou C, Pitel F, Gourichon D, Vignoles F, Tzika A, Tato P *et al.* (2011). Cryptic patterning of avian skin confers a developmental facility for loss of neck feathering. *PLoS biology* 9(3)*:*e1001028.

Muller P, Rogers KW, Jordan BM, Lee JS, Robson D, Ramanathan S *et al.* (2012). Differential diffusivity of Nodal and Lefty underlies a reaction-diffusion patterning system. *Science (New York, NY)* 336(6082)*:*721-724.

Murray JD, Oster GF, Harris AK (1983). A mechanical model for mesenchymal morphogenesis. *Journal of mathematical biology* 17(1)*:*125-129.

N'dri A, Mignon-Grasteau S, Sellier N, Beaumont C, Tixier-Boichard M (2007). Interactions between the naked neck gene, sex, and fluctuating ambient temperature on heat tolerance, growth, body composition, meat quality, and sensory analysis of slow growing meat-type broilers. *Livestock Science* 110(1)*:*33-45.

Nagorcka BN (1986). The reaction-diffusion system--a spatial organizer in the vertebrate epidermis. *Progress in clinical and biological research* 217A(319-323.

Nakamura T, Mine N, Nakaguchi E, Mochizuki A, Yamamoto M, Yashiro K *et al.* (2006). Generation of robust left-right asymmetry in the mouse embryo requires a self-enhancement and lateral-inhibition system. *Developmental cell* 11(4)*:*495-504.

Nelson WJ, Nusse R (2004). Convergence of Wnt, beta-catenin, and cadherin pathways. *Science (New York, NY)* 303(5663)*:*1483-1487.

Nemes Z, Steinert PM (1999). Bricks and mortar of the epidermal barrier. *Exp Mol Med* 31(5-19.

Nishijima K-i, Iijima S (2013). Transgenic chickens. *Development, Growth & Differentiation* 55(1)*:*207-216.

Nishita M, Itsukushima S, Nomachi A, Endo M, Wang Z, Inaba D *et al.* (2010). Ror2/Frizzled complex mediates Wnt5a-induced AP-1 activation by regulating Dishevelled polymerization. *Molecular and cellular biology* 30(14)*:*3610-3619.

Nitzsch CL (1867). Nitzsch's Pterylography / translated from the German ; edited by Philip Lutley Sclater London: Published for the Ray Society by R. Hardwicke.

Nohno T, Kawakami Y, Ohuchi H, Fujiwara A, Yoshioka H, Noji S (1995). Involvement of the Sonic Hedgehog Gene in Chick Feather Formation. *Biochemical and biophysical research communications* 206(1)*:*33-39.

Noji S, Koyama E, Myokai F, Nohno T, Ohuchi H, Nishikawa K *et al.* (1993). Differential expression of three chick FGF receptor genes, FGFR1, FGFR2 and

FGFR3, in limb and feather development. *Progress in clinical and biological research* 383B(645-654.

Nomachi A, Nishita M, Inaba D, Enomoto M, Hamasaki M, Minami Y (2008). Receptor tyrosine kinase Ror2 mediates Wnt5a-induced polarized cell migration by activating c-Jun N-terminal kinase via actin-binding protein filamin A. *The Journal of biological chemistry* 283(41)*:*27973-27981.

Noramly S, Morgan BA (1998). BMPs mediate lateral inhibition at successive stages in feather tract development. *Development (Cambridge, England)* 125(19)*:*3775-3787.

Noramly S, Freeman A, Morgan BA (1999). beta-catenin signaling can initiate feather bud development. *Development (Cambridge, England)* 126(16)*:*3509-3521.

Norell MA, Xu X (2005). Feathered Dinosaurs. *Annual Review of Earth and Planetary Sciences* 33(1)*:*277-299.

Novel G (1973a). Feather pattern stability and reorganization in cultured skin. *Journal of embryology and experimental morphology* 30(3)*:*605-633.

Novel G (1973b). Feather pattern stability and reorganization in cultured skin. *Journal of embryology and experimental morphology* 30(3)*:*605-633.

Nusse R, Varmus H (2012). Three decades of Wnts: a personal perspective on how a scientific field developed. *The EMBO journal* 31(12)*:*2670-2684.

O'Guin WM, Sawyer RH (1982). Avian scale development. VII. Relationships between morphogenetic and biosynthetic differentiation. *Developmental biology* 89(2)*:*485-492.

Oda K, Matsuoka Y, Funahashi A, Kitano H (2005). A comprehensive pathway map of epidermal growth factor receptor signaling. *Molecular Systems Biology* 1(2005.0010-2005.0010.

Olivera-Martinez I, Coltey M, Dhouailly D, Pourquie O (2000). Mediolateral somitic origin of ribs and dermis determined by quail-chick chimeras. *Development (Cambridge, England)* 127(21)*:*4611-4617.

Olivera-Martinez I, Missier S, Fraboulet S, Thelu J, Dhouailly D (2002). Differential regulation of the chick dorsal thoracic dermal progenitors from the medial dermomyotome. *Development (Cambridge, England)* 129(20)*:*4763-4772.

Ong SH, Guy GR, Hadari YR, Laks S, Gotoh N, Schlessinger J *et al.* (2000). FRS2 proteins recruit intracellular signaling pathways by binding to diverse targets on fibroblast growth factor and nerve growth factor receptors. *Molecular and cellular biology* 20(3)*:*979-989.

Ornitz DM, Leder P (1992). Ligand specificity and heparin dependence of fibroblast growth factor receptors 1 and 3. *Journal of Biological Chemistry* 267(23)*:*16305-16311.

Ornitz DM, Itoh N (2001). Fibroblast growth factors. *Genome biology* 2(3)*:*REVIEWS3005.

Ornitz DM, Itoh N (2015). The Fibroblast Growth Factor signaling pathway. *Wiley interdisciplinary reviews Developmental biology* 4(3)*:*215-266.

Oster GF, Murray JD, Harris AK (1983). Mechanical aspects of mesenchymal morphogenesis. *Journal of embryology and experimental morphology* 78(83-125.

Oulion S, Bertrand S, Escriva H (2012). Evolution of the FGF Gene Family. *International journal of evolutionary biology* 2012(298147.

Partanen J, Makela TP, Eerola E, Korhonen J, Hirvonen H, Claesson-Welsh L *et al.* (1991). FGFR-4, a novel acidic fibroblast growth factor receptor with a distinct expression pattern. *The EMBO journal* 10(6)*:*1347-1354.

Patel K, Makarenkova H, Jung HS (1999). The role of long range, local and direct signalling molecules during chick feather bud development involving the BMPs, follistatin and the Eph receptor tyrosine kinase Eph-A4. *Mechanisms of development* 86(1-2)*:*51-62.

Patstone G, Pasquale EB, Maher PA (1993). Different Members of the Fibroblast Growth Factor Receptor Family Are Specific to Distinct Cell Types in the Developing Chicken Embryo. *Developmental biology* 155(1)*:*107-123.

Pauling L, Corey RB (1951). Configurations of Polypeptide Chains With Favored Orientations Around Single Bonds: Two New Pleated Sheets. *Proceedings of the National Academy of Sciences of the United States of America* 37(11)*:*729-740.

Pauling L, Corey RB, Branson HR (1951). The structure of proteins; two hydrogen-bonded helical configurations of the polypeptide chain. *Proceedings of the National Academy of Sciences of the United States of America* 37(4)*:*205-211.

Pennycuick C, Klaassen M, Kvist A, Lindstr, Ouml, Aring (1996). Wingbeat frequency and the body drag anomaly: wind-tunnel observations on a thrush nightingale (Luscinia luscinia) and a teal (Anas crecca). *The Journal of experimental biology* 199(Pt 12)*:*2757-2765.

Peters KG, Marie J, Wilson E, Ives HE, Escobedo J, Del Rosario M *et al.* (1992). Point mutation of an FGF receptor abolishes phosphatidylinositol turnover and Ca2+ flux but not mitogenesis. *Nature* 358(6388)*:*678-681.

Pierce JW, Schoenleber R, Jesmok G, Best J, Moore SA, Collins T *et al.* (1997). Novel Inhibitors of Cytokine-induced IκBα Phosphorylation and Endothelial Cell Adhesion Molecule Expression Show Anti-inflammatory Effects in Vivo. *Journal of Biological Chemistry* 272(34)*:*21096-21103.

Pitel F, Berge R, Coquerelle G, Crooijmans RP, Groenen MA, Vignal A *et al.* (2000). Mapping the naked neck (NA) and polydactyly (PO) mutants of the chicken with microsatellite molecular markers. *Genetics, selection, evolution : GSE* 32(1)*:*73-86.

Pourquié O (2003). The Segmentation Clock: Converting Embryonic Time into Spatial Pattern. *Science (New York, NY)* 301(5631)*:*328-330.

Prum RO (1999). Development and evolutionary origin of feathers. *The Journal of experimental zoology* 285(4)*:*291-306.

Prum RO, Williamson S (2001). Theory of the growth and evolution of feather shape. *The Journal of experimental zoology* 291(1)*:*30-57.

Qiang J, Currie PJ, Norell MA, Shu-An J (1998). Two feathered dinosaurs from northeastern China. *Nature* 393(6687)*:*753-761.

Rapraeger AC, Krufka A, Olwin BB (1991). Requirement of heparan sulfate for bFGF-mediated fibroblast growth and myoblast differentiation. *Science (New York, NY)* 252(5013)*:*1705-1708.

Rawles ME (1963). Tissue Interactions in Scale and Feather Development as Studied in Dermal-Epidermal Recombinations. *Journal of embryology and experimental morphology* 11(765-789.

Reddi AH (1998). Role of morphogenetic proteins in skeletal tissue engineering and regeneration. *Nat Biotech* 16(3)*:*247-252.

Reddi AH (2005). BMPs: From bone morphogenetic proteins to body morphogenetic proteins. *Cytokine & Growth Factor Reviews* 16(3)*:*249-250.

Richardson RJ, Hammond NL, Coulombe PA, Saloranta C, Nousiainen HO, Salonen R *et al.* (2014). Periderm prevents pathological epithelial adhesions during embryogenesis. *The Journal of clinical investigation* 124(9)*:*3891-3900.

Ring DB, Johnson KW, Henriksen EJ, Nuss JM, Goff D, Kinnick TR *et al.* (2003). Selective glycogen synthase kinase 3 inhibitors potentiate insulin activation of glucose transport and utilization in vitro and in vivo. *Diabetes* 52(3)*:*588-595.

Roberts TM (1992). Cell biology. A signal chain of events. *Nature* 360(6404)*:*534-535.

Rogers GE (1985). Genes for Hair and Avian Keratins. *Annals of the New York Academy of Sciences* 455(1)*:*403-425.

Rohner N, Bercsényi M, Orbán L, Kolanczyk ME, Linke D, Brand M *et al.* (2009). Duplication of fgfr1 Permits Fgf Signaling to Serve as a Target for Selection during Domestication. *Current Biology* 19(19)*:*1642-1647.

Rothwarf DM, Zandi E, Natoli G, Karin M (1998). IKK-gamma is an essential regulatory subunit of the IkappaB kinase complex. *Nature* 395(6699)*:*297-300.

Saathoff M, Blum B, Quast T, Kirfel G, Herzog V (2004). Simultaneous cell death and desquamation of the embryonic diffusion barrier during epidermal development. *Experimental cell research* 299(2)*:*415-426.

Saka Y, Lhoussaine C, Kuttler C, Ullner E, Thiel M (2011). Theoretical basis of the community effect in development. *BMC systems biology* 5(54.

Sakou T (1998). Bone morphogenetic proteins: from basic studies to clinical approaches. *Bone* 22(6)*:*591-603.

Sampath TK, Coughlin JE, Whetstone RM, Banach D, Corbett C, Ridge RJ *et al.* (1990). Bovine osteogenic protein is composed of dimers of OP-1 and BMP-2A, two members of the transforming growth factor-beta superfamily. *The Journal of biological chemistry* 265(22)*:*13198-13205.

Sánchez-Duffhues G, Hiepen C, Knaus P, ten Dijke P (2015). Bone morphogenetic protein signaling in bone homeostasis. *Bone*.

Sasso SP, Gilli RM, Sari JC, Rimet OS, Briand CM (1994). Thermodynamic study of dihydrofolate reductase inhibitor selectivity. *Biochimica et biophysica acta* 1207(1)*:*74-79.

Saunders J (1958). Inductive specificity in the origin of integumentary derivatives in the fowl. In: The Chemical Basis of Development: The Johns Hopkins Press Baltimore, Maryland, pp. 239-253.

Savage C, Das P, Finelli AL, Townsend SR, Sun CY, Baird SE *et al.* (1996). Caenorhabditis elegans genes sma-2, sma-3, and sma-4 define a conserved family of transforming growth factor beta pathway components. *Proceedings of the National Academy of Sciences of the United States of America* 93(2)*:*790-794.

Sawada A, Shinya M, Jiang YJ, Kawakami A, Kuroiwa A, Takeda H (2001). Fgf/MAPK signalling is a crucial positional cue in somite boundary formation. *Development (Cambridge, England)* 128(23)*:*4873-4880.

Sawyer R, Knapp L, O'Guin WM (1986). Epidermis, Dermis and Appendages. In: Biology of the Integument. J Bereiter-Hahn, AG Matoltsy and KS Richards editors: Springer Berlin Heidelberg, pp. 194-238.

Sawyer RH, Abbott UK (1972). Defective histogenesis and morphogenesis in the anterior shank skin of the scaleless mutant. *The Journal of experimental zoology* 181(1)*:*99-110.

Sawyer RH, Craig KF (1977). Avian scale development. Absence of an "epidermal placode" in reticulate scale morphogenesis. *Journal of morphology* 154(1):83-93.

Sawyer RH, Glenn T, French JO, Mays B, Shames RB, Barnes GL *et al.* (2000). The Expression of Beta (β) Keratins in the Epidermal Appendages of Reptiles and Birds. *American Zoologist* 40(4):530-539.

Sawyer RH, Rogers L, Washington L, Glenn TC, Knapp LW (2005). Evolutionary origin of the feather epidermis. *Developmental dynamics : an official publication of the American Association of Anatomists* 232(2):256-267.

Scaal M, Fuchtbauer EM, Brand-Saberi B (2001). cDermo-1 expression indicates a role in avian skin development. *Anatomy and embryology* 203(1):1-7.

Scaal M, Prols F, Fuchtbauer EM, Patel K, Hornik C, Kohler T *et al.* (2002). BMPs induce dermal markers and ectopic feather tracts. *Mechanisms of development* 110(1-2):51-60.

Schneider P, Street SL, Gaide O, Hertig S, Tardivel A, Tschopp J *et al.* (2001). Mutations leading to X-linked hypohidrotic ectodermal dysplasia affect three major functional domains in the tumor necrosis factor family member ectodysplasin-A. *The Journal of biological chemistry* 276(22):18819-18827.

Sekelsky JJ, Newfeld SJ, Raftery LA, Chartoff EH, Gelbart WM (1995). Genetic characterization and cloning of mothers against dpp, a gene required for decapentaplegic function in Drosophila melanogaster. *Genetics* 139(3):1347-1358.

Sengel P, Abbott UK (1963). In Vitro Studies with the Scaleless Mutant. Interactions during Feather and Scale Differentiation. *The Journal of heredity* 54(255-262.

Sengel P (1975). Feather pattern development. *Ciba Foundation symposium* 0(29):51-70.

Sengel P (1976). Morphogenesis of skin: Cambridge University Press; Cambridge.

Sengel P (1990). Pattern formation in skin development. *The International journal of developmental biology* 34(1):33-50.

Sharrocks AD (2001). The ETS-domain transcription factor family. *Nature reviews Molecular cell biology* 2(11)*:*827-837.

Shen B, Zhang J, Wu H, Wang J, Ma K, Li Z *et al.* (2013). Generation of gene-modified mice via Cas9/RNA-mediated gene targeting. *Cell research* 23(5)*:*720-723.

Sheth R, Marcon L, Bastida MF, Junco M, Quintana L, Dahn R *et al.* (2012). Hox Genes Regulate Digit Patterning by Controlling the Wavelength of a Turing-Type Mechanism. *Science (New York, NY)* 338(6113)*:*1476-1480.

Singh C, Kumar D, Singh Y (2001). Potential usefulness of the plumage reducing Naked Neck (Na) gene in poultry production at normal and high ambient temperatures. *World's Poultry Science Journal* 57(02)*:*139-156.

Smart IH (1970). Variation in the plane of cell cleavage during the process of stratification in the mouse epidermis. *The British journal of dermatology* 82(3)*:*276-282.

Somes Jr R (1990). Mutations and major variants of plumage and skin in chickens. *Developments in Animal and Veterinary Sciences (Netherlands).*

Song H, Wang Y, Goetinck PF (1996). Fibroblast growth factor 2 can replace ectodermal signaling for feather development. *Proceedings of the National Academy of Sciences* 93(19)*:*10246-10249.

Song HK, Carver WE, Sawyer RH (1994). Pattern formation in chick feather development: distribution of beta 1-integrin in normal and scaleless embryos. *Developmental dynamics : an official publication of the American Association of Anatomists* 200(2)*:*129-143.

Song HK, Sawyer RH (1996). Dorsal dermis of the scaleless (sc/sc) embryo directs normal feather pattern formation until day 8 of development. *Developmental dynamics : an official publication of the American Association of Anatomists* 205(1)*:*82-91.

Song HK, Lee SH, Goetinck PF (2004). FGF-2 signaling is sufficient to induce dermal condensations during feather development. *Developmental dynamics : an official publication of the American Association of Anatomists* 231(4)*:*741-749.

Spearman RIC (1966). The Keratinization of Epidermal Scales, Feathers and Hairs. *Biological Reviews* 41(1)*:*59-95.

Spector I, Shochet NR, Kashman Y, Groweiss A (1983). Latrunculins: novel marine toxins that disrupt microfilament organization in cultured cells. *Science (New York, NY)* 219(4584)*:*493-495.

Staal FJ, Clevers H (2000). Tcf/Lef transcription factors during T-cell development: unique and overlapping functions. *The hematology journal : the official journal of the European Haematology Association / EHA* 1(1)*:*3-6.

Stettenheim PR (2000). The Integumentary Morphology of Modern Birds—An Overview. *American Zoologist* 40(4)*:*461-477.

Strutt D (2003). Frizzled signalling and cell polarisation in Drosophila and vertebrates. *Development (Cambridge, England)* 130(19)*:*4501-4513.

Sun L, Tran N, Liang C, Tang F, Rice A, Schreck R *et al.* (1999). Design, synthesis, and evaluations of substituted 3-[(3- or 4-carboxyethylpyrrol-2-yl)methylidenyl]indolin-2-ones as inhibitors of VEGF, FGF, and PDGF receptor tyrosine kinases. *Journal of medicinal chemistry* 42(25)*:*5120-5130.

Sung YH, Baek I-J, Kim DH, Jeon J, Lee J, Lee K *et al.* (2013). Knockout mice created by TALEN-mediated gene targeting. *Nat Biotech* 31(1)*:*23-24.

Tamai K, Semenov M, Kato Y, Spokony R, Liu C, Katsuyama Y *et al.* (2000). LDL-receptor-related proteins in Wnt signal transduction. *Nature* 407(6803)*:*530-535.

Tanaka S, Kato Y (1983). Epigenesis in developing avian scales. I. Qualitative and quantitative characterization of finite cell populations. *The Journal of experimental zoology* 225(2)*:*257-269.

Tanda N, Ohuchi H, Yoshioka H, Noji S, Nohno T (1995). A chicken Wnt gene, Wnt-11, is involved in dermal development. *Biochemical and biophysical research communications* 211(1)*:*123-129.

Tao H, Yoshimoto Y, Yoshioka H, Nohno T, Noji S, Ohuchi H (2002). FGF10 is a mesenchymally derived stimulator for epidermal development in the chick embryonic skin. *Mechanisms of development* 116(1-2)*:*39-49.

Thesleff I, Mikkola ML (2002). Death receptor signaling giving life to ectodermal organs. *Science's STKE : signal transduction knowledge environment* 2002(131):pe22.

Ting-Berreth SA, Chuong CM (1996). Sonic Hedgehog in feather morphogenesis: induction of mesenchymal condensation and association with cell death. *Developmental dynamics : an official publication of the American Association of Anatomists* 207(2):157-170.

Towers M, Signolet J, Sherman A, Sang H, Tickle C (2011). Insights into bird wing evolution and digit specification from polarizing region fate maps. *Nature communications* 2(426.

Trueb B (2011). Biology of FGFRL1, the fifth fibroblast growth factor receptor. *Cellular and molecular life sciences : CMLS* 68(6):951-964.

Tucker AS, Headon DJ, Schneider P, Ferguson BM, Overbeek P, Tschopp J *et al.* (2000). Edar/Eda interactions regulate enamel knot formation in tooth morphogenesis. *Development (Cambridge, England)* 127(21):4691-4700.

Turing AM (1952). The Chemical Basis of Morphogenesis. *Philosophical Transactions of the Royal Society of London Series B, Biological Sciences* 237(641):37-72.

Urist MR (1965). Bone: formation by autoinduction. *Science (New York, NY)* 150(3698):893-899.

van de Wetering M, Cavallo R, Dooijes D, van Beest M, van Es J, Loureiro J *et al.* (1997). Armadillo coactivates transcription driven by the product of the Drosophila segment polarity gene dTCF. *Cell* 88(6):789-799.

van Echten-Deckert G, Saathoff M, Kirfel G, Herzog V (2007). Specific distribution of barrier-relevant ceramides in the emerging epidermis and the periderm/subperiderm during chicken embryogenesis. *European journal of cell biology* 86(11-12):675-682.

Verkaar F, Zaman GJ (2010). A model for signaling specificity of Wnt/Frizzled combinations through co-receptor recruitment. *FEBS letters* 584(18):3850-3854.

Viallet JP, Prin F, Olivera-Martinez I, Hirsinger E, Pourquie O, Dhouailly D (1998). Chick Delta-1 gene expression and the formation of the feather primordia. *Mechanisms of development* 72(1-2)*:*159-168.

Wang EA, Rosen V, Cordes P, Hewick RM, Kriz MJ, Luxenberg DP *et al.* (1988). Purification and characterization of other distinct bone-inducing factors. *Proceedings of the National Academy of Sciences of the United States of America* 85(24)*:*9484-9488.

Wang F, Kan M, Yan G, Xu J, McKeehan WL (1995). Alternately spliced NH2-terminal immunoglobulin-like Loop I in the ectodomain of the fibroblast growth factor (FGF) receptor 1 lowers affinity for both heparin and FGF-1. *The Journal of biological chemistry* 270(17)*:*10231-10235.

Wang H, Yang H, Shivalila CS, Dawlaty MM, Cheng AW, Zhang F *et al.* (2013). One-step generation of mice carrying mutations in multiple genes by CRISPR/Cas-mediated genome engineering. *Cell* 153(4)*:*910-918.

Wang HY, Malbon CC (2003). Wnt signaling, Ca2+, and cyclic GMP: visualizing Frizzled functions. *Science (New York, NY)* 300(5625)*:*1529-1530.

Wang Y, Macke JP, Abella BS, Andreasson K, Worley P, Gilbert DJ *et al.* (1996). A large family of putative transmembrane receptors homologous to the product of the Drosophila tissue polarity gene frizzled. *The Journal of biological chemistry* 271(8)*:*4468-4476.

Wang Y, Li L, Zheng Y, Yuan G, Yang G, He F *et al.* (2012). BMP activity is required for tooth development from the lamina to bud stage. *Journal of dental research* 91(7)*:*690-695.

Wasylyk B, Hagman J, Gutierrez-Hartmann A (1998). Ets transcription factors: nuclear effectors of the Ras-MAP-kinase signaling pathway. *Trends in biochemical sciences* 23(6)*:*213-216.

Watt FM, Green H (1982). Stratification and terminal differentiation of cultured epidermal cells. *Nature* 295(5848)*:*434-436.

Watt FM (1998). Epidermal stem cells: markers, patterning and the control of stem cell fate. *Philos Trans R Soc Lond B Biol Sci* 353(1370)*:*831-837.

Wells KL, Hadad Y, Ben-Avraham D, Hillel J, Cahaner A, Headon DJ (2012). Genome-wide SNP scan of pooled DNA reveals nonsense mutation in FGF20 in the scaleless line of featherless chickens. *BMC genomics* 13(257.

Werner S, Duan DS, de Vries C, Peters KG, Johnson DE, Williams LT (1992). Differential splicing in the extracellular region of fibroblast growth factor receptor 1 generates receptor variants with different ligand-binding specificities. *Molecular and cellular biology* 12(1)*:*82-88.

Wessells NK (1965). Morphology and proliferation during early feather development. *Developmental biology* 12(1)*:*131-153.

Widelitz RB, Jiang TX, Noveen A, Chen CW, Chuong CM (1996). FGF induces new feather buds from developing avian skin. *The Journal of investigative dermatology* 107(6)*:*797-803.

Widelitz RB, Jiang TX, Chen CW, Stott NS, Jung HS, Chuong CM (1999). Wnt-7a in feather morphogenesis: involvement of anterior-posterior asymmetry and proximal-distal elongation demonstrated with an in vitro reconstitution model. *Development (Cambridge, England)* 126(12)*:*2577-2587.

Widelitz RB, Jiang TX, Lu J, Chuong CM (2000). beta-catenin in epithelial morphogenesis: conversion of part of avian foot scales into feather buds with a mutated beta-catenin. *Developmental biology* 219(1)*:*98-114.

Willert K, Nusse R (2012). Wnt Proteins. *Cold Spring Harbor Perspectives in Biology* 4(9).

Wisniewski SA, Kobielak A, Trzeciak WH, Kobielak K (2002). Recent advances in understanding of the molecular basis of anhidrotic ectodermal dysplasia: discovery of a ligand, ectodysplasin A and its two receptors. *Journal of applied genetics* 43(1)*:*97-107.

Witschi E (1935). Seasonal Sex Characters in Birds and Their Hormonal Control. *The Wilson Bulletin* 47(3)*:*177-188.

Wolpert L (1969). Positional information and the spatial pattern of cellular differentiation. *Journal of Theoretical Biology* 25(1)*:*1-47.

Wozney JM, Rosen V, Celeste AJ, Mitsock LM, Whitters MJ, Kriz RW *et al.* (1988). Novel regulators of bone formation: molecular clones and activities. *Science (New York, NY)* 242(4885)*:*1528-1534.

Wrench R, Hardy J, Spearman R (1980). Sebokeratocytes of avian epidermis with mammalian comparisons. *The skin of vertebrates:*47-56.

Xu X, Zhou Z, Prum RO (2001). Branched integumental structures in Sinornithosaurus and the origin of feathers. *Nature* 410(6825)*:*200-204.

Xu X, Zhou Z, Wang X, Kuang X, Zhang F, Du X (2003). Four-winged dinosaurs from China. *Nature* 421(6921)*:*335-340.

Xu X, Norell MA, Kuang X, Wang X, Zhao Q, Jia C (2004). Basal tyrannosauroids from China and evidence for protofeathers in tyrannosauroids. *Nature* 431(7009)*:*680-684.

Xu X, Zhang F (2005). A new maniraptoran dinosaur from China with long feathers on the metatarsus. *Naturwissenschaften* 92(4)*:*173-177.

Xu X, Wang K, Zhang K, Ma Q, Xing L, Sullivan C *et al.* (2012). A gigantic feathered dinosaur from the Lower Cretaceous of China. *Nature* 484(7392)*:*92-95.

Yamasaki E, Soma Y, Kawa Y, Mizoguchi M (2003). Methotrexate inhibits proliferation and regulation of the expression of intercellular adhesion molecule-1 and vascular cell adhesion molecule-1 by cultured human umbilical vein endothelial cells. *The British journal of dermatology* 149(1)*:*30-38.

Yan M, Wang LC, Hymowitz SG, Schilbach S, Lee J, Goddard A *et al.* (2000). Two-amino acid molecular switch in an epithelial morphogen that regulates binding to two distinct receptors. *Science (New York, NY)* 290(5491)*:*523-527.

Yang H, Wang H, Shivalila CS, Cheng AW, Shi L, Jaenisch R (2013). One-step generation of mice carrying reporter and conditional alleles by CRISPR/Cas-mediated genome engineering. *Cell* 154(6)*:*1370-1379.

Yayon A, Klagsbrun M, Esko JD, Leder P, Ornitz DM (1991). Cell surface, heparin-like molecules are required for binding of basic fibroblast growth factor to its high affinity receptor. *Cell* 64(4)*:*841-848.

Yu M, Yue Z, Wu P, Wu DY, Mayer JA, Medina M *et al.* (2004). The biology of feather follicles. *The International journal of developmental biology* 48(2-3)*:*181-191.

Yue Z, Jiang T-X, Widelitz RB, Chuong C-M (2005). Mapping stem cell activities in the feather follicle. *Nature* 438(7070)*:*1026-1029.

Zhao D, McBride D, Nandi S, McQueen HA, McGrew MJ, Hocking PM *et al.* (2010). Somatic sex identity is cell autonomous in the chicken. *Nature* 464(7286)*:*237-242.

Zhou S, Lo WC, Suhalim JL, Digman MA, Gratton E, Nie Q *et al.* (2012). Free extracellular diffusion creates the dpp morphogen gradient of the Drosophila wing disc. *Current biology : CB* 22(8)*:*668-675.

Zhou Z, Barrett PM, Hilton J (2003). An exceptionally preserved Lower Cretaceous ecosystem. *Nature* 421(6925)*:*807-814.

Zou H, Niswander L (1996). Requirement for BMP signaling in interdigital apoptosis and scale formation. *Science (New York, NY)* 272(5262)*:*738-741.